12-15-2014 12:00 AM

Polyglyoxylates: a new class of triggerable self-immolative polymers

Bo Fan
The University of Western Ontario

Supervisor
Elizabeth Gillies
The University of Western Ontario

Graduate Program in Chemistry
A thesis submitted in partial fulfillment of the requirements for the degree in Master of Science

«POLYGLYOXYLATES: A NEW CLASS OF TRIGGERABLE SELF-IMMOLATIVE POLYMERS »

(Thesis format: Integrated Article)

by

Bo Fan

Graduate Program in Chemistry

A thesis submitted in partial fulfillment
of the requirements for the degree of
Master of Science

The School of Graduate and Postdoctoral Studies
The University of Western Ontario
London, Ontario, Canada

Abstract

Self-immolative polymers, which degrade by an end-to-end depolymerization mechanism in response to the cleavage of a stabilizing end-cap from the polymer terminus, are of increasing interest for a wide variety of applications ranging from sensors to controlled release. However, the preparation of these materials often requires expensive, multi-step monomer syntheses and the degradation products such as quinone methides or phthalaldehydes are potentially toxic to humans and the environment. We demonstrate here that polyglyxoylates can serve as a new and versatile class of self-immolative polymers. Polymerization of the commercially available monomer ethyl glyoxylate, followed by end-capping with a 6-nitroveratryl carbonate provides a poly(ethyl glyoxylate) that depolymerizes selectively upon irradiation with UV light. Via ozonolysis of corresponding fumaric or maleic acid derivatives, a series of different glyoxylates were synthesized and polymerized, providing polyglyoxylates with different physical properties. Furthermore, using a multifunctional end-cap that is UV-responsive and also enables the conjugation of another polymer block via an azide-alkyne "click" cycloaddition, amphiphilic self-immolative block copolymers were prepared and self-assembled into light responsive micelles for drug delivery. Lastly, stimuli-responsive end-caps other than those responsive to UV light were also installed at the termini of poly(ethyl glyoxylate) to achieve polyglyoxylates responsive to other stimuli. Overall, these strategies are expected to greatly expand the utility of self-immolative polymers by providing access for the first time to self-immolative polymers with tunable properties that can be readily obtained from simple monomers and which depolymerize into non-toxic products.

Keywords

Self-immolative polymers, polyglyoxylates, degradation, ozonolysis, amphiphilic block copolymer, UV light sensitive, micelles, drug delivery, depolymerization, stimuli-responsive.

Co-Authorship Statement

The research described in this thesis is a result of contribution from the author as well as coworkers from Western University and supervisor Dr. Elizabeth Gillies. The detailed contributions for each chapter are as follows:

Chapter 1 was written collaboratively by the author and Dr. Gillies.

Chapter 2 describes a project proposed by Dr. Gillies with additional conception of the monomers from fumaric acid and maleic acid by Dr. John Trant and Andrew Wong. The author conducted all the synthesis and characterization experiments under the supervision of Dr. Gilllies. Chomatographic analysis of the polymers was performed by Gillies lab technician, Aneta Borecki. The manuscript was prepared by the author and was revised with the assistance of Dr. Gillies, Dr. Trant and Andrew Wong.

Chapter 3 describes a project proposed by Dr. Gillies and further developed by the author. The author conducted all the experiments under the supervision of Dr. Gillies. The chapter was written by the author and edited by Dr. Gillies.

Chapter 4 describes work jointly conceived by the author and Dr. Gillies. All of the experimental work was carried out by the author. The chapter was written by the author and edited by Dr. Gillies.

Chapter 5 was written by the author and edited by Dr. Gillies.

Acknowledgements

In the first place, I would like to give my sincere thanks to my supervisor Dr. Gillies. I thank her for accepting me as a member of this caring, mutually helping and creative research group. Research is hard work, and it is sure I met lots of difficulties in the past two years with my own research. Some of them were really frustrating, but each time after I talked with Dr. Gillies, I would feel energetic and devote into it my research again until we finally worked it out. Therefore, I would also like to thank Dr. Gillies for her guidance and encouragement along this way.

My thanks would also go to all the past and present members of Gillies group. Thank you all for creating a caring and mutually helping research environment. You leave me with lots of unforgettable memories during the past two years. Especially, I will thank Dr. John Trant for his mentoring and lots of excellent suggestions for my research. I also want to thank our laboratory technician, Aneta Borecki, for helping with the tons of SEC samples. Furthermore, I would like to thank Andrew Wong, Dr. Ali Nazemi and all the other members in our group.

I also would like to thank my thesis examiners Dr. Luyt, Dr. Stillman, and Dr. Xu for taking time to read through my thesis. Many thanks to all the faculty and staff in the Department of Chemistry as well, without whom this thesis would not be possible.

Furthermore, I would like to thank all my friends both in Canada and out of Canada.

Lastly but not the least, I want to give the deepest thanks to my parents, without the constant love, supporting and encouragement from both of you, nothing will be possible for me.

Thank all the people who helped me along this way!

Table of Contents

List of Tables

List of Figures

List of Schemes

List of Abbreviations

Bn	Benzyl
BnG	Benzyl glyoxyalte
Bu	Butyl
BuG	Butyl glyoxylate
CuAAC	Copper-assisted azide-alkyne cycloaddition
CR	Counter rate
DBTL	Dibutyltin dilaurate
DLS	Dynamic light scattering
DSC	Differential scanning calorimetry
DTT	Dithiothereitol
DMAP	4-Dimethylaminopyridine
DMF	*N*, *N*-Dimethylformamide
DMSO	Dimethyl sulfoxide
$Đ$	Dispersity
EDC	1-Ethyl-3-(3-dimethylaminopropyl)carbodiimide
Et	Ethyl
EtG	Ethyl glyoxylate
EtGH	Ethyl glyoxylate hydrate
FT-IR	Fourier transform infrared spectroscopy
Me	Methyl
M_n	Number average molecular weight
M_w	Weight average molecular weight
MWCO	Molecular weight cut-off
MSDS	Material safety data sheets
NEt_3	Triethyl amine
NMR	Nuclear magnetic resonace
NVOC	6-Nitroveratryloxycarbonyl
NVOC-Cl	6-Nitroveratryloxycarbonyl chloride
OPA	*o*-phthalaldehyde

PBnG	Poly(benzyl glyoxylate)
PBuG	Poly(butyl glyoxylate)
PDI	Polydispersity index
PEtG	Poly(ethyl glyoxylate)
PEG	Poly(ethylene glycol)
PMeG	Poly(methyl glyoxylate)
PMA	Poly(methyl acrylate)
PPHA	Poly(phthalaldehyde)
PS	Polystyrene
SEC	Size exclusion chromatography
SIP	Self-immolative polymer
TGA	Thermogravimetric analysis
THF	Tetrahydrofuran
TEM	Transmission electron microscopy
T_o	On-set degradation temperature
T_p	Peak degradation temperature
T_{98}	Maximum temperature at which 98% of mass is still present
T_g	Glass transition temperature
T_m	Melting point temperature
UV	Ultraviolet

Chapter 1

1 Self-immolative Polymers

1.1 Introduction

In recent years there has been significant interest in the development of stimuli-responsive polymers for a wide range of applications. For example, thermoresponsive polymers can serve as valves in microfluidic devices,[1] while polymers responding to intrinsic biological stimuli such as enzymes, or changes in pH or redox potential can be used to selectively deliver drug molecules to diseased sites *in vivo*.[2] There are several established mechanisms by which polymers can respond to stimuli. The stimulus can trigger a change in the charge state or solubility of the polymer backbone or pendant functional group along the polymer backbone (Fig. 1.1a). For example, polyamines undergo protonation-deprotonation in a pH-dependent manner, which can result in water-soluble material at neutral and acidic pH, and water-insoluble material at basic pH.[3] Alternatively, a stimulus can result in the cleavage of pendant groups along the polymer backbone (Fig. 1.1b). For example, pendant cyclic acetal groups undergo hydrolysis at acid pH, resulting in the transformation of the pendant hydrophobic groups to hydrophilic ones, changing the polymer from water-insoluble to water-soluble.[4] Stimuli can also trigger cleavage of the polymer backbone and ultimately its degradation into small molecules (Fig. 1.1c). For example, polymers with pH-sensitive acetals,[5] reduction-sensitive disulfides,[6] and photochemically-cleavable *o*-nitrobenzyl ester moieties[7] in their backbones have been reported.

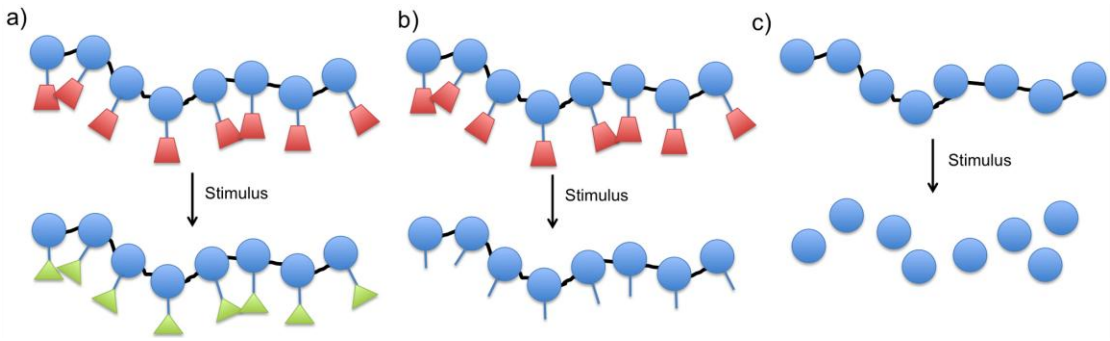

Figure 1. 1 Schematic representations of the mechanisms by which polymers can respond to stimuli: a) Change in solubility of the polymer backbone or pendant groups; b) Cleavage of pendant groups from the backbone; c) Cleavage of the polymer backbone.

A limitation to most of the approaches described above is that multiple stimuli-mediated events are required in order to effect significant changes in the polymer properties. For example, multiple stimuli-mediated cleavages of pendant groups or backbone moieties are required to change the solubility of a polymer or to break it down to small molecules. While large changes in chemical environment and high concentrations of stimuli are easily achieved in the laboratory, in real applications the changes in environmental conditions are generally more subtle and the concentrations of stimuli are much lower. Therefore, there is significant interest in the development of approaches that can amplify the response of materials to stimuli. Self-immolative dendrimers were developed in 2004 almost simultaneously by the groups of McGrath,[8] de Groot,[9] and Shabat[10] with the aim of amplifying responses to stimuli. These molecules employed the self-immolative spacer concept initially developed for prodrugs in which cleavage of a trigger moiety initiates a spontaneous intramolecular reaction such as an elimination or cyclization, to release a drug molecule (Fig. 1.2).[11] The linkage of multiple self-immolative spacers sequentially in branched form led to dendrimers that could fragment, releasing multiple molecules from the dendrimer periphery upon cleavage or activation of a trigger moiety at the dendrimer focal point (Fig. 1.3a).[8-10]

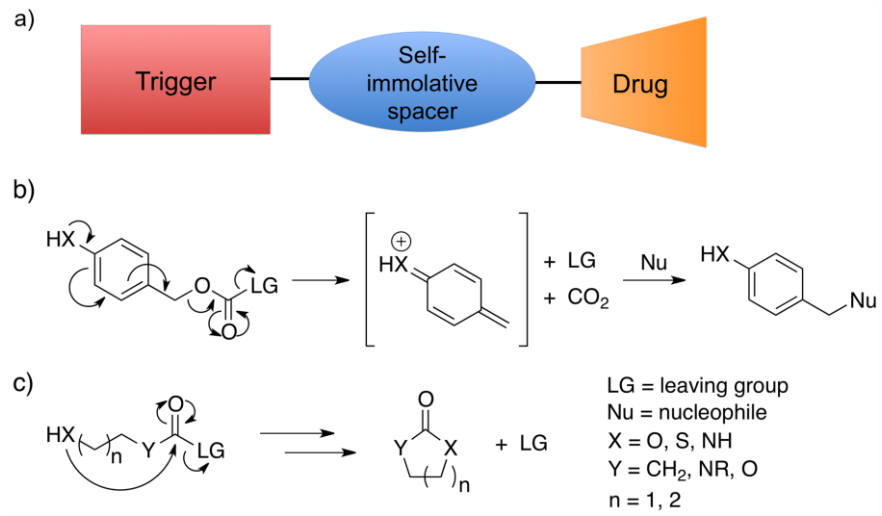

Figure 1. 2 a) Schematic of a prodrug employing a self-immolative spacer and trigger; b) General scheme for an elimination spacer; c) General scheme for a cyclization spacer.

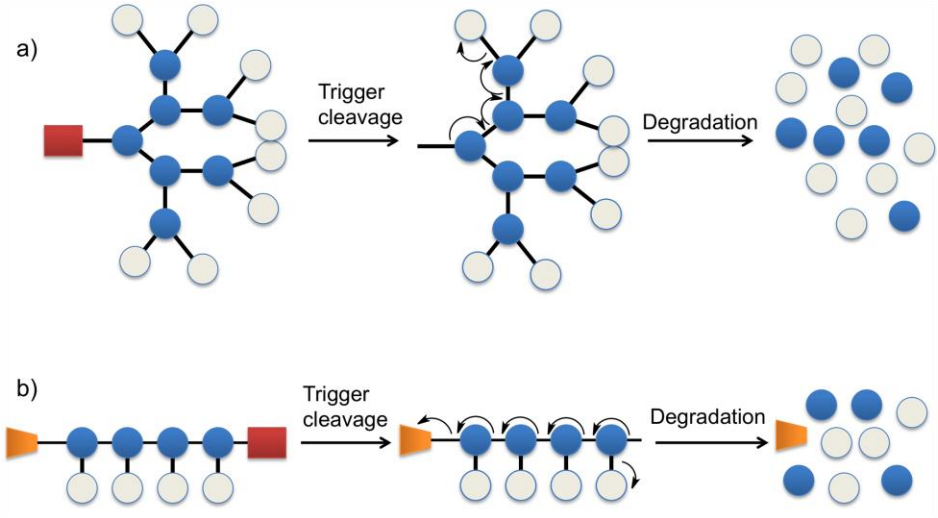

Figure 1. 3 Cleavage of a trigger moiety by a stimulus initiates fragmentation of a self-immolative a) dendrimer and b) oligomer.

Since their conception, a wide range of self-immolative dendrimers have been developed, with potential applications ranging from drug delivery vehicles[12] to chemical sensors.[13] Self-immolative spacers have also been combined in oligomeric form through step-wise synthesis in order to enable the release of terminal as well as multiple pendant

groups upon triggering (Fig. 1.3b).[14] However, limitations of these systems include their tedious, step-wise synthesis, as well as issues of steric hindrance in the case of dendrimers, which limits the number of branching layers (i.e., generations) that can be prepared and thus the extent of signal amplification.

The preparation of linear self-immolative polymers (SIPs) through one-step polymerization reactions offers a possibility to overcome the limitations of multi-step dendrimer and oligomer syntheses, as well as the steric hindrance issues associated with dendrimers. Their design is similar to that of the above described dendrimers in that activation or cleavage of a trigger moiety at the polymer terminus initiates a cascade of reactions that results in depolymerization (Fig. 1.4). Indeed the concept of depolymerization has been known for decades in the context of polymers with low ceiling temperatures (T_c). For example, polyformaldehyde was developed by DuPont as the first engineering plastic, but required stabilization via acetate end-capping. [15] It has a ceiling temperature of ~120 °C in its unend-capped form, above which the entropy gained through depolymerization overrides the relatively small enthalpic gain of polymerization, but this is increased to >200 °C through end-capping. [16]

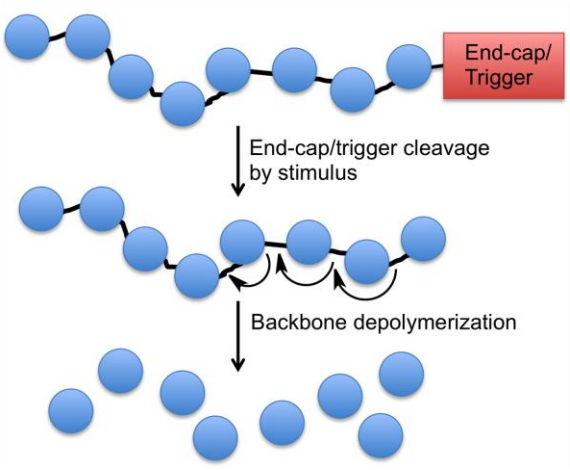

Figure 1. 4 Schematic illustrating how cleavage of a terminal end-cap/trigger moiety initiates depolymerization of a SIP.

Despite many decades of knowledge on polymer T_c and depolymerization, the use of stimuli-responsive end-caps in combination with backbones that depolymerize by sequences of well-defined reactions has enabled a new level of control over this degradation process, allowing SIPs to be exploited for signal amplification and stimuli-responsive materials.[17] Described here is the development of several classes of self-immolative linear polymers including poly(benzyl carbamate)s, polycarbamates and polythiocarbamates that depolymerize via cyclization reactions, polyacetals, and poly(benzyl ether)s, including their syntheses and depolymerization mechanisms. Their application in functional materials including sensors, capsules, nanoscale polymer assemblies, and microscale pumps is described. The depolymerization kinetics is also summarized, as this is a key feature that distinguishes the degradation of self-immolative polymers from that of traditional biodegradable polymers. Finally, the current state-of-the-art for the field and future outlook are discussed.

1.2 Poly(benzyl carbamate)s

The first linear SIP backbone was introduced in 2008 by Shabat and coworkers.[18] It was based on the 4-aminobenzyl alcohol spacer that had previously been widely exploited in prodrugs[11a-c] and previous self-immolative dendrimers[13a] and oligomers[14b, 14d]. When incorporated into electron withdrawing groups such as carbamates, the aniline nitrogen is insufficiently electron-donating to undergo an elimination reaction, but upon activation, revealing the electron donating aniline, the molecule undergoes a 1,6-elimination reaction to generate an azaquinone methide and release the substituent on the benzylic position (Fig. 1.5). The released azquinone methide can further react with surrounding nucleophiles such as water, regenerating aromaticity. The approach of Shabat and coworkers involved the preparation of a phenyl carbamate derivative of 4-aminobenzyl alcohol.[18] This derivative was quite stable at room temperature, but underwent polymerization in the presence of dibutyltin dilaurate (DBTL) at high temperature (100 °C), followed by reaction with an alcohol-functionalized end-cap molecule to provide the

target self-immolative polycarbamate (Fig. 1.6). Cleavage of the end-cap revealed the aniline, triggering depolymerization via alternating 1,6-elimination and loss of CO_2.

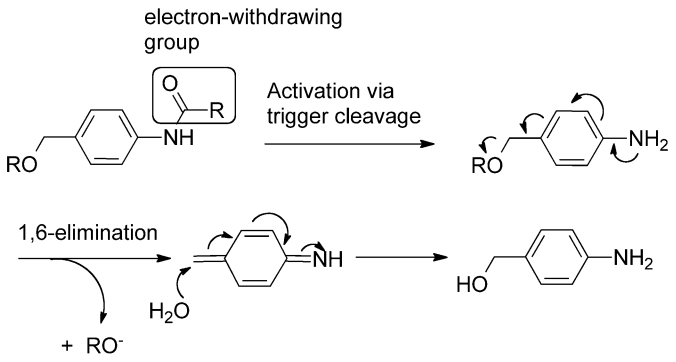

Figure 1. 5 Mechanism of the 1,6-elimination reaction.

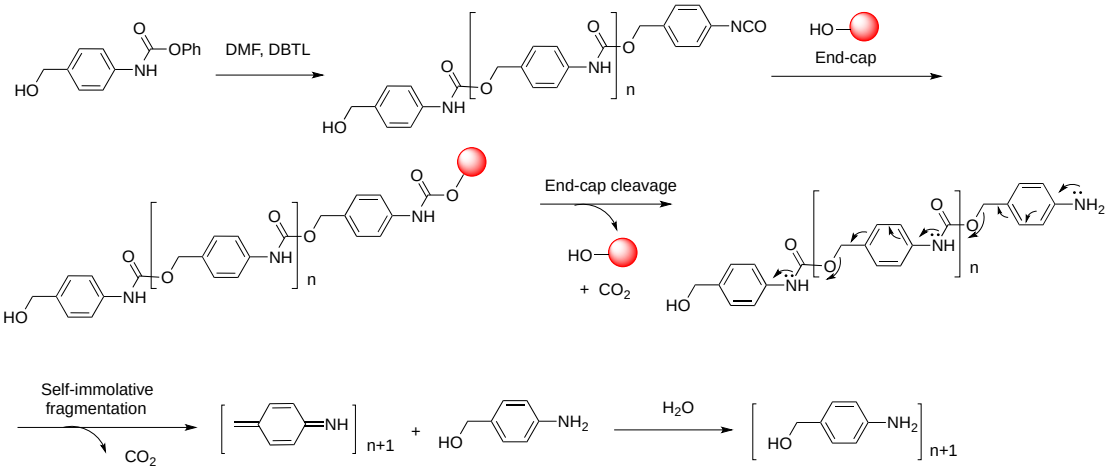

Figure 1. 6 Synthesis of a self-immolative poly(benzyl carbamate) and its depolymerization following end-cap cleavage.

In this initial work of Shabat and coworkers, 4-hydroxy-2-butanone was used as the end-cap.[18] In the presence of bovine serum albumin (BSA), this end-cap was removed via β-elimination, triggering depolymerization (Fig. 1.7). In order to detect depolymerization and to enable use of the polymer as a turn-on fluorescent sensor for BSA, the 4-hydroxybenzyl alcohol monomer was modified with an acrylate substituent *ortho* to the amine (Fig. 1.7). When the amine was functionalized as a carbamate, this monomer exhibited only weak fluorescence, but upon release of the amine, the monomer exhibited

strong fluorescence emission at 510 nm. Thus, the production of the free amine upon depolymerization in the presence of BSA led to a significant increase in fluorescence emission. In addition, while the pendant carboxylic acid group of the acrylate could be protected as a *t*-butyl ester during polymerization, cleavage of these *t*-butyl protecting groups from the resultant polymer provided many ionizable carboxylic acid groups, imparting water solubility to the material.

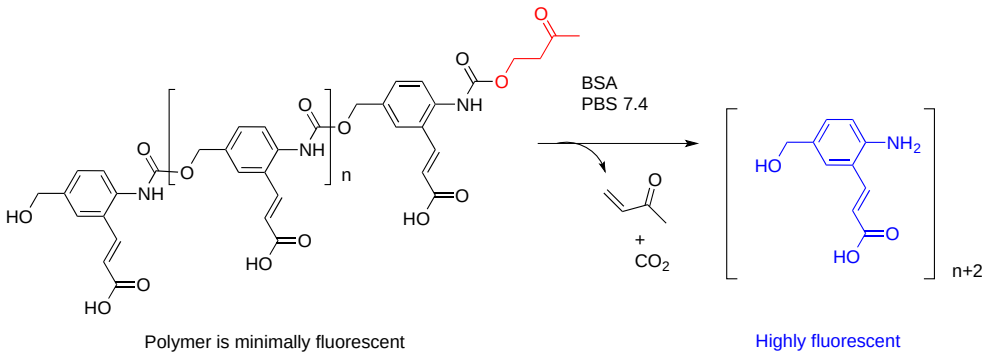

Figure 1. 7 A water-soluble poly(benzyl carbamate) with pendant carboxylic acid groups that undergoes depolymerization in the presence of BSA to release fluorescent monomer units.

In subsequent work, Shabat and coworkers modified the design to incorporate the pendant 4-nitroaniline groups into each monomer.[19] Depolymerization was activated by the cleavage of the 4-hydroxy-2-butanone end-cap by piperidine, and a subsequent 1,6-elimination of the depolymerized monomers released the 4-nitroaniline reporter molecules (Fig. 1.8). In this case, the solubility of the polymer required that the depolymerization be performed in organic solvent, where it is relatively slow. This was addressed through the synthesis and polymerization of a dimeric monomer with a protected carboxylic acid group on one unit and a 4-nitroaniline reporter molecule on the other. This polymer was end-capped with a phenylacetamide moiety, designed for cleavage by penicillin-G amidase (PGA). Following deprotection of the carboxylic acid moieties on the resulting polymer, the molecule was water-soluble and could be triggered by PGA to depolymerize, releasing the reporter molecules.

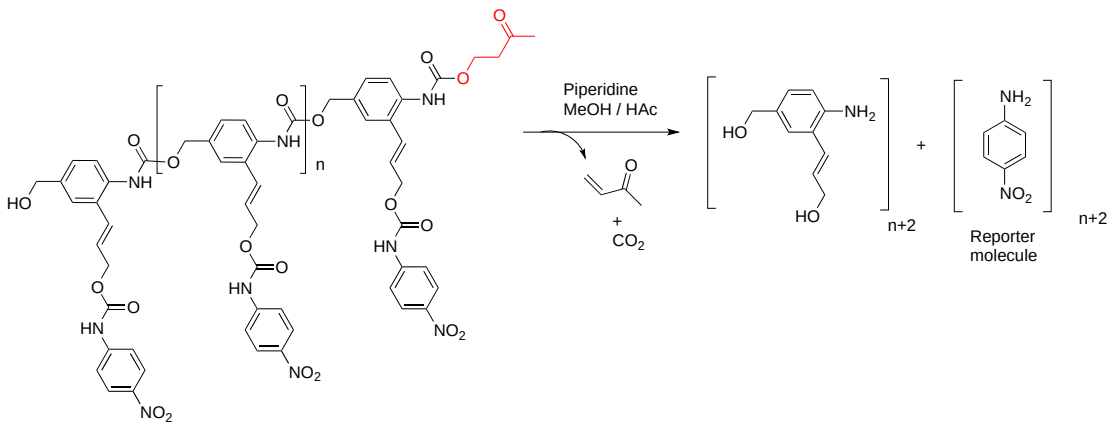

Figure 1. 8 Depolymerization of a poly(benzyl carbamate) releases 4-nitroaniline reporter molecules.

Because the azaquinone methide intermediate generated upon depolymerization is highly reactive, in addition to water molecules, it can also react with other nucleophiles. Shabat and coworkers have used this reactivity for the activity-linked labeling of enzymes (Fig. 1.9).[20] The phenylacetamide and 4-hydroxy-2-butanone end-caps described above were used to impart sensitivity to PGA and a catalytic antibody Ab38C2 respectively. Following small molecule model studies, it was demonstrated that the labeling of both PGA and Ab38C2 could be achieved following cleavage of the SIPs by these enzymes. Following labeling, PGA did not exhibit a significant reduction in its activity. However, the activity of Ab38C2 did decrease as the concentration of the SIP probe increased in the reaction, suggesting that labeling of the active site lysine ε-amine interfered with catalytic activity. It was also demonstrated that SIPs could provide enhanced levels of labeling while preserving higher catalytic activity in comparison with self-immolative monomers or oligomers. This was attributed to the gradual breakdown of the SIP over seconds to minutes, during which time the SIP could diffuse farther from the active site, allowing azaquinone methide species to be released in the vicinity of protein nucleophiles whose modification would not affect catalytic activity. Despite this possibility for polymer diffusion, when both an activating and non-activating protein were present during the reaction, the labeling of the activating protein was 8-fold higher than that of the non-activating protein.

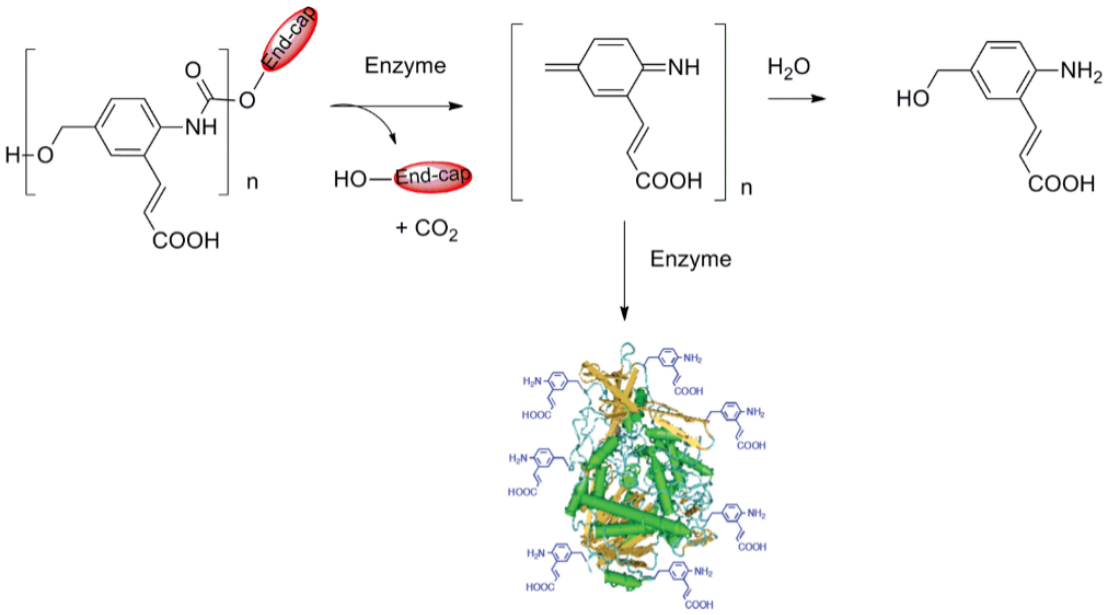

Figure 1. 9 Activity-linked labeling of enzymes through the reaction of azaquinone methide species with nucleophilic groups on proteins. Adapted with permission from reference [20]. Copyright 2009 American Chemical Society.

In addition to the initial enzyme sensors described by Shabat, poly(benzyl carbamate) SIPs have also been used in a variety of other sensor devices. For example, Phillips and coworkers incorporated polycarbamate oligomers with H_2O_2-sensitive aryl boronate end-caps as phase-switching agents in quantitative time-based assays.[21] The principle behind this design is that upon depolymerization the SIP changes from a hydrophobic, water-impermeable layer to hydrophilic, water-soluble degradation products, allowing water to wick through the layered, paper-based device, dissolving food-coloring in a subsequent layer (Fig. 1.10). The resulting brightly-colored solution provides a simple visual read-out for the device, the only required measurable being time for the signal to be produced, which depends on the concentration of H_2O_2. This aspect makes these devices promising for applications in resource-limited environments including the developing world. It was found that the use of oligomers improved the detection limit of the device by 4 orders of magnitude to 6 nM H_2O_2, in comparison with an analogous device using a small molecules[22] due to the amplification effect afforded by the depolymerization mechanism. It was proposed that the sensitivity could be further improved by using longer polymers,

but only if they depolymerized more rapidly than the residence time in the device. The same team has recently expanded this assay to employ a cascade of events involving aptamers and enzymatic reactions to ultimately trigger cleavage of the aryl boronate end-cap. This has enabled the detection of inorganic ions including Pb^{2+} and Hg^{2+}, with the possibility to expand to other analytes including small molecules, enzymes, and other inorganic ions.[23]

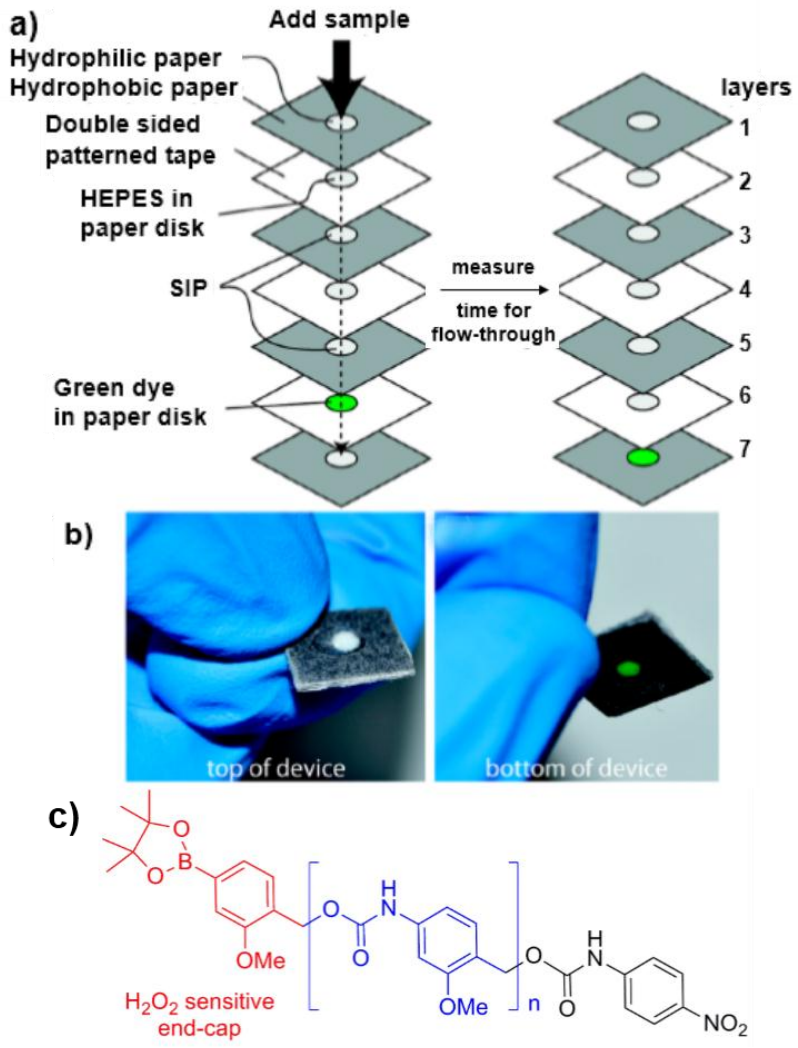

Figure 1. 10 a) Schematic of the design of a phase-switching, time-based assay; b) Observed read-out on the actual device; c) Chemical structure of the SIP employed in this device. Adapted with permission from reference [21]. Copyright 2013 American Chemical Society.

While the sensors developed by Phillips and coworkers successfully demonstrated the potential utility of the self-immolative polycarbamates, they also highlighted one of their limitations. The degradation rate of these SIPs is relatively slow in polar environments, and is even slower or may not occur at all in environments with low dielectric constant. They suggested that as depolymerization is proposed to occur via less aromatic transition states resembling azaquinone methides, it should be possible to reduce the energy penalty and thus increase the depolymerization rate by two possible approaches.[24] One approach involved reducing the aromaticity of the parent structure (Fig. 1.11a) by replacing the benzene ring with a naphthalene (Fig. 1.11b). A second approach involved the addition of a methoxy group to the aromatic ring in order to increase electron density and raise the highest occupied molecular orbital (HOMO) (Fig. 1.11c). This approach was successful with the naphthalene derivative providing a 113-fold enhancement and the methoxy derivative providing a 143-fold enhancement in the rate of depolymerization. Thus, this work provided important guideline on the design of rapidly-degradable poly(benzyl carbamates).

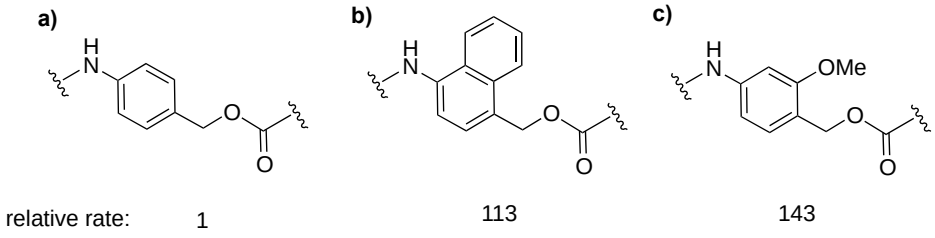

Figure 1. 11 Chemical structures of 4-aminobenzyl alcohol derivatives with increased rates of 1,6-elimination: a) parent structure; b) naphthalene derivative; c) methoxy derivative.

In addition to the end-caps described above, Boydston and coworkers have recently used a bicyclic 1,2-oxazine end-cap to afford thermal triggering of self-immolative polycarbamates.[25] As shown in Fig. 1.12a, it was anticipated that heating would result in cycloreversion of the oxazine to an unstable carbamoylnitroso intermediate which following hydrolysis would rapidly decarboxylate to generate the free amine, initiating depolymerization.[26] Poly(*N*,*N*-dimethylacrylamide) (PDMA) was synthesized by atom

transfer radical polymerization (ATRP) from a pentamethylcyclopentadiene-based initiator and then reacted with hydroxyurea end-capped SIP under oxidative conditions to afford a diblock copolymer via *in situ* oxidation to the nitroso followed by cycloaddition reaction (Fig. 1.12b). It was shown that the resulting block copolymer underwent depolymerization in a temperature-dependent manner in 9:1 DMSO-d_6:D_2O. In comparison, depolymerization was slower for a control polymer with a non-responsive end-cap, though some depolymerization was observed for the control polymer at higher temperatures, suggesting that hydrolysis is also involved at greater than 60 °C. Trapping studies with cyclohexadiene further supported the role of the carbamoylnitroso intermediate and thus the proposed thermolysis mechanism. Thus in addition to chemical stimuli it is also possible to use heat to trigger depolymerization of SIPs.

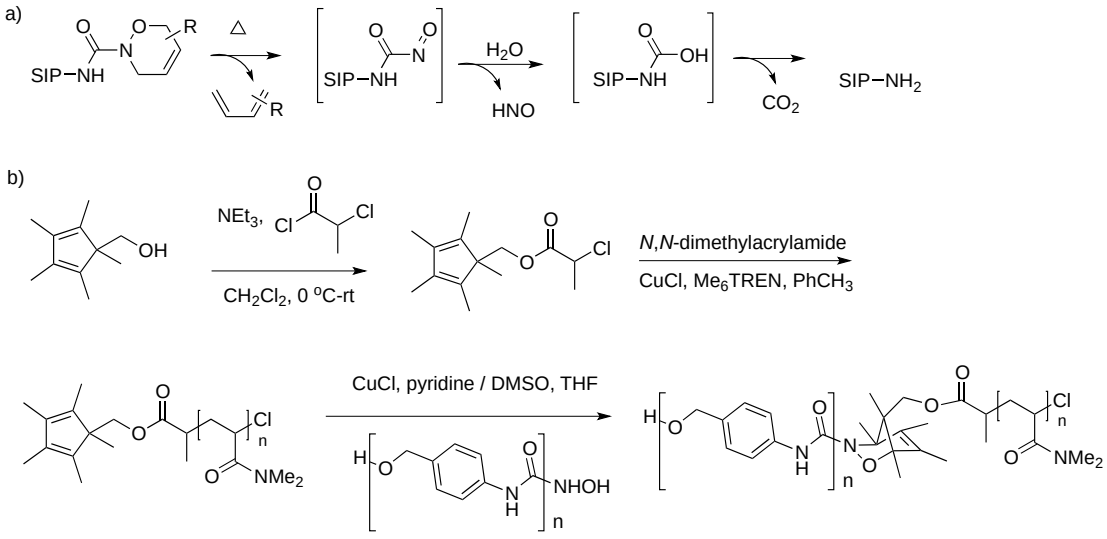

Figure 1. 12 a) Proposed mechanism of thermally-activated end-cap clavage; b) Synthesis of a block copolymer containing a SIP and a heat-sensitive linkage between the blocks.

Through the incorporation of pendant *t*-butyldimethylsilyl (TBDMS) protected hydroxyl groups along the backbone of this polymer, Moore and coworkers prepared cross-linkable SIPs based on poly(benzyl carbamate)s.[27] *t*-Butyloxycarbonyl (Boc) and fluorenylmethyloxycarbonyl (Fmoc) end-caps were used, providing sensitivity to acid and base respectively. After removal of the TBDMS groups, the hydroxyl groups were

converted to isocyanates by reaction with excess 2,4-toluene diisocyanate (2,4-TDI) (Fig. 1.13a). An emulsion of water with gum arabic as a surfactant and viscosity modifier, and ethyl phenylacetate as the organic phase containing the isocyanate-functionalized polymers was prepared. Interfacial cross-linking was performed using butandiol. Microcapsules with sizes ranging from 5 μm to 40 μm containing ethyl phenylacetate in their cores were produced. Upon triggering with either HCl (Boc capsules) or piperidine (Fmoc capsules) the capsules released their core contents over a period of 24-48 hours. In contrast, capsules prepared from a non-self-immolative control polymer released negligible core contents over this period. In addition, electron microscopy revealed that the triggered capsules became cracked and deflated, whereas control capsules were unaffected by the acidic or basic triggering conditions (Fig. 1.13b). These results suggest that such capsules are promising for potential applications such as drug delivery and self-healing materials.

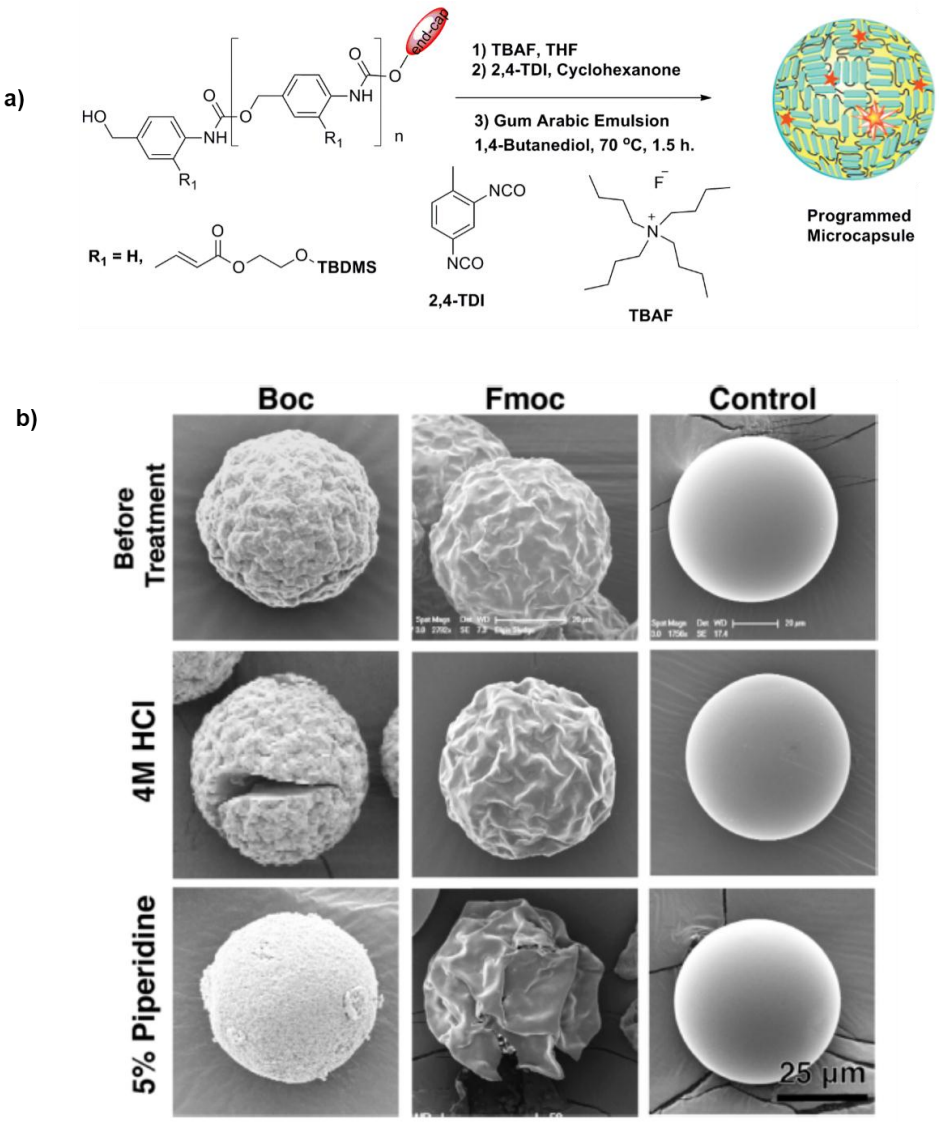

Figure 1. 13 a) Preparation of microcapsules from a self-immolative poly(benzyl carbamate); b) Changes in capsule shell morphology under different conditions. Adapted with permission from reference [27]. Copyright 2010 American Chemical Society.

Poly(benzyl carbamate)s have also been incorporated into block copolymers. As the parent poly(benzyl carbamate) is water-insoluble, its linkage to a hydrophilic block provides an amphiphilic block copolymer that can self-assemble in aqueous solution to form nanoassemblies. Liu and coworkers synthesized poly(benzyl carbamate) by the

previously reported method[18] and incorporated end-caps including perylen-3-yl methanol, 2-nitrobenzyl alcohol, and diethanol disulfide which are visible light-, UV-light-, and reduction-responsive end-caps respectively (Fig. 1.14) or a noncleavable benzyl alcohol end-cap.[28] The remaining alcohol termini were then functionalized with a reversible addition-fragmentation chain transfer (RAFT) agent. RAFT polymerization was then used to grow hydrophilic poly(*N*,*N*-dimethylacrylamide) (PDMA) block, resulting in block copolymers with hydrophilic fractions on the order of 60-70 wt%. Self-assembly of the polymers in aqueous solution was then investigated. The assemblies were studied by transmission electron microscopy (TEM), scanning electron microscopy (SEM), confocal laser scanning microscopy, and dynamic light scattering. It was found that these block copolymers formed vesicles with diameters ranging from 200 to 580 nm. This behavior was despite their relatively high hydrophilic fraction in comparison to the expected volume fraction of ~ 25-45 wt% for vesicle-forming block copolymers.[29] This was attributed to the strong hydrogen-bonding interactions between the carbamate groups. Upon end-cap cleavage with light or reducing conditions, the vesicles were shown by microscopy, NMR spectroscopy, and size exclusion chromatography (SEC) to depolymerize and disintegrate. The release of 4-aminobenzyl alcohol was also demonstrated.

Liu and coworkers also exploited the capabilities of vesicles to incorporate hydrophilic payloads in their aqueous core and hydrophobic payloads in their membranes.[28] Using the reduction-sensitive disulfide system, they encapsulated hydrophilic doxorubicin as its HCl salt and hydrophobic camptothecin. They demonstrated selective release of both drugs in the presence of the reducing agent glutathione. Encapsulation and release of the photosensitizer eosin was also investigated. Furthermore, using different combinations of the light- and reduction-responsive vesicles, OR, AND, and XOR logic gate-type programmed enzymatic reactions were constructed.

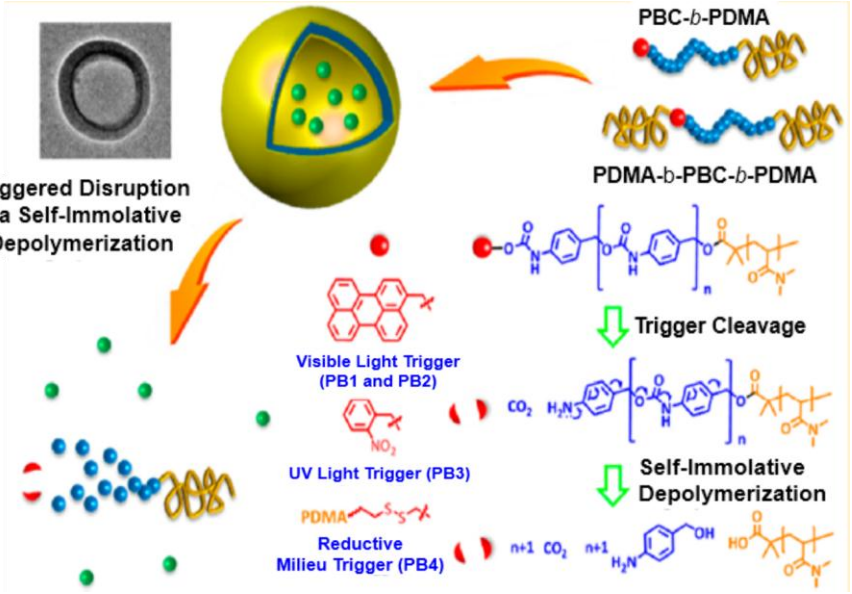

Figure 1. 14 Synthesis of diblock copolymers containing self-immolative blocks with light- and reduction-sensitive linkers and their self-assembly into vesicles. End-cap cleavage lead to the release of cargo from the vesicles. Adapted with permission from reference [28]. Copyright 2014 American Chemical Society.

In contrast to using the SIP in the shell of vesicles or capsules, Cornelissen and coworkers have encapsulated water-soluble self-immolative polycarbamates with pendant acrylic acid groups (as in Figure 1.7 above) into the cores of Cowpea Chlorotic Mottle Virus (CCMV) capsids.[30] The SIP was capped with a 5-methoxy-2-nitrobenzyl carbamate to afford depolymerization in response to UV light. Upon irradiation with 350 nm light, depolymerization occurred, resulting in a significant increase in the fluorescence emission at 490 nm indicative of depolymerization, and resulting monomers were released through the capsid pores. Dynamic light scattering and transmission electron microscopy (TEM) suggested that in the the capsid underwent a morphological change and shrinkage upon depolymerization, a phenomenon that was not observed for capsids containing nondegradable poly(styrene sulfonate) that were irradiated. The presence of Mg^{2+} ions was found to stabilize the capsules with respect to this morphological change, likely through binding to the pores, yet it did not prevent depolymerization or the release

of monomers. Overall, this concept offers an alternative strategy for the loading and noninvasively triggered release of small molecules from capsids.

1.3 SIPs Degrading via Cyclization Reactions

In addition to the self-immolative poly(benzyl carbamates) that depolymerize via 1,6-elimination reactions and loss of CO_2, another important category of SIPs is those incorporating cyclization reactions. As described below, these cyclization reactions can be used to tune the depolymerization rate when used in combination with the 1,6-elimination, CO_2 elimination sequence, and they also reduce the generation of potentially toxic quinone methide species[31] that arise from the 1,6-elimination. Using an activated monomer based on 4-hydroxylbenzyl alcohol and *N*,*N*'-dimethylethylenediamine, Gillies and coworkers prepared a self-immolative polycarbamate capped with a Boc group.[32] As shown in Fig. 1.15, in the presence of base as well as 5 mol% of Boc protected monomer as an end-cap, the amines on the monomers reacted with the 4-nitrophenyl carbonates on other monomers to provide a polycarbamate. Upon removal of the Boc group and incubation in pH 7.4 phosphate buffer:acetone (3:2), the SIP underwent depolymerization by a sequence of cyclization, 1,6-elimination, and loss of CO_2 to afford *N*,*N*'-dimethylimidazolidinone, 4-hydroxybenzyl alcohol, and CO_2.

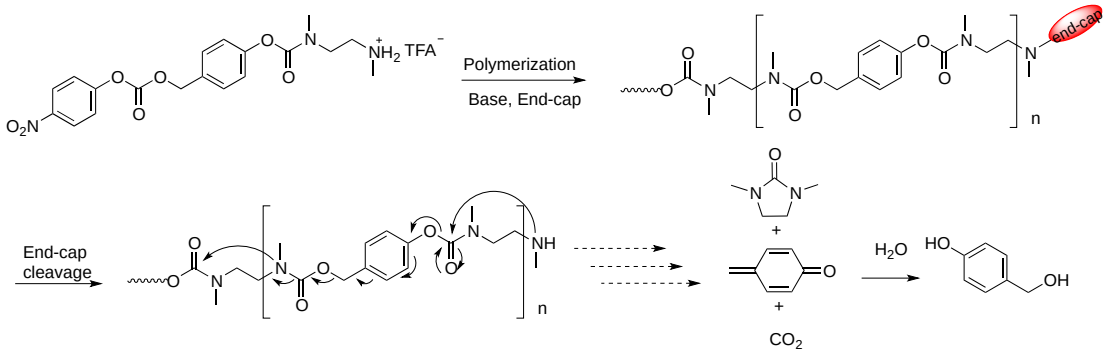

Figure 1. 15 Synthesis of a polycarbamate based on 4-hydroxylbenzyl alcohol and *N*,*N*'-dimethylethylenediamine as well as its depolymerization via a sequence of reactions involving cyclization, 1,6-elimination, and loss of CO_2.

In the same study, Gillies and coworkers also demonstrated that it was possible to incorporate a poly(ethylene glycol) (PEG) end-cap using a 4-nitrophenyl carbonate-activated PEG as an end-cap in the polymerization. This resulted in an amphiphilic block copolymer that self-assembled in aqueous solution to afford micellar-type nanoaggregates (Fig. 1.16).[32-33] Upon cleavage of a single ester group between the PEG and SIP blocks, depolymerization was initiated, ultimately resulting in disintegration of the nanoaggregates. Encapsulation of a model payload nile red was demonstrated, and its release throughout the depolymerization process was suggested by a significant decrease in its fluorescence, as the dye is well known to aggregate upon its release into the aqueous environment resulting in significant quenching of fluorescence.

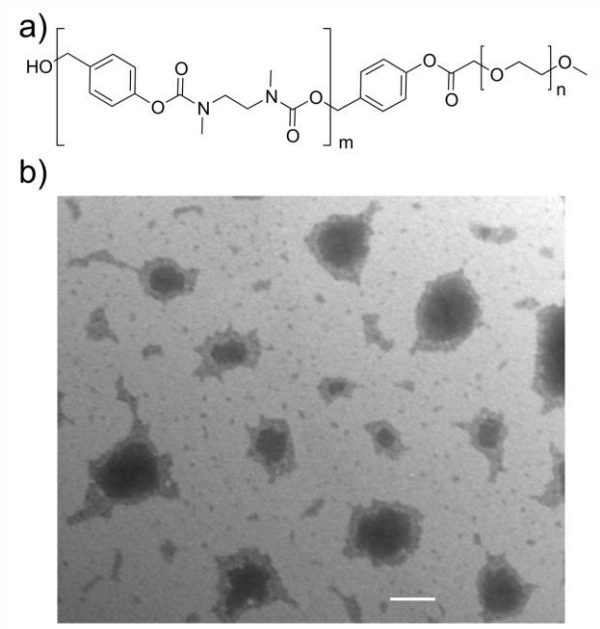

Figure 1. 16 a) Chemical structure of an amphiphilic self-immolative block copolymer; b) Transmission electron microscopy image of assemblies of this block copolymer formed in aqueous solution (scale bar = 100 nm). Adapted with permission from reference [32]. Copyright 2009 American Chemical Society.

In 2012, Almutairi and coworkers introduced UV light- and near infrared (NIR) light-sensitive *o*-nitrobenzyl and 4-bromo-7-hydroxycoumarin end-caps respectively to this polycarbamate backbone (Fig. 1.17).[34] Complete depolymerization of the resulting

polymers was demonstrated by size exclusion chromatograpy (SEC) and ^{1}H NMR spectroscopy following relatively short irradiation times. Using a single emulsion procedure, these SIPs were used to prepare nanoparticles. Following UV or NIR light irradiation the nanoparticles were disrupted, resulting in a burst release of encapsulated nile red. Furthermore, the depolymerization products were found to exhibit minimal cytotoxicity to RAW 264.7 macrophage cells in an MTT assay, suggesting the potential of these stimuli-responsive nanoparticles for drug delivery applications.

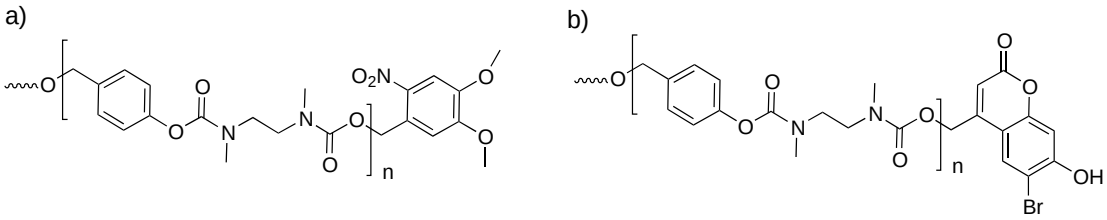

Figure 1. 17 Chemical structure of a) UV and b) NIR light-responsive polycarbamates.

Although the self-immolative polycarbamates both with and without cyclization spacers have been successfully synthesized and demonstrated to depolymerize in response to a variety of stimuli for different applications including sensors and materials for controlled release, their depolymerization rates are relatively slow. This was highlighted as a potential limitation in the flow-through sensors developed by Phillips.[23b] In addition, in the work of Gillies[32] and Almutairi,[34] the polycarbamates containing the *N*,*N*'-dimethylethylenediamine spacer required days to weeks to depolymerize, depending on the conditions. To address this limitation, Phillips and coworkers have tuned the chemical structures of 1,6-elimination spacers to afford rapid elimination and slow background hydrolysis as described above.[24, 35] Gillies and coworkers have also developed 4-aminobutyric acid spacers that cyclize in seconds in pH 7.4 aqueous buffer.[36] Most of these new spacers have not yet been incorporated into polymer backbones, likely due to synthetic challenges. However, Gillies and coworkers have incorporated two simple modifications to the *N*,*N*'-dimethylethylenediamine spacer, in order to afford rapidly-depolymerizing polycarbamates based on 4-hydroxybenzyl

alcohol.[37] As shown in Fig. 1.18a, the replacement of one amino group of *N*,*N*'-dimethylethylenediamine with an oxygen converted a backbone carbamate into a carbonate, which was more electrophilic and facilitated the cyclization reaction. Through this modification, the time required for depolymerization was reduced from days for the parent polycarbamate to hours for the poly(carbamate-carbonate). Replacement of the other amino amino group with a thiol provided even slightly faster depolymerization (Fig. 1.18b).

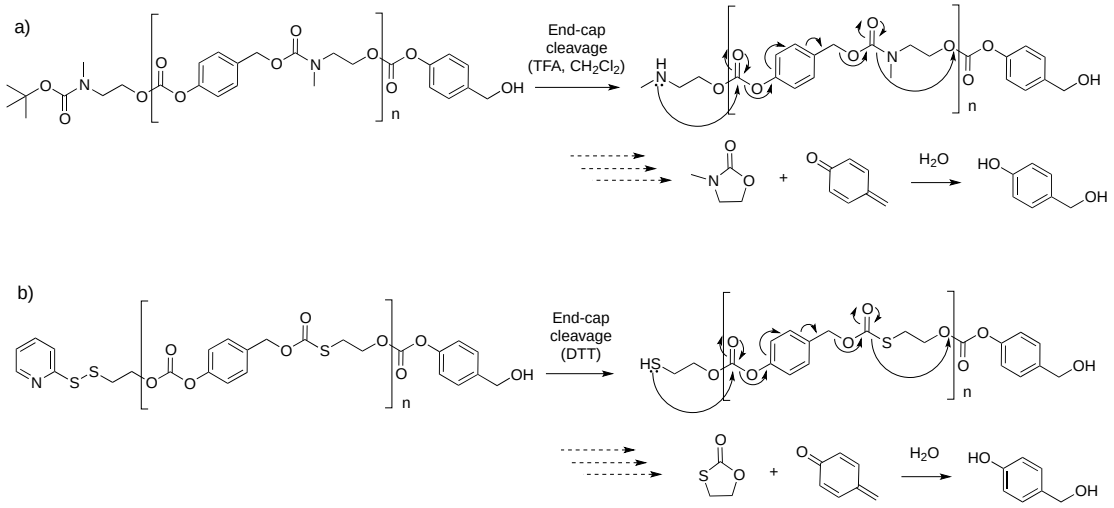

Figure 1. 18 Chemical structures and depolymerization mechanisms for SIPs similar to those in Figure 15, but where the depolymerization rate is accelerated by a) replacement of a backbone carbamate with a carbonate and b) replacement of the amine nucleophile in the cyclization reaction with a thiol.

Currently there are mixed data concerning the potential toxicity of quinone methide and azaquinone methide depolymerization products.[31] For biomedical applications in particular, the potential for these reactive species to react irreversible with proteins is a significant concern.[20] To address this potential issue, Gillies and coworkers developed a SIP derived from *N*,*N*'-dimethylethylenediamine and 2-mercaptoethanol, which degraded entirely by cyclization reactions, without the generation of reactive quinone methides (Fig. 1.19).[38] This polymer had a reduction-sensitive disulfide end-cap, with the potential to be cleaved under physiological conditions such as within cells where the concentration

of the biological reducing agent glutathione is 0.5-10 mM in comparison with 2-20 μM in the extracellular environment,[39] or within hypoxic tumor tissue,[40] where it is proposed to be about fourfold higher than in normal tissue. However, this polymer backbone involved relatively slow cyclization reactions and required 10-14 days to depolymerize upon end-cap cleavage, suggesting that further optimization of the backbone would be required for many applications. In addition, approximately 20% of the polymer did not depolymerize, which was attributed to the presence of cyclic species lacking end-caps and therefore initiation sites for depolymerization.

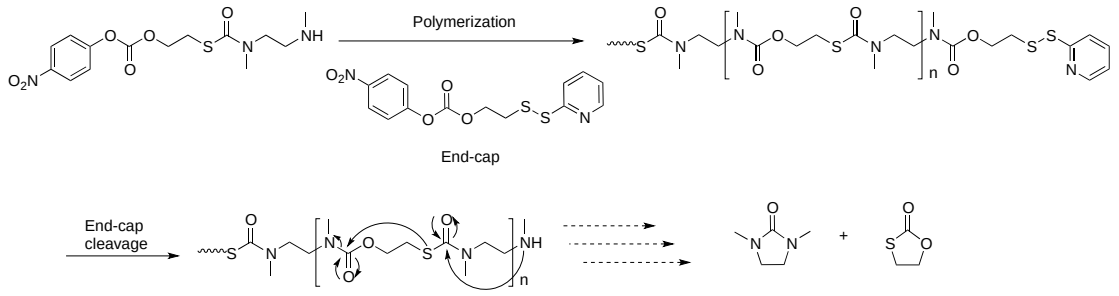

Figure 1. 19 Chemical structure and depolymerization mechanism for a SIP that degrades entirely by cyclization reactions.

1.4 Poly(phthalaldehyde) (PPHA) Derivatives

Another important category of SIPs is the polyacetals, including polyphthalaldehyde (PPHA) and its copolymers. Polyacetals depolymerize due to their relatively low ceiling temperatures (T_c).[15] For example non-end-capped PPHA is well known to have a ceiling temperature of approximately -40 ^oC and therefore depolymerizes spontaneously at room temperature.[41] This can be attributed to the unstable hemiacetal termini, which undergo rapid head-to-tail depolymerization (Fig. 1.20). However, with proper end-capping, they can be stable well above the T_c of the uncapped polymer.[41] Because of the high dipole moment of the carbonyl bond of aldehydes, they are susceptible to ionic polymerization by both anionic and cationic mechanisms, with the required polymerization temperature dependent on the T_c.

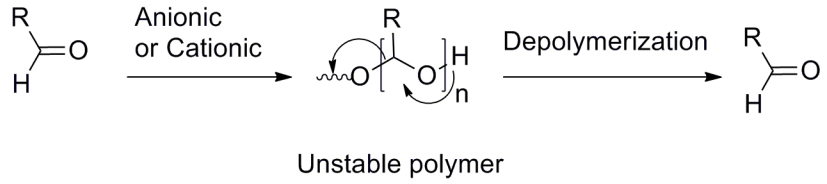

Figure 1. 20 General synthesis and depolymerization of a polyacetal.

PPHA and its depolymerization chemistry have been known for decades. For example, it was used by Fréchet, Ito, and Wilson in photoresist chemistry, where backbone cleavage of a stable, end-capped PPHA initiated by a photoacid generator resulted in complete depolymerization.[41c, 42] However, it was much more recently that Phillips and coworkers recognized the potential of using stimuli-responsive end-caps with PPHA, to afford a new level of control over PPHA depolymerization and thus materials that were selective to various chemical signals. In their initial work, they used *n*-butyllithium (*n*-BuLi) to anionically polymerize *o*-phthalaldehyde (OPA) at -80 ^{o}C over a period of 10 days and end-capped it with functional moieties responsive to stimuli including Pb(0), fluoride, and a control polymer (Fig. 1.21).[43] After end-capping, the PPHAs were stable for at least 15 hours in THF, but once the end-caps were removed by the desired conditions, the polymers completely depolymerized in minutes. They also prepared stimuli-responsive plastics by patterning a cylinder of the fluoride-responsive polymer in a control polymer (Fig. 1.22a). Upon exposure to fluoride, the polymer depolymerized to produce a cylindrical hole in the plastic (Figure 1.22b).

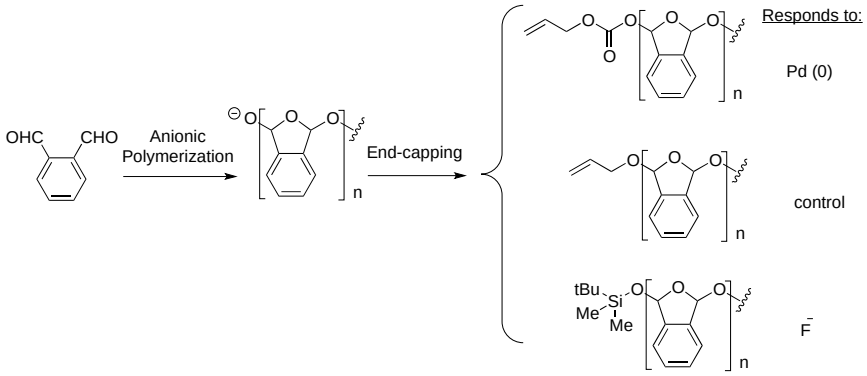

Figure 1. 21 Synthesis of PPHA end-capped with moieties reponsive to different stimuli.

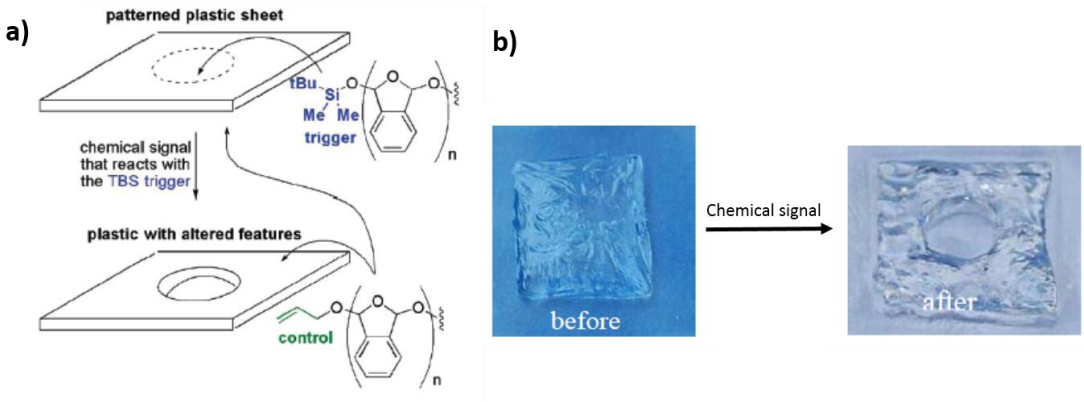

Figure 1. 22 a) Preparation of a stimuli-responsive plastic by the patterning of a cylinder of fluoride-responsive polymer in a control non-responsive polymer. b) Exposure to fluoride results in the production of a cylinidrical hole in the plastic. Adapted with permission from reference [43]. Copyright 2010 American Chemical Society.

One limitation to expanding the scope of application of PPHAs was the long polymerization time of more than 10 days noted above. Using a modification of a protocol developed by Hedrick and coworkers,[44] Phillips and coworkers developed a scalable and reproducible synthesis of PPHA using 1-*tert*-butyl-2,2,4,4,4-pentakis (dimethylamino)-2λ^5,4λ^5-catenadi-(phosphazene) (P_2-*t*-Bu) as a nitrogen-base catalyst.[45]

This procedure allowed PPHA to be synthesized in 3 h, instead of multiple days, and allowed various different end-caps to be incorporated at either the initiating or terminal end of the polymer. In addition, control of PPHA molecular weight could be achieved based on the amount of initiator alcohol added. Purity of the 1,2-benzenedicarboxaldehyde monomer was found to be critical in order to obtain good yields of polymer. An additional development in this study was the demonstration that depolymerization PPHA could occur rapidly in the solid state upon exposure of a photochemically-sensitive PPHA to UV light, even in the absence of solvent.

Phillips, Sen, and coworkers have also explored the application of PPHAs in single-use self-powered microscale pumps that would be turned on by specific stimuli.[46] A *t*-butyldimethylsilyl end-capped PPHA insoluble film served as the basis of this technology. Exposure of the polymer film to fluoride ions as the signal resulted in end-cap cleavage, and depolymerization to more than 100 monomers per polymer chain, thereby amplifying the signal and and creating a concentration gradient that pumped fluids and insoluble particles away from the bulk polymer by a diffusiophoretic mechanism (Fig. 1.23a). The pumping speed of this type of micropump ranged from 0.1 μm s^{-1} to 11μm s^{-1} , depending on the concentration of the signaling molecule. Furthermore, the pump was capable of moving particles around corners and over distances of approximately 5 mm. It was also demonstrated that the PPHA pump could be tuned to be responsive to different analytes, including enzymes.[45-46] For example, a β-D-glucuronidase sensitive glucose derivative with a self-immolative spacer that released fluoride ion upon glucose cleavage by the enzyme was incorporated, such that released fluoride would turn on the pumping system (Fig. 1.23b).

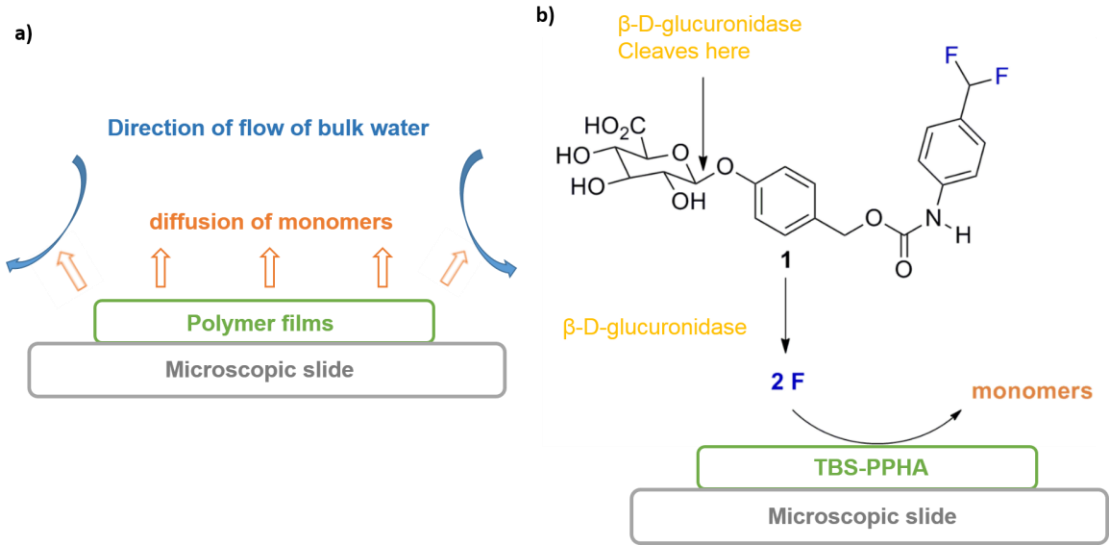

Figure 1. 23 a) Design principle of a self-powered micrometer-scale pump based on PPHA; b) Variation of the design incorporating a β-glucuronidase-sensitive small molecule that produces fluoride ions to trigger the depolymerization.

In general, when end-capped SIPs are used as solid-state materials, such as in the micrometer-scale pumps described above, it is necessary that the end-caps be accessible for cleavage in the liquid and therefore accessible at the solid-liquid interface. Phillips and coworkers used the micrometer-scale pump as a test system to evaluate the effect of end-cap polarity and polymer length on end-cap accessibility, as this would provide the functional output of tracer particle movement that could be measured.[47] In this study, the β-D-glucuronidase system described above was used. Silyl ether derivatives with varying hydrophilicities including a *t*-butyl group, a hydrophilic oligo(ethylene glycol), or a 30-carbon-long hydrocarbon were used, and varying molecular weights of PPHA were prepared with each end-cap. It was found that for short to moderate length polymers (e.g., M_n of 8 - 35 kg/mol), fasting pumping and thus faster PPHA depolymerization were observed for the more hydrophilic silyl end-caps. This was attributed to the increased concentration of silane end-cap at the polymer film surface for the more hydrophilic end-caps, which was supported by analysis of the films by x-ray photoelectron spectroscopy (XPS). However, for longer PPHA (e.g. 60 kg/mol), the pumping speeds were similar for all end-caps. At such lengths, the rate of pumping was thought to no longer be limited by

the rate of end-cap cleavage, but rather the low end-cap content, and therefore the depolymerization time itself. Overall, this study provided a new understanding of how to tune the accessibility of end-caps at solid liquid interfaces and ultimately the pumping speed. It is envisoned that these “turn on” micro-pumps will have applications in microanalysis, microfluids and diagnostic devices.

Phillips, Weitz, and coworkers have also prepared microcapsules from TBDMS end-capped PPHA.[48] As for the previously described polycarbamate microcapsules developed by Moore and coworkers,[27] the aim was to utilize the amplification effect afforded by SIPs to increase the sensitivity of the capsules to stimuli. In this study, a flow-focusing fabrication technique was used, which is ideal for the preparation of capsules containing aqueous cores under mild conditions without the requirement of chemical reactions for the incorporation of the polymer into the shell wall. The polymer was dissolved in chloroform and microfluidic flow-focusing was used to encapsulate fluorescein isothiocyanate (FITC) labeled dextran (Fig. 1.24a). Poly(vinyl alchol) (PVA) was added to both the core and external aqueous solutions to balance the osmotic pressure. The thickness of the shell wall was controlled by varying the flow rates of the different phases and the PPHA concentration. The resulting microcapsules had smooth surfaces and diameters of the microcapsules were approximately 150 μm. It was found that exposure to fluoride resulted in the formation of holes in the capsule wall and the release of FITC-dextran (Fig. 1.24b). Capsules with thinner walls released FITC-dextran more rapidly. Those composed of shorter PPHA chains also released their contents more rapidly for the same reasons described above for the micrometer-scale pumps.

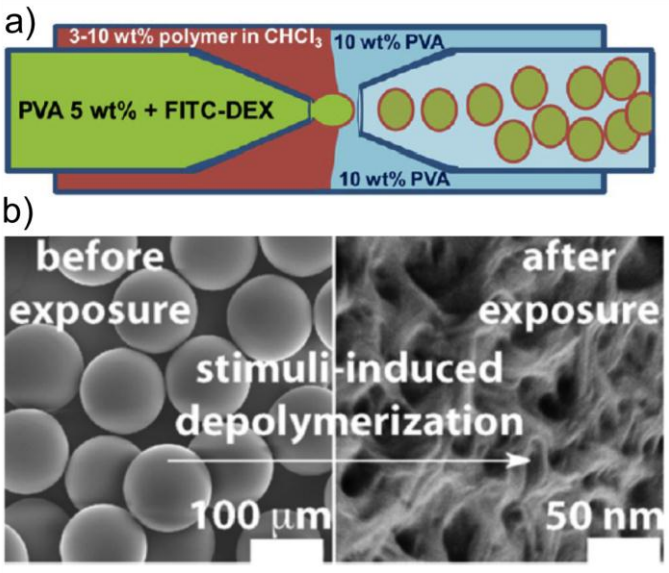

Figure 1. 24 a) Schematic illustrating the preparation of PPHA microcapsules by a microfluidic flow-focusing technique; b) SEM images illustrating the destruction of the capsule wall upon exposure to fluoride. Adapted with permission from reference [48]. Copyright 2013 American Chemical Society.

While PPHA is promising for many applications due to its rapid depolymerization, even in solid state, as well as the commercial availability of OPA as a polymerization monomer, the chemical modification of this polymer is challenging because of the sensitivity of the polymer backbone and because functionalizable derivatives of the monomer are neither commercially available or easy to access synthetically. To address this limitation and expand the potential ultility of PPHA in new applications, Moore and coworkers have explored the copolymerization of OPA with substituted benzaldehydes to introduce functional groups for further modification of this polymer.[49] They hypothesized that while the ceiling temperature of polybenzaldehyde itself is too low to enable polymerization under accessible conditions due to its low enthalpic gain relative to entropic cost of polymerization, the more exothermic nature of hydrate formation with electron-deficient benzaldehyde derivatives would translate into higher polymerizability. Through a series of copolymerization experiments, they found that benzyladehyde derivatives with Hammett values higher than 0.92 were incorporated into the polymers (Fig. 1.25). The incorporation of functional groups such as halides or aldehydes provides

sites for the subsequent functionalization of the polymers. For example, the aromatic halides underwent Stille and Sonogashira couplings to provide alkene or alkyne groups for cross-linking or "click" functionalization (Fig. 1.26a). Pendant aldehyde groups could be reduced to alcohols and reacted with isocyanates to afford cross-linking or used as initiation sites for the synthesis of polylactide (Fig. 1.26b). While this work was performed with acetate as an end-cap, making the polymers stimuli-responsive mainly through backbone cleavage, it should be feasible to readily extend this approach to PPHA with stimuli-responsive end-caps.

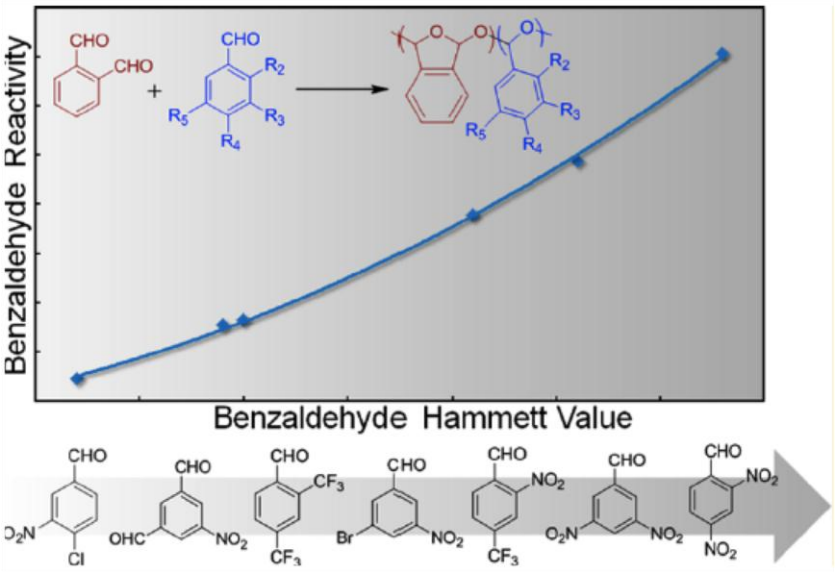

Figure 1. 25 The polymerizability of benzaldehyde derivatives increases with increasing Hammett values. Reproduced with permission from reference [49]. Copyright 2013 American Chemical Society.

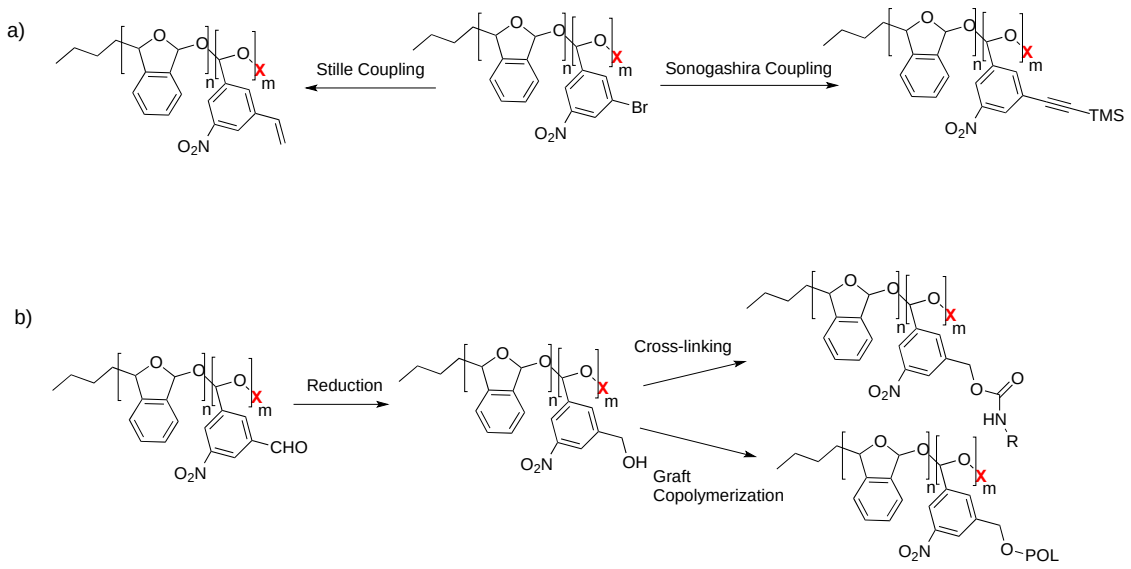

Figure 1. 26 a) Reactions of halide-functionalized benzaldehydes incorporated into PPHA; b) Reactions of aldehyde-functionalized benzaldehydes incorporated into PPHA.

In addition to the anionic polymerization approach used in the work described above, cationic polymerization is another possible route for the synthesis of PPHA. However, the cationic polymerization method had been much less explored until recently. In 2009, Ribitsch and coworkers[50] found that PPHA prepared using a $BF_3{\cdot}OEt_2$ initiator could be isolated without end-capping, suggesting stability above its ceiling temperature. While the authors of this study speculated possible chain entanglements at high molecular weight as the reason for the unexpected stability, Moore and coworkers investigated this cationic polymerization in more detail in order to better understand the end-capping.[51] They found that the cationic polymerization was much more rapid than the anionic polymerization, providing polymer within minutes, compared to hours for the anionic polymerization. In addition, while end-cap peaks were clearly visible in the NMR spectra of anionically synthesized PPHA, no end-cap peaks were observed in the spectra of cationically prepared PPHA of similar molecular weight. This led the authors to propose that the products of the cationic polymerization were cyclic species, a hypothesis that was confirmed by careful matrix-assisted laser desorption/inionization-time of flight mass spectrometry (MALDI-TOF MS) and size exclusion chromatography (SEC) analysis of

the polymers. Furthermore, they found that the macrocyclization is reversible in nature, with the possibility to reopen the ring and expand or contract it in the presence of $BF_3{\cdot}OEt_2$, depending on the monomer concentration (Fig. 1.27). While these cyclic polymers also do not contain stimuli-responsive end-caps, this intriguing behavior, resulting from polymerization near the ceiling temperature offers a new approach for the preparation of highly pure cyclic polymers, which are challenging to prepare by other processes, while at the same time providing dynamic properties. Based on this discovery, Moore and coworkers have further demonstrated that these cyclic polymers of OPA and its derivatives can ring open to depolymerize and exchange monomers to form cyclic new block copolymers and even random copolymers under the cationic polymerization condition (Fig. 1.28).[52]

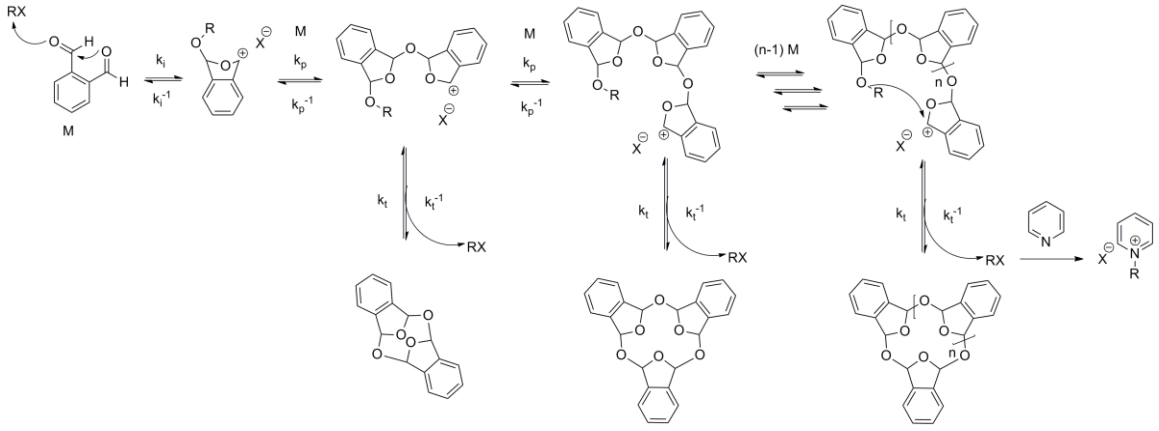

Figure 1. 27 Proposed mechanisms for the formation of cyclic PPHA by cationic polymerization and for its ring expansion-contraction. Adapted with permission from reference [51]. Copyright 2013 American Chemical Society.

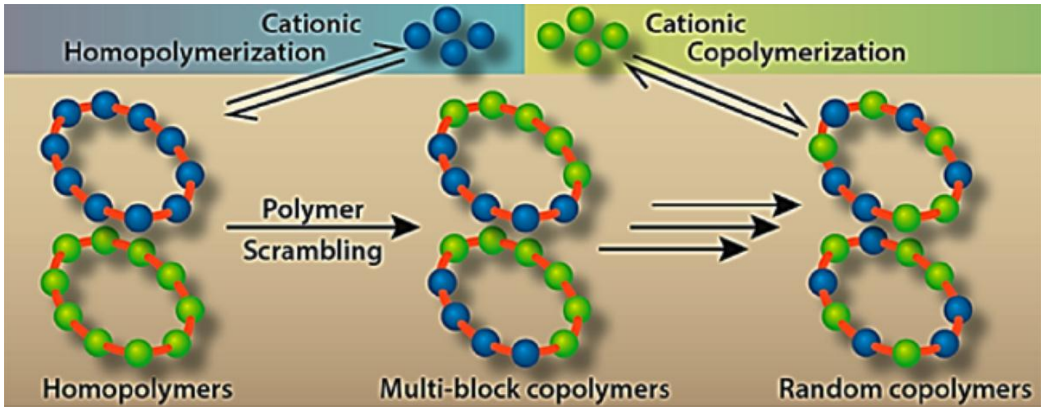

Figure 1. 28 Schematic illustration of the synthesis of PPHA macrocycles and their scrambling. Reproduced with permission from reference [52]. Copyright 2013 American Chemical Society.

Moore, Boydston, and coworkers have also recently demonstrated the mechanically triggered depolymerization of PPHA and its subsequent repolymerization as a model of the continuous remodelling of biomaterials including bone.[53] They prepared cyclic PPHA with M_ns of 16.5, 58.2, and 254 kg/mol by cationic polymerization using $BF_3{\cdot}OEt_2$, as well as a high molecular weight (M_n = 86.4 kg/mol) poly(methyl acrylate) (PMA) control polymer. Mechanical scission was induced by pulsed ultrasound, resulted in depolymerization of the higher molecular weight PPHAs as demonstrated by SEC. Consistent with previous results on the ultrasound-induced depolymerization of polystyrene, which showed that a molecular weight threshold of 30 kg/mol was required for chain scission,[54] the smallest PPHA did not undergo ultrasound-induced depolymerization. The PMA control sample, underwent some degree of chain scission in response to ultrasound, but was not broken down to monomer units, demonstrating the fundamental difference between the low ceiling temperature, depolymerizable PPHA and the PMA control. Molecular dynamics calculations as well as trapping studies suggested that PPHA was cleaved by a heterolytic scission mechanism which is unusual in the context of mechanochemical bond scission. In addition, using an anionic polymerization initiated by *n*-butyllithium in THF at -78 °C, it was possible to repolymerize the product monomer to regenerate polymer. This suggests the potential application of these polymers in self-healing materials.

1.5 Poly(benzyl ethers)

Phillips and coworkers developed end-capped self-immolative poly(benzyl ethers) with the aim of introducing a SIP that is easily prepared with lengths up to hundreds or thousands of repeat units, stability to acid, base, and heat, easy functionalization with an end-cap, solubility in common solvents, and rapid depolymerization in a wide range of environments.[55] Their approach built on the work of McGrath and coworkers on benzyl ether oligomers.[8, 56] They employed methyl substituents on the monomer to prevent its uncontrolled polymerization as well as a pendant phenyl group that would provide an enthalpic driving force for depolymerization through conjugation with the quinone methide (Fig. 1.29). The polymerization was conducted anionically using isopropanol or methanol as an initiator and P_2-*t*-Bu as a catalyst at -10 ^{o}C for 1 hour. Depending on the initiator to monomer ratio, polymerization time and temperature, and even purity of the monomer, the molecular weights of the polymers ranged from 3.6 kg/mol to 484 kg/mol. After polymerization, they reacted the polymers with a series of end-caps that were sensitive to fluoride ions, UV light and palladium(0). The depolymerization rate depended on the polarity of solvent. For example, depolymerization occurred in minutes in DMF and less than 2 days in THF, but required more than 1 week in toluene. Nevertheless, these depolymerization rates were still faster than many of the SIP backbones described above. In addition, compared to the previously investigated SIPs, this poly(benzyl ether) has better stability to acid, base and heat, which may be useful in applications where poor stability and/or slow depolymerization prevent the use of other backbones.

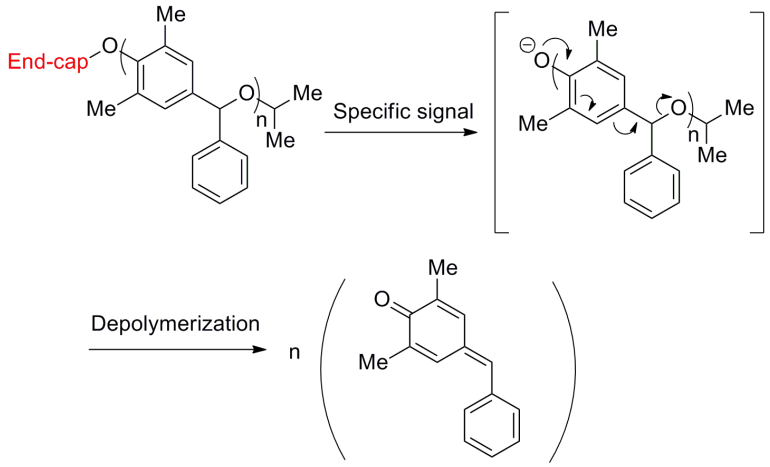

Figure 1. 29 Chemical structure and depolymerization mechanism of a poly(benzyl ether).

1.6 Kinetics of Depolymerization

It is intuitive that longer SIPs should require longer depolymerization times than shorter SIPs of the same backbone, owing to the requirement for more reactions to occur in order to completely break down the polymer backbone to small molecules. Recently, Gillies and coworkers have performed detailed kinetic studies using their previously reported polycarbamate backbone derived from 4-hydroxybenzyl alcohol and *N*,*N*'-dimethylethylene diamine (Fig. 1.15) to explicitly demonstrate this property.[67] They prepared a series of monodisperse oligomers (monomer, dimer, tetramer, and octamer) by step-wise synthesis, and used a design of experiments to optimize the conditions for preparation of two linear polymers with varying chain lengths (M_n = 5250 g/mol with $Đ$ of 1.47 and M_n = 13,600 g/mol with $Đ$ of 1.58). All of these molecules were prepared with Boc end-caps as the protonated amine terminus arising from cleavage of the end-cap with acid is stable to depolymerization until transferred to buffer, allowing end-cap cleavage to be decoupled from depolymerization.

A kinetic model was developed in which cyclization was assumed to be slower than 1,6-elimination under the conditions of the study, and therefore the depolymerization could be described as a series of first-order intramolecular reactions:

$$P_n \underset{k_n}{\overset{-M}{\rightarrow}} P_{n-1} \underset{k_{n-1}}{\overset{-M}{\rightarrow}} \cdots \underset{k_2}{\overset{-M}{\rightarrow}} P_1 \underset{k_1}{\overset{-M}{\rightarrow}} M \quad (1)$$

where P_i is the polymer chain of length *i*, M is the released monomer unit, and k_i is the rate of intramolecular cyclization for a terminal cyclization spacer on a polymer chain of length *i*. Using the assumption that the rate constant for intramolecular cyclization was independent of chain length, equation (1) was reduced to a set of linear differential equations:

$$\frac{d[P_n]}{dt} = -k[P_n] \quad \textbf{(2)}$$

$$\frac{d[P_i]}{dt} = k([P_{i+1}]-[P_i]) \quad \forall\ i \leq n-1 \quad \textbf{(3)}$$

where $[P_i]$ is the concentration of polymer chains of length *i* and *t* is the time elapsed in the degradation process. Equations (2) and (3) were then reduced using an integrating factor to:

$$[P_{n-i}] = e^{-kt} \sum_{j=0}^{i} \frac{(kt)^{i-j}}{(i-j)!} [P_{n-j}]_0 \quad \textbf{(4)}$$

Released monomer was the most easily measured quantity during the depolymerization process. Although it is not a direct measure of polymer molecular weight, it is inversely related to molecular weight and could be used to measure polymer degradation according to equations 5 and 6:

$$\frac{d[M]}{dt} = k \sum_{i=1}^{n} P_i \quad \textbf{(5)}$$

$$D(t)=\frac{M(t)}{M_{\infty}}=\frac{M(t)}{\sum_{i=1}^{n} i[P_i]_0} \quad \textbf{(6)}$$

In the case of the monodisperse oligomers, equations 2, 3, and 5 can be algebraically solved and then substituted into equation 6 to provide the following equation describing the self-immolative depolymerization:

$$D(t)=\frac{M(t)}{n[P_n]_0}=[P_n]_0\left(1-e^{-kt}n^{-1}\sum_{i=1}^{n}\sum_{j=1}^{i}\frac{(kt)^{j-1}}{(j-1)!}\right) \quad \textbf{(7)}$$

Oligomer depolymerization was studied in 3:2 pH 7.4 phosphate buffer:acetone at 37 ℃ by ^{1}H NMR spectroscopy and the data were fit to equation 7 using non-linear regression (Fig. 1.30a). It was found that indeed the rate constant for one monomer cyclization was independent of chain length within experimental error, and that the time to 50% depolymerization (t_{50}), as a measured of the depolymerization time, increased linearly with chain length (Table 1.1).

Depolymerization of the polymers was studied under the same conditions as the oligomers, and their degradation profiles were fit to the above depolymerization model using a non-linear regression algorithm in which a numerical solution from equations 2, 3, and 5 was applied to the SEC chromatograms as an indicator of the molecular weight distributions of the polymers (Fig. 1.30b). Again, good fits were obtained and the time to 50% depolymerization was proportional to chain length with the shorter polymer having a t_{50} of 17.4 minutes and the longer polymer having a t_{50} of 41.5 minutes; however, a limitation of this model is the requirement for a priori knowledge of the distribution of absolute polymer lengths, which is challenging to obtain and can only be approximated by SEC.

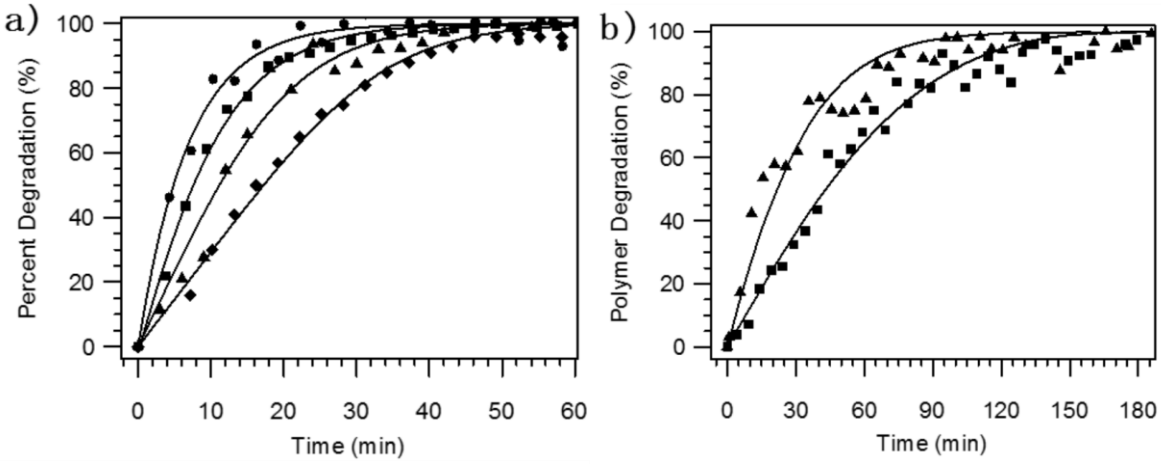

Figure 1. 30 Degradation kinetics of as measured by ^{1}H NMR spectroscopy in 0.1 M phosphate buffer (D_2O):acetone-d_6 (3:2) at 37˚C. a) Monomer (●), dimer (■), tetramer (▲), octamer (◆). Solid lines correspond to the regressed fits of Eq. (7). b) Degradation kinetics of polymers M_n = 5250 g/mol with *Đ* of 1.47 (▲) and M_n = 13,600 g/mol with *Đ* of 1.58 (■). Overlayed lines correspond to the self-immolative model fits for both polymers. Reproduced with permission from reference [67]. Copyright 2013 American Chemical Society.

Compound	k ×10^{1} (min^{-1})^{a}	t_{50} (min)^{b}
Monomer	1.61 ± 0.37	4.5 ± 0.9
Dimer	1.48 ± 0.10	8.1 ± 0.9
Tetramer	1.60 ± 0.38	13.2 ± 1.7
Octamer	1.73 ± 0.34	23.9 ± 4.3

Table 1. 1 Kinetic parameters for the degradation of monodisperse oligomers. Reproduced with permission from reference [67]. Copyright 2013 American Chemical Society.[a]Rate constant for monomer cyclization; [b]Time for 50% polymer degradation.

As noted by McBride and Gillies,[67] an analysis of the depolymerization kinetics of SIPs reveals an interesting mixed-mode phenomenon relatively unique to this class of polymers. In contrast to conventional biodegradable polymers that degrade by random backbone cleavage and typically display pseudo first-order degradation kinetics, SIPs exhibit an initial pseudo zero-order phase, followed by a transition to pseudo-first-order behavior during the course of depolymerization (Fig. 1.31). This behavior arises because the concentration of polymer chains does not change until they are completely degraded to monomer units. Both experimental data and simulation studies indicate that this mixed-mode phenomenon is most apparent in monodisperse or low polydispersity samples, whereas as $Đ$ is increased, the kinetics become more heavily weighted towards both short and long chains, resulting in a increased dispersity in times over which the transition from zero-order to first-order behavior occurs. For this reason, the depolymerization kinetics of SIPs may appear to be first-order; however, the fitting of such data to first-order models is not strictly correct.

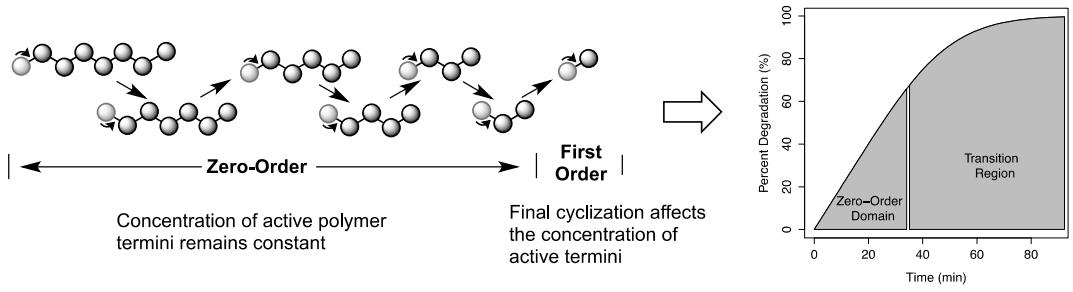

Figure 1. 31 Mixed-mode degradation profile for the depolymerization of linear self-immolative polymers involving an initial zero-order domain followed by a gradual transition towards first-order behavior. Reproduced with permission from reference [57]. Copyright 2013 American Chemical Society.

1.7 Scope of the Thesis

In the context of the literature described above, two major limitations to the wide-spread application of SIPs can be identified. First, most monomers for the preparation of SIPs

require multi-step syntheses, which increase the cost of the final polymers and likely the scale on which they can be prepared. This would limit their application to niche areas. Secondly, most of the backbones depolymerize to generate potentially toxic species such as quinone methides[58] or OPA[59]. This would restrict their use in biomedical applications. Thus, the major goal of this thesis was to develop a new backbone that would overcome these limitations. Specifically, there are three goals for this thesis: 1) The development of a new class of SIPs that can be derived from commercially available monomers and degrade into non-toxic products; 2) Modifications to these SIPs by changing of side-groups, end-caps and forming block copolymers; 3) Application of the new SIP towards drug delivery. The detailed work described in each chapter is as follows.

Chapter 2 will describe the background and detailed procedures for the development and demonstration of poly(ethyl glyoxylate) as a new SIP by installation of UV responsive end-caps at the polymer termini. Further expansion of this new class of SIPs by changing the side-group via a two-step synthesis for new poly(glyoxylate)s and the formation of block copolymers are explored. In addition, the physical properties and stimuli-responsive degradation of these new poly(glyoxylate)s are studied.

Chapter 3 focuses on the self-assembly of poly(ethyl glyoxylate) based amphiphilic block copolymers for drug delivery applications. The assembly procedures, morphology confirmation, disassembly, model drug loading and release behaviour are described.

Chapter 4 describes the exploration of other possible stimuli-responsive end-caps for polyglyoxylates. Specifically, oxidation-responsive (H_2O_2) and reduction-responsive (DTT) end-caps are synthesized and installed on poly(ethyl glyoxylate). The corresponding degradation of these polymers in the absence and presence of stimuli are monitored and demonstrated via ^{1}H NMR spectroscopy.

Lastly, Chapter 5 summarizes all of the key results of previous chapters and outlines the future directions of this project.

1.8 References

1. Chunder, A.; Etcheverry, K.; Londe, G.; Cho, H. J.; Zhai, L., *Colloids Surf., A* **2009,** *333*, 187.

2. Ge, Z.; Liu, S., *Chem. Soc. Rev.* **2013,** *42*, 7289.

3. (a) Lee, E. S.; Na, K.; Bae, Y. H., *Nano Lett.* **2005,** *5*, 325; (b) Lee, Y.; Ishii, T.; Cabral, H.; Kim, H. J.; Seo, J. H.; Nishiyama, N.; Oshima, H.; Osada, K.; Kataoka, K., *Angew. Chem. Int. Ed.* **2009,** *48*, 5309.

4. Gillies, E. R.; Fréchet, J. M. J., *Chem. Commun.* **2003,** (14), 1640.

5. Hefferman, M. J.; Murthy, N., *Bioconjugate Chem.* **2005,** *16* (6), 1340.

6. Lin, C.; Zhong, Z. Y.; Lok, M. C.; Jiang, X. L.; Hennink, W. E.; Feijan, J.; Engbersen, J. F. J., *Bioconjugate Chem.* **2007,** *18* (1), 138.

7. Zhao, H.; Sterner, E. S.; Coughlin, E. B.; Theato, P., *Macromolecules* **2012,** *45*, 1723.

8. Szalai, M. L.; Kevwitch, R. M.; McGrath, D. V., *J. Am. Chem. Soc.* **2003,** *125*, 15688.

9. Groot, F. M. H. d.; Albrecht, C.; Koekkoek, R.; Beusker, P. H.; Scheeren, H. W., *Angew. Chem. Int. Ed.* **2003,** *42*, 4490.

10. Amir, R. J.; Pessah, N.; Shamis, M.; Shabat, D., *Angew. Chem. Int. Ed.* **2003,** *42*, 4494.

11. (a) Carl, P. L.; Chakravarty, P. K.; Katzenellenbogen, J. A., *J. Med. Chem.* **1981,** *24* (5), 479; (b) Kratz, F.; Müller, I. A.; Ryppa, C.; Warnecke, A., *ChemMedChem* **2008,** *3*, 20; (c) Wakselman, M., *Nouv. J. Chem.* **1983,** *7*, 439; (d) Shan, D.; Nicolaou, M. G.; Borchardt, R. T.; Wang, B., *J. Pharm. Sci.* **1997,** *86* (7), 765.

12. (a) Shamis, M.; Lode, H. N.; Shabat, D., *J. Am. Chem. Soc.* **2004,** *126*, 1726; (b) Erez, R.; Segal, E.; Miller, K.; Satchi-Fainaro, R.; Shabat, D., *Bioorg. Med. Chem.* **2009,** *17*, 4327.

13. (a) Sella, E.; Shabat, D., *Chem. Commun.* **2008,** *2008* (44), 5701; (b) Sella, E.; Shabat, D., *J. Am. Chem. Soc.* **2009,** *131*, 9934; (c) Sella, E.; Weinstain, R.; Erez, R.; Burns, N. Z.; Baran, P. S.; Shabat, D., *Chem. Commun.* **2010,** *46* (35), 6575.

14. (a) Meyer, Y.; Richard, J. A.; Massonneau, M.; Renard, P. Y.; Romieu, A., *Org. Lett.* **2008,** *10* (8), 1517; (b) de Groot, F. M. H.; Loos, W. J.; Koekkoek, R.; van Berkom, L. W.

A.; Busscher, G. F.; Seelen, A. E.; Albrecht, C.; de Brujin, P.; Scheeren, H. W., *J. Org. Chem.* **2001,** *66* (26), 8815; (c) Weinstain, R.; Segal, E.; Satchi-Fainaro, R.; Shabat, D., *Chem. Commun.* **2010,** *46*, 553; (d) Warnecke, A.; Kratz, F., *J. Org. Chem.* **2008,** *73*, 1546.

15. Vogl, O., *J. Polym. Sci. A: Polym. Chem.* **2000,** *38*, 2293.
16. Bryant, W. M. D.; Thompson, J. B., *J. Polym. Sci. A-1* **1971,** *9*, 2523.
17. (a) Wong, A. D.; DeWit, M. A.; Gillies, E. R., *Adv. Drug Delivery Rev.* **2012,** *64*, 1031; (b) Peterson, G. I.; Larsen, M. B.; Boydston, A. J., *Macromolecules* **2012,** *45* (18), 7317; (c) Phillips, S. T.; DiLauro, A. M., *ACS Macro Lett.* **2014,** *3* (4), 298; (d) Phillips, S. T.; Robbins, J. S.; DiLauro, A. M.; Olah, M. G., *J. Appl. Polym. Sci.* **2014,** *131*.
18. Sagi, A.; Weinstain, R.; Karton, N.; Shabat, D., *J. Am. Chem. Soc.* **2008,** *130*, 5434.
19. Weinstain, R.; Sagi, A.; Karton, N.; Shabat, D., *Chem. Eur. J.* **2008,** *14*, 6857.
20. Weinstain, R.; Baran, P. S.; Shabat, D., *Bioconjugate Chem.* **2009,** *20*, 1783.
21. Lewis, G. G.; Robbins, J. S.; Phillips, S. T., *Anal. Chem.* **2013,** *85*, 10432.
22. Lewis, G. G.; DiTucci, M. J.; Phillips, S. T., *Angew. Chem. Int. Ed.* **2012,** *51*, 12707.
23. (a) Lewis, G. G.; Robbins, J. S.; Phillips, S. T., *Chem. Commun.* **2014,** *50*, 5352; (b) Lewis, G. G.; Robbins, J. S.; Phillips, S. T., *Macromolecules* **2013,** *46*, 5177.
24. Robbins, J. S.; Schmid, K. M.; Phillips, S. T., *J. Org. Chem.* **2013,** *78*, 3159.
25. Peterson, G. I.; Church, D. C.; , N. A. Y.; Boydston, A. J., *Polymer* **2014,** *09*, 048.
26. Zeng, B.; Huang, J.; Wright, M.; King, S., *Med. Chem. Lett.* **2004,** *14*, 5565.
27. Esser-Kahn, A. P.; Sottos, N. R.; White, S. R.; Moore, J. S., *J. Am. Chem. Soc.* **2010,** *132*, 10266
28. Liu, G.; Wang, X.; Hu, J.; Zhang, G.; Liu, S., *J. Am. Chem. Soc.* **2014,** *136*, 7492.
29. Discher, D. E.; Eisenberg, A., *Science* **2002,** *297*, 967.
30. Brasch, M.; Voets, I. K.; Koay, M. S. T.; Cornelissen, J. J. L. M., *Faraday Discuss.* **2013,** *166*, 47.
31. Monks, T.; Jones, D., *Drug Metab.* **2002,** *3*, 425.
32. DeWit, M. A.; Gillies, E. R., *J. Am. Chem. Soc.* **2009,** *131*, 18327.
33. DeWit, M. A.; Nazemi, A.; Karamdoust, S.; Gillies, E. R., *ACS Symp. Ser.* **2011,** *1066*, 9.

34. de Gracia Lux, C.; McFearin, C. L.; Joshi-Barr, S.; Sankaranarayanan, J.; Fomina, N.; Almutairi, A., *ACS Macro. Lett.* **2012,** *1*, 922.

35. Schmid, K. M.; Jensen, L.; Phillips, S. T., *J. Org. Chem.* **2012,** *77*, 4363.

36. DeWit, M. A.; Gillies, E. R., *Org. Biomol. Chem.* **2011,** *9*, 1846.

37. Chen, E. K. Y.; McBride, R. A.; Gillies, E. R., *Macromolecules* **2012,** *45*, 7364.

38. Dewit, M. A.; Beaton, A.; Gillies, E. R., *J. Polym. Sci. Pol. Chem.* **2010,** *48*, 3977.

39. (a) Kuppusamy, P.; Li, H.; Ilangovan, G.; Cardounel, A. J.; Zweier, J. L.; Yamada, K.; Krishna, M. C.; Mitchell, J. B., *Cancer Res.* **2002,** *62*, 307; (b) Wu, G.; Fang, Y. Z.; Yang, S.; Lupton, J. R.; Turner, N. D., *J. Nutr.* **2004,** *134* (2004), 489.

40. Kuppusamy, P.; Afeworki, M.; Shankar, R. A.; Coffin, D.; Krishna, M. C.; Hahn, S. M.; Mitchell, J. B.; Zweier, J. L., *J. L. Cancer Res.* **1998,** *58*, 1562.

41. (a) Aso, C.; Tagami, S.; Kunitake, T., *J. Polym. Sci. A: Polym. Chem.* **1969,** *7*, 497; (b) Wilson, C. G.; Ito, H.; Frechet, J. M. J.; Tessier, T. G.; Houlihan, F. M., *J. Electrochem. Soc.* **1986,** *133*, 181; (c) MacDonald, S. A.; Willson, C. G.; Frechet, J. M. J., *Acc. Chem. Res.* **1994,** *27*, 151.

42. Ito, H.; Willson, C. G., *Polym. Eng. Sci.* **1983,** *23*, 1012.

43. Seo, W.; Phillips, S. T., *J. Am. Chem. Soc.* **2010,** *132*, 9234.

44. Coulembier, O.; Knoll, A.; Pires, D.; Gotsmann, B.; Duerig, U.; Frommer, J.; Miller, R. D.; Dubois, P.; Hedrick, J. L., *Macromolecules* **2010,** *43*, 572.

45. DiLauro, A. M.; Robbins, J. S.; Phillips, S. T., *Macromolecules* **2013,** *46*, 2963.

46. Zhang, H.; Yeung, K.; Robbins, J. S.; Pavlick, R. A.; Wu, M.; Liu, R.; Sen, A.; Phillips, S. T., *Angew. Chem. Int. Ed.* **2012,** *51*, 2400.

47. DiLauro, A. M.; Zhang, H.; Baker, M. S.; Wong, F.; Sen, A.; Phillips, S. T., *Macromolecules* **2013,** *46*, 7257.

48. DiLauro, A. M.; Abbaspourrad, A.; Weitz, D. A.; Phillips, S. T., *Macromolecules* **2013,** *46*, 3309.

49. Kaitz, J. A.; Moore, J. S., *Macromolecules* **2013,** *46*, 608.

50. Köstler, S.; Zechner, B.; Trathnigg, B.; Fasl, H.; Kern, W.; Ribitsch, V., *J. Polym. Sci. Pol. Chem.* **2009,** *47*, 1499.

51. Kaitz, J. A.; Diesendruck, C. E.; Moore, J. S., *J. Am. Chem. Soc.* **2013,** *135*, 12755.

52. Kaitz, J. A.; Diesendruck, C. E.; Moore, J. S., *Macromolecules* **2013,** *46*, 8121.

53. Diesendruck, C. E.; Peterson, G. I.; Kulik, H. J.; Kaitz, J. A.; Mar, B. D.; May, P. A.; White, S. R.; Martinez, T. J.; Boydston, A. J.; Moore, J. S., *Nat. Chem.* **2014,** *6*, 623.

54. Nguyen, T. Q.; Liang, Q. Z.; Kausch, H.-H., *Polymer* **1997,** *38*, 3783.

55. Olah, M. G.; Robbins, J. S.; Baker, M. S.; Phillips, S. T., *Macromolecules* **2013,** *46*, 5924.

56. (a) Li, S.; Szalai, M. L.; Kevwitch, R. M.; McGrath, D. V., *J. Am. Chem. Soc.* **2003,** (125), 10516; (b) Kevwitch, R. M.; Shanahana, C. S.; McGrath, D. V., *New J. Chem.* **2012,** *36*, 492.

57. McBride, R. A.; Gillies, E. R., *Macromolecules* **2013,** *46*, 5157.

58. Monks, T. J.; Jones, D. C. *Curr. Drug Metab.* **2002**, *3*, 425.

59 Anderson, S.; Umbright, C.; Sellamuthu, R.; Fluharty, K.; Kashon, M.; Franko, J.; Jackson, L.; Johnson, V.; Joseph, P. *Toxicol. Sci.* **2010**, *115*, 435.

Chapter 2

2 Development of Polyglyoxylates as a New Class of Self-immolative Polymers.

2.1 Introduction

In recent years, there has been significant interest in the development of degradable polymers for a wide range of applications including environmentally friendly plastics, adhesives, biomedical sutures, tissue engineering scaffolds, and drug delivery vehicles.[1-4] The preparation of biodegradable polymeric materials based on monomers derived from renewable, non-petroleum resources is particularly attractive as these materials are potentially more sustainable than hydrocarbon-based materials and often degrade into non-toxic metabolic intermediates.[5-6] The development of stimuli-responsive polymers has also been a highly active area of research over the past couple of decades. Many examples of polymers undergoing changes in solubility or bond cleavage events in response to stimuli such as light,[7] changes in pH,[8] or redox potential,[9] and even mechanical force[10] have been reported with the aim of changing the properties of materials for applications such as tissue engineering, drug delivery, responsive coatings, and microfluidic values.

Self-immolative linear polymers are materials that undergo end-to-end backbone depolymerization in response to the cleavage of stimuli-responsive end-caps.[11-13] They combine the features of both degradable and stimuli-responsive polymers, while having unique features such as a predictable dependence of degradation time of chain length[14] and the possibility to change the stimulus to which a given backbone responds, simply by changing the end-cap. Over the past several years, the field of self-immolative linear polymers has grown significantly and several different backbones have been developed including polycarbamates,[15-18] poly(carbamate-thiocarbamate)s,[19] polyphthalaldehydes[20-23] and poly(benzyl ether)s.[24] Their application in a wide range of areas including sensors,[15,17] shape-changing plastics,[25] self-powered microscale pumps,[26] membranes,[27] and controlled

release systems[16,28-30] has been explored. However, the multistep synthesis of monomers required for the preparation of these materials, as well as their degradation into potentially toxic species such as quinone methides[31] and *o*-phthaldehyde,[32] are potential barriers to the widespread application of these materials.

Polyglyoxylates are a potentially versatile new class of readily accessible self-immolative linear polymers. They are particularly attractive, as monomers such as ethyl glyoxylate are directly available commercially on large scale. For example, ethyl glyoxylate (EtG) is prepared industrially via step-wise oxidation of acetaldehyde, which is a large-scale commodity chemical that can be obtained from petroleum feedstocks but also from bioethanol.[33] Poly(methyl glyoxylate) (PMeG) and poly(ethyl glyoxylate) (PEtG) have been previously reported, but rapidly depolymerize if not end-capped.[34-37] To address this, isocyanates, including phenyl isocyanate have been introduced as end-capping agents.[37,38] Capped PEtG and PMeG have been shown to degrade by a combination of random backbone cleavage and depolymerization[39] to the corresponding alcohol as well as glyoxylic acid hydrate,[36,40] an intermediate in the glyoxylic acid cycle, and ultimately to CO_2 in the environment.[41] These degradation products have been demonstrated to be non-toxic in invertebrate models and in plant ecotoxicity models.[41] To the best of our knowledge this class of materials has not yet been imparted with stimuli-responsive degradation properties, which should enable them to degrade selectively by the end-to-end depolymerization mechanism as shown in Scheme 2.1, making them a new class of self-immolative polymers.

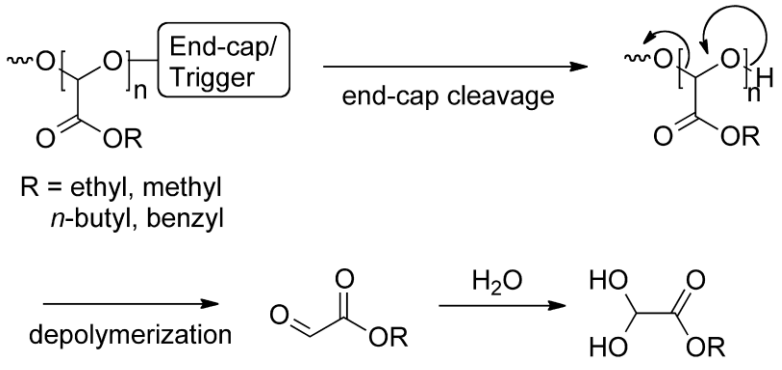

Scheme 2. 1 Depolymerization of polyglyoxylates upon end-cap cleavage.

Using UV light as a model stimulus, we demonstrate that PEtG can serve as a new self-immolative linear polymer. Furthermore, we demonstrate that various other glyoxylates including methyl glyoxylate (MeG), *n*-butyl glyoxylate (BuG), and benzyl glyoxylate (BnG) can be prepared in two steps from starting materials such as fumaric acid, which is a large-scale industrial chemical that can be prepared from petroleum sources[42] or from the agricultural byproduct furfural.[43] Both homopolymers and copolymers of these monomers with EtG can also be prepared. Moreover, amphiphilic block copolymers can be prepared using a multifunctional end-cap. All of these polymers exhibit stimuli-responsive self-immolative degradation. The accessibility of the polymerization monomers, both from petroleum and renewable resources, as well as the depolymerization of PEtG in particular to non-toxic metabolic intermediates is anticipated to open numerous new prospects for self-immolative polymers.

2.2 Results and Discussion

2.2.1 Synthesis and Characterization of PEtG with a Stimuli-responsive End-cap

Because of the availability of EtG from commercial sources on a large scale, this monomer was selected to demonstrate the feasibility of using polyglyoxylates as self-immolative materials. Purification of EtG is an essential prerequisite to obtain high molecular weight PEtG, as excess initiation and transfer reactions resulting from glyoxylate hydrate, water or other impurities result in low molecular weight products. In our hands, the most effective purification protocol involved two successive distillations of the crude EtG at 130 ℃ over phosphorus pentoxide under argon at atmospheric pressure. The high temperature of the distillation ensured cracking of the glyoxylate oligomers and the drying agent removed any liberated water. As shown in Scheme 2.2, the optimized conditions for polymerization involved the use of CH_2Cl_2 as a solvent at -20 ℃ in the presence of NEt_3. Under these conditions, residual trace water or ethyl

glyoxylate hydrate (EtGH) initiates the polymerization providing PEtG **2.1**, which can be isolated by precipitation in methanol.

PEtG **2.1** can be end-capped *in situ*, by reaction with phenyl isocyanate in the presence of dibutyltin dilaurate (DBTL) to provide the control PEtG **2.2** as previously reported.[37,38] It was found that chloroformates also serve as efficient end-capping agents in the presence of additional NEt_3. For example, capping with benzyl chloroformate provided control PEtG **2.3** with a carbonate end-cap. To prepare a stimuli-responsive PEtG, 6-nitroveratryl chloroformate (NVOC-Cl) was selected as an end-cap to provide the nitroveratryl carbonate (NVOC) end-capped PEtG **2.4**. While the chloroformate chemistry can be used to potentially introduce a variety of end-caps, the NVOC group is ideal in the current work as a model end-cap because it is well known that it can be cleanly cleaved with UV light (λ = 340nm) under neutral conditions, which was expected to initiate the depolymerization of the polymer (Scheme 2.1).

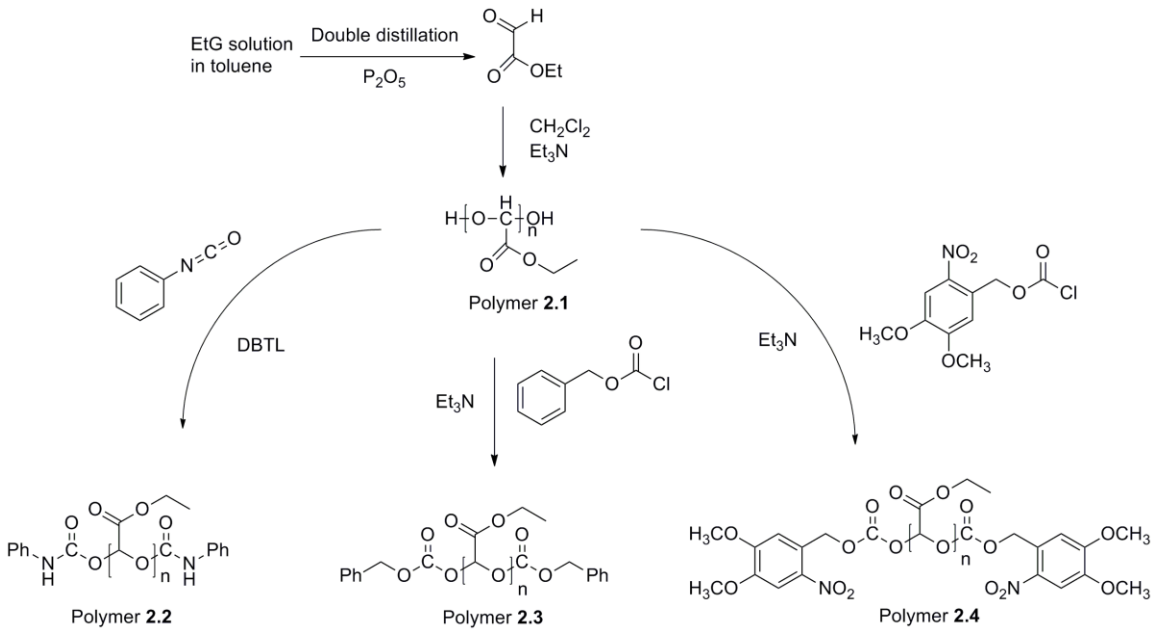

Scheme 2. 2 Synthesis of PEtG

Polymer	M_n (NMR) (kDa)	M_n (SEC) (kDa)	M_w (SEC) (kDa)	Dispersity ($Đ$)
2.1[a]	----	103	266	2.6
2.2[b]	----	27	66	2.5
2.3	79	31	59	1.9
2.4	32	53	91	1.7
2.11	7.3	3.8	4.8	1.3
2.12	6.3	5.0	9.8	1.9
2.13	4.3	2.1	3.5	1.6
2.14	69	40	81	2.0
2.15	13	11	22	2.0
2.19	64	42	88	2.1
2.21	43	40	85	2.1

Table 2. 1 Molecular weight measured from NMR and SEC for the polymers, SEC measured in THF relative to polystyrene standards. [a]End-cap integration is not possible due to no end-cap. [b]End-cap integration is not possible due to overlap with the residual NMR solvent ($CHCl_3$) peak.

All of the PEtGs were characterized by ^1H and ^{13}C NMR spectroscopy, IR spectroscopy, and size exclusion chromatography (SEC). The spectral data were consistent with the expected chemical structures of the materials (Appendix 2). As shown in Table 2.1, SEC results showed that PEtGs **2.1** – **2.4** have number average molecular weights (M_n) ranging from 27 - 103 kDa and weight average molecular weights (M_w) ranging from 66 kDa to 266 kDa. The higher molar mass of the unend-capped polymer **2.1** may reflect the selective precipitation of the higher molar mass fraction of **2.1** as lower molar mass PEtG has been observed to precipitate slowly from methanol, which could allow depolymerization to occur during this process. However, it is also possible that the end-capping process, carried out at ambient temperature to increase the rate of end-capping, could potentially result in some degree of depolymerization and may favor chains with lower degrees of polymerization, which are more reactive. It was also noted that both the yield (e.g. 62% for **2.4**) and molar mass were higher for the polymers end-capped with chloroformates in comparison with the less reactive isocyanate (e.g. 45%

yield), suggesting that rapid end-capping may be important for preserving the degree of polymerization.

Polymer	$T_{98\%}$ (ºC)	T_o (ºC)	T_p (ºC)	T_g (ºC)	T_m (ºC)
2.1	84	148	165	-32	-----
2.2	168	190	202	-1	-----
2.3	161	173	203	-3	-----
2.4	164	202	228	-9	-----
2.11	139	196	220	25	-----
2.12	180	218	247	-30	-----
2.13	147	195	229	12	-----
2.14	169	181	203	15	-----
2.15	164	208	236	-10	-----
2.21	160	203 (375)[a]	232 (398)[a]	-5	46

Table 2. 2 Thermal properties of polyglyoxylates measured by TGA and DSC. [a] The values in brackets represent the values for the second stage of a two-stage decomposition, T_{98} = maximum temperature at which 98% of mass is still present; T_o = onset degradation temperature; T_p = peak degradation temperature.

The thermal properties of the polymers were measured by thermogravimetric analysis (TGA) and differential scanning calorimetry (DSC). TGA was particularly useful for differentiating between capped and uncapped polymers. Based on the maximum temperature at which 98% of mass is still present (T_{98}, Table 2.2 and Figure 2.1), as well as all other measures of thermal stability, the unend-capped PEtG **2.1** was less stable than the end-capped PEtGs **2.2** – **2.4**. The data suggest that **2.1** likely degrades thermally by depolymerization, whereas PEtGs **2.2** – **2.4** require a backbone or end-cap cleavage to initiate the thermal degradation process. All of the PEtGs were amorphous and exhibited glass transition temperatures (T_g) of -32 ºC for the uncapped PEtG **2.1** and -9 to -1 ºC for end-capped PEtGs **2.2** – **2.4** (Table 2.2).

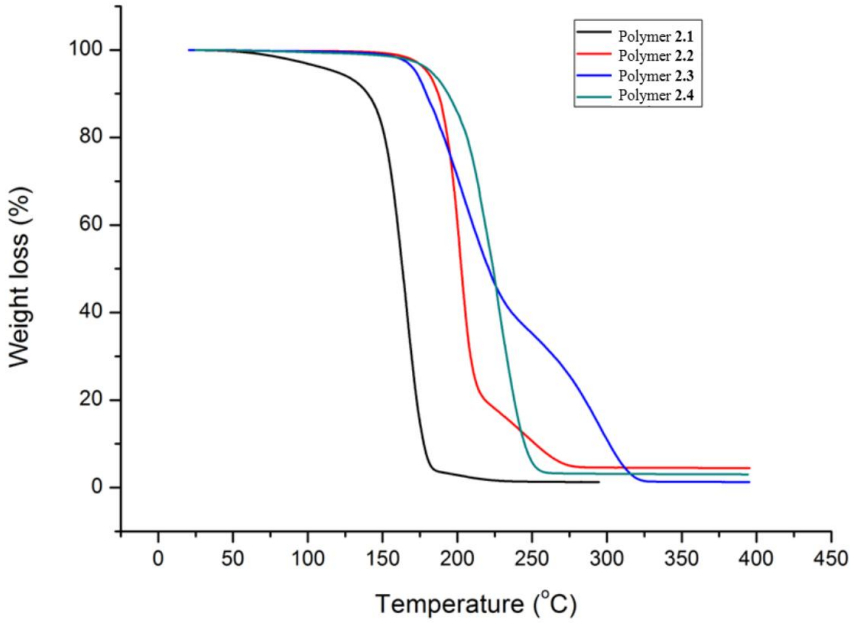

Figure 2. 1 TGA results from polymer 2.1-2.4

2.2.2 Stimuli-responsive Degradation of PEtG

The triggered degradation of PEtG **2.4** in response to irradiation with UV light was studied both in solution and in polymer films. PEtG was insoluble in fully aqueous conditions, but dissolved in 9:1 CD_3CN:D_2O at 15 mg/mL, a concentration sufficient for NMR studies. First, UV-visible spectroscopy was used to determine the required irradiation time for NVOC cleavage in this solution and it was found that 80 min of irradiation with a low energy UV light source (300 - 350 nm) was sufficient to effect complete removal of the NVOC end-cap (Appendix 2).

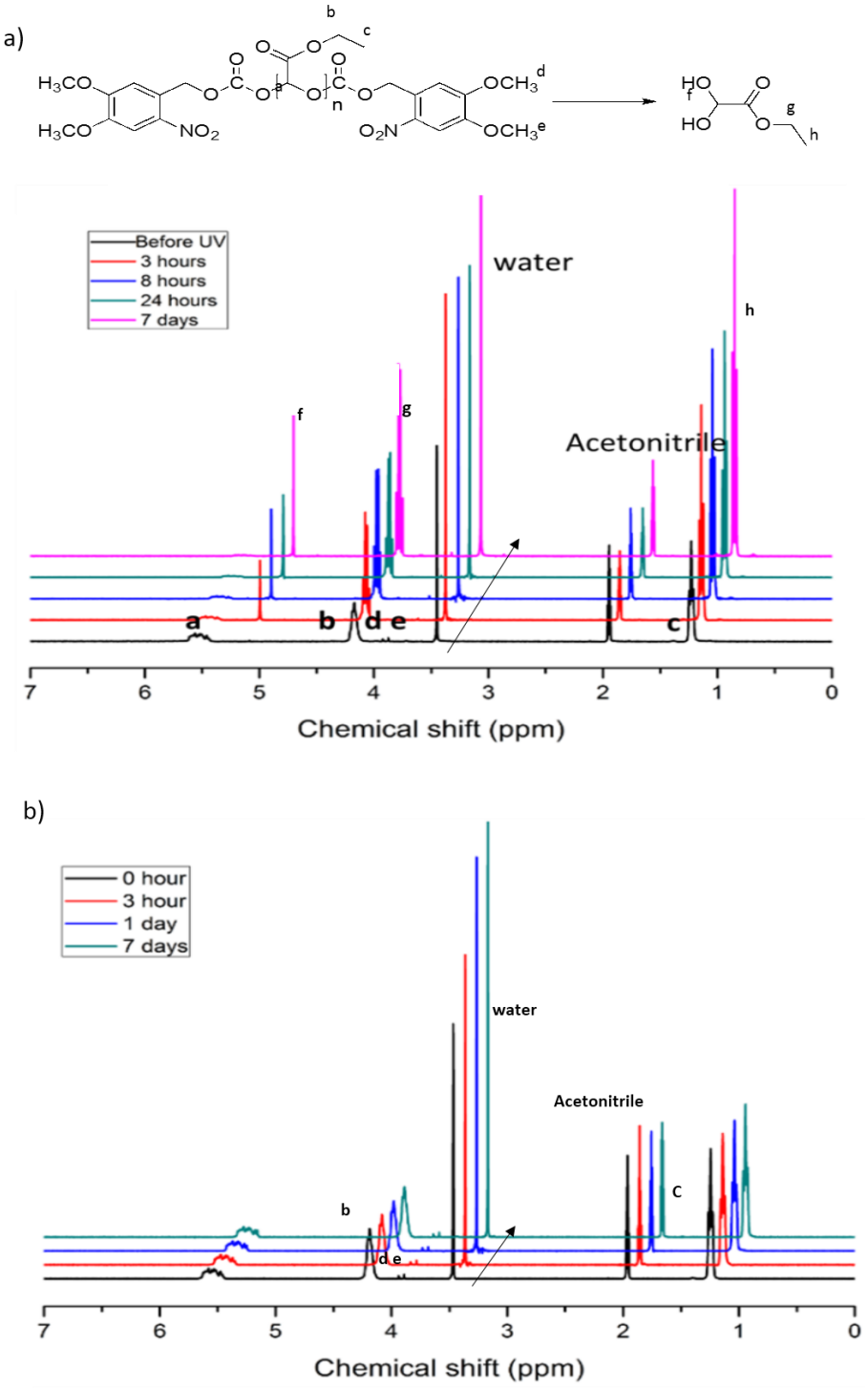

Figure 2. 2 ^{1}H NMR spectra of PEtG 2.4: a) after UV irradiation and b) without UV irradiation, following incubation in 9:1 CD_3CN:D_2O at 21 °C for varying time periods. Spectra are offset to allow the progression over time to be clearly observed.

A comparison of the NMR spectra before and after irradiation supports the successful cleavage of the end-cap. Before irradiation, the spectrum consisted of three broad peaks attributable to the PEtG backbone and peaks corresponding to the two methoxy groups (4.06 ppm and 3.97 ppm) on the NVOC moiety were also observable (Figure 2.2). However, after irradiation and incubation in the solution at ambient temperature (21 °C) for 3 h, the peaks corresponding to the methoxy groups had disappeared, resulting in a series of small singlets between 3 and 4 ppm. This confirmed that the NVOC group had indeed been cleaved. In addition, as shown in Figure 2.2a, the broad peak at 5.5 ppm corresponding to the acetal hydrogens along the polymer backbone decreased in intensity while a new sharp peak at 5.1 ppm corresponding to the expected degradation product EtGH emerged. Sharpening of the peaks corresponding to the ethyl group was also consistent with depolymerization to EtGH. Based on the relative peak integrations, about 50% of the PEtG had depolymerized into EtGH after 3 h, increasing to more than 70% after 24 h. In contrast, as shown in Figure 2.2b, a non-irradiated sample of PEtG **2.4** did not undergo any detectable degradation after 7 days in solution. In addition, PEtG **2.3** with the benzyl carbonate end-cap remained unchanged after UV irradiation and 7 days in solution (Appendix 2). Combined, this data confirms that the depolymerization of PEtG **2.4** indeed results from backbone depolymerization induced by end-cap cleavage and not by random backbone cleavage induced by UV light or hydrolytic reactions.

PEtG's insolubility in water allows for the preparation and study of PEtG film degradation under aqueous conditions. Films were subjected to UV irradiation, then immersed in a pH 7.4 phosphate buffer solution. At time points ranging from 1 - 17 days, the films were removed, rinsed and dried, and then the remaining mass of polymer was measured. As shown in Figure 2.3a, the irradiated films of PEtG **2.4** exhibited steady mass loss over the 17 days, at which point they had completely degraded. In contrast, non-irradiated films of PEtG lost less than 4% of their mass during this same time period. This small amount of weight loss is likely due to a small degree of ester hydrolysis and backbone degradation, as PEtGs are known to gradually degrade in water.[40]

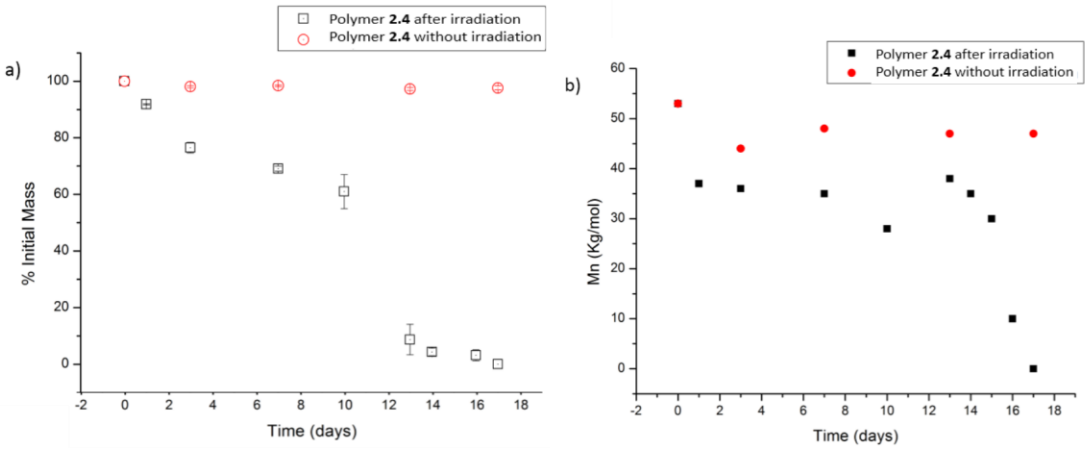

Figure 2. 3 a) Mass loss from films of PEtG 2.4 with and without UV irradiation upon incubation in pH 7.4 phosphate buffer. The UV irradiation was conducted in a UV box (5 mW/cm^3) for 17 hours. Error bars represent the standard error of mean on the measurement of 3 films; b) Evolution of molar mass in the same films as measured by SEC (one measurement per time point).

After the measurement of mass loss, the material remaining on the slide was analyzed by SEC to determine to what degree depolymerization had occurred, as small levels of non-specific hydrolysis and/or slow depolymerization would result in a lower molecular weight, but may not result in dissolution of the material from the film. As shown in Figure 2.3b, the initial M_n of polymer **2.4** was 53 kDa, but after UV irradiation the M_n of polymer **2.4** decreased to about 37 kDa in the first day. Over the next 12 days, the M_n exhibited very little change but at the same time the mass of the film kept decreasing. This suggests that the film was likely disintegrating via a surface erosion process during this time period so the M_n of the bulk material that remained unexposed to water was not affected. From days 13 to 17, a rapid reduction in molecular weight was observed, which as shown in Figure 2.3b, correlated to the loss of the remaining 10% of material from the films. At this stage, with only a thin film of material remaining on the slides, the percentage of material exposed to water and thus depolymerizing, progressively increased, resulting in a reduction of M_n for the measured sample. In comparison, the M_n of the non-irradiated control remained very close to that of the starting polymer throughout the experiement. However, it seemed there was an acceleration of mass loss at the time period between 10

days and 13 days, and the molecular weight of the samples also showed little decreasing at the 10 days, therefore, further detailed study may needed to get a conclusive results.

2.2.3 Development of Stimuli-responsive Polyglyoxylates with Diverse Ester Side Chains

Having shown that PEtG can selectively undergo depolymerization in response to a stimulus, it was of interest to demonstrate that the simple structure of the monomer allows for the rapid generation of structurally diverse polymers using alternate glyoxylates. Glyoxylates other than EtG are available from specialty chemical suppliers, but at high cost. Therefore, we aimed to develop an improved synthetic route to access these monomers. The most common synthetic approach towards glyoxylates is the oxidative cleavage of dialkyl tartrates.[44-46] However, this introduces oxidative impurities, such as the corresponding acid, that can be challenging to remove.[47,48] While the purity is sufficient for most synthetic applications, higher purity monomer is required for polymerization. To address this, ozonolysis of dialkyl fumarates and maleates was used as an alternative strategy.

As shown in Scheme 2.3, methyl maleate (**2.5**), *n*-butyl fumarate (**2.6**) and benzyl fumarate (**2.7**) were first prepared by standard esterification procedures. Ozonolysis with quenching by dimethyl sulfide, followed by distillation, provided the corresponding glyoxylates **2.8** – **2.10**. These monomers were polymerized using the same procedures as for PEtG **2.4** to provide poly(methyl glyoxylate) (PMeG, **2.11**), poly(*n*-butyl glyoxylate (PBuG, **2.12**), and poly(*n*-benzyl glyoxylate) (PBnG, **2.13**), each having a NVOC end-cap.

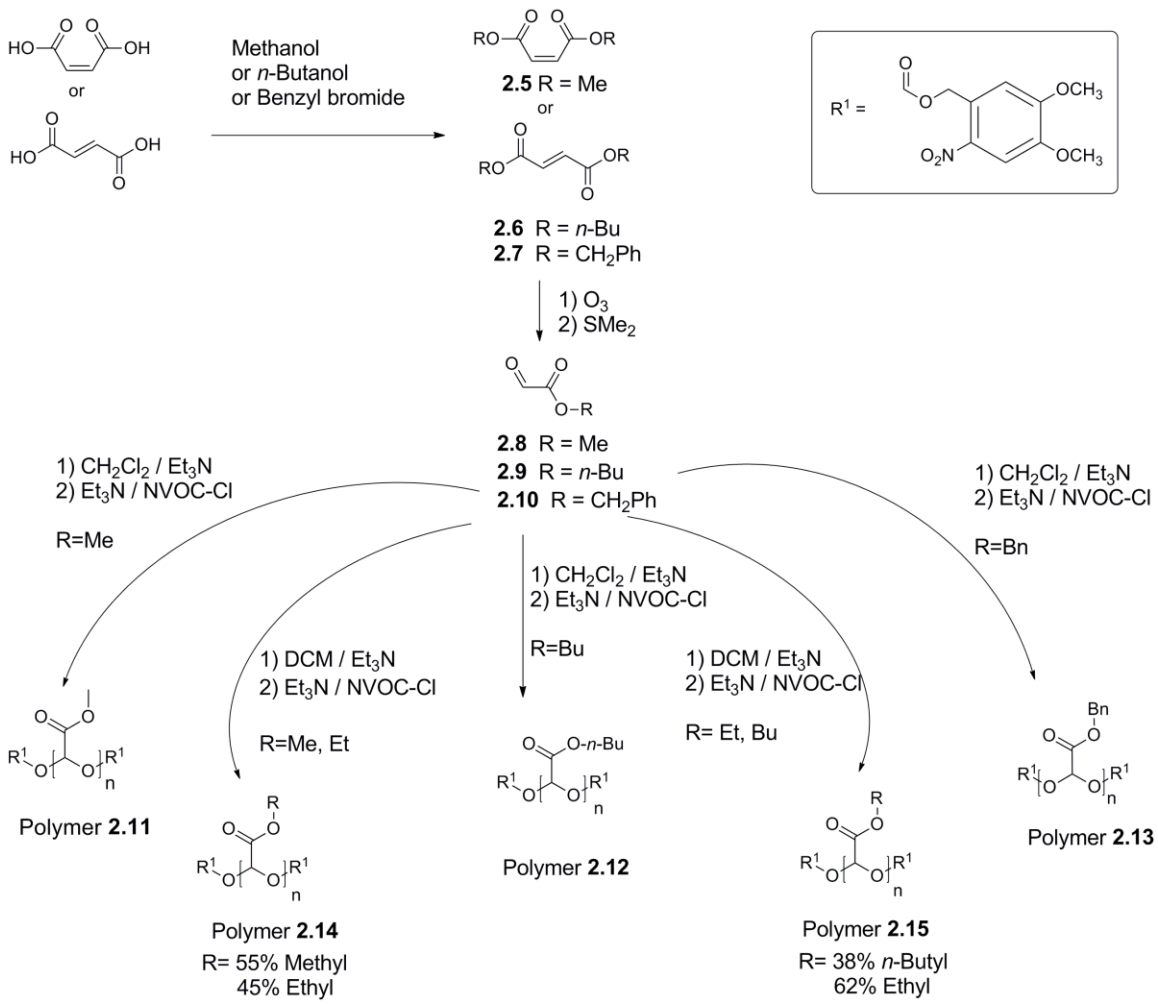

Scheme 2. 3 Synthesis of glyoxylate monomers and polyglyoxylates.

As shown in Table 2.1, the molecular weights of polyglyoxylates **2.11** – **2.13** were significantly lower than those of the PEtGs, with M_n ranging from 2.1 - 5.0 kDa and M_w ranging from 3.5 - 9.8 kDa. These values were in reasonable agreement with the M_n values obtained by ^{1}H NMR spectroscopy. This may be related to lower reactivities of these monomers, but also may relate to the challenge of purifying these monomers to the same degree as for EtG. However, this limitation was overcome by preparing copolymers. Copolymerization of MeG **2.8** and EtG in a 55:45 feed ratio provided copolymer **2.14** comprising approximately 46:54 methyl:ethyl side chains and with an M_n of 40 kDa, comparable to that of the PEtGs despite the high MeG content. Similarly, *n*-BuG **2.9** was copolymerized with EtG in a 38:62 feed ratio to afford copolymer **2.15** comprising approximately 33:67 *n*-butyl:ethyl side chains.

As shown in Table 2.2, the thermal stabilities of these polyglyoxylates are similar to those of the end-capped PEtGs (**2.2** – **2.4**). DSC revealed that these polymers are amorphous materials with T_g ranging from -30 to 25 °C. The T_g decreases as the length of the pendant alkyl group increases from methyl to butyl, which is expected as these flexible groups facilitate chain motion. On the other hand, polymer **2.13** with the less flexible benzyl side chain has an intermediate T_g of 12 °C. Copolymers **2.14** and **2.15** have T_g that are in between those of their corresponding homopolymers.

Polyglyoxylates **2.11** – **2.15** exhibited similar solubility properties to PEtG, and their stimuli-responsive degradation was therefore studied as described above for PEtG. In each case, irradiation with UV light in 9:1 CD_3CN:D_2O followed by incubation at 21 °C resulted in conversion of the broad peaks corresponding to the polymers in the ^{1}H NMR spectra to sharp peaks corresponding to the expected glyoxylate hydrates over a period of 7 days. The degradation rates of the different polyglyoxylates are summarzied in Figure 2.4 and individual graphs are provided in Appendix 2. In each case, the degradation approached completion in less than 10 days, with a small fraction of the resulting glyoxylate existing in its oligomerized form under these conditions. The differences in rates can likely be attributed to a combination of factors including differences in chain

lengths,[14] the susceptibilities of the different polymers to depolymerization, and the reoligomerization of the liberated monomers under these conditions. In each case, non-irradiated samples were also studied and did not show any signs of degradation (Appendix 2). Overall, these results suggest that the different polyglyoxylates and their copolymers degrade similarly to PEtG, thereby opening prospects for the preparation of a wide variety of glyoxylate-based polymers.

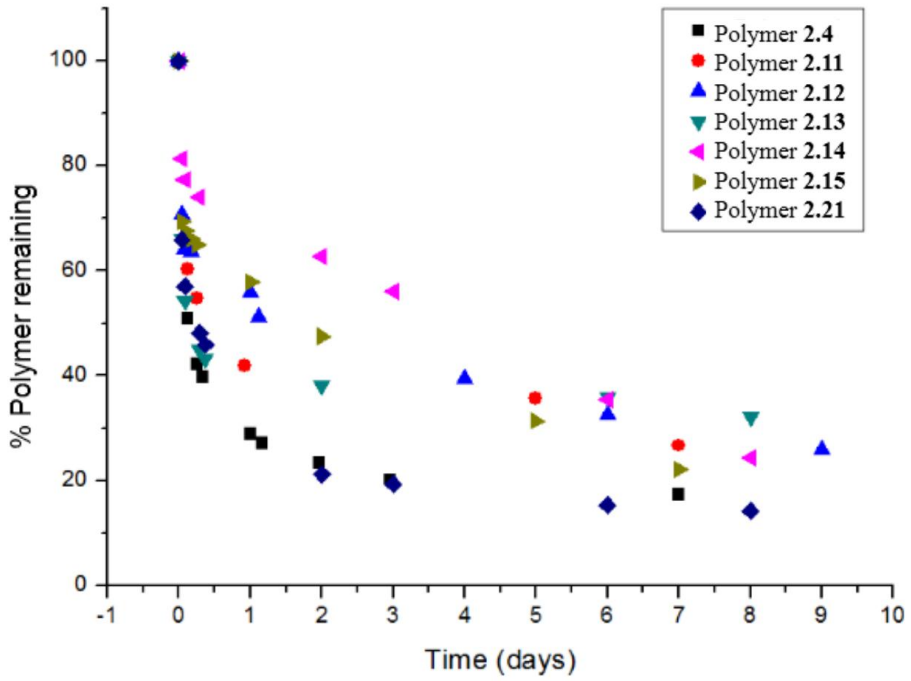

Figure 2. 4 Depolymerization of different end-capped polyglyoxylates following cleavage of the NVOC end-caps by UV irradiation in 9:1 CD_3CN:D_2O following by incubation at ambient temperature (21°C).

2.2.4 Synthesis of a Polyglyoxylate Block Copolymer

The preparation of block polymers is another strategy routinely used to modify the properties of polymeric materials. In the current work, we demonstrate this approach by the incorporation of a hydrophilic block to the relatively hydrophobic PEtG block, thereby preparing an amphiphilic block copolymer. Poly(ethylene glycol) (PEG) was selected as the hydrophilic block as it is a water-soluble polymer that is still being extensively studied in a wide range of applications from coatings to drug delivery vehicles.[49-50] To incorporate the PEG block while at the same time retaining the ability of the PEtG to undergo stimuli-responsive depolymerization, it was necessary to develop a new multifunctional end-cap. As shown in Scheme 2.4, starting from the previously reported alcohol **2.16**[51], the propargyl amide **2.17** was synthesized through an EDC-mediated coupling. Next, the alcohol group was converted into a chloroformate by reaction with phosgene to obtain the target linker end-cap **2.18**.

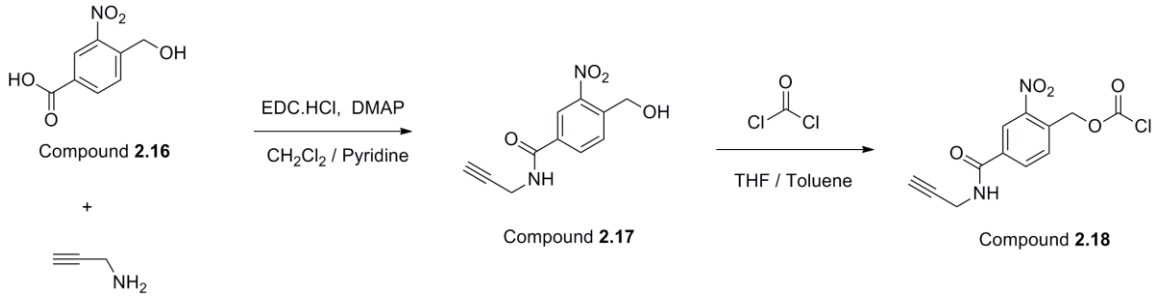

Scheme 2. 4 Synthesis of a multifunctional end-cap.

As shown in Scheme 2.5, PEtG was prepared and end-capped with chloroformate **2.18** to provide polymer **2.19**. A copper assisted azide-alkyne "click" cycloaddition (CuAAC) between **2.19** and azide-terminated PEG **2.20**[52] with a molar mass of 2 kDa provided PEG-PEtG-PEG triblock copolymer **2.21**. Excess PEG was removed by dialysis in water. As shown in Table 2.1, SEC of **2.21** did not show any significant change in molar mass relative to polymer **2.19**, but it confirmed the absence of uncoupled PEG, and the presence of the expected amount of PEG in the ^{1}H NMR spectrum of **2.21** confirmed the

successful coupling. As shown in Table 2.2, TGA showed a two-phase degradation process for the material, with the initial mass loss corresponding to the PEtG block and the second phase corresponding to PEG. The relative mass losses for these two phases were consistent with the relative content of PEtG and PEG in **2.21**. Incorporation of the PEG also imparted semicrystalline properties to the material, with a T_g of -5 °C and a T_m of 46 °C. As shown in Figure 2.4, triblock copolymer **2.21** also underwent depolymerization triggered by UV light at a rate very similar to that of PEtG in $CD_3CN:D_2O$ (9:1).

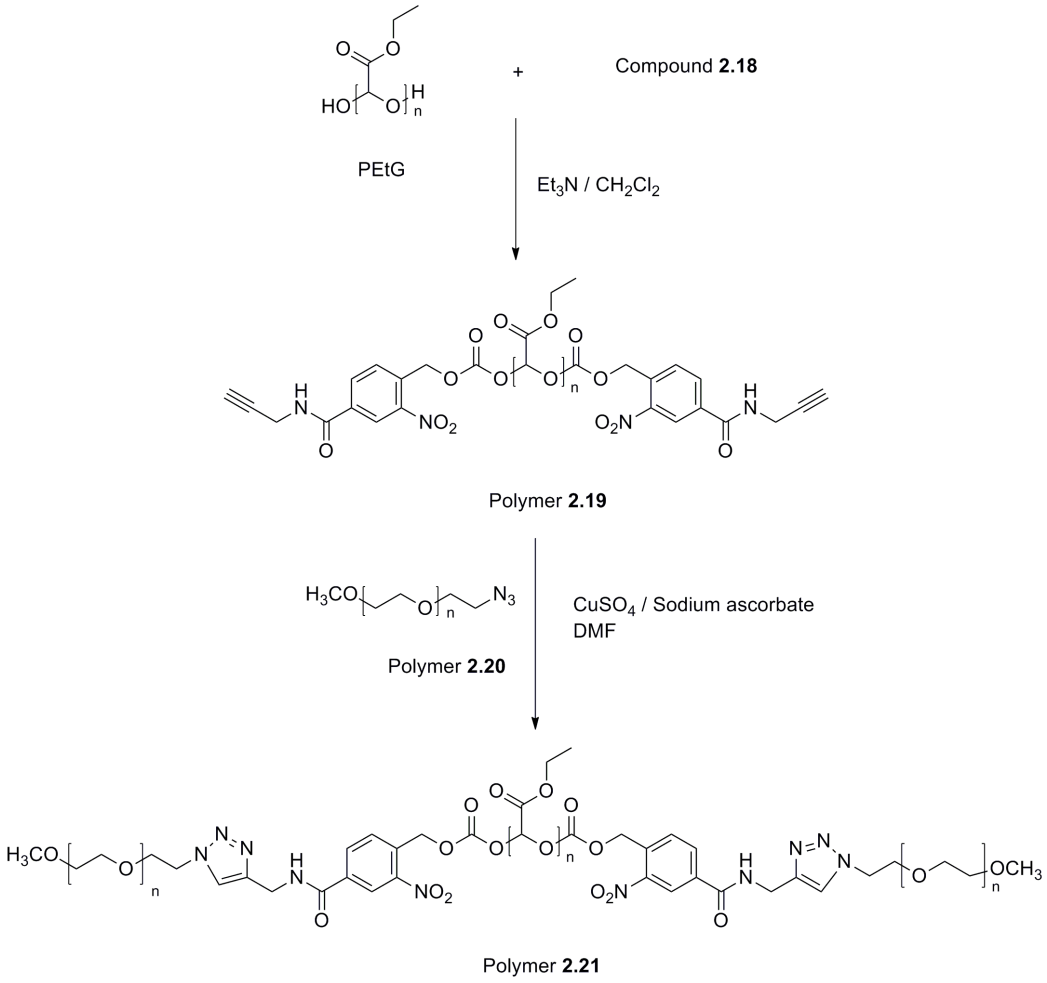

Scheme 2. 5 Synthesis of a PEG-PEtG-PEG triblock copolymer.

2.3 Conclusions

It was demonstrated for the first time that through the use of stimuli-responsive end-caps, polyglyoxylates serve as a new class of self-immolative linear polymer backbones. The use of chloroformates provides an effective end-capping strategy as demonstrated by the preparation and study of control PEtGs as well as a triggerable PEtG **2.4** with a UV light-cleavable end-cap. This will allow a variety of end-caps responsive to different stimuli to be incorporated into polyglyoxylates. It was also shown that glyoxylates with various side chains can be prepared by simple two-step synthetic processes starting from alcohols and fumaric or maleic acid, and these can be homopolymerized or copolymerized with EtG to provide materials with a range of properties and molar masses. Furthermore, using a multifunctional end-cap, it is possible to prepare glyoxylate-based triblock copolymers, which provides an additional means of tuning polymer properties. All of the above materials underwent depolymerization to the expected products selectively upon cleavage of the end-cap, while the untriggered polymers were stable under the studied conditions. These new materials are particularly attractive as the component monomers can be derived not only from petroleum-based sources, but also from renewable resources. In addition, while the toxicity of other alcohol derivatives remains to be explored, PEtG depolymerizes to ultimately provide the benign products glyoxylic acid hydrate and ethanol. This should open many new prospects for the field of self-immolative polymers. Future work will involve studies of the toxicity and properties of various polyglyoxyates available through this chemistry as well as the development of polyglyoxylate coatings and aqueous assemblies for controlled release, sensing, and other applications.

2.4 Experimental

2.4.1 General Procedures and Materials

Ethyl glyoxylate in toluene solution (50% w/w), phenyl isocyanate, dibutyltin dilaurate

(DBTL), benzyl chloroformate, 4-bromomethyl-3-nitrobenzoic acid, methanesulfonyl chloride and benzyl bromide were obtained from Alfa Aesar (Canada). Fumaric acid and maleic acid were purchased from Acros Organics (USA). 6-Nitroveratryl chloroformate (NVOC-Cl) was obtained from Chem-Impex International, Inc. (USA). Propargyl amine was purchased from AK Scientific, Inc. (USA). Dimethyl sulfide, sodium azide (NaN3), phosgene solution (15 wt. % in toluene) and poly(ethylene glycol) methyl ether (2 kDa) were purchased from Sigma-Aldrich (USA). 1-Ethyl-3-(3-dimethylaminopropyl) carbodiimide hydrochloride (EDC·HCl) was purchased from Creo Salus (USA). Triethylamine (Et3N), pyridine, and dichloromethane were distilled from calcium hydride before use. Anhydrous tetrahydrofuran (THF) and N,N-dimethylformamide (DMF) were obtained from a solvent purification system using aluminum oxide columns. All the other chemicals were of reagent grade and used without further purification unless otherwise noted. 1H NMR spectra were obtained at 400 MHz or 600 MHz on Varian Inova instruments. NMR chemical shifts (δ) are reported in ppm and are calibrated against residual solvent signals of CDCl3 (δ 7.27), CD3CN (δ 1.94), (CD3)2SO (δ 2.50) or D2O (δ 4.75). Fourier transform infrared spectra (FT-IR) were obtained using a Bruker tensor 27 instrument with films drop cast from CH2Cl2 on KBr plates. High-resolution mass spectrometry (HRMS) was performed using a Finnigan MAT 8400 electron impact (EI) mass spectrometer. The SEC instrument was equipped with a Viscotek GPC Max VE2001 solvent module. Samples were analyzed using the Viscotek VE3580 RI detector operating at 30 ̊C. The separation technique employed two Agilent Polypore (300x7.5mm) columns connected in series and to a Polypore guard column (50x7.5mm). Samples were dissolved in THF (glass distilled grade) in approximately 5mg/mL concentrations and filtered through 0.22 μm syringe filters. Samples were injected using a 100 μL loop. The THF eluent was filtered and eluted at 1ml/min for a total of 30 minutes. A calibration curve was obtained from Polystyrene samples with molecular weight ranges of 1,540-1,126,000/mol. DSC and TGA were performed on a Mettler Toledo DSC 822e. For TGA the heating rate was 10 ℃/min between 50-400 ℃ under nitrogen. For DSC, the heating/cooling rate was 10 ℃/min from -100 to +170 ℃. Glass transition temperatures were obtained from the second heating cycle.

2.4.2 Synthesis of Monomers

Synthesis of Dimethyl Maleate (2.5). Maleic acid (25.0 g, 216 mmol) was dissolved in methanol (250 mL). Concentrated sulfuric acid (2.5 mL) was then added dropwise. After refluxing at 75 ℃ for 16 hours, the methanol was removed by rotary evaporator. Ethyl acetate (100 mL) was then added to the residue, and the solution was washed twice with saturated sodium bicarbonate (20 mL), and then with deionized water (20 mL). The organic layer was then dried over $MgSO_4$, filtered and concentrated under reduced pressure to provide a clear, colorless, oily liquid (30.0 g, 97%) after distillation of the oil at 140 ℃ (190 mbar). ^{1}H NMR (400 MHz, $CDCl_3$): δ 6.26 (s, 2H), 3.79 (s, 6H). Spectral data are consistent with published values.[53]

Synthesis of Dibutyl Fumarate (2.6). Synthesis of Fumaric acid (20.0 g, 172 mmol) was dissolved in *n*-butanol (250 mL). Concentrated sulfuric acid (2.5 mL) was then added dropwise. After stirring at 120 ℃ for 16 hours, the residual *n*-butanol was removed *in vacuo*. Ethyl acetate (100 mL) was then added to the residue, and the solution was washed with saturated sodium bicarbonate (20 mL) solution twice, and deionized water (20 mL) once. The organic layer was then dried over $MgSO_4$, filtered and concentrated under reduced pressure to provide a clear, colorless, oily liquid (36.8 g, 94%) after distillation at 100 ℃ (40 mbar). ^{1}H NMR (400 MHz, $CDCl_3$): δ 6.85 (s, 2H), 4.20 (t, J = 6.6 Hz, 4H), 1.63-1.70 (m, 4H), 1.36-1.46 (m, 4H), 0.95 (t, J = 7.4 Hz, 6H). Spectral data are consistent with published values.[54]

Synthesis of Dibenzyl Fumarate (2.7). Fumaric acid (10.0 g, 86 mmol, 1.0 equiv.) was dissolved in anhydrous DMF (200 mL), and then triethylamine (24.0 mL, 172 mmol, 2.0 equiv.) was added dropwise to the stirring solution. Benzyl bromide (19.5 mL, 164 mmol, 1.9 equiv.) was then injected into the reaction mixture. After stirring at 100 ℃ for 16 hours, the solution was precipitated into deionized water (800 mL) to provide a pale yellow solid (18.8 g, 78%) after filtration and drying. ^{1}H NMR (400 MHz, $CDCl_3$): δ 7.31-7.41 (m, 10H), 6.94 (s, 2H), 5.24 (s, 4H). Spectral data are consistent with published values.[55]

Synthesis of Methyl Glyoxylate (2.8). Diester **2.5** (20.0 g, 139 mmol, 1.0 equiv.) was dissolved in dichloromethane (200 mL), and the solution was cooled to -78 ℃ in a dry ice/acetone bath. Ozone was bubbled into the solution under stirring until the solution turned blue. The solution was then purged with oxygen. Dimethyl sulfide (12.2 mL, 167 mmol, 1.2 equiv.) was added dropwise to quench the system. After stirring for 5 hours, and warming to room temperature, the solvent and residual dimethyl sulfide were removed by distillation at 70 ℃ under argon. A pale yellow liquid (18.3 g, 75%) was obtained via distillation at 100 ℃ under a slightly reduced pressure. ^{1}H NMR (400 MHz, $CDCl_3$): δ 9.33 (s, 1H), 3.86 (s, 3H). Spectral data are consistent with published values.[56]

Synthesis of *n*-Butyl Glyoxylate (2.9). Diester **2.6** (26.0 g, 114 mmol, 1.0 equiv.) was dissolved in CH_2Cl_2 (300 mL), and the solution was cooled to -78 ℃ in a dry ice/acetone bath. Ozone was bubbled into the solution under stirring until the solution turned into blue, and then the solution was purged with oxygen. Dimethyl sulfide (10.0 mL, 137 mmol, 1.2 equiv.) was then added dropwise to quench the system. After stirring for 5 h, and warming to room temperature, the solvent and the residual dimethyl sulfide were removed by distillation at 70 ℃ under argon. A pale yellow liquid (15.3 g, 52%) was obtained after distillation at 150 ℃ (200 mbar) over P_2O_5. ^{1}H NMR (400 MHz, $CDCl_3$): δ 9.39 (s, 1H), 4.31 (t, *J* = 6.6 Hz, 2H), 1.68-1.76 (m, 2H), 1.37-1.47 (m, 2H), 0.94 (t, *J* = 7.4 Hz, 3H). ^{13}C NMR (150 MHz, $(CD_3)_2SO$): δ 184.2, 159.7, 65.3, 30.0, 18.6, 13.4. MS calc'd. for $[M+H]^+$ $C_6H_{11}O_3$: 131.07082; found: 131.07088.

Synthesis of Benyzl Glyoxylate (2.10). Diester **2.7** (10.0 g, 34 mmol, 1.0 equiv.) and Sudan Red III (20.0 mg) were dissolved in dichloromethane (100 mL), and the solution was cooled to -78 ℃ by dry ice/acetone bath. Ozone was then bubbled into the stirred solution until the red solution turned clear and colorless, and then the solution was immediately purged with oxygen. Dimethyl sulfide (3.0 mL, 41 mmol, 1.2 equiv.) was then added dropwise into the solution to quench the ozonide. The mixture was stirred for an additional 5 hours, and allowed to warm to ambient temperature. The solvent and the residual dimethyl sulfide were then removed by distillation at 70 ℃ under argon to

provide a pale yellow liquid (6.0 g, 55%) following distillation at 150 ℃ (40 mbar) from P_2O_5. ^{1}H NMR (400 MHz, $CDCl_3$): δ 9.43 (s, 1H), 7.21-7.51 (m, 5H), 5.35 (s, 2H). Spectral data are consistent with published values.[57]

2.4.3 Synthesis of Polymers

Due to the highly reactive nature of these monomers, even trace water can lead to oligomerization or polymerization. Therefore, immediately before polymerization, a second vacuum distillation with P_2O_5 was conducted to crack any oligomers and remove any remaining traces of water.

Synthesis of Polymer 2.1. Ethyl glyoxylate in toluene solution (20 mL) was fractionally distilled under vacuum (55 ℃, 125 mbar) over P_2O_5 to remove toluene and trace water in the first, discarded fraction. The residue was then distilled twice successively over P_2O_5 at atmospheric pressure under argon protection at 130 ℃ to obtain the highly pure monomer. This pale yellow liquid (5.0 mL, 50 mmol, 1.0 equiv.) was dissolved in dichloromethane (5.0 mL) and Et_3N (3.5 μL, 25 μmol, 0.0005 equiv.). The solution was stirred for one hour at -20 ℃, and the resulting polymer was purified by precipitation into methanol. After drying *in vacuo* for 48 hours, polymer **2.1** was obtained (1.8 g, 35%). ^{1}H NMR (400 MHz, $CDCl_3$): δ 5.48-5.75 (m, 100H), 4.12-4.38 (m, 204H), 1.24-1.44 (m, 298H). ^{13}C NMR (150 MHz, $CDCl_3$): δ 164.7-167.1, 90.6-93.8, 61.7, 13.5. SEC: M_n = 103 kDa, M_w = 266 kDa, $Đ$ = 2.6. T_g = -32 ℃.

Synthesis of Polymer 2.2. The same distillation and polymerization procedure was conducted to obtain poly(ethyl glyoxylate) as described for polymer **2.1**; however, prior to precipitation, phenyl isocyanate (100 μL, 920 μmol, 0.018 equiv.) was added to end-cap the polymer along with 3 drops of DBTL. The solution was then stirred for 24 hours at room temperature and a further 16 hours at 40 ℃. Purification was achieved by precipitation of the crude reaction mixture into methanol. After decanting the excess methanol, the residue was dried *in vacuo* for 48 hours to provide polymer **2.2** (2.3 g, 45%). ^{1}H NMR (400 MHz, $CDCl_3$): δ 7.26-7.43 (m, 10H), 5.48-5.73 (m, 79H), 4.10-4.30

(m, 171H), 1.17-1.36 (m, 249H). ^{13}C NMR (150 MHz, $CDCl_3$): δ 164.7-166.9, 90.3-94.8, 61.7, 13.5. FT-IR (KBr, thin film): 2982, 1762, 1447, 1376, 1020 cm^{-1}. SEC: M_n = 27 kDa, M_w = 66 kDa, $Đ$ = 2.5. T_g = -1 ℃.

Synthesis of Polymer 2.3. Poly(ethyl glyoxylate) was prepared as described for polymer **2.1**. Following polymerization, but prior to precipitation, benzyl chloroformate (100 μL, 710 μmol, 0.014 equiv.) was added at 0 ℃ along with Et_3N (99.0 μL, 710 μmol, 0.014 equiv.). The solution was stirred for 24 hours at room temperature and a further 16 hours at 40 ℃. Purification was achieved by precipitation of the crude reaction mixture into methanol. After the solvent was decanted, the residue was dried *in vacuo* for 48 hours to provide polymer **2.3** (2.6 g, 50%). ^{1}H NMR (400 MHz, $CDCl_3$): δ 7.26-7.41 (m, 15H), 5.48-5.82 (m, 750H), 5.20 (s, 4H), 4.05-4.32 (m, 1562H), 1.19-1.49 (m, 2349H). ^{13}C NMR (150 MHz, $CDCl_3$): δ 165.0-167.5, 127.2-128.9, 90.6-94.0, 62.0, 13.8. FT-IR (KBr, thin film): 2982, 1762, 1448, 1379, 1020 cm^{-1}. SEC: M_n = 31 kDa, M_w = 59 kDa, $Đ$ = 1.9. T_g = -3 ℃.

Synthesis of Polymer 2.4. EtG in toluene solution (20 mL) was fractionally distilled under vacuum (55 ºC, 125 mbar) over P_2O_5 to remove toluene and trace water in the first, discarded fraction. The residue was then distilled twice successively over P_2O_5 at atmospheric pressure under argon at 130 ºC to obtain the highly pure monomer. The resulting pale yellow liquid (5.0 mL, 50 mmol, 1.0 equiv.) was dissolved in CH_2Cl_2 (5.0 mL) and Et_3N (3.5 μL, 25 μmol, 0.0005 equiv.). The solution was stirred for 1 h at -20 ºC. NVOC-Cl (0.2 g, 730 μmol, 0.014 equiv.) and Et_3N (100 μL, 730 μmol, 0.014 equiv.) were added at 0 ºC to end-cap the polymer. The solution was stirred for 24 h at room temperature and a further 16 h at 40 ºC. Purification was achieved by precipitation of the crude reaction mixture into methanol. After decanting the excess methanol, the residue was dried in vacuo for 48 h to provide 3.2 g of a white, sticky polymer in 62% yield. ^{1}H NMR (400 MHz, $CDCl_3$): δ 7.75 (s, 0.04H), 7.01 (s, 0.02H), 5.48-5.75 (m, 312H), 4.06-4.34 (m, 642H), 4.05 (s, 6H), 3.97 (s, 6H), 1.17-1.45 (m, 963H). ^{13}C NMR (150 MHz,

$CDCl_3$): δ 164.8-166.4, 148.1, 107.9, 90.1-94.0, 86.9, 66.7, 61.9, 56.5, 55.1, 13.7. FT-IR (KBr, thin film): 2985, 1757, 1448, 1377, 1022 cm^{-1}. SEC: M_n = 53 kg/mol, M_w = 91 kg/mol, $Đ$ = 1.7. T_g = -9 ºC.

Synthesis of Polymer 2.11. Freshly distilled methyl glyoxylate (5.0 mL, 63 mmol, 1.0 equiv.) was dissolved in dichloromethane (5.0 mL) and Et_3N (4.4 μL, 32 μmol, 0.0005 equiv.). After the solution had been stirred for one hour at -20 ℃, Et_3N (0.2 mL, 1.5 mmol, 0.023 equiv.) and NVOC-Cl (0.4 g, 1.5 mmol, 0.023 equiv.) were added into the mixture to end-cap the polymer. The solution was then stirred for 24 hours at room temperature and a further 16 hours at 40 ℃. Purification was achieved by precipitation of the crude reaction mixture into methanol. After decanting the excess methanol, the residue was dried *in vacuo* for 48 hours, to provide polymer **2.11** (3.3 g, 59%). ^{1}H NMR (400 MHz, $CDCl_3$): δ 7.75 (s, 1.8H), 7.14 (s, 1.2H), 5.55-5.78 (m, 83H), 4.06 (s, 6H), 3.97 (s, 6H), 3.73-3.86 (m, 262H). ^{13}C NMR (150 MHz, $CDCl_3$): δ 164.7-166.5, 153.8, 148.1, 109.2, 107.6, 90.0-93.9, 86.7, 66.8, 56.4, 56.2, 52.6. FT-IR (KBr, thin film): 2960, 1760, 1440, 1019 cm^{-1}. SEC: M_n = 3800 Da, M_w = 4800 Da, $Đ$ = 1.3. T_g = 24 ℃, T_m = 72 ℃.

Synthesis of Polymer 2.12. Freshly distilled *n*-butyl glyoxylate (5.0 mL, 38 mmol, 1.0 equiv.) was dissolved in dichloromethane (5.0 mL) and Et_3N (2.7 μL, 19 μmol, 0.0005 equiv.). After the solution was stirred for one hour at -10 ℃, Et_3N (0.2 mL, 1.5 mmol, 0.038 equiv.) and NVOC-Cl (0.4 g, 1.5 mmol, 0.038 equiv.) were added into the mixture to end-cap the polymer. The solution was then stirred for 24 hours at room temperature and a further 16 hours at 40 ℃. The solvent was removed by high vacuum and the crude polymer was re-dissolved in tetrahydrofuran (5.0 mL) and dialyzed against water for 24 hours (200 mL, 2 solvent changes) using a regenerated cellulose membrane (6000-8000 Da MWCO). The residual content was then lyophilized to afford polymer **2.12** (2.2 g, 44%).^{1}H NMR (400 MHz, $CDCl_3$): δ 7.75 (s, 3H), 7.09 (s, 2.9H), 5.46-5.77 (m, 49H), 4.06-4.24 (m, 83H), 4.05 (s, 6H), 3.96 (s, 6H), 1.55-1.73 (m, 88H), 1.25-1.45 (m, 82H), 0.81-1.04 (m, 120H). ^{13}C NMR (150 MHz, $CDCl_3$): δ 164.1-166.4, 153.9, 147.5, 109.2,

107.6, 90.2-94.3, 65.7, 56.6, 56.3, 30.2, 18.8, 13.6. FT-IR (KBr, thin film): 2963, 2936, 2876, 1759, 1464, 1379, 1219, 1016 cm^{-1}. SEC: M_n = 5000 Da, M_w = 9800 Da, $Đ$ = 1.9. T_g = -30 ℃.

Synthesis of Polymer 2.13. Freshly distilled benzyl glyoxylate (5.0 mL, 36 mmol, 1.0 equiv.) was dissolved in dichloromethane (5.0 mL) and Et_3N (2.5 μL, 18 μmol, 0.0005 equiv.). After the solution was stirred for one hour at 0 ℃, Et_3N (0.2 mL, 1.5 mmol, 0.042 equiv.) and NVOC-Cl (0.40 g, 1.5 mmol, 0.042 equiv.) were added into the mixture to end-cap the polymer. The solution was then stirred for 24 hours at room temperature and a further 16 hours at 40 ℃. The solvent was removed under high vacuum and the crude polymer was re-dissolved in DMF (5.0 mL) and dialyzed against DMF for 24 hours (200 mL, 2 solvent changes) and water for 24 hours (200 mL, 2 solvent changes) using a regenerated cellulose membrane (6000-8000 Da MWCO). The residual content was then lyophilized to afford polymer **2.13** (1.9 g, 36%). ^{1}H NMR (400 MHz, $CDCl_3$): δ 7.69 (s, 1.7H), 6.89-7.36 (m, 106H), 5.46-5.83 (m, 26H), 4.74-5.20 (m, 50H), 3.93 (s, 6H), 3.73 (s, 6H). ^{13}C NMR (150 MHz, $CDCl_3$): δ 164.6-166.6, 153.9, 147.4, 134.8, 128.2, 109.1, 107.7, 91.1-94.2, 67.4, 56.5, 56.3. FT-IR (KBr, thin film): 3034, 2968, 1763, 1583, 1522, 1500, 1456, 1217, 974, 746, 696 cm^{-1}. SEC: M_n = 2100 Da, M_w = 3500 Da, $Đ$ = 1.6. T_g = 12 ℃.

Synthesis of Polymer 2.14. Freshly distilled methyl glyoxylate (4.0 mL, 50 mmol, 1.0 equiv.) and ethyl glyoxylate (4.0 mL, 40 mmol, 0.8 equiv.) were dissolved in dichloromethane (8.0 mL) and Et_3N (12.6 μL, 90 μmol, 0.001 equiv.). After the solution was stirred for one hour at -20 ℃, Et_3N (0.2 mL, 1.5 mmol, 0.03 equiv.) and NVOC-Cl (0.4 g, 1.5 mmol, 0.03 equiv.) were added into the mixture to end-cap the polymer. The solution was then stirred for 24 hours at room temperature and a further 16 hours at 40 ℃. Purification was achieved by precipitation of the crude reaction mixture into methanol. After decanting the excess methanol, the residue was dried *in vacuo* for 48 hours to provide polymer **2.14** (4.8 g, 57%). ^{1}H NMR (400 MHz, $CDCl_3$): δ 7.75 (s, 3H), 7.09 (s,

2H), 5.48-5.78 (m, 770H), 4.16-4.32 (m, 840H), 4.05 (s, 6H), 3.97 (s, 6H), 3.73-3.86 (m, 1072H), 1.21-1.39 (m, 1253H). ^{13}C NMR (150 MHz, $CDCl_3$): δ 164.6-166.8, 148.1, 107.9, 90.1-94.4, 66.8, 61.9, 56.2, 52.5, 13.6. FT-IR (KBr, thin film): 2960, 1759, 1445, 1377, 1016 cm^{-1}. SEC: M_n = 40 kDa, M_w = 81 kDa, $Đ$ = 2.0. T_g = 15 ℃.

Synthesis of Polymer 2.15. Freshly distilled *n*-butyl glyoxylate (3.0 mL, 25 mmol, 1.0 equiv.) and ethyl glyoxylate (4.0 mL, 40 mmol, 1.6 equiv.) were dissolved in dichloromethane (7.0 mL) and Et_3N (9.0 μL, 65 μmol, 0.001 equiv.). After the solution was stirred for one hour at -10 ℃, Et_3N (0.2 mL, 1.5 mmol, 0.023 equiv.) and NVOC-Cl (0.40 g, 1.5 mmol, 0.023 equiv.) were added into the mixture to end-cap the polymer. The solution was then stirred for 24 hours at room temperature and a further 16 hours at 40 ℃. After that the solvent was removed by high vacuum and the crude polymer was re-dissolved into DMF (5.0 mL) and dialyzed against DMF for 24 hours (200 mL, 2 solvent changes) and distilled water for 24 hours (200 mL, 2 solvent changes) using a regenerated cellulose membrane (6000-8000 Da MWCO). The residual content was then lyophilized to afford polymer **2.15** (3.4 g, 45%). ^{1}H NMR (400 MHz, $CDCl_3$): δ 7.75 (s, 1.7H), 7.16 (s, 0.8H), 5.46-5.75 (m, 108H), 4.09-4.43 (m, 221H), 4.05 (s, 6H), 3.97 (s, 6H), 1.57-1.73 (m, 72H), 1.17-1.46 (m, 294H), 0.84-0.99 (m, 95H). ^{13}C NMR (150 MHz, $CDCl_3$): δ 164.7-166.7, 153.7, 148.2, 141.4, 126.7, 109.9, 107.9, 90.4-94.5, 66.8, 65.7, 61.9, 56.7, 56.3, 30.2, 18.8, 13.8,13.6. FT-IR (KBr, thin film): 2964, 2939, 2876, 1765, 1468, 1381, 1219, 1024 cm^{-1}. SEC: M_n = 11 kDa, M_w = 22 kDa, $Đ$ = 2.0. T_g = -10 ℃.

Synthesis of Polymer 2.19. Poly(ethyl glyoxylate) was prepared as described for polymer **1**. Following polymerization, but prior to precipitation, compound **18** (0.22 g, 730 μmol, 0.014 equiv.) was added at 0 ℃ to end-cap the polymer along with Et_3N (100 μL, 730 μmol, 0.014 equiv.). The solution was stirred for 24 hours at room temperature and a further 16 hours at 40 ℃. Purification was achieved by precipitation of the crude reaction mixture into methanol. After decanting the excess methanol, the residue was dried *in vacuo* for 48 hours to provide polymer **2.19** (2.8 g, 56%). ^{1}H NMR (400 MHz,

$CDCl_3$): δ 8.65 (s, 1.9H), 8.19 (s, 2H), 7.82 (s, 2.8H), 5.46-5.71 (m, 627H), 4.12-4.30 (m, 1303H), 2.29 (s, 4H), 1.12-1.40 (m, 1949H). ^{13}C NMR (150 MHz, $CDCl_3$): δ 169.4, 164.9-166.7, 128.3, 90.9-94.5, 81.7, 62.9, 62.2, 29.9, 13.9. FT-IR (KBr, thin film): 2988, 1759, 1468, 1379, 1021, 1028 cm^{-1}. SEC: M_n = 42 kDa, M_w = 89 kDa, $Đ$ = 2.1.

Synthesis of Polymer 2.21. Polymer **2.20**[52] (150 mg, 75 μmol, 3 equiv.) and polymer **2.19** (500 mg, 25 μmol, 1 equiv.) were dissolved into DMF (5 mL). After removing the air and refilling with argon, $CuSO_4$ (4 mg, 25 μmol, 1 equiv.) and sodium ascorbate (5 mg, 25 μmol, 1 equiv.) were added into the solution, and the mixture was stirred at 40 ℃ for 16 hours. Then it was transferred into a regenerated cellulose membrane (50 kDa MWCO) and dialyzed against deionized water for 48 hours (300 mL, 6 solvent changes). The dialyzed material was then lyophilized to afford polymer **2.21** (430 mg, 79%). ^1H NMR (400 MHz, $CDCl_3$): δ 8.71 (s, 27H), 8.24 (s, 31H), 7.83 (s, 38H) 5.47-5.75 (m, 421H), 4.15-4.31 (m, 769H), 3.65 (s, 364H), 3.39 (s, 6H), 1.17-1.40 (m, 1152H). ^{13}C NMR (150 MHz, $CDCl_3$): δ 164.7-166.3, 127.5, 124.1, 90.8-93.9, 71.8, 70.5, 62.0, 13.7. FT-IR (KBr, thin film): 2985, 2941, 2908, 2876, 1759, 1447, 1377, 1231, 1021 cm^{-1}. SEC: M_n = 40 kDa, M_w = 85 kDa, $Đ$ = 2.1. T_g = -5 ℃.

2.4.4 Synthesis of the Multifunctional End-cap

Synthesis of Propargyl Amide 2.17. Compound **2.16** (580 mg, 2.9 mmol, 1.0 equiv.) was dissolved in solvent (12 mL of 5:1 CH_2Cl_2:pyridine), then EDC·HCl (690 mg, 3.5 mmol, 1.2 equiv.), propargyl amine (1.1 mL, 17.7 mmol, 6 equiv.) and DMAP (430 mg, 3.5 mmol, 1.2 equiv.) were added into the stirring mixture under argon. After stirring at room temperature for 6 h, the reaction was diluted with ethyl acetate (60 mL) and washed with saturated $NaHCO_3$ solution (1 × 30 mL), 1M HCl (3 × 30 mL) and deionized water (1 × 30 mL) successively. The organic phase was dried with $MgSO_4$, filtered and the solvent removed under reduced pressure to yield compound **2.17** (395 mg, 57%) as a brown solid. ^1H NMR (400 MHz, $(CD_3)_2SO$): δ 9.26 (t, J = 5.3 Hz, 1H), 8.53 (d, J = 1.2 Hz, 1H), 8.22 (dd, J = 7.6 Hz, 1.2 Hz, 1H), 7.94 (d, J = 7.6 Hz, 1H), 5.67 (t, J = 5.3 Hz, 1H), 4.87 (d, J

=5.3 Hz, 2H), 4.09 (dd, *J* = 5.3 Hz, 2.4 Hz, 2H) 3.16 (t, *J* = 2.4 Hz, 1H). ^{13}C NMR (150 MHz,$(CD_3)_2SO$): δ 163.7, 146.4, 141.6, 133.0, 132.0, 128.4, 123.1, 80.7, 73.0, 59.8, 28.6. MS calc'd for $[M]^+$ $C_{11}H_{10}O_4N_2$, 234.0641; found, 234.0642.

Synthesis of Chloroformate 2.18. WARNING: Phosgene is a highly toxic gas and must be handled with great care, refer to MSDS before using. Compound **2.17** (390 mg, 1.6 mmol, 1.0 equiv.) was dissolved in THF (7 mL). The resulting solution was then added dropwise into a phosgene solution (15 wt% in toluene, 3.5 mL, 4.8 mmol, 3.0 equiv.) under an argon atmosphere at room temperature and was stirred for 40 h. The residual phosgene and solvent was then removed by high vacuum to yield compound **2.18** (482 mg 98%) as a brown solid. Phosgene collected in the liquid nitrogen-cooled trap was then quenched with methanol (10 mL) and saturated sodium hydroxide solution (10 mL). ^{1}H NMR (400 MHz, $CDCl_3$): δ 8.59 (d, *J* = 2.0 Hz, 1H), 8.17 (dd, *J* = 8.2 Hz, 2.0 Hz, 1H), 7.79 (d, *J* = 8.2 Hz, 1H), 6.36 (s, 1H), 5.81 (s, 2H), 4.31 (dd, *J* = 5.1 Hz, 2.3 Hz, 2H) 2.35 (t, *J* = 2.3 Hz, 1H). ^{13}C NMR (150 MHz, $CDCl_3$): δ 164.1, 150.6, 135.49, 133.4, 132.8, 132.3, 129.5, 124.1, 78.8, 72.8, 69.1, 30.4. MS calc'd for $[M]^+$ $C_{12}H_9O_5N_2Cl$, 296.0200; found, 296.0201.

2.4.5 Degradation Study

Study of PEtG 2.4 Degradation in Solution (general procedure for the study of polymer degradation). PEtG **2.4** (15 mg) was dissolved into a 9:1 mixture of CD_3CN:D_2O (1.2 mL) at ambient temperature (21 °C). The solution was then transferred into two NMR tubes and the tubes were promptly sealed. One tube was exposed to UV light (wavelength: 300-350 nm, 5.3 $mWcm^{-2}$) to initiate the removal of the photo-labile end-cap, and the absorbance at 340 nm was monitored by UV-vis spectroscopy to ensure the complete deprotection of the polymer (approximately 80 minutes). Another NMR tube was stored in a light-impermeable box over this time, and was prepared as a control for any background polymer degradation. Then, ^{1}H NMR spectra were recorded at defined intervals to monitor the depolymerization of the materials. At the same time, polymer **2.3** also underwent the

same irradiation and NMR study, serving as a non-triggerable control. This same protocol was also applied to study the degradation of polymers **2.11** – **2.15** and **2.21**.

Mass Loss and SEC Degradation Study of PEtG 2.4 Films. PEtG **2.4** (3.0 g) was dissolved in CH_2Cl_2 (15 mL) and drop-cast onto sixty individual glass slides to provide films. After the solvent was evaporated *in vacuo* for 48 h in a desiccator, the mass of each film was recorded. 30 films were placed into a UV box as described above for 17 h to remove the end-cap. During this time the remaining slides were stored in the dark. Next, all the slides were placed into a phosphate buffer solution (100 mM, pH = 7.4) at ambient temperature (21 ºC). At selected times, three plates from each treatment were removed from the buffer solution, rinsed, and dried under house vacuum for 48 h and then weighed. After each set of samples was weighed, 5.0 mg from one slide of each treatment was analyzed by SEC.

2.5 References

1. Marin, E.; Briceno, M. I.; Caballero-George, C. *Int. J. Nanomed.* **2012**, *8*, 3071.
2. Lenz, R. W.; Marchessault, R. H. *Biomacromolecules* **2005**, *6*, 1.
3. Liu, X.; Holzwarth, J. M.; Ma, P. X. *Macromol. Biosci.* **2012**, *12*, 911.
4. Bakhru, S. H.; Furtado, S.; Morello, A. P.; Mathiowitz, E. *Adv. Drug Delivery Rev.* **2013**, *65,* 811.
5. Mooney, B. P. *Biochem. J.* **2009**, *418*, 219.
6. Alessandro, G. *Macromolecules* **2008**, *41*, 9491.
7. Gohy, J.-F.; Zhao, Y. *Chem. Soc. Rev.* **2013**, *42*, 7117.
8. Prathamesh M. Kharkar; Kiick, K. L.; Kloxin, A. M. *Chem. Soc. Rev.* **2013**, *42*, 7335.
9. Huo, M.; Yuan, J.; Wei, Y. *Polym. Chem.* **2014**, *5*, 1519.
10. Wiggins, K. M.; Brantleya, J. N.; Bielawski, C. W. *Chem. Soc. Rev.* **2013**, *42*, 7130.
11. Wong, A. D.; DeWit, M. A.; Gillies, E. R. *Adv. Drug Delivery Rev.* **2012**, *64*, 1031.
12. Phillips, S. T.; DiLauro, A. M. *ACS Macro Lett.* **2014**, *3*, 298.

13. Peterson, G. I.; Larsen, M. B.; Boydston, A. J. *Macromolecules* **2012**, *45*, 7317.

14. McBride, R. A.; Gillies, E. R. *Macromolecules* **2013**, *46*, 5157.

15. Sagi, A.; Weinstain, R.; Karton, N.; Shabat, D. *J. Am. Chem. Soc.* **2008**, *130*, 5434.

16. DeWit, M. A.; Giliies, E. R. *J. Am. Chem. Soc.* **2009**, *131*, 18327.

17. Lewis, G. G.; Robbins, J. S.; Phillips, S. T. *Macromolecules* **2013**, *46*, 5177.

18. Robbins, J. S.; Schmid, K. M.; Phillips, S. T. *J. Org. Chem.* **2013**, *78*, 3159.

19. DeWit, M. A.; Beaton, A.; Gillies, E. R. *J. Polym. Sci. A: Polym. Chem.* **2010**, *48*, 3977.

20. DiLauro, A. M.; Robbins, J. S.; Phillips, S. T. *Macromolecules* **2013**, *46*, 2963.

21. DiLauro, A. M.; Zhang, H.; Baker, M. S.; Wong, F.; Sen, A.; Phillips, S. T. *Macromolecules* **2013**, *46*, 7257.

22. Kaitz, J. A.; Moore, J. S. *Macromolecules* **2013**, *46*, 608.

23 Kaitz, J. A.; Diesendruck, C. E.; Moore, J. S. *J. Am. Chem. Soc.* **2013**, *135*, 12755.

24. Olah, M. G.; Robbins, J. S.; Baker, M. S.; Phillips, S. T. *Macromolecules* **2013**, *46*, 5924.

25. Seo, W.; Phillips, S. T. *J. Am. Chem. Soc.* **2010**, *132*, 9234.

26. Zhang, H.; Yeung, K.; Robbins, J. S.; Pavlick, R. A.; Wu, M.; Liu, R.; Sen, A.; Phillips, S. T. *Angew. Chem. Int. Ed.* **2012**, *51*, 2400.

27. DiLauro, A. M.; Abbaspourrad, A.; Weitz, D. A.; Phillips, S. T. *Macromolecules* **2013**, *46*, 3309.

28. de Gracia Lux, C.; McFearin, C. L.; Joshi Barr, S.; Sankaranarayanan, J.; Fomina, N.; Almutairi, A. *ACS Macro Lett.* **2012**, *1*, 922.

29. Esser-Kahn, A. P.; Odom, S. A.; Sottos, N. R.; White, S. R.; Moore, J. S. *Macromolecules* **2011**, *44*, 5539.

30. Liu, G.; Wang, X.; Hu, J.; Zhang, G.; Liu, S. *J. Am. Chem. Soc.* **2014**, *136*, 7492.

31. Monks, T. J.; Jones, D. C. *Curr. Drug Metab.* **2002**, *3*, 425.

32. Anderson, S.; Umbright, C.; Sellamuthu, R.; Fluharty, K.; Kashon, M.; Franko, J.; Jackson, L.; Johnson, V.; Joseph, P. *Toxicol. Sci.* **2010**, *115*, 435.

33. Mattioda, G.; Christidis, Y. in *Ullmann's Encyclopedia of Industrial Chemistry*; Wiley-VCH Verlag GmbH & Co.: Weinheim, 2000.

34. Crutchfield M. M.; Papanu V. D.; Warren C. B. *United States Patent* **1979**, No. 4144226.

35. Brachais, C. H.; Duclos, R.; Vaugelade, C.; Huguet, J.; Capelle-Hue, M.-L.; Bunel, C. *Int. J. Pharm.* **1998**, *169*, 23.

36. Brachais, C. H.; Huguet, J.; Bunel, C.; Brachais, L. *Polymer* **1998**, *39*, 883.

37. Burel, F.; Rossignol, L.; Pontvianne, P.; Hartman, J.; Couesnon, N.; Bunel, C. *e-Polymers* **2003**, *3*, 407.

38. Brachais, C. H.; Huguet, J.; Bunel, C. *Polymer* **1997**, *38*, 4959.

39. Belloncle, B.; Burel, F.; Bunel, C. *Poylm. Preprints* **2007**, *48*, 633.

40. Belloncle, B.; Burel, F.; Oulyadi, H.; Bunel, C. *Polym. Deg. Stability* **2008**, *93*, 1151.

41. Belloncle, B.; Bunel, C.; Menu-Bouaouiche, L.; Lesouhaitier, O.; Burel, F. *J. Polym. Environ.* **2012**, *20*, 726.

42. Volhard, J. *Justus Lieb. Ann. Chem.* **2006**, *268*, 255.

43. Milas, N. A. *Org. Syn.* **1943**, *2*, 302.

44. Wolf, F. J.; Weijlard, J. *Org. Syn.* **1955**, *35*, 18.

45. Kelly, T. R.; Schmidt, T. E.; Haggerty, J. G. *Synthesis* **1972**, 544.

46. Hook, J. M. *Synth. Commun.* **1984**, *14*, 83.

47. Viski, P.; Szeverenyi, Z.; Simandi, L. I. *J. Org. Chem.* **1986**, *51*, 3213.

48. Fujii, T.; Ueno, H.; *Japanese Patent* **1997**, No. 09124553.

49. Qi, W.; Ghoroghchian, P. P.; Li, G.; Hammerd, D. A.; Therien, M. J. *Nanoscale* **2013**, *5*, 10908.

50. Gao, H.; Tang, Y.; Hu, Z.; Guan, Q.; Shi, X.; Zhua, F.; Wu, Q. *Polym. Chem.* **2013**, *4*, 1107.

51. Eisenfuhr, A.; Arora, P. S.; Sengle, G.; Takaoka, L. R.; Nowick, J. S.; Famulok, M. *Bioorg. Med. Chem.* **2003**, *11*, 235.

52. Nguyen, P. K.; Snyder, C. G.; Shields, J. D.; Smith, A. W.; Elbert, D. L. *Macromol. Chem. Phys.* **2013**, *214*, 948.

53. Pankaj Dawara; M. Bhagavan Rajub; Ramakrishna, R. A., *Tet. Lett.* **2011,** *52*, 4262.

54. Choi, T.-L.; Lee, C. W.; Chatterjee, A. K.; Grubbs, R. H., *J. Am. Chem. Soc.* **2001,** *123*, 10417.

55. Chan, T. M.; Jianshe, K.; McNamara, P.; Wong, J. K., *Synth. Commun.* **2008,** *38*, 2252.

56. Donohoe, T. J.; Fishlock, L. P.; Procopiou, P. A., *Org. Lett.* **2007,** *10*, 285.

57. Bishop, J. E.; OConnell, J. F.; Rapoport, H., *J. Org. Chem.* **1991,** *56*, 5079.

Chapter 3

3 Self-assembly of Poly(ethyl glyoxylate) Block Copolymers

3.1 Introduction

Amphiphilic block copolymers contain both hydrophobic and hydrophilic polymer blocks. In aqueous solution, they can undergo self-assembly in order to minimize the potential energy induced by interaction between the hydrophobic blocks and water molecules.[1] The self-assembly of amphiphilic block copolymers into functionl nano-aggregates, such as micelles[2] and vesicles[3], has garnered significant interest in recent years,[4-7] as these nano-aggregates can serve as a drug carriers and delivery systems[8-9] to solve the solubility problems of many current or potential drug candidates during blood circulation. In addition, with more sophisticated drugs emerging, particularly in the anti-cancer area,[10] targeted drug release,[11] which can improve the efficiency of drugs and decrease the impairment of drug to healthy tissues, are in demand.

Drug release from carriers can occur by simple diffusion of drugs out of the assembly.[12] It can also occur in response to stimuli. For example, the hydrophobic block of the copolymer can undergo a hydrophobic to hydrophilic transition that results in disruption of the aggregate[13-15] or cleavage of the hydrophobic block in response to a large excess of stimuli can occur.[16-17] However, there are problems with these approaches.[18] For example, the diffusion of drugs from assembly may take a long time, thereby decreasing the efficacy of drugs. In addition, the transition from hydrophobic to hydrophilic may not be complete and therefore may not result in the disintegration of the assembly. In addition, a large excess of stimuli is needed and is not readily achievable under real conditions. To address these limitations, over the past decade, a completely new class of triggerable and degradable polymers, termed self-immolative polymers

(SIPs) has emerged.[19-22] These polymers, which undergo head-to-tail depolymerization in response to stimuli, introduce a new possibility to solve current drug delivery challenges. Coupling of a hydrophobic self-immolative polymer with a hydrophilic polymer through a stimuli-responsive linker to form a self-immolative amphiphilic block copolymer, provides a new approach to self-assembled nanocarriers for drug delivery. In comparison with the approach involving a hydrophobic to hydrophilic transition, the complete breakage of the hydrophobic block should result in higher release efficiency. In comparison with the above-described approach involving backbone cleavage of the hydrophobic block, less stimuli will be needed. Therefore, the self-immolative amphiphilic block copolymer assembly holds great promise for the triggering of drug release in the presence of low concentrations of stimuli. However, at present only few examples of self-immolative polymers have been reported. In these examples, multiple synthesis steps were needed to obtain the required monomers, which makes the final polymers costly and only suited for small-scale applications.[19,22] Furthermore, the degradation intermediates such as quinone methides or azaquinone methides are potentially toxic,[23-24] which greatly limits their potential for medical applications.

In Chapter 2, a family of polyacetal based self-immolative polymers were described.[25] Among all of them, PEtG is especially interesting and attractive, because the final degradation products of this polymer are just ethanol and glyoxylic acid hydrate, both of which are expected to exhibit low toxicity.[26-27] The biological effects of ethanol are well known, and glyoxylic acid hydrate is a metabolic intermediate in the glyoxylic acid cycle that has been shown to be non-toxic in both plant and animal models.[28] In this chapter, the self-assembly of PEG-PEtG-PEG triblock copolymers is described. In addition, the release of nile red, a model drug from the resulting nano-carriers in response to UV light is studied to test the feasibility and practicability of our self-immolative micelles for drug delivery.

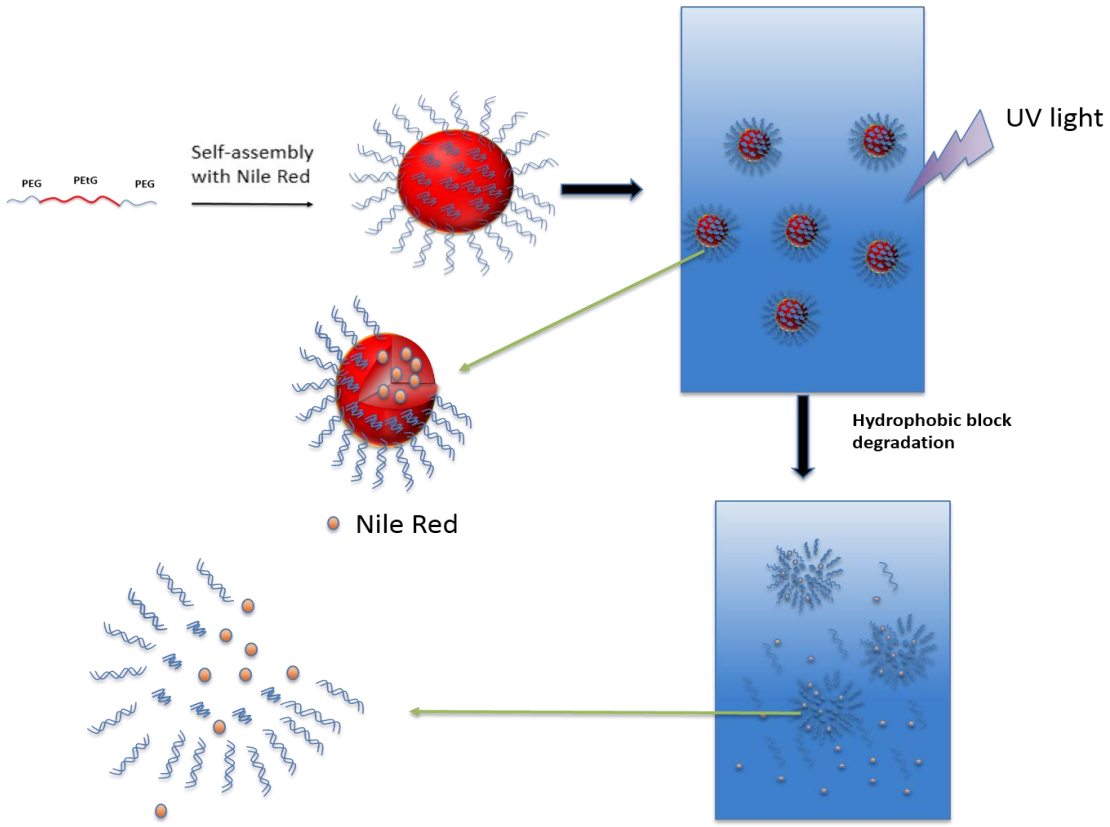

Scheme 3. 1 Self-assembly and disassembly of micelles formed from self-immolative block copolymers in response to UV light.

3.2 Results and Discussion

3.2.1 Assembly of PEG-PEtG-PEG Triblock Copolymers in Aqueous Solution

The synthesis of block copolymer PEG-PEtG-PEG **3.2** prepared using 2 kDa PEG was described in Chapter 2. PEG-PEtG-PEG **3.1** and PEG-PEtG-PEG **3.3** were synthesized from PEG 750 Da and 5 kDa respectively using the same methods. Using a standard nanoprecipitation procedure, the polymer was dissolved into DMSO and rapidly injected into stirring deionized water or buffer solution to obtain nano-aggregates. The DMSO

was then removed by dialysis against deionized water or buffer solution. The sizes and size distributions of the nano-aggregates were characterized by dynamic light scattering (DLS). The results are summarized in Table 3.1 and Figures 3.1-3.3. The Z-average diameters of the nano-aggregates were all below 100 nm for polymer **3.1**, **3.2** and **3.3**. The polydispersity indices (PDI) suggest that nano-aggregates from polymer **3.2** had quite a narrow distribution of sizes. In contrast, the PDIs for polymers **3.1** and **3.3** were relatively high, indicating a wider distribution of sizes.

Triblock copolymers	Micelles		
	z-average (nm)	Micelle PDI	Hydrophilic block mass fraction
PEG-PEtG (59 kDa)-PEG (750 Da) **3.1**	78	0.12	2.48 %
PEG-PEtG (42 kDa)-PEG (2 kDa) **3.2**	52	0.06	8.70 %
PEG-PEtG (48 kDa)-PEG (5 kDa) **3.3**	89	0.19	17.24 %

Table 3. 1 DLS characterization data for assemblies formed from PEG-PEtG-PEG block copolymers

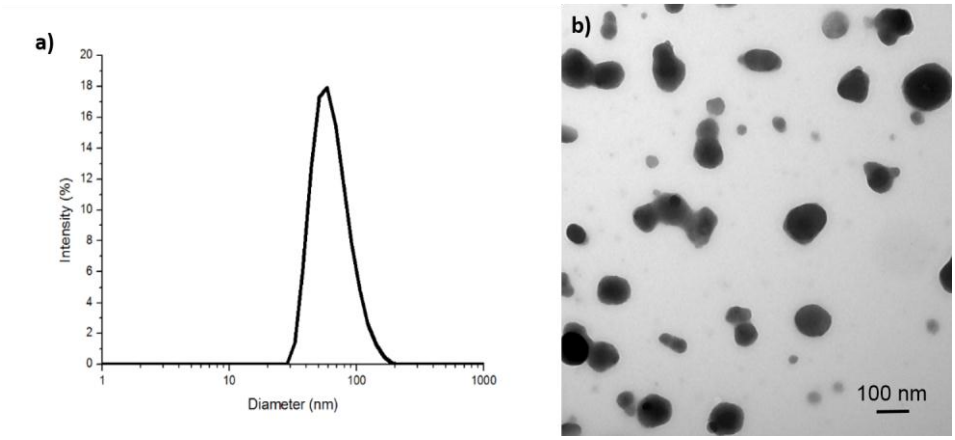

Figure 3. 1 a) DLS traces and b) TEM image for micelle formed from triblock polymer 3.1

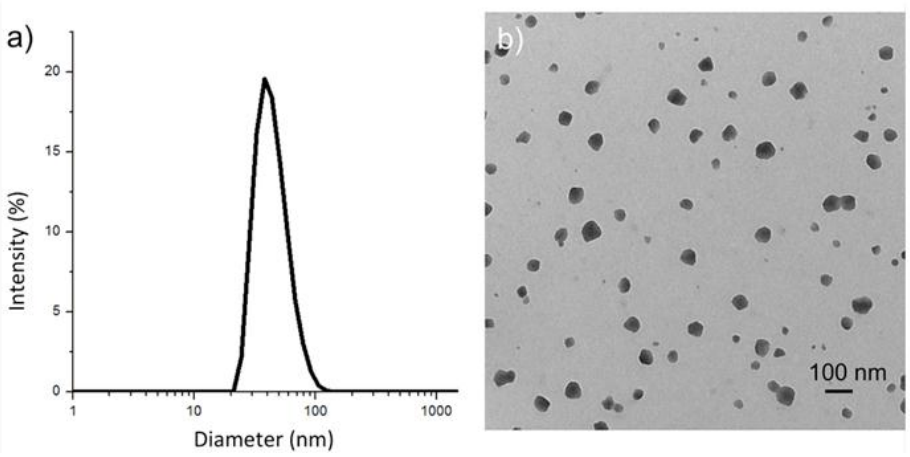

Figure 3. 2 a) DLS traces and b) TEM image for micelle formed from triblock polymer 3.2

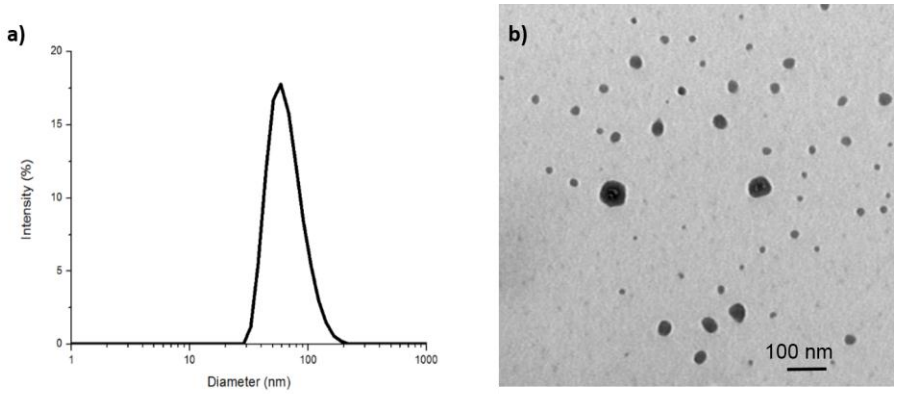

Figure 3. 3 a) DLS traces and b) TEM image for micelle formed from triblock polymer 3.3

Transmission electron microscopy (TEM) was also used to confirm the presence of the nano-aggregates and their morphologies. TEM images showed that all of the copolymers formed solid spherical aggregates, which suggests that they formed micelles or compound micelles. However, the diameters of the micelles shown from TEM were disperse, this is especially true for micelles obtained from polymer **3.1** and polymer **3.3**, which is in a general agreement with polydispersities from DLS. Because of the high polydispersity of these two samples, the z-average diameters from DLS did not precisely

reflect the real size of micelles, and TEM images should be more reliable and accurately reflect the real size of micelles. Given the low hydrophilic mass fractions of **3.1** and **3.2**, it was expected that they would form vesicles, and the formation of stable micellar structures was somewhat unexpected based on the guidelines of Discher and Eisenberg[3] which suggest that the vesicles will be formed if the hydrophilic fraction was less than 40%. However, in the case of the polyglyoxylates, the hydrophobic block is quite hydrophilic in comparison with conventional hydrophobic blocks such as polybutadiene or polystyrene.

3.2.2 Micelle Degradation Studied by DLS

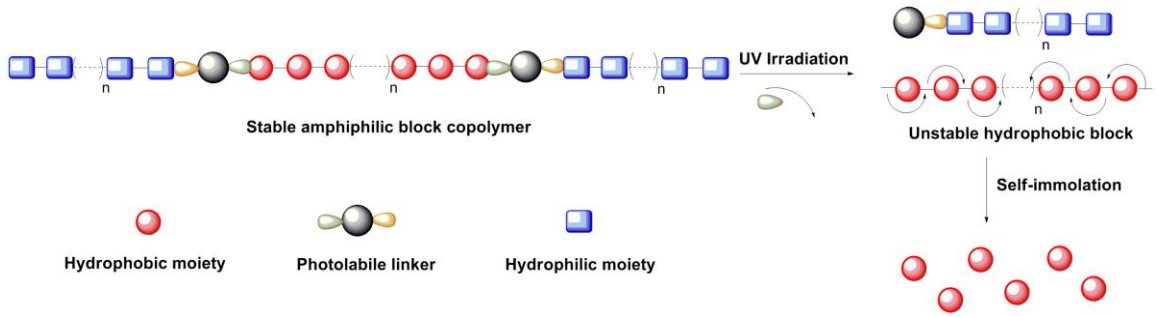

Scheme 3. 2 Cartoon illustrating the degradation mechanism of amphiphilic block copolymer PEG-PEtG-PEG

The linker molecule connecting the PEtG and PEG is photo-cleavable. Therefore, with UV irradiation, it is possible to separate the triblock polymer into its constituent blocks and initiate the depolymerization of the hydrophobic PEtG. This should lead to the disassembly of the micelles (Scheme 3.2). By DLS with a fixed detector attenuation, it was possible to monitor the disintegration of the micelles by the change in count rate (CR), as the count rate is proportional to the number of scattering species and their sizes. In this study, polymer **3.3** was chosen for micelle suspension preparation because a longer hydrophilic block can usually provide a stable micelle morphology[3]. The micelle suspensions were prepared in two different buffer solutions, one at pH 7.4, and another at

pH 5.0. After the initial micelle suspensions were measured by DLS, the samples were put into a UV box (23 mW/cm^2) and irradiated for 20 minutes. The irradiation time was previously determined by a series of control studies in which irradiation was performed for periods ranging from 5 minutes to 60 minutes. As shown in Figure 3.4, after UV irradiation, reductions of almost 90% and 50% in the count rate were observed at pH 7.4 and pH 5.0, respectively. These changes in count rates suggest a much faster degradation rate of PEtG in a fully aqueous system than what was described in Chapter 2 in the mixture of 9:1 acetonitrile:water. Moreover, the data suggest that the micelles disintegrated more rapidly in neutral conditions than in acidic conditions. This likely relates to the relative stabilities of the terminal hemiacetals on the polymers in these different conditions, after the linker molecule (end-cap) was removed. Depolymerization is not expected to occur via a cationic mechanism (Scheme 3.3a), which would be similar to simple backbone cleavage and which is not observed in part due to the electron-withdrawing effect of the adjacent ester. On the other hand, a mechanism involving an oxyanion is much more likely (Scheme 3.3b) and this would be expected to be faster at neutral or basic pH.

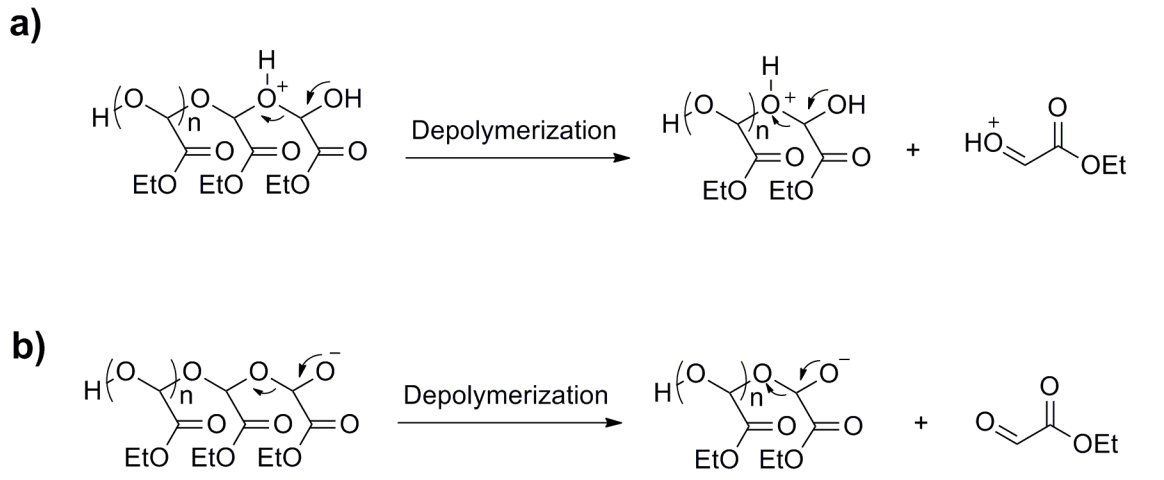

Scheme 3. 3 Degradation mechanism of unprotected PEtG in a) acid condition and b) basic condition.

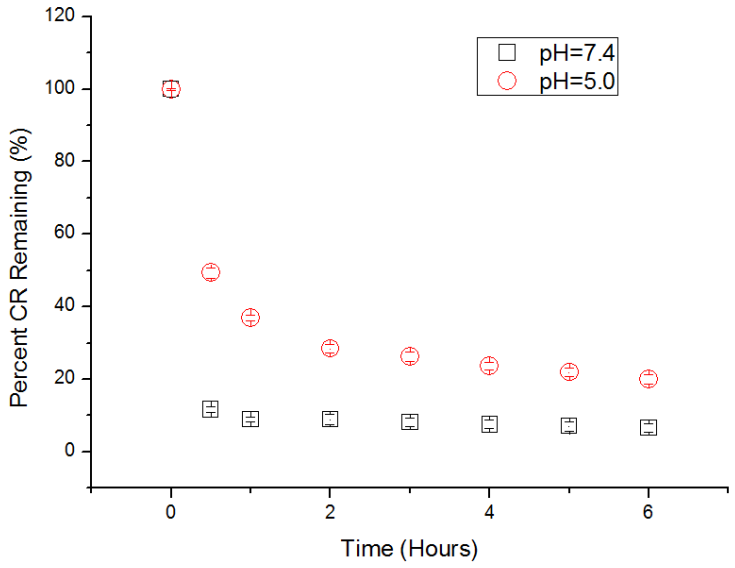

Figure 3. 4 DLS degradation study of micelles formed from polymer 3.3, error bars represent the standard error of mean on the measurement of 3 samples.

3.2.3 Micelle Degradation Studied by NMR Spectroscopy

The self-assembly and depolymerization were also studied by ^{1}H NMR spectroscopy. In this case, the assemblies were prepared by nanoprecipitation of a DMSO-d_6 solution of the polymer into pH 7.4 phosphate buffered D_2O (DMSO-d_6:D_2O = 1:5). For practical reasons, the DMSO-d_6 was not removed by dialysis. Consistent with the self-assembly of **3.2** into micelles under these conditions, only the peak corresponding to the PEG block, and no peaks corresponding to the PEtG block were observed in the NMR spectrum prior to UV irradiation (Figure 3.5). However, a ^{1}H NMR spectrum taken immediately following UV irradiation showed greater than 90% degradation of PEtG block (Figure 3.7), as measured by the appearance of peaks corresponding to EtGH. Subsequently, the resulting EtGH underwent ~45% hydrolysis to glyoxylic acid and ethanol over 24 h at 37 °C. These results confirm that the depolymerization following end-cap cleavage is much faster in these buffered aqueous conditions than in 9:1 CD_3CN:H_2O, and also that the nanoscale dispersion of PEtG into water through self-assembly of copolymer **3.2** results in

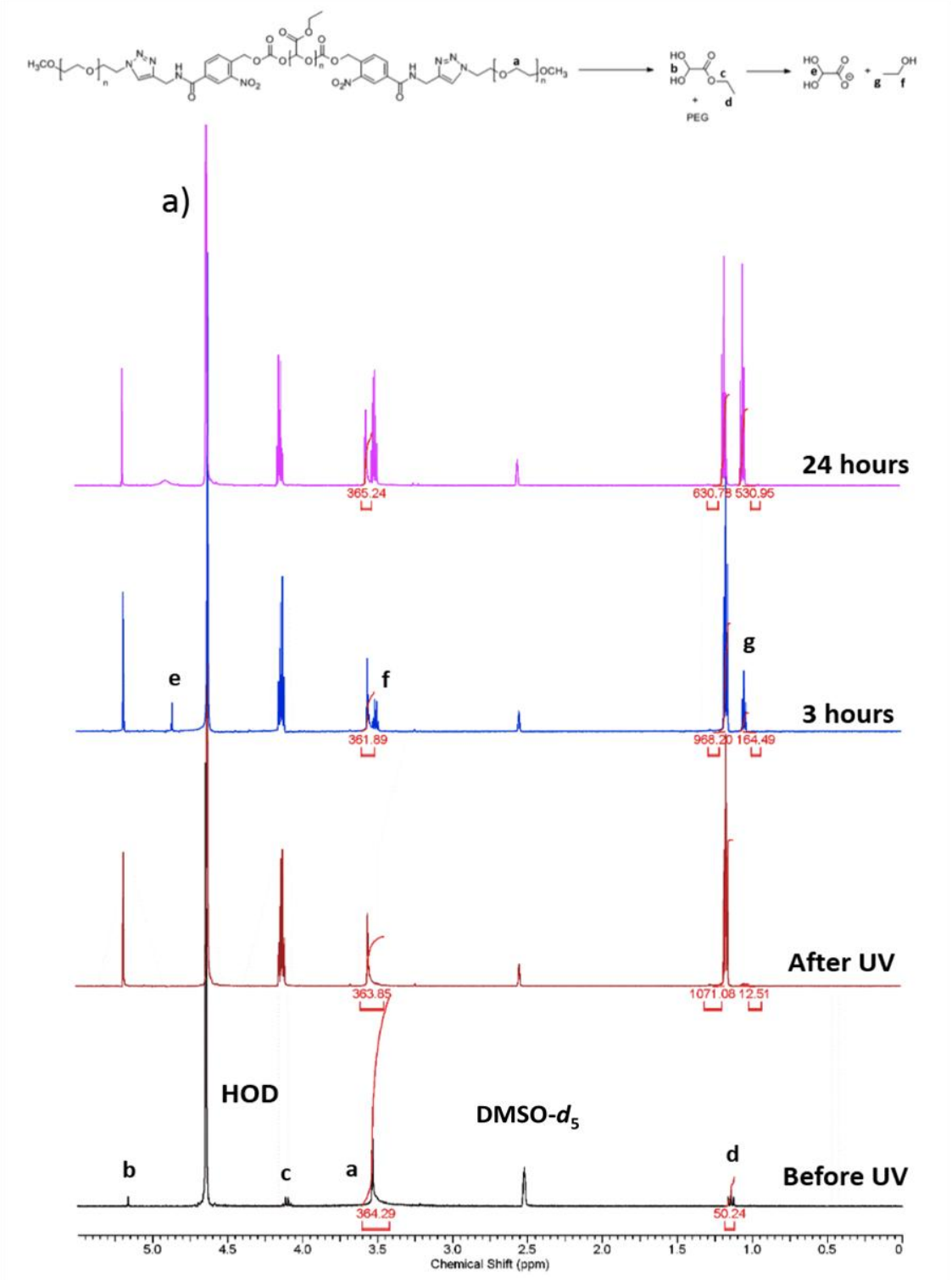

Figure 3. 5 Representative ^{1}H NMR spectra of micelles over time following UV irradiation and incubation in 5:1 pH 7.4 phosphate buffered D_2O:DMSO-d_6.

much more rapid depolymerization than in the films of pure PEtG described in Chapter 2. In contrast, a control sample of micelles that was not irradiated underwent less than 10% degradation over 24 h. (Figure 3.6 and 3.7)

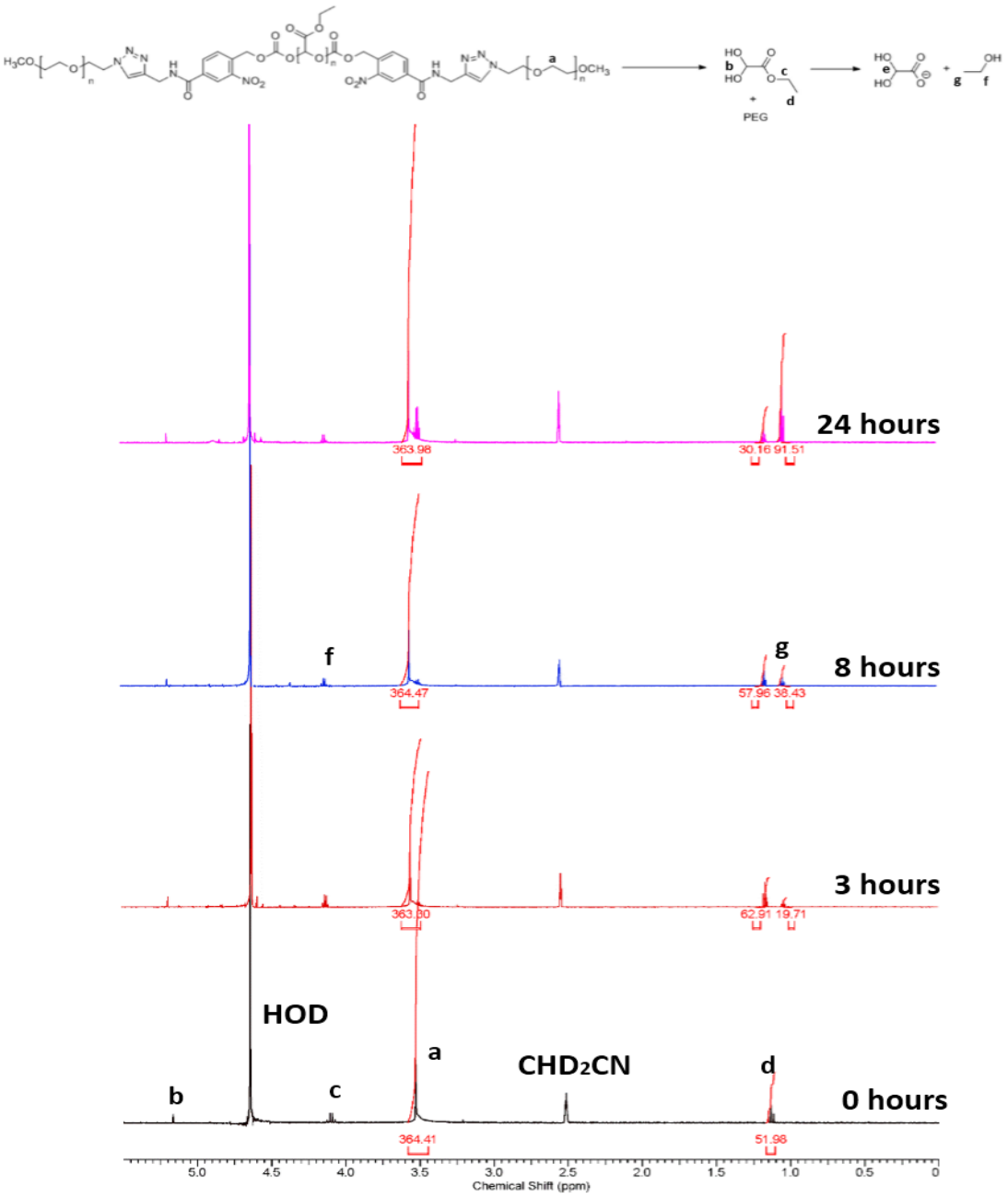

Figure 3. 6 Representative ^{1}H NMR spectra of micelles over time without UV irradiation but with incubation in 5:1 pH 7.4 phosphate buffered D_2O:DMSO-d_6.

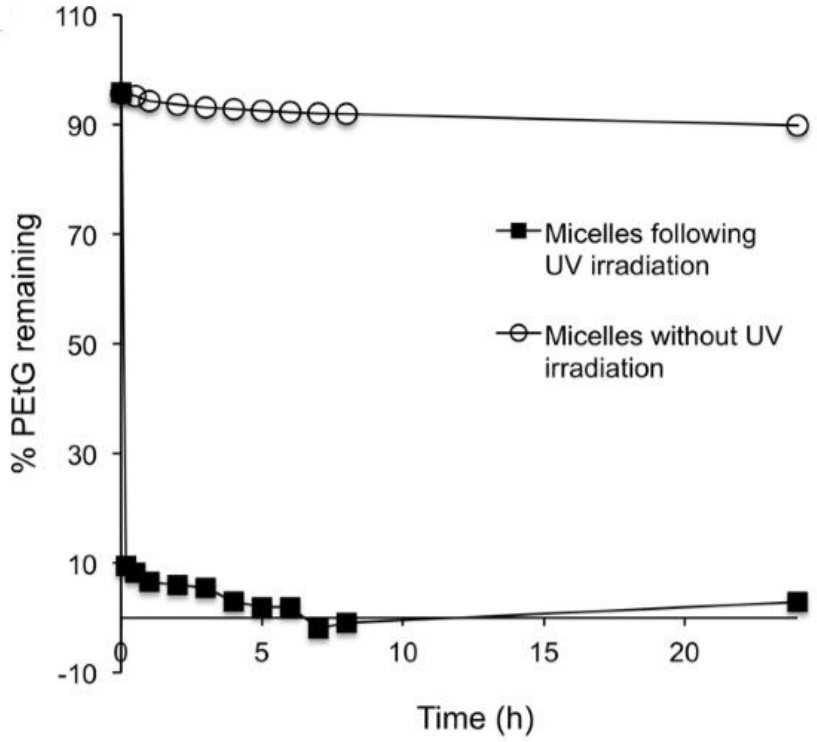

Figure 3. 7 Depolymerization of PEtG in micelles formed from polymer 3.2 following UV irradiation in 5:1 100 mM, pH 7.4 phosphate buffered D_2O:DMSO-d_6 at 37 °C and comparison with a control non-irradiated sample of the micelles

The NMR degradation study of the micelles was also extended to copolymer **3.3** at different pHs. At pH 7.4, the PEtG showed fast degradation with more than 90% of the polymer degraded by the first measurement (Figure 3.8, 5 min). However, in pH 5.0 buffer solution, only ~ 50% of PEtG had degraded by the first measurement. These results are consistent with the DLS studies, and also confirm that the disassembly of micelles observed by DLS were the result of the degradation of PEtG block upon end-cap cleavage by UV irradiation. In addition, TEM imaging showed there were almost nothing left after UV irradiation, again suggesting disassembly of the micelles.

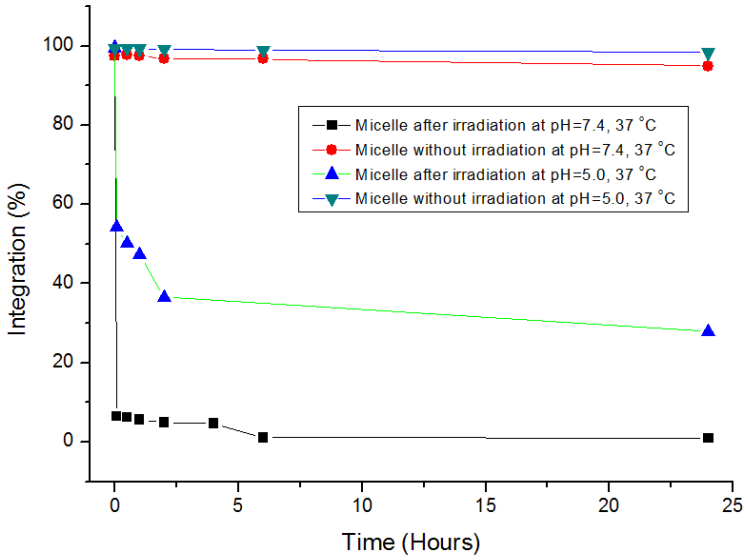

Figure 3. 8 Depolymerization of PEtG in micelles formed from polymer 3.3 following UV irradiation in 5:1 100 mM, pH 7.4 and pH 5.0 buffered D_2O:DMSO-d_6 at 37 °C and comparison with a control non-irradiated sample of the micelles

3.2.4 Model Drug Incorporation and Release Studies

In order to demonstrate the encapsulation and release abilities of the micelles, the hydrophobic dye nile red was used as a model drug. This molecule has strong fluorescence emission at 550 nm when it is dissolved into organic solvent or incorporated into a hydrophobic core of a micelle, but the emission is negligible in water due to aggregation and quenching.[29] This allows its release from the micelle core to be directly probed. In this experiment, both micelles formed from copolymer **3.2** and **3.3** were used. The micelle suspensions (in water) were irradiated for time periods ranging from 1 minute to 64 minutes, and then the fluorescence intensity was record immediately after each irradiation. As shown in Figures 3.9a, 3.9b and 3.9d, the intensity of nile red fluorescence in micelles both from **3.2** and **3.3** showed dramatic decreases for the first 16 minutes irradiation, but after about 30 minutes of irradiation, the intensity almost did not

decrease significantly further. This experiment provides an indication of the irradiation time (range from 16 minutes to 32 minutes) needed for complete disintegration of micelles containing the dye. In addition, nile red dissolved in ethanol served as a control. When subject to the same irradiation periods as the micelles, no detectable decrease in intensity was observed (Figure 3.9c and 3.9d). This confirms that the decreases in nile red fluorescence were indeed due to its release from the micelles rather than photodegradation of the dye.

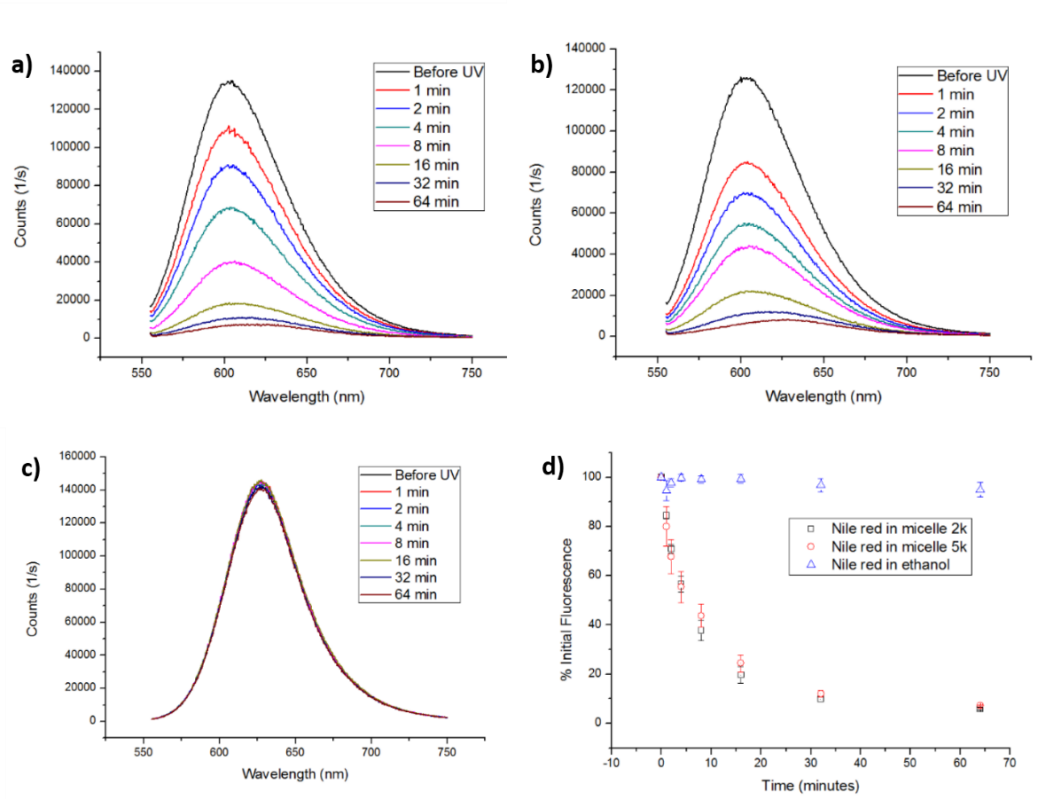

Figure 3. 9 Changes in fluorescence intensities of nile red with different irradiation times for (a) micelles formed from 3.2, (b) micelles formed from 3.3, (c) nile red in ethanol; (d) a plot of percent initial fluorescence versus irradiation time

The release study was then conducted in different buffer solutions at the 37 ^{o}C with micelles formed from **3.3**. As shown in Figures 3.10a and 3.10b, there was an almost 50% decrease in fluorescence intensity after 10 minutes of irradiation and more than 80%

decrease after 20 minutes of irradiation at pH 7.4. However, for the micelle suspension at pH 5.0 only a 20% intensity decrease was observed after 10 minutes and another 40% decrease was observed after 20 minutes irradiation. In addition, when the micelles were subsequently incubated over longer time periods, the fluorescence intensity continued to decrease at pH 5.0. In contrast, no further decrease was observed for the suspension at pH 7.4 suggesting that release was already complete at 20 min. Therefore, the micelles can undergo a rapid burst release of nile red at neutral conditions, whereas the release is more gradual at slightly acidic conditions. This result is consistent with the degradation of the micelles studied by DLS and NMR.

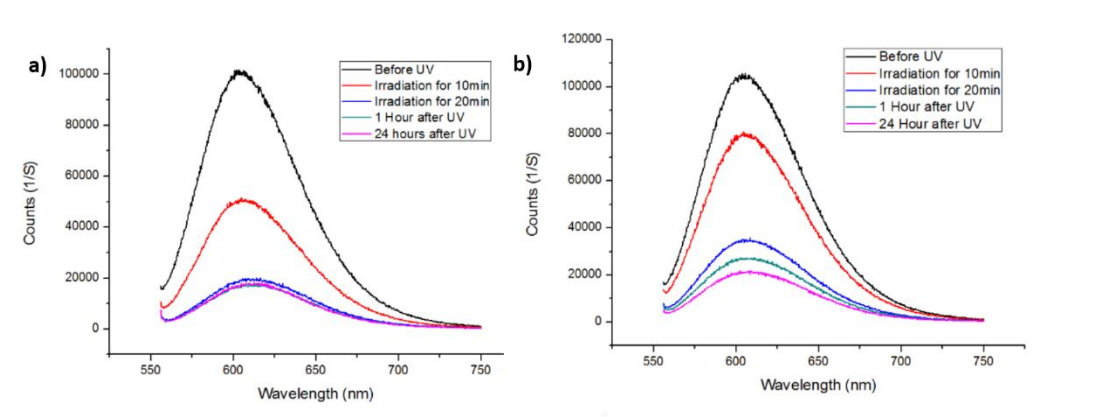

Figure 3. 10 Changes in fluorescence intensity of nile red with different irradiation times of micelles at a) pH 7.4 and b) pH 5.0, the sample was incubated at 37 ºC.

3.3 Conclusions

In conclusion, self-immolative block copolymers PEG-PEtG-PEG were successfully assembled into micelles with average diameters below 100 nm using a nanoprecipitation method. Because the micelles contained self-immolative polymer blocks and a UV-responsive trigger, their disassembly was achieved by UV irradiation due to the fast depolymerization of the hydrophobic PEtG. DLS and NMR degradation studies showed that the micelles in aqueous solvent had much faster disassembly rates than the

degradation of PEtG observed in 9:1 acetonitrile:water, owing to the more polar solvent system. In addition, the depolymerization and micelle disassembly was significantly faster at neutral than at mildly acidic pH. Finally, nile red was used as a model drug to demonstrate the excellent loading and release abilities of this new class of micelles.

3.4 Experimental

3.4.1 General Procedures and Materials

Nile red was purchased from Sigma-Aldrich and was used without further purification. Ultrapure water was obtained from a Barnstead EASYpure II system. Dialyses were performed using Spectra/Por regenerated cellulose membranes with 3500 g/mol MWCO. ^{1}H NMR spectra were obtained at 400 MHz. NMR chemical shifts are reported in ppm and were calibrated against the residual solvent signal of D_2O (δ 4.61). The sizes and size distributions of the micelles were measured by dynamic light scattering (Zetasizer Nano Series, Malvern Instruments, UK) at room temperature (25 ℃) in a 1 cm pathlength glass cuvette at a concentration of 0.8 mg/ml suspension of polymer assemblies. TEM imaging was performed using a Phillips CM10 microscope operating at an acceleration voltage of 80 kV. 3 μL of micelle suspension (0.08 mg / mL) was placed onto a copper grid. The resulting sample was air-dried for overnight before imaging.

3.4.2 Synthesis of Block Copolymers

The synthesis of polymer **3.2**, PEG-N_3, and PEtG end-capped by **2.18** were referred to Chapter 2.

Synthesis of Polymer 3.1. PEG-N_3 (750 Da, 56 mg, 75 μmol, 1.5 equiv.) and PEtG end-capped by **2.18** (59 kDa, 1.0 g, 25 μmol, 1 equiv.) were dissolved into DMF (5 mL). After removing the air and refilling with argon, $CuSO_4$ (4 mg, 25 μmol, 1 equiv.) and sodium ascorbate (5 mg, 25 μmol, 1 equiv.) were added into the solution, and the mixture was stirred at 40 ℃ for 16 hours. It was then transferred into a regenerated cellulose membrane (50 kDa MWCO) and dialyzed against deionized water for 48 hours (300 mL,

6 solvent changes). The dialyzed material was then lyophilized to afford polymer **3.1** (860 mg, 81%). ^{1}H NMR (400 MHz, $CDCl_3$): δ 5.47-5.75 (m, 473 H), 4.15-4.31 (m, 854H), 3.65 (s, 136H), 3.39 (s, 6H), 1.17-1.40 (m, 1269H). SEC: M_n = 68 kDa, M_w = 130 kDa, $Đ$ = 1.9.

Synthesis of Polymer 3.3. PEG-N_3 (5 kDa, 375 mg, 75 μmol, 1.5 equiv.) and PEtG end-capped by **2.18** (47 kDa, 0.5 g, 25 μmol, 1 equiv.) were dissolved in DMF (5 mL). After removing the air and refilling with argon, $CuSO_4$ (4 mg, 25 μmol, 1 equiv.) and sodium ascorbate (5 mg, 25 μmol, 1 equiv.) were added into the solution, and the mixture was stirred at 40 ℃ for 16 hours. It was then transferred into a regenerated cellulose membrane (50 kDa MWCO) and dialyzed against deionized water for 48 hours (300 mL, 6 solvent changes). The dialyzed material was then lyophilized to afford polymer **3.3** (580 mg, 77%). ^{1}H NMR (400 MHz, $CDCl_3$): δ 5.47-5.75 (m, 578H), 4.15-4.31 (m, 1023H), 3.65 (s, 909H), 3.39 (s, 6H), 1.17-1.40 (m, 1502H). SEC: M_n = 50 kDa, M_w = 95 kDa, $Đ$ = 1.9.

3.4.3 Representative Micelle Preparation

8 mg of block copolymer was fully dissolved into 1.0 mL of DMSO (stirring for overnight) to form a homogenous solution. Then, 0.1 ml of the resulting solution was injected quickly into 0.9 mL of rapidly stirring deionized water. After stirring for 0.5 hours, the micelle suspension was then transferred into a regenerated cellulose membrane (3 kg/mol MWCO) and dialyzed against deionized water for 12 hours (300 mL, 2 solvent changes) to remove DMSO, affording an aqueous suspension of micelles.

3.4.4 Representative DLS Study of Micelle Degradation

The micelles were formed by the procedure described above, except that the DMSO solutions were precipitated into either 100 mM pH 7.4 phosphate buffer solution or 100 Mm pH 5.0 citrate buffer solution and dialyzed against the same buffer. The formed

micelles were then transferred into quartz cuvette and the CR was measured by DLS while fixing the attenuator at 7. The samples were then irradiated for 20 min in the UV box (wavelength: 300-350 nm, 23 mW cm^{-2}), the samples were incubated at 37 ^{o}C and the CR was measured at selected time points.

3.4.5 NMR Degradation Study of the Micelles

16 mg of block copolymer **3.2** was fully dissolved in 0.8 mL of DMSO-d_6. 0.2 mL of the resulting solution was rapidly injected into 1.0 mL of 100 mM, pH 7.4 phosphate or 100 mM, pH 5.0 citrate buffered D_2O. After stirring for 0.5 h, the micelle suspension was transferred into two NMR tubes. One tube was then irradiated for 10 min in with UV light (wavelength: 300-350 nm, 23 mWcm^{-2}), while the other one was kept in the dark. A ^{1}H NMR spectrum was obtained immediately following irradiation (10 min time point in the graph), then the samples were incubated at 37 ^{o}C and spectra were obtained at regular intervals over 24 h. Complete depolymerization was confirmed for the irradiated sample as the sum of the integration of the methyl peaks corresponding to EtGH and ethanol (1.0-1.2 ppm) plateaud at a very similar (1198) value to that of the methyl peak at 1.17-1.45 ppm in the block copolymer **3.2** taken in $CDCl_3$ (integration 1152) when setting the PEG peak integral to 364. The % polymer remaining was calculated as 100 - (sum of integration from 1.0-1.2 ppm/1198))*100.

3.4.6 Representative Procedure for the Study of Nile Red Release

8 mg of block copolymer and 0.16 mg (2 wt% relative to polymer) of nile red were fully dissolved into 1 mL DMSO to form a homogenous solution. Then, 0.1 mL of the resulting solution was injected quickly into 0.9 mL of stirring deionized water or different buffer solutions. After stirring for 2 minutes, the micelle suspension was then transferred into a regenerated cellulose membrane (3500 g/mol MWCO) and dialyzed against deionized water or different buffer solutions for 12 hours (300ml, 2 solvent changes) to remove DMSO. After the initial fluorescence emission of the micelle suspension was measured, the micelle suspension was put into a UV box and irradiated for different times

(wavelength: 300-350 nm, 23 $mWcm^{-2}$). The fluorescence emission was measured after the different irradiation times. In the case of Figure 3.11, the maximum irradiation time was 20 minutes, but the sample was incubated at 37 ^{o}C following the 20 minutes irradiation time and the fluorescence spectra were obtained at 1 hour and 24 hours.

3.5 References

1. Mai, Y.; Eisenberg, A., *Chem. Soc. Rev.* **2012**, *41*, 5969.
2. Zhang, L. F.; Eisenberg, A. *Science* **1995**, *268*, 1728.
3. Discher, D. E.; Eisenberg, A. *Science* **2002**, *297*, 967.
4. McIntosh, J. T.; Nazemi, A.; Bonduelle, C. V.; Lecommandoux, S.; Gillies, E. R., *Can. J. Chem.* **2015,** *93*, 1.
5. Chen, H.; Lu, Y.; Shen, L.; Liu, X.; Zhang, G., *Polymer* **2008,** *49*, 2095.
6. Gohr, K.; Pakula, T.; Tsutsumi, K.; Schärtl, W., *Macromolecules* **1999,** *32*, 7156.
7. Kim, J.-K.; Garripelli, V. K.; Jeong, U.-H.; Park, J.-S.; Repka, M. A.; Jo, S., *Int. J. Pharm.* **2010,** *401*, 79.
8. Ding, J.; Chen, L.; Xiao, C.; Chen, L.; Zhuang, X.; Chen, X., *Chem. Commun.* **2014,** *50*, 11274.
9. Huang, Y.; Dong, R.; Zhu, X.; Yan, D., *Soft Matter.* **2014,** *10*, 6121.
10. Pignatti, F.; Ehmann, F.; Hemmings, R.; Jonsson, B.; Nuebling, M.; Papaluca-Amati, M.; Posch, M.; Rasi, G., *Clin. Cancer Res.* **2014,** *20*, 1458.
11. Min, K. H.; Kim, J. H.; Bae, S. M.; Shin, H.; Kim, M. S.; Park, S.; Lee, H.; Park, R. W.; Kim, I. S.; Lee, D. S., *J. Control. Release* **2010,** *144*, 259.
12. Lavasanifar, A.; Samuel, J.; Kwon, G. S., *Adv. Drug Delivery Rev.* **2002,** *54*, 169-190.
13. Fomina, N.; Sankaranarayanan, J.; Almutairi, A., *Adv. Drug Delivery Rev.* **2012,** *64*, 1005.
14. Zhao, Y., *Macromolecules* **2012,** *45*, 3647.
15. Zhao, H.; Sterner, E. S.; Coughlin, E. B.; Theato, P., *Macromolecules* **2012,** *45*, 1723.

16. Johnson, J. A.; Lu, Y. Y.; Burts, A. O.; Lim, Y. H.; Finn, M. G.; Koberstein, J. T.; Turro, N. J.; Tirrell, D. A.; Grubbs, R. H., *J. Am. Chem. Soc.* **2011,** *133*, 559.
17. Trenor, S. R.; Shultz, A. R.; Love, B. J.; Long, T. E., *Chem. Rev.* **2004,** *104*, 3059.
18. Liu, G.; Liu, W.; Dong, C.-M., *Polym. Chem.* **2013,** *4*, 3431.
19. Sagi, A.; Weinstain, R.; Karton, N.; Shabat, D., *J. Am. Chem. Soc.* **2008,** *130*, 5434.
20. Liu, G.; Wang, X.; Hu, J.; Zhang, G.; Liu, S., *J. Am. Chem. Soc.* **2014,** *136*, 7492.
21. DeWit, M. A.; Gillies, E. R., *J. Am. Chem. Soc.* **2009,** *131*, 18327.
22. Dewit, M. A.; Beaton, A.; Gillies, E. R., *J. Polym. Sci. Pol. Chem.* **2010,** *48*, 3977.
23. Anderson, S.; Umbright, C.; Sellamuthu, R.; Fluharty, K.; Kashon, M.; Franko, J.; Jackson, L.; Johnson, V.; Joseph, P., *Toxicol Sci.* **2010,** *115* (2), 435.
24. Monks, T. J.; Jones, D. C. *Curr. Drug Metab.* **2002**, *3*, 425.
25. Fan, B.; Trant, J. F.; Wong, A. D.; Gillies, E. R., *J. Am. Chem. Soc.* **2014,** *136*, 10116.
26. B. Belloncle; F. Burel; H. Oulyadi; Bunel, C., **2008,** *93* (9), 1151.
27. Belloncle, B.; Bunel, C.; Menu-Bouaouiche, L.; Lesouhaitier, O.; Burel, F., *J Polym Environ* **2012,** *20* (3), 726.
28. Belloncle, B.; Bunel, C.; Menu-Bouaouiche, L.; Lesouhaitier, O.; Burel, F. *J. Polym. Environ.* **2012**, *20*, 726.
29. Maiti, N. C.; Krishna, M. M. G.; Britto, P. J.; Periasamy, N., *J. Phys. Chem. B* **1997,** *101*, 11051-11060.

Chapter 4

4 Development of Self-immolative Poly(ethyl glyoxylate)s responsive to Different Stimuli

4.1 Introduction

The development of biodegradable polymers is a research area of increasing interest in the past decades.[1-2] For example, degradable polymers can work as environmentally friendly substituents for commodity plastics to solve the urgent environmental concerns with white pollution.[3] In addition, biodegradable polymers can also have other advanced applications in medicine, such as sutures, implants and drug delivery systems.[4] At present, the most common biodegradable polymers are based on polyesters such as poly(lactic acid), poly(glycolic acid), polycarprolactone.[5-9] These materials are attractive as they are broken down to nontoxic products. However, the degradation of these polymers cannot easily be controlled. Once they are made, the random degradation begins and continues at varying rates in different environments. This may be undesirable if the material degrades while it is still performing its function.

To address this problem, in 2008, Shabat and co-workers first introduced the concept of self-immolative linear polymers (SIPs).[10] As shown in Scheme 4.1, SIPs constitute a class of degradable polymers that is stable in the presence of end-caps, but once the end-caps are removed, the polymer can degrade in the time scale from seconds to days depending on the backbone structure and its environment.[11-12] This class of polymers can be designed to respond to different external stimuli such as light,[13] fluoride ions,[14] redox change,[15] enzymes,[16] and even mechanical force,[17] just by changing the end-caps, therefore endowing them with much wider applications, such as molecular sensors,[10] micropumps,[18] responsive drug delivery systems,[19] and microcapsules for self-damage healing.[20]

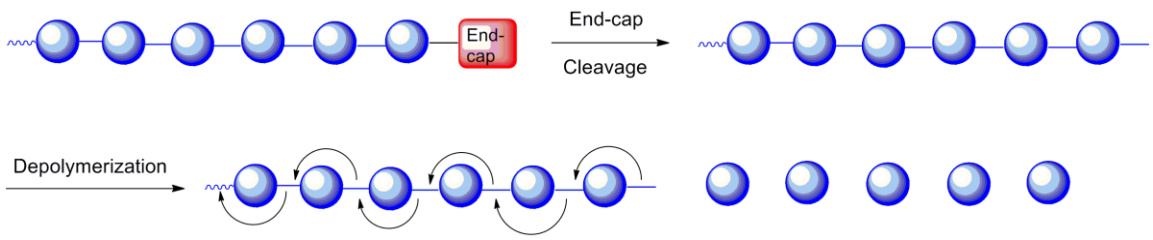

Scheme 4. 1 Degradation mechanism of self-immolative polymer

In chapter 2, through the incorporation of UV light-sensitive end-cap, we successfully demonstrated that polyglyoxylates could serve as a versatile class of SIPs that can be easily synthesized from petroleum sources or the agricultural byproducts, and more interestingly, they degrade into metabolic intermediates.[21] Furthermore, using a UV light-sensitive linker molecule, PEtG-based amphiphilic triblock polymers were developed and in the Chapter 3, we described the self-assembly of these copolymers into functional nanoscale micelles for drug delivery. With UV irradiation, the micelles could immediately break down and release loaded molecules. However, it is well known that UV light can lead to permanent damage to human tissue,[22] therefore, the model study cannot directly be applied to practical applications. In order to solve this problem and further explore the possible applications of polyglyoxylate-based SIPs, in this chapter, we describe the development of a series of other stimuli-responsive end-caps for polyglyoxylates. These end-caps expand the sensitivity of polyglyoxyates to stimuli including hydrogen peroxide[26] and reducing agents such as dithiothreitol (DTT)[15] and hydrazine.

4.2 Results and Discussion

4.2.1 Synthesis and Characterization of PEtG with Different Stimuli-responsive End-caps

In previous work, we found that PEtG obtained from anionic polymerization can be properly end-capped by reaction with chloroformates. Therefore, we sought different

stimuli-sensitive end-caps that could be converted into chloroformates. For example, as shown in the Scheme 4.2, the hydroxyl groups in compounds **4.1** to **4.3** were easily converted into chloroformates by reaction with phosgene with above 90 % yield. The phenylboronic acid pinacol ester in chloroformate **4.4** can readily react with hydrogen peroxide to provide a phenol, which can then initiate a 1,6-elimination to form a quinone methide, followed by the release of carbon dioxide. Therefore, this molecule is extremely sensitive to hydrogen peroxide, and it was proposed that this process could initiate depolymerization (Scheme 4.3a). In chloroformate **4.5**, the disulfide linkage is sensitive to reducing conditions. With one equivalent of reductive agent, such as DTT, the disulfide linkage can be easily reduced and then the resulting thiol was proposed to undergo cyclization to release the hemiacetal terminated polymer (Scheme 4.3b). Chloroformate **4.6** is an azo-compound, which was recently explored as a reductive sensitive end-cap by our group.[27] It can be reduced by reaction with either hydrazine or DTT to provide a secondary amine, which can lead to 1,6-elimination, followed by loss of CO_2 to initiate depolymerization (Scheme 4.3c).

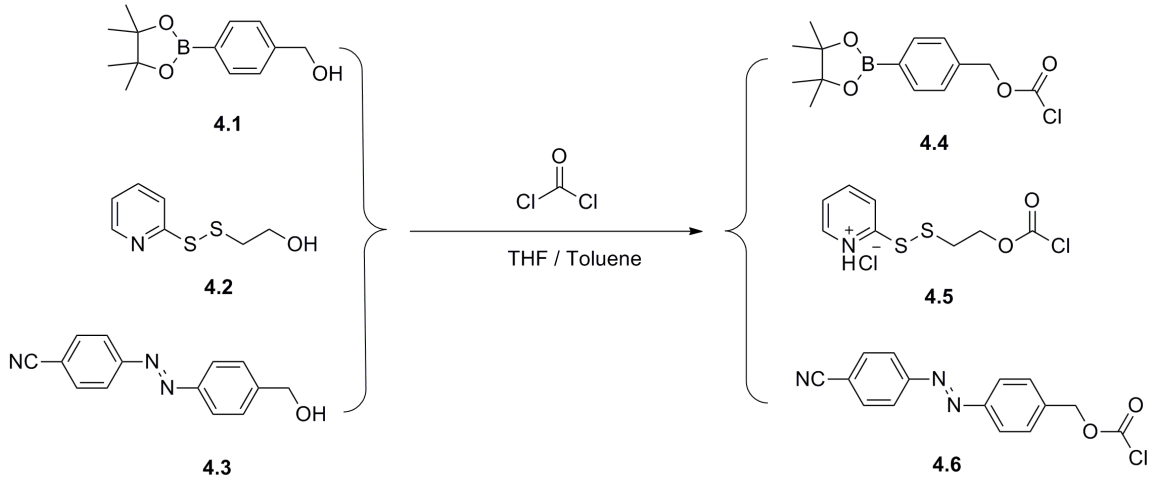

Scheme 4. 2 Synthesis of chloroformate based end-caps.

With all of these chloroformate end-caps in hand, polymerization of ethyl glyoxylate was conducted via anionic polymerization at -20 ^{o}C, then the polymer was end-capped *in situ* by reaction with chloroformates **4.4**, **4.5**, and **4.6**, to afford polymers **4.7**, **4.8** and **4.9**

that are sensitive to hydrogene peroxide, DTT and hydrazine (Scheme 4.4) respectively. The M_ns of these polymers were all above 100 kg/mol from SEC results in THF relative to polystyrene (PS) standards. There are two possible reasons for the significantly increased molecular weights of the polymers here relative to those reported in Chapter 2. One possibility is the minor technical improvements in the monomer distillation and polymerization, which have reduced contamination with water and ethyl glyoxylate hydrate, thereby increasing the monomer:initiator ratio. Another possible explanation is highly reactive properties of these chloroformates that serve as excellent end-capping agents to quickly react with polymer terminal groups and stop undesired depolymerization during the end-capping reaction.

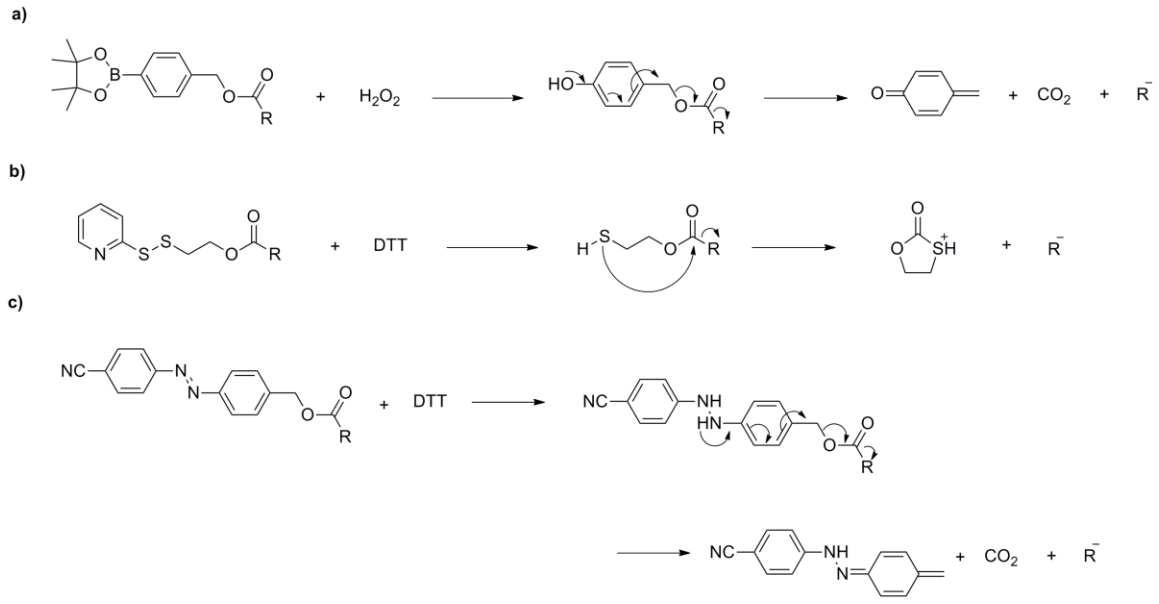

Scheme 4. 3 Triggering mechanism of different end-caps

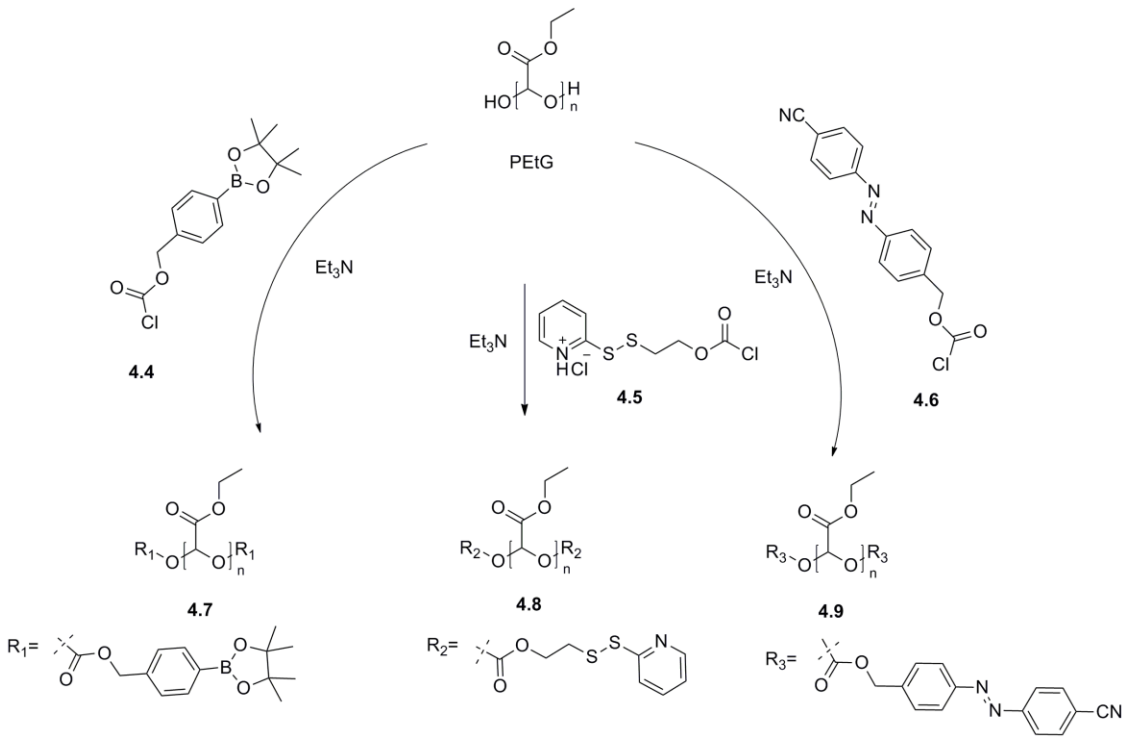

Scheme 4. 4 Synthesis of poly(ethyl glyoxylates) with different end-caps.

Polymer	M_n(SEC) (kDa)	M_w(SEC) (kDa)	Dispersity ($Đ$)	$T_{98\%}$ (ºC)	T_g (ºC)
4.7	131	305	2.3	193	-1
4.8	250	425	1.7	151	-7
4.9	246	461	1.9	108	-7

Table 4. 1 Molecular weights, measured by SEC in THF, relative to PS standards for the polymers. Thermal properties of polyglyoxylates measured by TGA and DSC. T_{98} = maximum temperature at which 98% of mass is still present, T_g is the glass transition temperature.

As shown from the TGA results (Table 4.1 and Figure 4.1), polymer **4.9** had a much lower T_{98} compared to **4.7 and 4.8**, and there were two stages on the TGA curve for polymer **4.9**. This suggests that polymer **4.9** may not have been completely end-capped.

One possibility is that polymers **4.9** had a much longer chain length compared to our previously reported examples (Chapters 2 and 3). This may make end-capping more difficult. In addition, with higher molecular weight the polymer can precipitate in methanol more rapidly, so there is less chance to selectively remove unend-capped polymers during this purification procedure. However, the TGA results indicate that there was at least 70% of polymer **4.9** properly end-capped, which was sufficient for preliminary depolymerization studies. Although polymer **4.8** had a relatively lower T_{98} compared to polymer **4.7** and previous samples in Chapter 2, no two-phase degradation was observed, so the polymer was deemed to be well end-capped. The lower T_{98} may result from the limited stability of the disulfide linkage in the end-cap above 150 °C.

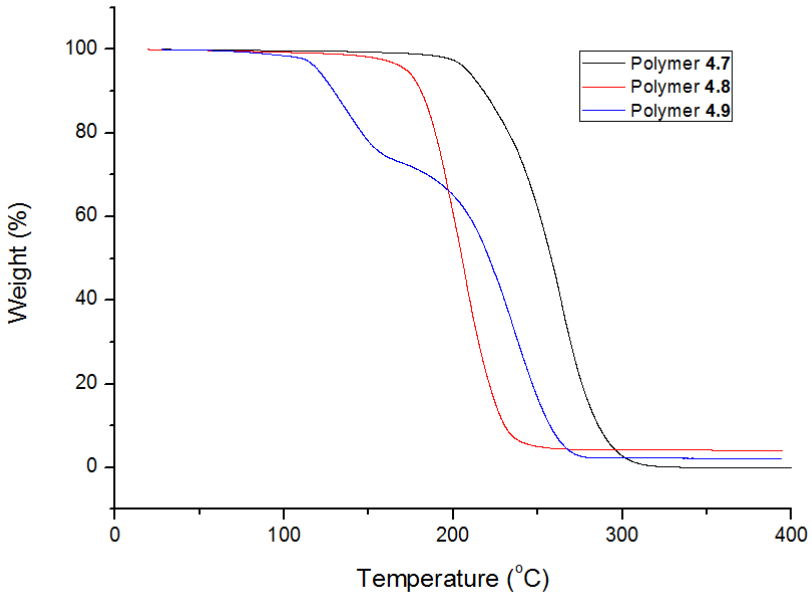

Figure 4. 1 TGA results for PEtGs with different end-caps

4.2.2 Degradation Study of PEtG by NMR Spectroscopy

Despite the possibly incomplete end-capping of polymer **4.9**, the degradation of these polymers was studied in the presence and absence of the stimuli. The triggered

degradation of PEtG **4.7** in response to H_2O_2 was studied in solution first. Using the same procedure described in Chapter 2, PEtG **4.7** was dissolved in 9:1 CD_3CN:D_2O at 15 mg/mL, a concentration sufficient for NMR studies. A comparison of the NMR spectra with and without addition of H_2O_2 (132 mM) supports the successful cleavage of the end-cap by H_2O_2 (Figure 4.2). Before addition of H_2O_2, the spectrum consisted of three broad peaks attributable to the PEtG backbone. Unfortunately, because of the extremely high molecular weight of this batch of polymer, the end-caps could not be detected from the NMR spectroscopy. However, following the addition of H_2O_2, the broad peak at 5.5 ppm corresponding to the acetal hydrogens along the polymer backbone decreased in intensity while two new sharp peaks at 5.3 ppm and 5.1 ppm emerged. The sharp peak at 5.1 ppm can be assigned to the degradation product EtGH as observed in Chapter 2. The new peak at 5.3 ppm can likely be attributed to a reaction product of ethyl glyoxylate with H_2O_2 due to the increased nucleophilicity of H_2O_2 compared to water. However, to conclusively identify this product further studies must be performed. At the same time, sharpening of the peaks corresponding to the ethyl group were also consistent with depolymerization to small molecules. Based on the relative peak integrations, about 70% (Figure 4.4) of the PEtG had depolymerized into small molecules just after the addition of H_2O_2. In contrast, as shown in Figure 4.2b and Figure 4.4, PEtG **4.7** without the addition of H_2O_2 only showed less than 3% degradation after 3 days in solution. In addition, PEtG **2.3** with the benzyl carbonate end-cap remained unchanged with same amount of H_2O_2 after 7 days in solution. Combined, these data confirm that the depolymerization of PEtG **4.7** indeed resulted from backbone depolymerization induced by end-cap cleavage and not by random backbone cleavage induced by H_2O_2 or hydrolytic reactions. As for the polymers described in Chapter 2, the percent depolymerization plateaued at ~81% after 6 hours, which is believed to result from the presence of an equilibrium concentration of oligomers under these mainly-organic solvent conditions.

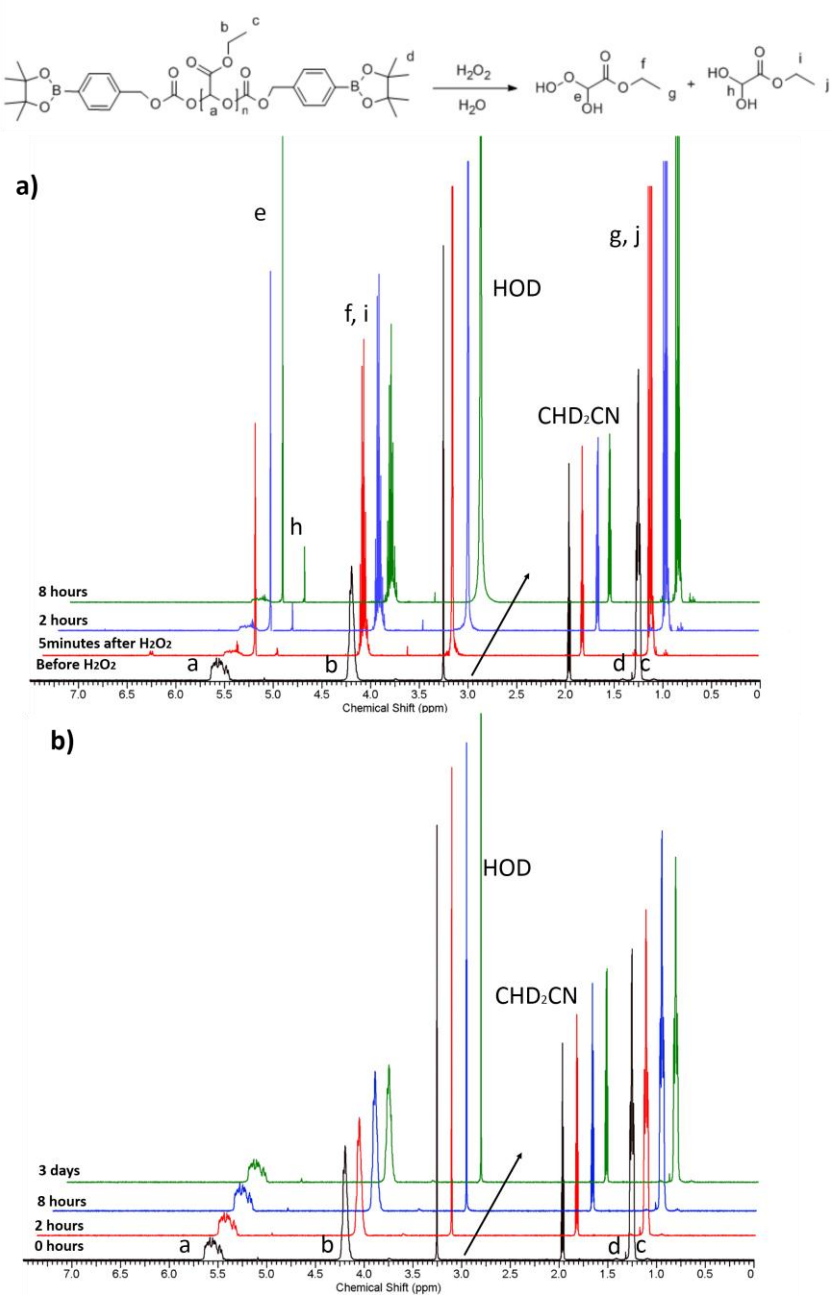

Figure 4. 2 ^{1}H NMR spectra of polymer 4.7 dissolved in 9:1 CD_3CN:D_2O (a) with and (b) without addition of H_2O_2. Spectra are offset to allow the progression over time to be clearly observed.

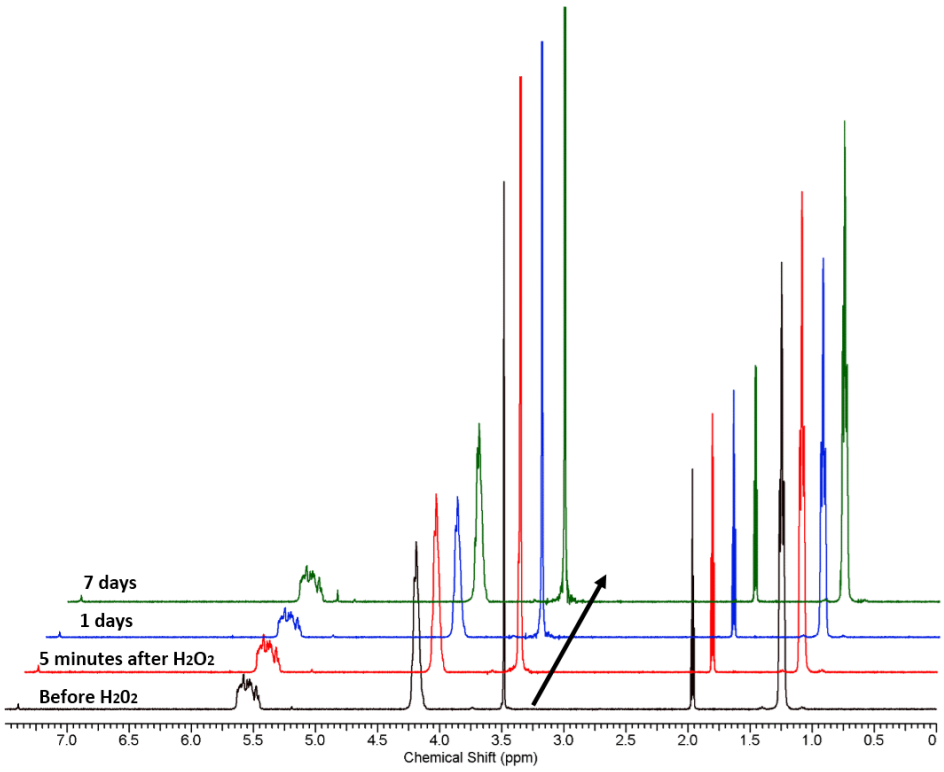

Figure 4. 3 ^{1}H NMR spectra of polymer 2.3 dissolved in 9:1 CD_3CN:D_2O with addition of H_2O_2. No changes were observed, indicating that the polymer is stable under these conditions and H_2O_2 does not cleave the polymer backbone.

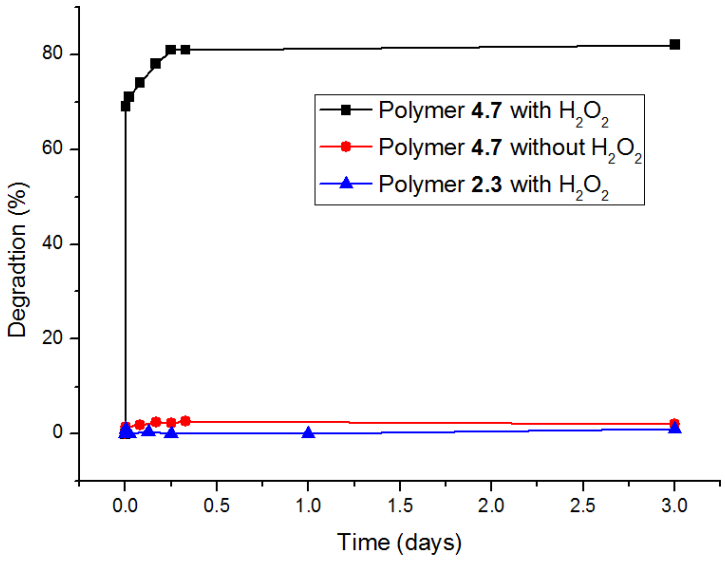

Figure 4. 4 Percent degradation of polymer 4.7 with control groups.

The same NMR degradation study was conducted with polymer **4.8** as well. In this case, because the polymer was functionalized with a reduction-responsive end-cap, dithiothreitol (DTT), which is a common reducing agent to reduce the disulfide bonds of proteins, was chosen as the trigger for depolymerization. However, because DTT is also a very strong nucleophile, it can react very rapidly with depolymerized monomers compared to water molecules. Therefore, in order to ensure that there was enough DTT to break down the end-caps, 880 equivalents (110 mM) of DTT was added into the NMR tubes. As shown in Figures 4.5a and 4.7, 50% of the polymer degraded immediately after addition of DTT, and after 1 hour 97% polymer was degraded. In contrast, the control sample of polymer **4.8** without DTT underwent only ~5% degradation after 3 days (Figure 4.5b). The benzyl chlorformate end-capped control polymer **2.3** (Figure 4.6 and Figure 4.7), underwent only about 4% and 5% degradation after 4 hours and 1 day, respectively, even with same amount of DTT. Combined, these data suggest that the polymer was at least 95% end-capped, and that addition of the reducing agent DTT selectively triggered rapid depolymerization.

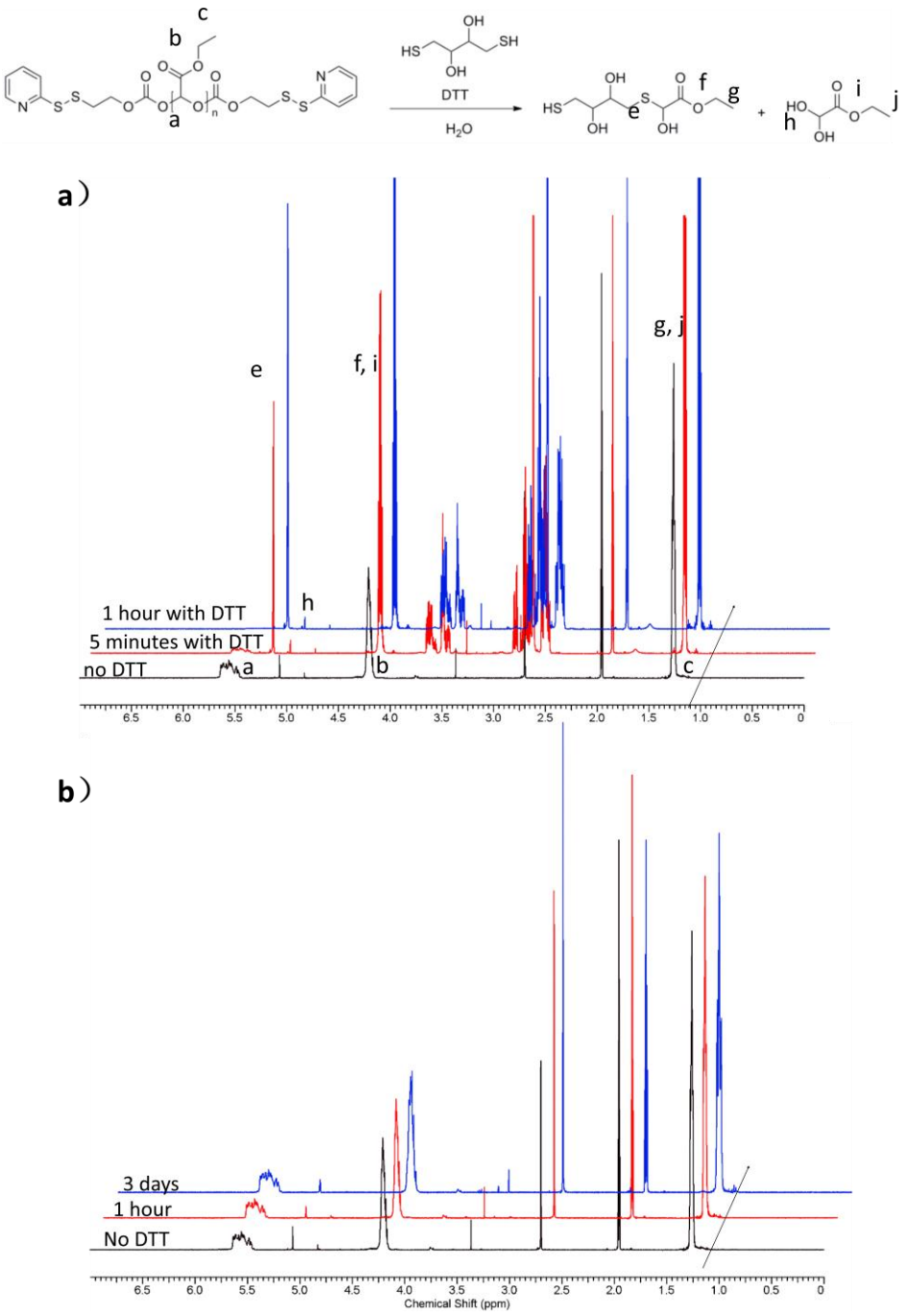

Figure 4. 5 ^{1}H NMR spectrum of polymer 4.8 dissolved in 9:1 CD_3CN:D_2O with and without addition of DTT. Spectra are offset to allow the progression over time to be clearly observed.

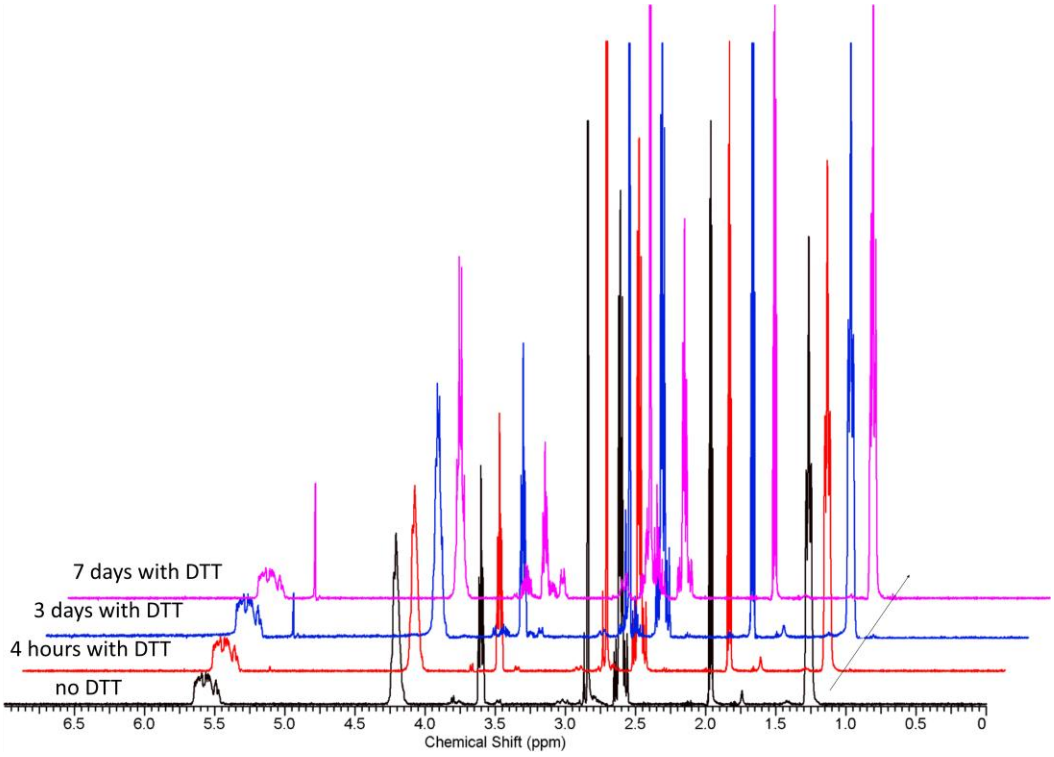

Figure 4. 6 ^{1}H NMR spectrum of polymer 2.3 dissolved in 9:1 CD_3CN:D_2O with addition of DTT.

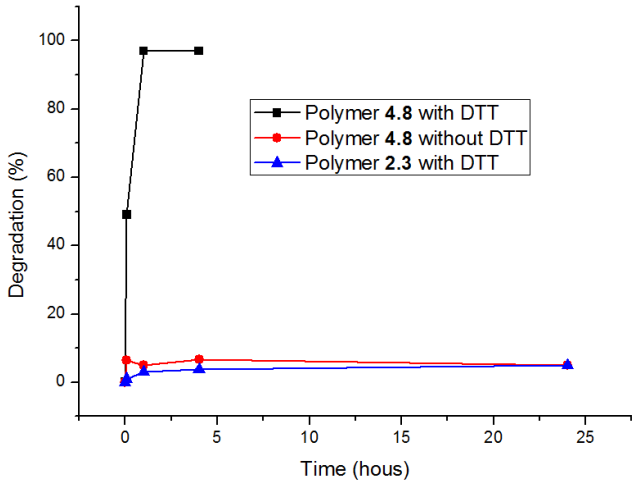

Figure 4. 7 Percent degradation of polymer 4.8 with control groups.

Lastly, the degradation profile of polymer **4.9** was investigated. This end-cap should be easily cleaved by hydrazine, making polymer **4.9** sensitive to hydrazine. When hydrazine (100 mM) was added into polymer **4.9** solution, the polymer did degrade immediately. Unfortunately, the control polymer **2.3** that was end-capped by benzyl choroformate degraded as well, suggesting that hydrazine can generally cleave carbonates under these conditions and therefore the trigger was not very specific. As demonstrated by our group[28], the azo-compound can also be reduced by DTT, albeit with slower rate. Therefore, polymer **4.9** was also subjected to DTT as the trigger for depolymerization. As shown from Figures 4.8a and Figure 4.9, approximately 50% of the polymer degraded after 1 day with addition of DTT (110 mM). This rate is much slower compared to polymer **4.8**, which underwent 97% degradation in just 1 hour. The degradation finally plateaued at the fourth day with 75% depolymerization, likely because of the consumption or background oxidation of DTT. As shown from Figures 4.8b and Figure 4.9, approximately 20% of polymer **4.9** depolymerized in the absence of DTT, consistent with the incomplete end-capping observed by TGA. In addition, at the concentrations of DTT employed in this study, about 14% of control polymer **2.3** depolymerized over the time period of this experiment (Figure 4.6 and 4.9). It can still be concluded that polymer **4.9** undergoes depolymerization in response to reducing agents. Further work will be required to optimize the end-capping efficiency as well as to increase the sensitivity of the azobenzene to DTT, thereby enhancing the reduction rate. However, the slower response to DTT in the case of this polymer relative to polymer **4.8** might be useful for some applications.

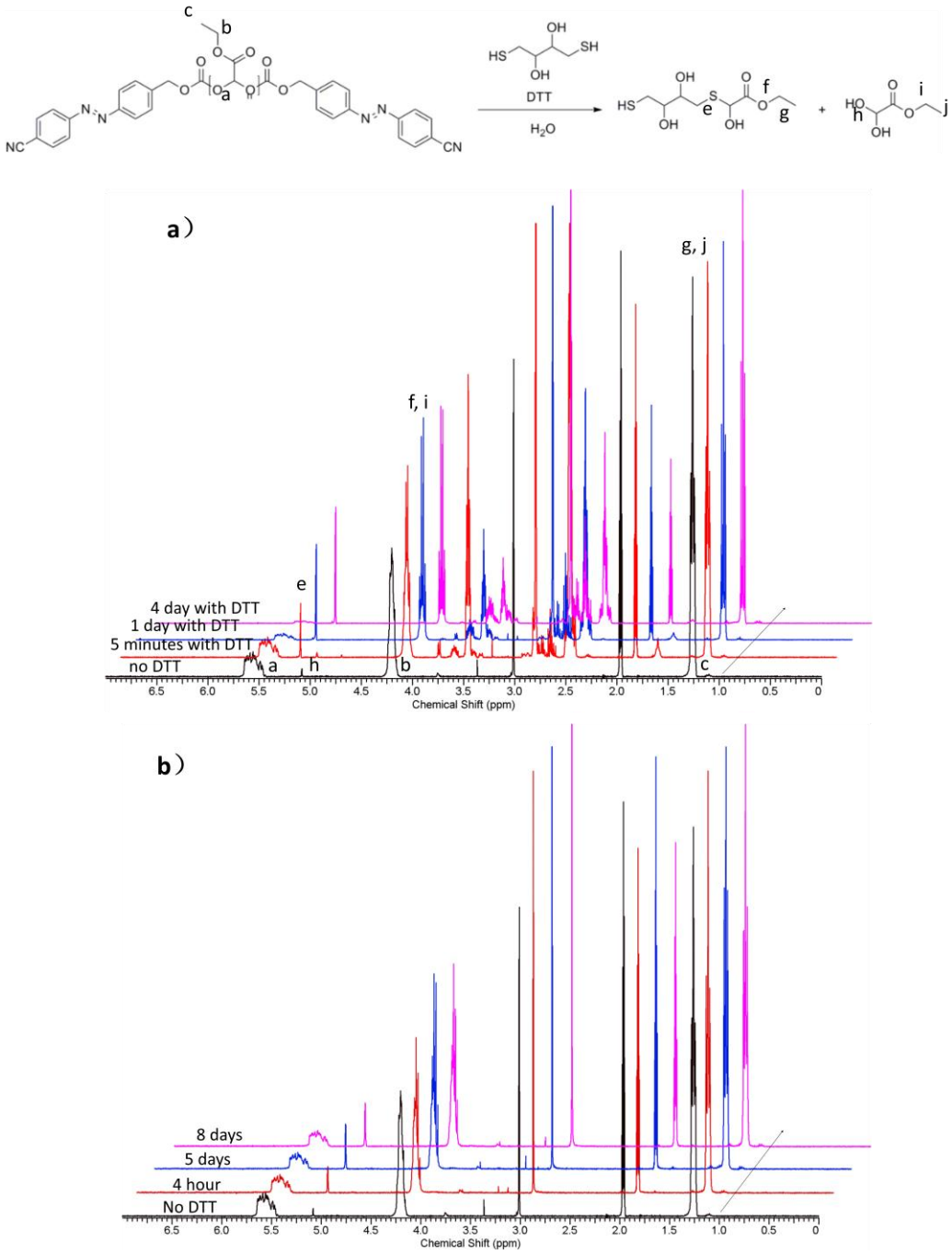

Figure 4. 8 ^{1}H NMR spectrum of polymer 4.8 dissolved in 9:1 CD_3CN:D_2O with and without addition of DTT. Spectra are offset to allow the progression over time to be clearly observed.

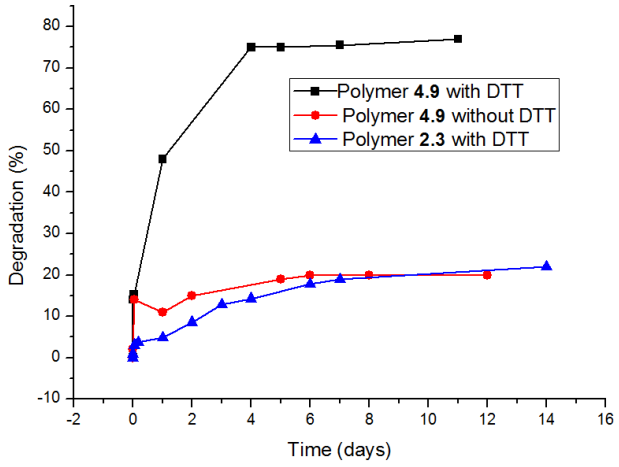

Figure 4. 9 Percent degradation of polymer 4.9 with control groups

4.3 Conclusions

In conclusion, three different stimuli-sensitive molecules with hydroxyl groups were converted into chlorofromates by reaction with phosgene in high yield. These end-caps were installed at the termini of PEtG to afford polymers that were responsive to hydrogen peroxide, and reducing conditions. As demonstrated by ^{1}H NMR spectroscopy, these polymers underwent depolymerization to small molecules in response to signals in their environment. Moreover, by comparing the degradation rates of polymers end-capped by molecules with disulfide linkages versus azobenzenes, we found another way to tune the rate of polymer degradation by installing of different end-caps.

4.4 Experimental

4.4.1 General Procedures and Materials

Ethyl glyoxylate in toluene solution (50% w/w) was obtained from Alfa Aesar (Canada). 4-(Hydroxymethyl)phenylboronic acid pinacol ester and hydrogen peroxide solution (50 wt%) in water, hydrazine hydrate, and phosgene solution (15 wt. % in toluene) were

purchased from Sigma-Aldrich (USA). Triethylamine, pyridine, and dichloromethane were distilled from calcium hydride before use. Anhydrous tetrahydrofuran was obtained from a solvent purification system using aluminum oxide columns. All the other chemicals were of reagent grade and used without further purification. ^{1}H NMR spectra were obtained in $CDCl_3$ at 400 MHz or 600 MHz on Varian Inova instruments. NMR chemical shifts (δ) are reported in ppm and are calibrated against residual solvent signals of $CDCl_3$ (δ 7.27), CD_3CN (δ 1.94), (δ 2.50) or D_2O (δ 4.75). FT-IR were obtained using a Bruker tensor 27 instrument with films drop cast from CH_2Cl_2 on KBr plates. High-resolution mass spectrometry (HRMS) was performed using a Finnigan MAT 8400 electron impact (EI) mass spectrometer. The SEC instrument was equipped with a Viscotek GPC Max VE2001 solvent module. Samples were analyzed using the Viscotek VE3580 RI detector operating at 30 ˚C. The separation technique employed two Agilent Polypore (300x7.5mm) columns connected in series and to a Polypore guard column (50x7.5mm). Samples were dissolved in THF (glass distilled grade) in approximately 5mg/mL concentrations and filtered through 0.22 μm syringe filters. Samples were injected using a 100 μL loop. The THF eluent was filtered and eluted at 1ml/min for a total of 30 minutes. A calibration curve was obtained from Polystyrene samples with molecular weight ranges of 1,540-1,126,000/mol. DSC and TGA were performed on a Mettler Toledo DSC 822e. For TGA the heating rate was 10 ℃/min between 50-400 ℃ under nitrogen. For DSC, the heating/cooling rate was 10 ℃/min from -100 to +100 ℃. Glass transition temperatures were obtained from the second heating cycle.

Synthesis of Chloroformate 4.4.WARNING: Phosgene is a highly toxic gas and must be handled with great care. Refer to the MSDS before using. 4-(Hydroxymethyl)phenylboronic acid pinacol ester, compound **4.1** (800 mg, 3.4 mmol, 1.0 equiv.) was dissolved in THF (7 mL). The resulting solution was then added dropwise into a phosgene solution (15 wt% in toluene, 7.5 mL, 10.3 mmol, 3.0 equiv.) under an argon atmosphere at room temperature and was stirred for 24 h. The residual phosgene and solvent were then removed by high vacuum to yield chloroformate **4.4** (920 mg, 91%) as a pale brown liquid. Phosgene collected in the liquid nitrogen-cooled trap was then

quenched with methanol (20 mL) and saturated sodium hydroxide solution (20 mL). ^{1}H NMR (400 MHz, $CDCl_3$): δ 7.86 (d, *J* = 8.2 Hz, 2H), 7.39 (d, *J* = 8.2 Hz, 2H), 5.32 (s, 2H), 1.36 (s, 12H). Spectral data are consistent with published values.[23]

Synthesis of Chloroformate 4.5. Compound **4.2**[24] (500 mg, 2.7 mmol, 1.0 equiv.) was dissolved in THF (10 mL). The resulting solution was then added dropwise into a phosgene solution (15 wt% in toluene, 5.8 mL, 8.1 mmol, 3.0 equiv.) under an argon atmosphere at room temperature and was stirred for 24 h. The residual phosgene and solvent were then removed by high vacuum to yield chloroformate **4.5** (750 mg, 98%) as a pale brown liquid. Phosgene collected in the liquid nitrogen-cooled trap was then quenched with methanol (20 mL) and saturated sodium hydroxide solution (20 mL). ^{1}H NMR (400 MHz, $CDCl_3$): δ 8.81 (s, 1H), 8.26 (t, *J* = 7.0 Hz, 1H), 8.17 (d, *J* = 8.2 Hz, 1H) 7.69 (t, *J* = 7.0 Hz, 1H), 4.61 (t, *J* = 5.9 Hz, 2H), 3.34 (t, *J* = 5.9 Hz, 2H). ^{13}C NMR (150 MHz, $CDCl_3$): δ 156.9, 150.5, 145.2, 142.9, 125.0, 123.9, 68.8, 37.8. MS calc'd. for $[M]^+$ $C_8H_8ClNO_2S_2$: 248.9685; found: 248.9689.

Synthesis of Chloroformate 4.6. Compound **4.3**[25] (200 mg, 0.84 mmol, 1.0 equiv.) was dissolved in THF (8 mL). The resulting solution was then added dropwise into a phosgene solution (15 wt% in toluene, 1.8 mL, 2.5 mmol, 3.0 equiv.) under an argon atmosphere at room temperature and was stirred for 24 h. The residual phosgene and solvent were then removed by high vacuum to yield chloroformate **4.5** (230 mg, 91%) as a pale brown liquid. Phosgene collected in the liquid nitrogen-cooled trap was then quenched with methanol (20 mL) and saturated sodium hydroxide solution (20 mL). ^{1}H NMR (400 MHz, $CDCl_3$): δ 8.02 (d, *J* = 8.2 Hz, 1H), 8.00 (d, *J* = 8.8 Hz, 1H), 7.85 (d, *J* = 8.8 Hz, 1H), 7.59 (d, *J* = 8.2 Hz, 1H), 5.40 (s, 2H).

Synthesis of Polymer 4.7. EtG in toluene solution (20 mL) was fractionally distilled under vacuum (55 ºC, 125 mbar) over P_2O_5 to remove toluene and trace water in the first, discarded fraction. The residue was then distilled twice successively over P_2O_5 at atmospheric pressure under argon at 130 ºC to obtain the highly pure monomer. Purified ethyl glyoxylate (5.0 mL, 50 mmol, 1.0 equiv.) was dissolved in CH_2Cl_2 (5.0 mL) and

Et_3N (3.5 μL, 25 μmol, 0.0005 equiv.). The solution was stirred for 1 h at -20 °C. Chloroformate **4.4** (0.22 g, 730 μmol, 0.014 equiv.) and Et_3N (100 μL, 730 μmol, 0.014 equiv.) were added at 0 °C to end-cap the polymer. The solution was stirred for 24 h at room temperature and a further 16 h at 40 °C. Purification was achieved by precipitation of the crude reaction mixture into methanol. After decanting the excess methanol, the residue was dried in vacuo for 48 h to provide 3.3 g of a white, sticky polymer in 63% yield. ^{1}H NMR (400 MHz, $CDCl_3$): δ 7.80 (d, *J* = 8.6 Hz, 2H), 7.53 (d, *J* = 8.6 Hz, 2H), 5.46-5.78 (m, 675H), 4.10-4.33 (m, 1367H), 1.34 (s, 12H), 1.21-1.44 (m, 2000H). ^{13}C NMR (150 MHz, $CDCl_3$): δ 164.6-166.5, 90.0-93.9, 61.7, 13.5. FT-IR (KBr, thin film): 2986, 2943, 2908, 1759, 1469, 1446, 1377, 1302, 858, 735, 702 cm^{-1}. SEC: M_n = 131 kg/mol, M_w = 304 kg/mol, Đ = 2.3. T_g = -1 °C.

Synthesis of Polymer 4.8. Purified ethyl glyoxylate (2.5 mL, 25 mmol, 1.0 equiv.) was dissolved in CH_2Cl_2 (2.5 mL) and Et_3N (1.8 μL, 13 μmol, 0.0005 equiv.). The solution was stirred for 1 h at -20 °C. Chloroformate **4.5** (0.11 g, 365 μmol, 0.014 equiv.) and Et_3N (100 μL, 730 μmol, 0.028 equiv.) were added at 0 °C to end-cap the polymer. The solution was stirred for 24 h at room temperature and a further 16 h at 40 °C. Purification was achieved by precipitation of the crude reaction mixture into methanol. After decanting the excess methanol, the residue was dried in vacuo for 48 h to provide 1.5 g of a white, sticky polymer in 60% yield. ^{1}H NMR (400 MHz, $CDCl_3$): δ 5.48-5.75 (m, 2500H), 4.12-4.33 (m, 5150H), 1.34 (s, 12H), 1.20-1.37 (m, 7645H). ^{13}C NMR (150 MHz, $CDCl_3$): δ 165.4-166.1, 91.0-94.43, 62.4, 14.2. FT-IR (KBr, thin film): 2986, 2939, 2367, 1765, 1468, 1385, 1302, 1229, 1146, 1020, 966, 8568cm^{-1}. SEC: M_n = 250 kg/mol, M_w = 425 kg/mol, Đ = 1.7. T_g = -7 °C.

Synthesis of Polymer 4.9. Purified ethyl glyoxylate (2.5 mL, 25 mmol, 1.0 equiv.) was dissolved in CH_2Cl_2 (2.5 mL) and Et_3N (1.8 μL, 13 μmol, 0.0005 equiv.). The solution was stirred for 1 h at -20 °C. Chloroformate **4.6** (0.12 g, 365 μmol, 0.014 equiv.) and Et_3N (50 μL, 365 μmol, 0.014 equiv.) were added at 0 °C to end-cap the polymer. The solution was stirred for 24 h at room temperature and a further 16 h at 40 °C. Purification was

achieved by precipitation of the crude reaction mixture into methanol. After decanting the excess methanol, the residue was dried in vacuo for 48 h to provide 1.2 g of a white, sticky polymer in 48% yield. ^{1}H NMR (400 MHz, $CDCl_3$): δ 5.47-5.76 (m, 2548H), 4.09-4.31 (m, 5299H), 1.25-1.42 (m, 7798H). ^{13}C NMR (150 MHz, $CDCl_3$): δ 165.9-166.7, 91.2-94.3, 62.1, 13.8. FT-IR (KBr, thin film): 2986, 2947, 1767, 1468, 1379, 1300, 1229, 1144, 1026, 964, 858 cm^{-1}. SEC: M_n = 246 kg/mol, M_w = 461 kg/mol, Đ = 1.9. T_g = -7 °C.

Study of PEtG 4.7 degradation in solution. PEtG **4.7** (15 mg) was dissolved in a 9:1 mixture of CD_3CN:D_2O (1.2 mL) at ambient temperature (21 °C). The solution was then transferred into two NMR tubes and 4 μL H_2O_2 (50 wt% in water solution) was added to one tube to initiate the removal of the H_2O_2-labile end-cap, then the tubes were promptly sealed. ^{1}H NMR spectra were recorded at defined intervals to monitor the depolymerization of the materials. At the same time, benzyl chloroformate end-capped PEtG **2.3** was also exposed to the same amount of H_2O_2 and its depolymerization was monitored by NMR spectroscopy.

Study of PEtG 4.8 and 4.9 degradation in solution. PEtG **4.8** or **4.9** (15 mg) was dissolved in a 9:1 mixture of CD_3CN:D_2O (1.2 mL) at ambient temperature (21 °C). The solution was then transferred into two NMR tubes and 10 mg DTT was added to one tube to initiate the removal of the end-cap, then the tubes were promptly sealed. ^{1}H NMR spectra were recorded at defined intervals to monitor the depolymerization of the materials. At the same time, benzyl chloroformate end-capped PEtG **2.3** was also exposed to the same amount of DTT and its depolymerization was monitored by NMR spectroscopy.

4.5 References

1. A. Ashwin Kumar; Karthick. K; K. P. Arumugam, *Int. J. Chem. Eng. Appl.* **2011,** *2*, 164.
2. Alessandro, G., *Macromolecules* **2008,** *41*, 9491.

3. Billingham, N. C., *Polym. Degrad. Stabil.* **1996,** *53*, 269.
4. Bakhru, S. H.; Furtado, S.; Morello, A. P.; Mathiowitz, E., *Adv. Drug Deliver. Rev.* **2013,** *65*, 811.
5. Gilding, D. K.; Reed, A. M. *Polymer* **1979**, *20*.
6. Reed, A. M.; Gilding, D. K. *Polymer* **1981**, *22*, 494.
7. Li, Y.; Thouas, G. A.; Chen, Q.Z. *RSC Adv.* **2012**, *2*, 8229.
8. Langer, R.; Vacanti, *Science* **1993**, *260*, 920.
9. Jeong, B.; Bae, Y. H.; Lee, D. S.; Kim, S. W. *Nature* **1997**, *388*.
10. Sagi, A.; Weinstain, R.; Karton, N.; Shabat, D., *J. Am. Chem. Soc.* **2008,** *130*, 5434.
11. A.McBride, R.; Gillies, E. R., *Macromolecules* **2013,** *46*, 5157.
12. Chen, E. K. Y.; McBride, R. A.; Gillies, E. R., *Macromolecules* **2012,** *45*, 7364.
13. Lux, C. d. G.; McFearin, C. L.; Joshi-Barr, S.; Sankaranarayanan, J.; Fomina, N.; Almutairi, A., *ACS Macro. Lett.* **2012,** *1*, 922.
14. Seo, W.; Phillips, S. T., *J. Am. Chem. Soc.* **2010,** *132*, 9234.
15. Dewit, M. A.; Beaton, A.; Gillies, E. R., *J. Polym. Sci. Pol. Chem.* **2010,** *48*, 3977.
16. Weinstain, R.; Baran, P. S.; Shabat, D., *Bioconjugate Chem.* **2009,** *20*, 1783.
17. Diesendruck, C. E.; Peterson, G. I.; Kulik, H. J.; Kaitz, J. A.; Mar, B. D.; May, P. A.; White, S. R.; Martinez, T. J.; Boydston, A. J.; Moore, J. S., *Nat. Chem.* **2014,** *6*, 623.
18. Zhang, H.; Yeung, K.; Robbins, J. S.; Pavlick, R. A.; Wu, M.; Liu, R.; Sen, A.; Phillips, S. T., *Angew. Chem. Int. Ed.* **2012,** *51*, 2400.
19. Liu, G.; Wang, X.; Hu, J.; Zhang, G.; Liu, S., *J. Am. Chem. Soc.* **2014,** *136*, 7492.
20. Esser-Kahn, A. P.; Sottos, N. R.; White, S. R.; Moore, J. S., *J. Am. Chem. Soc.* **2010,** *132*, 10266.
21. Fan, B.; Trant, J. F.; Wong, A. D.; Gillies, E. R., *J. Am. Chem. Soc.* **2014,** *136*, 10116.
22. Felton, S.; Navid, F.; Schwarz, A.; Schwarz, T.; Gläser, R.; Rhodes, L. E., *Photochem. Photobiol. Sci.* **2013,** *12*, 29.
23. Chung, C.; Srikun, D.; Lim, C. S.; Chang, C. J.; Cho, B. R., *Chem. Commun.* **2011,** *47*, 9618.
24. Jia, L.; Cui, D.; Bignon, J.; Cicco, A. D.; Wdzieczak-Bakala, J.; Liu, J.; Li, M. H., *Biomacromolecules* **2014,** *15*, 2206

25. Valley, D. T.; Onstott, M.; Malyk, S.; Benderskii, A. V., *Langmuir* **2013,** *29*, 11623.
26. Lewis, G. G.; Robbins, J. S.; Phillips, S. T., *Macromolecules* **2013,** *46*, 5177.
27. Wong, A. D.; Güngör, T. M.; Gillies, E. R., *ACS Macro. Lett.* **2014,** *3*, 1191.

Chapter 5

5 Conclusions and Future Perspectives

Overall, this thesis described the design, synthesis, characterization and studies towards the biomedical application of a completely new class of self-immolative polymers. In the Chapter 2, we firstly demonstrated that poly(ethyl glyoxylate), which is a previously reported low-ceiling temperature polymer, can function as a new self-immolative polymer by installation of a UV-responsive end-cap on both termini. This work expanded the family of linear self-immolative polymers, of which there are currently still retaively few examples. In addition, compared to previous self-immolative polymers, which usually need multiple steps for the syntheses of monomers, the commercially available monomer for poly(ethyl glyoxylate) could promise a low cost final product that would allow for wide-spread applications. In addition, the high toxic degradation products of previous self-immolative polymers greatly limited their applications, but the introduction of poly(ethyl glyoxylate) addresses this problem as its final degradation products are ethanol and glyoxylic acid hydrate.

Furthermore, via the ozonolysis of corresponding fumaric and maleic derivatives, methyl glyoxylate, butyl glyoxylate and benzyl glyoxylate were also synthesized. Via either homopolymerization or copolymerization with ethyl glyoxylate and installation of photo-responsive end-cap, a series of poly(glyoxylate) based self-immolative polymers with different physical properties were obtained. Specifically, poly(methyl glyoxylate) and poly(benzyl glyoxylate) are white solids at room temperature, a property that may allow them to serve as self-immolative plastics. Poly(ethyl glyoxylate) may serve as a stimuli-responsive adhesive because it is sticky at room temperature. Poly(butyl glyoxylate) on the other hand is a gel-like polymer. In order to further modify the properties of this new class of self-immolative polymers, poly(ethyl glyoxylate) was used

as a hydrophobic block to form an amphiphilic block copolymer by coupling with hydrophilic poly(ethylene glycol) via a UV sensitive linker molecule.

In Chapter 3, the synthesized amphiphilic block copolymer was self-assembled into functional nanoscale self-immolative micelles with the aim of pursuing drug delivery applications. Because those two blocks were linked by a light sensitive linker molecule, UV irradiation resulted in the linkage between the two blocks being cleaved and the hydrophobic poly(ethyl glyoxylate) undergoing head-to-tail degradation. This resulted in disassembly of micelles as demonstrated by DLS, ^{1}H NMR spectroscopy and TEM. Moreover, nile red was used as a model drug to testify the capacity of this micelle system for drug incorporation and release. In the future, additional work is required to incorporate real drugs into the micelles, and to investigate drug release, cytotoxicity, biodistribution, and efficacy in preclinical models. In addition to micelles, another morphology of interest is vesicles, which are able to carry both hydrophobic and hydrophilic molecules. However, so far the tuning of the mass fraction of the hydrophilic blocks of copolymer, did not result in vesicle formation. One possible reason is that poly(ethyl glyoxylate) is not hydrophobic enough. Therefore, in the future more hydrophobic poly(glyoxylate)s, such as poly(butyl glyoxylate) and poly(benzyl glyoxylate), may be coupled with poly(ethylene glycol) and self-assembled into vesicles or other morphologies.

Lastly, in Chapter 4, a series of different stimuli-responsive end-caps were synthesized and installed on the termini of poly(ethyl glyoxylate) to achieve self-immolative polyglyoxylates that were responsive to H_2O_2 and reducing conditions. In the future, the azobenzene end-capping requires further optimization and there are also many possibilities to explore end-caps responsive to other stimuli such as acid and enzymes. It is also possible to form block copolymers from these different stimuli-responsive poly(glyoxylate)s and assemble them into micelles and vesicles that can be responsive to external stimuli other than UV light.

Appendix 1: Permission to Reuse Copyrighted Material

Copyright Clearance Center RightsLink®

Home | Account Info | Help | Live Chat

ACS Publications
Most Trusted. Most Cited. Most Read.

Title:	Polyglyoxylates: A Versatile Class of Triggerable Self-Immolative Polymers from Readily Accessible Monomers
Author:	Bo Fan, John F. Trant, Andrew D. Wong, et al
Publication:	Journal of the American Chemical Society
Publisher:	American Chemical Society
Date:	Jul 1, 2014

Copyright © 2014, American Chemical Society

Logged in as:
Bo Fan
Account #:
3000851023
LOGOUT

PERMISSION/LICENSE IS GRANTED FOR YOUR ORDER AT NO CHARGE

This type of permission/license, instead of the standard Terms & Conditions, is sent to you because no fee is being charged for your order. Please note the following:

- Permission is granted for your request in both print and electronic formats, and translations.
- If figures and/or tables were requested, they may be adapted or used in part.
- Please print this page for your records and send a copy of it to your publisher/graduate school.
- Appropriate credit for the requested material should be given as follows: "Reprinted (adapted) with permission from (COMPLETE REFERENCE CITATION). Copyright (YEAR) American Chemical Society." Insert appropriate information in place of the capitalized words.
- One-time permission is granted only for the use specified in your request. No additional uses are granted (such as derivative works or other editions). For any other uses, please submit a new request.

BACK | CLOSE WINDOW

Copyright © 2014 Copyright Clearance Center, Inc. All Rights Reserved. Privacy statement.
Comments? We would like to hear from you. E-mail us at customercare@copyright.com

PERMISSION/LICENSE IS GRANTED FOR YOUR ORDER AT NO CHARGE

PERMISSION/LICENSE IS GRANTED FOR YOUR ORDER AT NO CHARGE

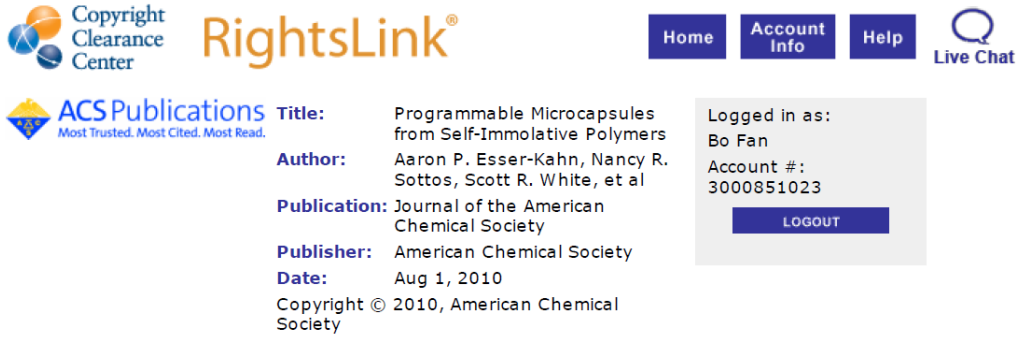

PERMISSION/LICENSE IS GRANTED FOR YOUR ORDER AT NO CHARGE

Title: Copolymerization of o-Phthalaldehyde and Ethyl Glyoxylate: Cyclic Macromolecules with Alternating Sequence and Tunable Thermal Properties

Author: Joshua A. Kaitz, Jeffrey S. Moore

Publication: Macromolecules

Publisher: American Chemical Society

Date: Aug 1, 2014

Copyright © 2014, American Chemical Society

Logged in as:
Bo Fan
Account #:
3000851023
LOGOUT

PERMISSION/LICENSE IS GRANTED FOR YOUR ORDER AT NO CHARGE

Title: End-Capped Poly(benzyl ethers): Acid and Base Stable Polymers That Depolymerize Rapidly from Head-to-Tail in Response to Specific Applied Signals

Author: Michael G. Olah, Jessica S. Robbins, Matthew S. Baker, et al

Publication: Macromolecules

Publisher: American Chemical Society

Date: Aug 1, 2013

Copyright © 2013, American Chemical Society

Logged in as:
Bo Fan
Account #:
3000851023
LOGOUT

PERMISSION/LICENSE IS GRANTED FOR YOUR ORDER AT NO CHARGE

Title: Kinetics of Self-Immolative Degradation in a Linear Polymeric System: Demonstrating the Effect of Chain Length

Author: Ryan A. McBride, Elizabeth R. Gillies

Publication: Macromolecules

Publisher: American Chemical Society

Date: Jul 1, 2013

Copyright © 2013, American Chemical Society

Logged in as:
Bo Fan
Account #:
3000851023
LOGOUT

PERMISSION/LICENSE IS GRANTED FOR YOUR ORDER AT NO CHARGE

Appendix 2: Supporting Information for Chapter 2

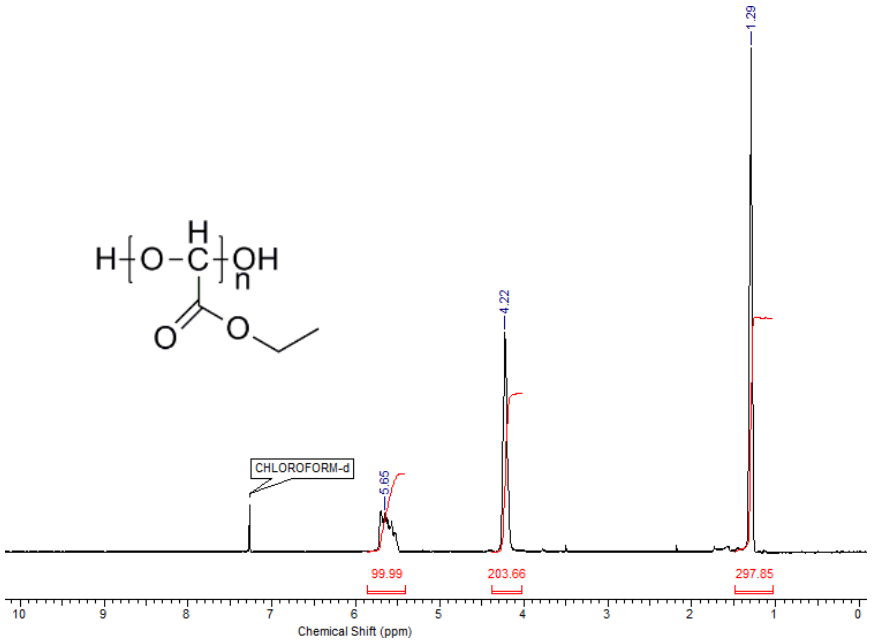

Figure A2. 1 ^{1}H NMR spectrum of poly(ethyl glyoxylate) without end-cap (Polymer 2.1) ($CDCl_3$, 400 MHz).

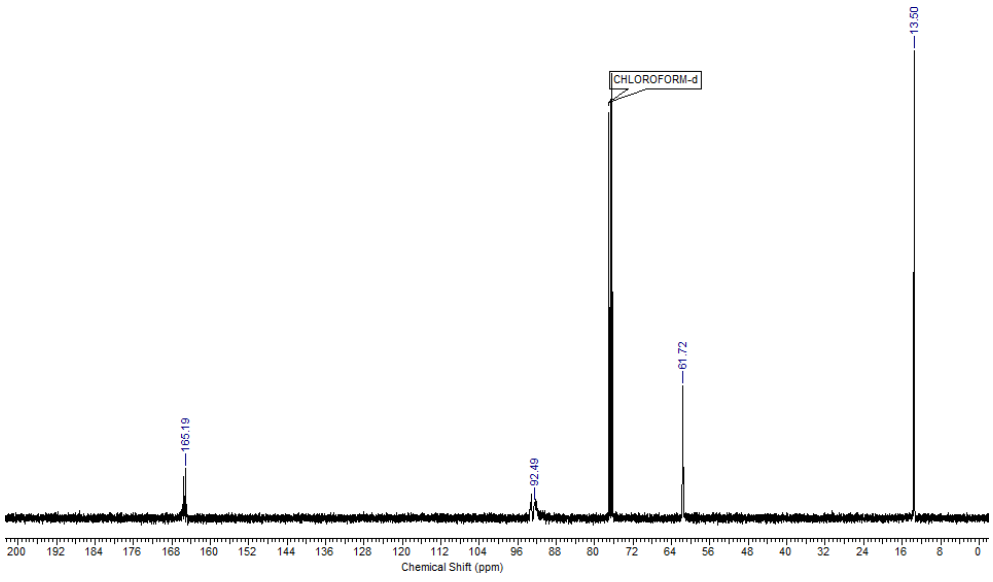

Figure A2. 2 ^{13}C NMR spectrum of poly(ethyl glyoxylate) without end-cap (Polymer 2.1) ($CDCl_3$, 150 MHz).

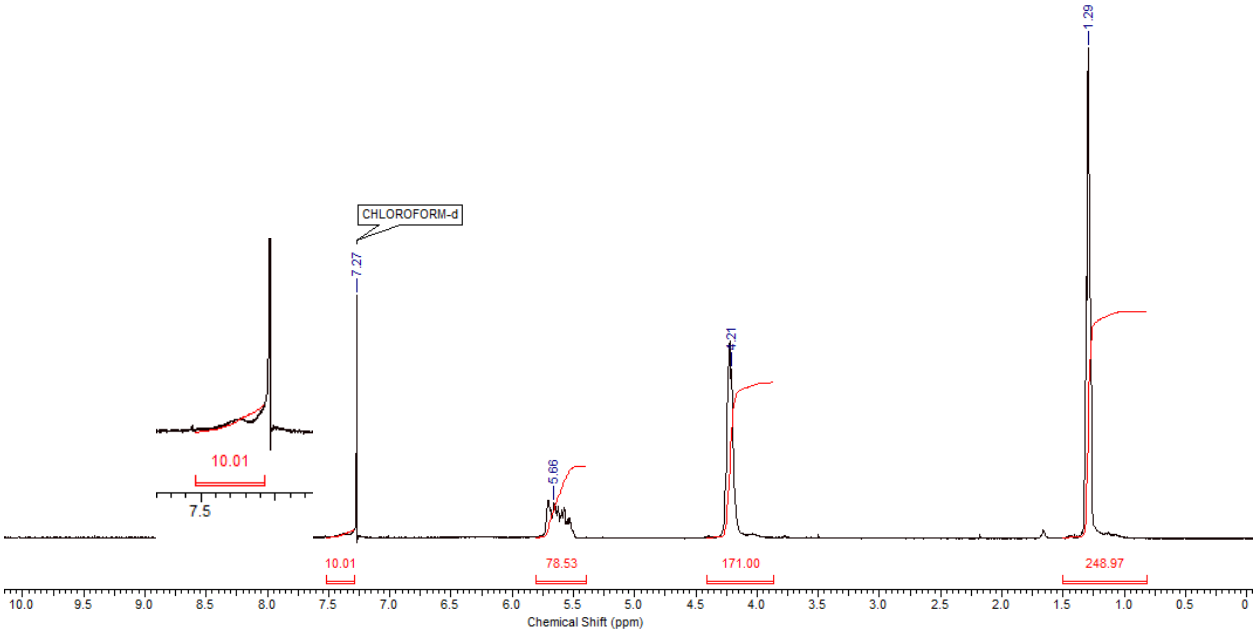

Figure A2. 3 ^{1}H NMR spectrum of poly(ethyl glyoxylate) end-capped by phenyl isocyanate (Polymer 2.2) ($CDCl_3$, 400 MHz).

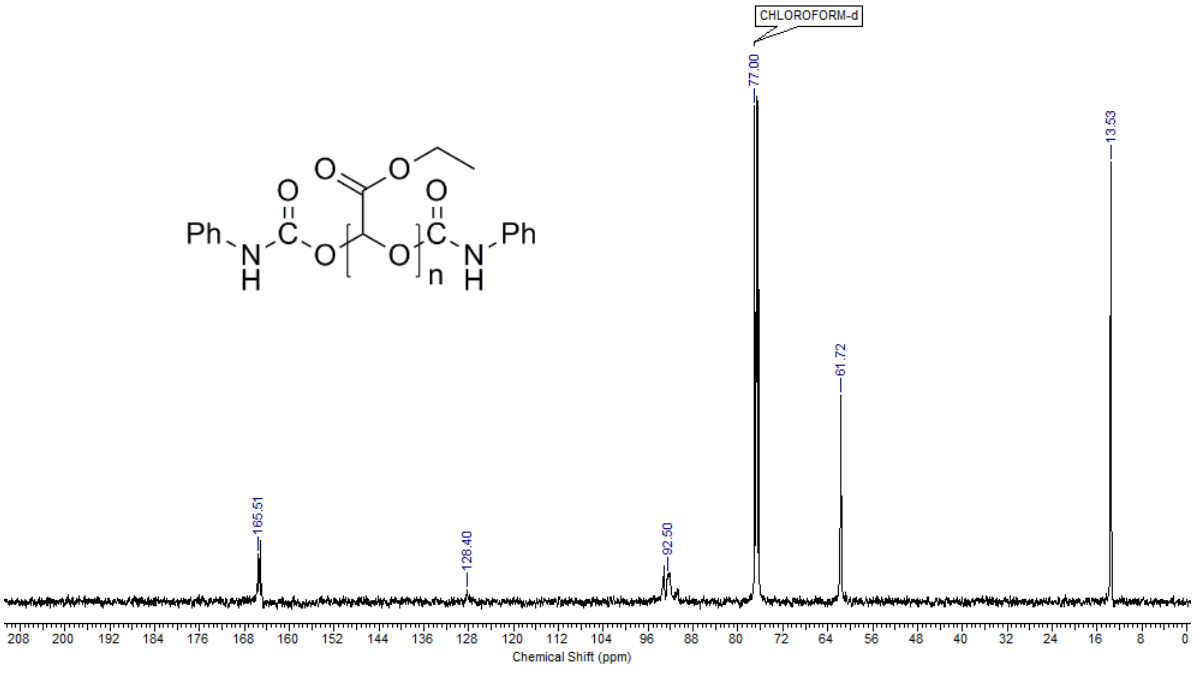

Figure A2. 4 ^{13}C NMR spectrum of poly(ethyl glyoxylate) end-capped by phenyl isocyanate (Polymer 2.2) ($CDCl_3$, 150 MHz).

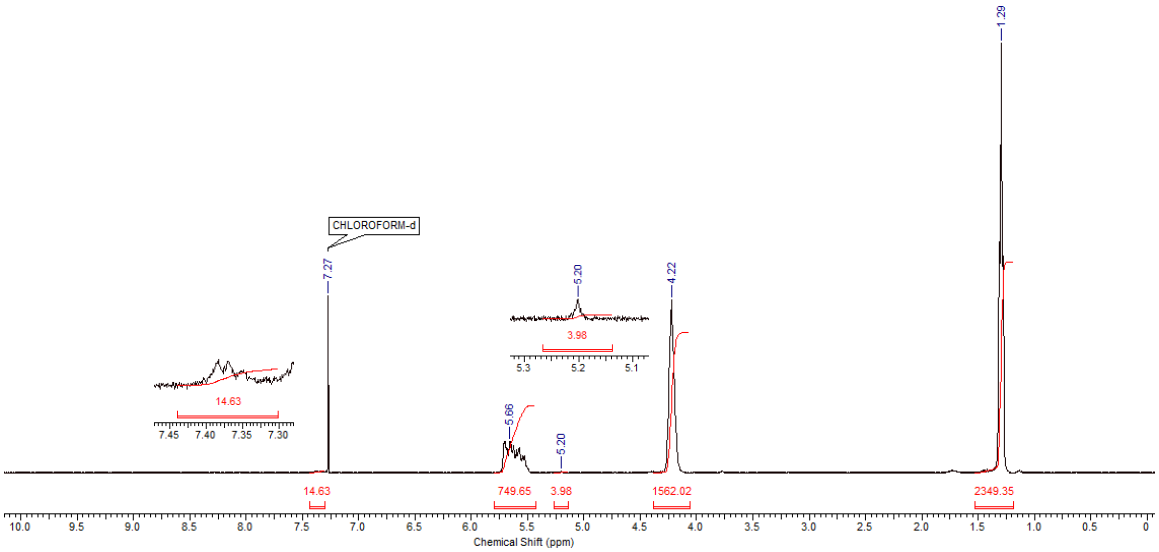

Figure A2. 5 ^{1}H NMR spectrum of poly(ethyl glyoxylate) end-capped by benzyl chloroformate (Polymer 2.3) ($CDCl_3$, 400 MHz).

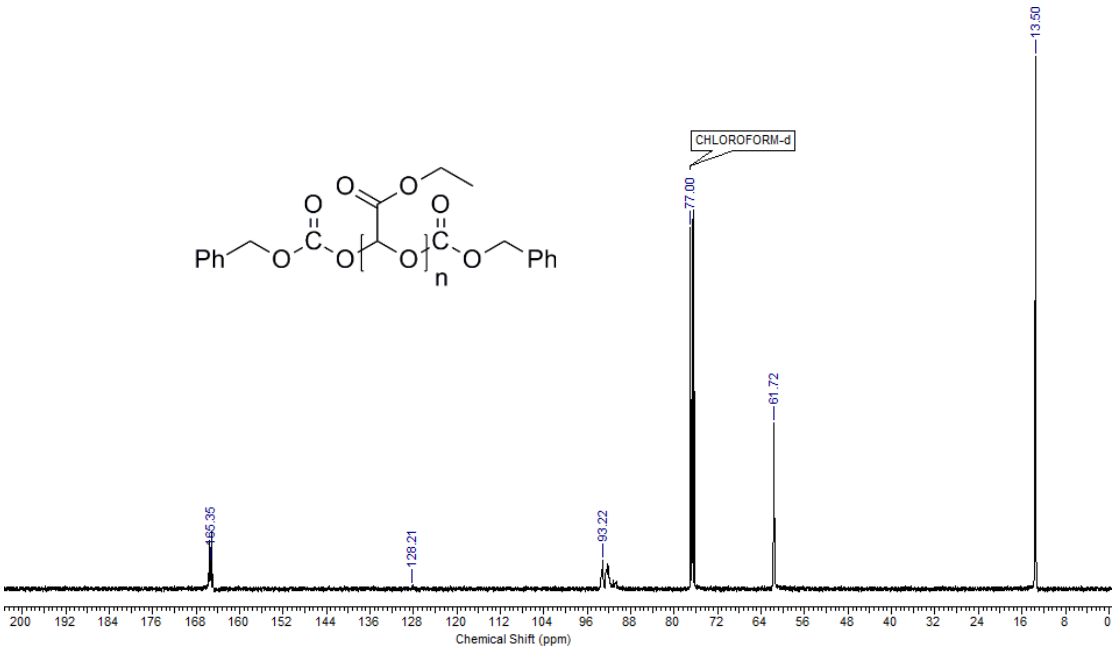

Figure A2. 6 ^{13}C NMR spectrum of poly(ethyl glyoxylate) end-capped by benzyl chloroformate (Polymer 2.3) ($CDCl_3$, 150 MHz).

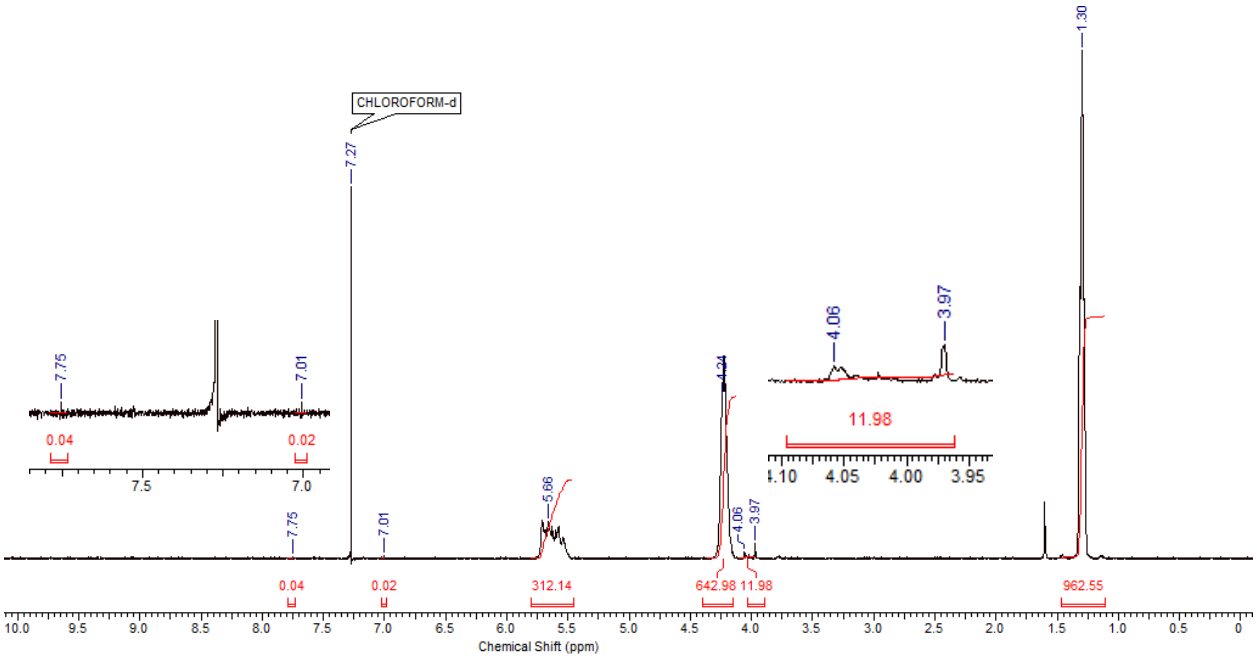

Figure A2. 7 ^{1}H NMR spectrum of poly(ethyl glyoxylate) end-capped by NVOC-Cl (Polymer 2.4) ($CDCl_3$, 400 MHz).

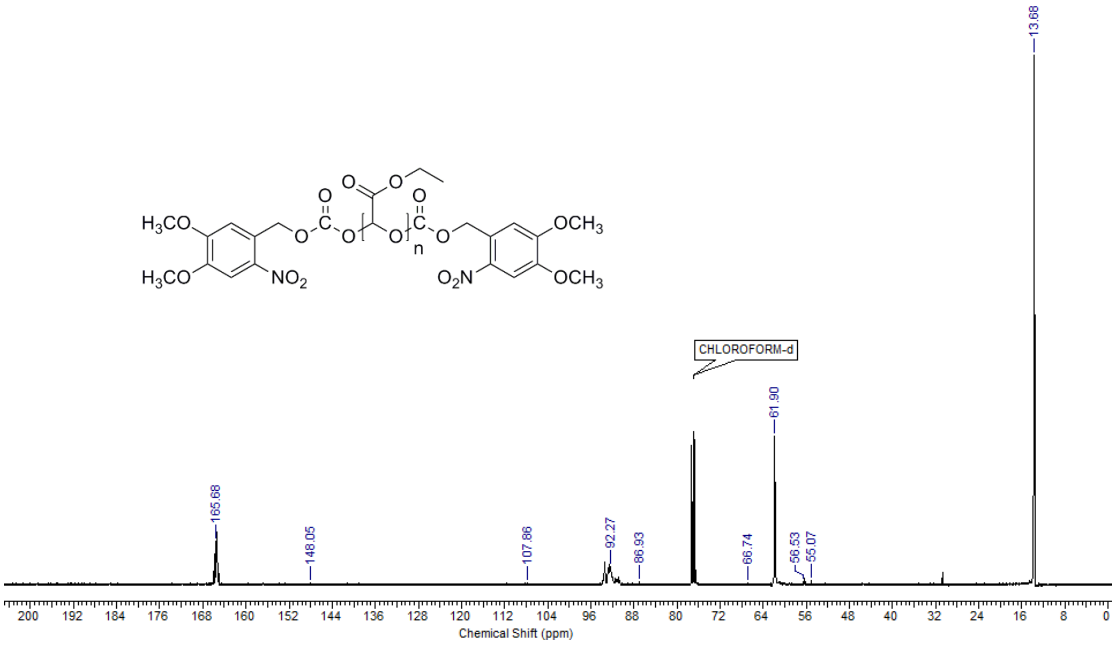

Figure A2. 8 ^{13}C NMR spectrum of poly(ethyl glyoxylate) end-capped by NVOC-Cl (Polymer 2.4) ($CDCl_3$, 150 MHz).

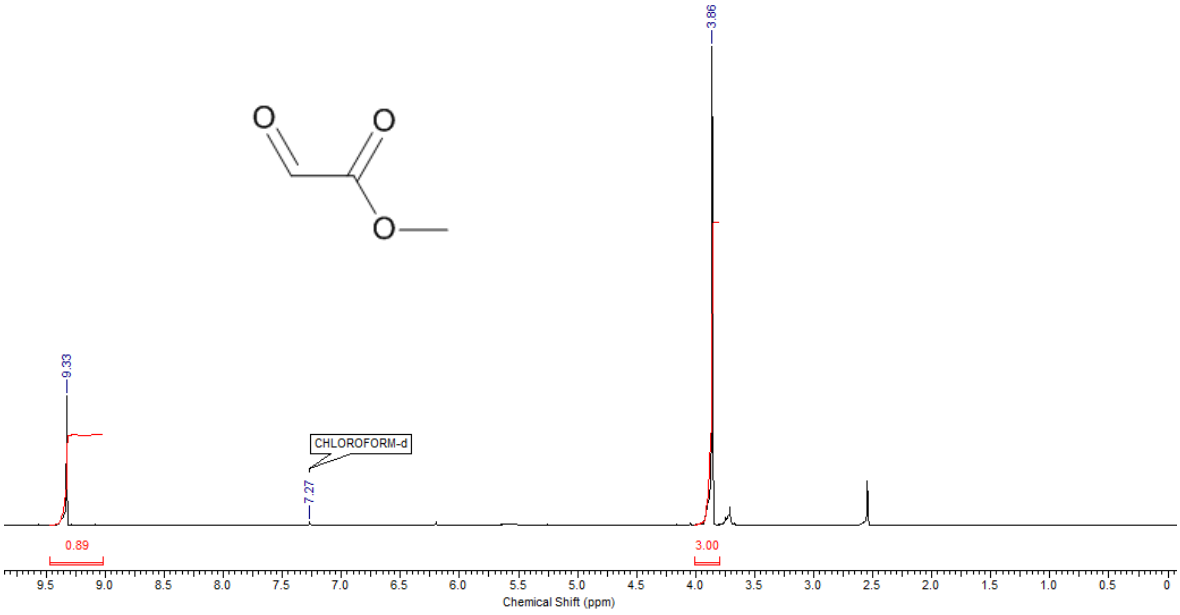

Figure A2. 9 ^{1}H NMR spectrum of methyl glyoxylate compound 2.8 ($CDCl_3$, 400 MHz).

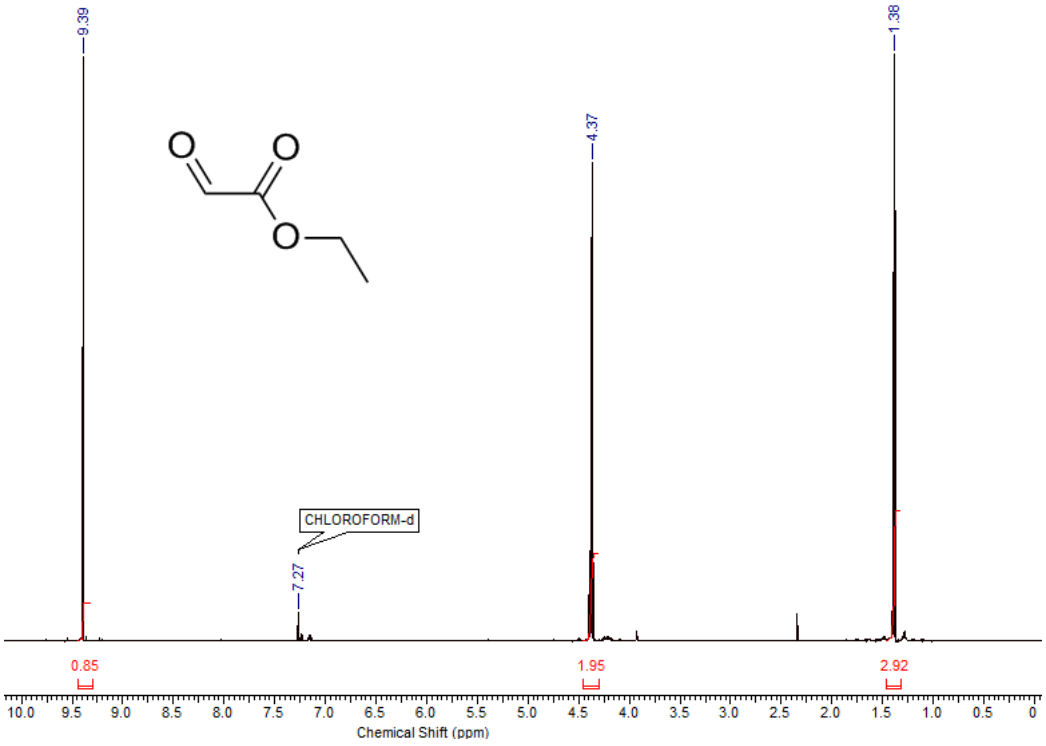

Figure A2. 10 ^{1}H NMR spectrum of ethyl glyoxylate ($CDCl_3$, 400 MHz).

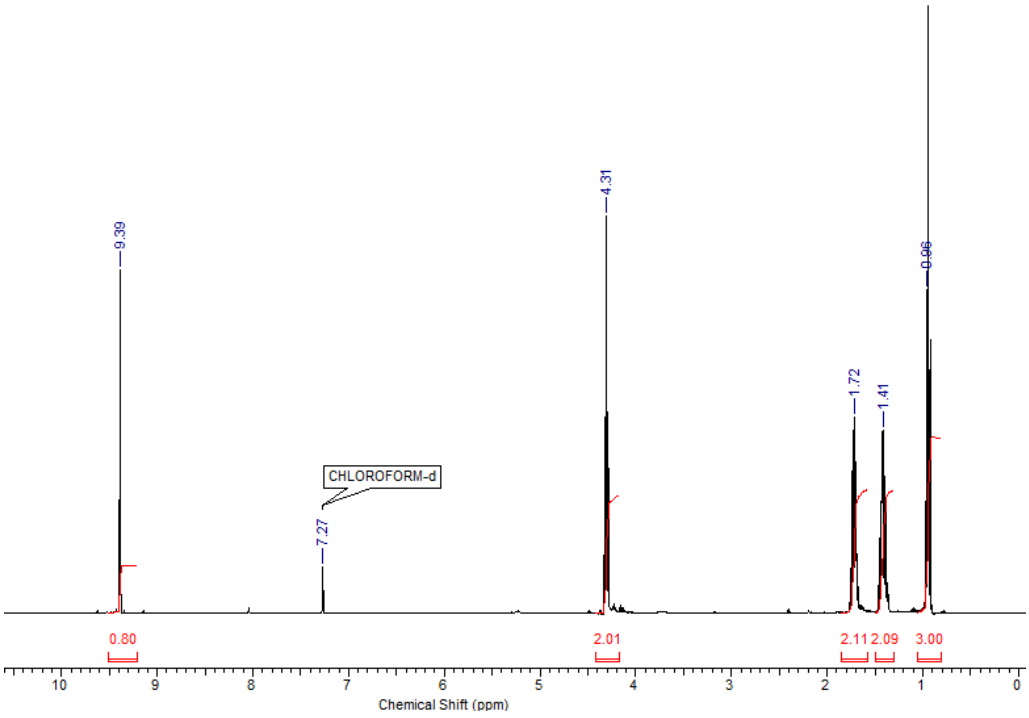

Figure A2. 11 ^{1}H NMR spectrum of *n*-butyl glyoxylate compound 2.9 ($CDCl_3$, 400 MHz).

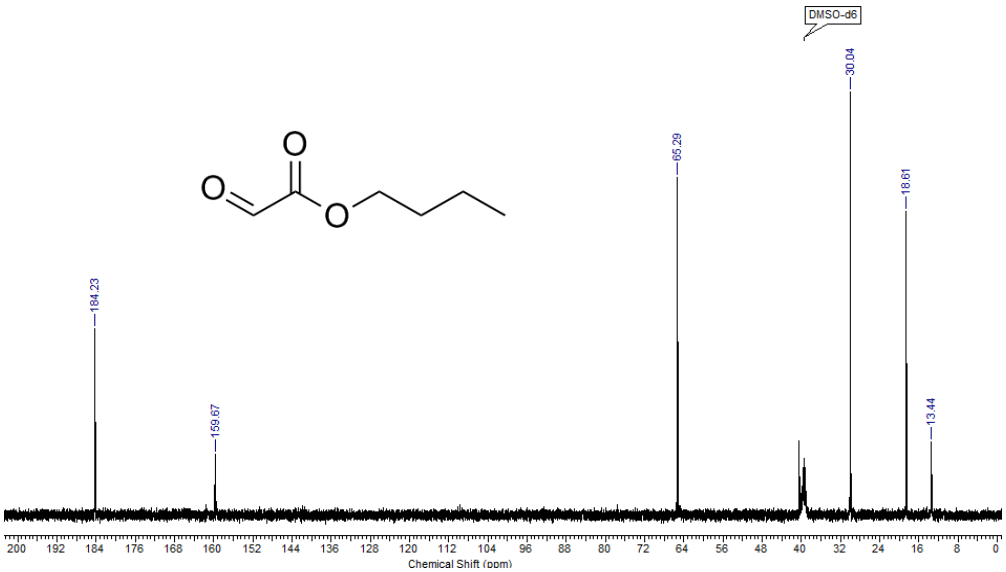

Figure A2. 12 ^{13}C NMR spectrum of *n*-butyl glyoxylate compound 2.9 ($CDCl_3$, 150 MHz).

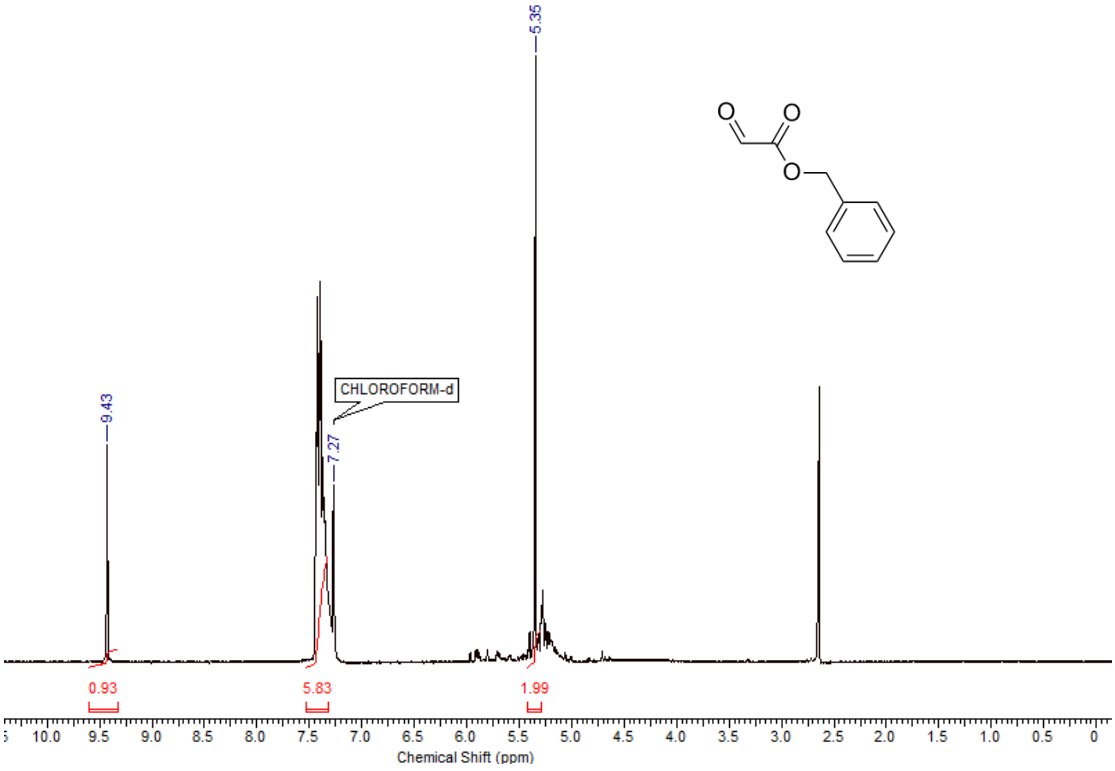

Figure A2. 13 ^{1}H NMR spectrum of benzyl glyoxylate compound 2.10 ($CDCl_3$, 400 MHz).

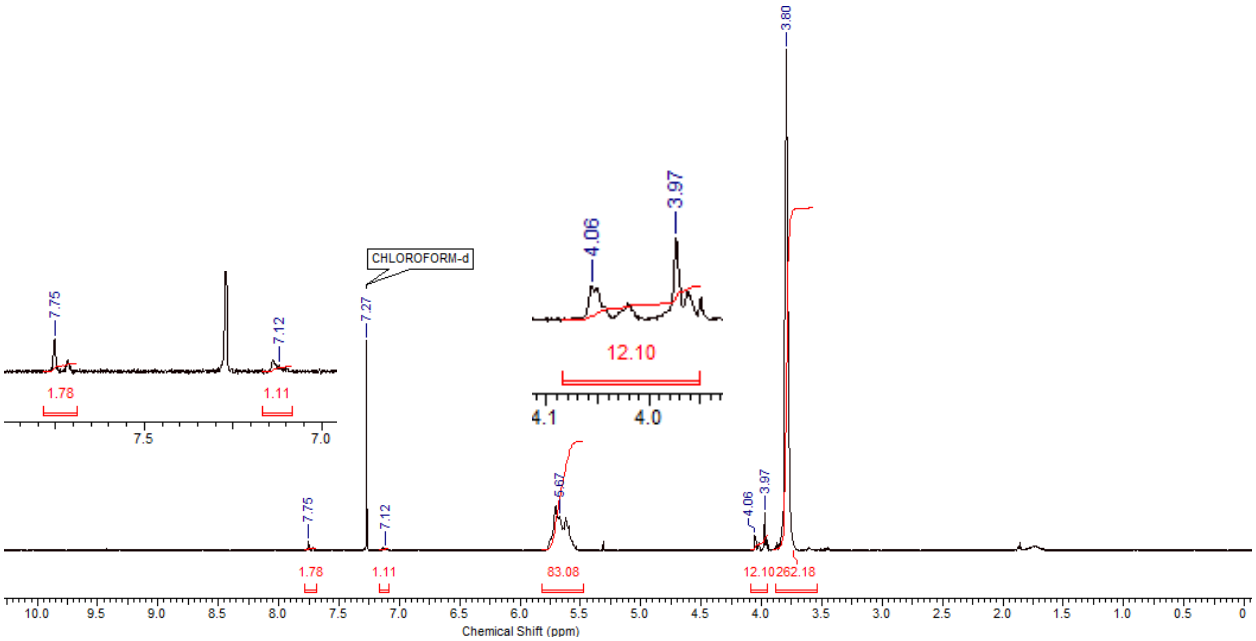

Figure A2. 14 ^{1}H NMR spectrum of poly(methyl glyoxylate) end-capped by NVOC-Cl (Polymer 2.11) ($CDCl_3$, 400 MHz).

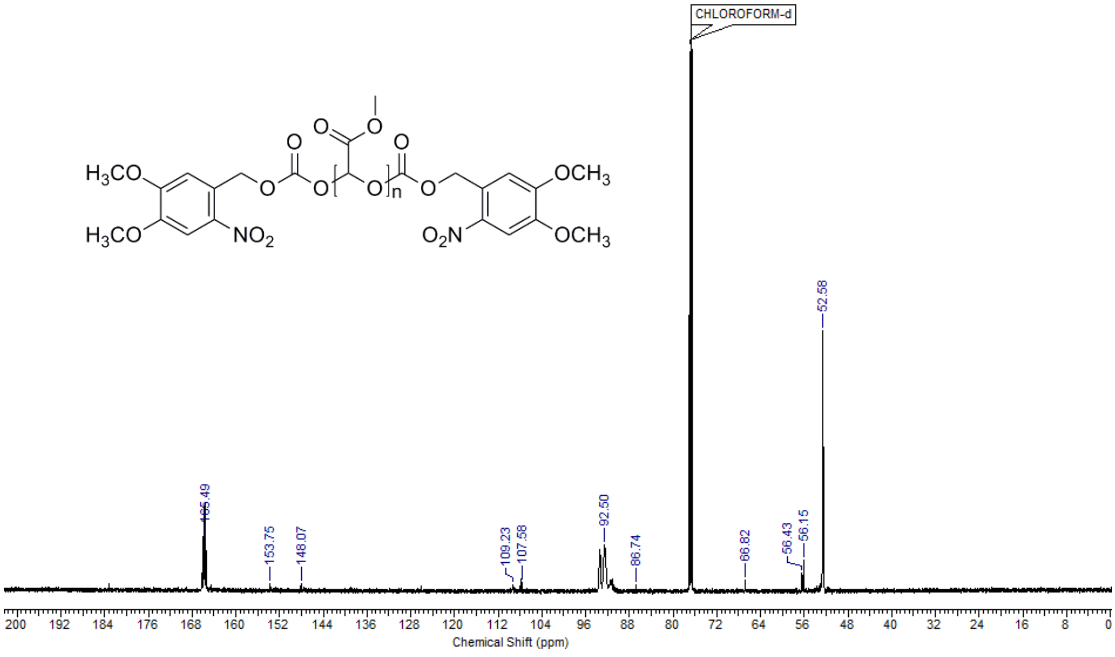

Figure A2. 15 ^{13}C NMR spectrum of poly(methyl glyoxylate) end-capped by NVOC-Cl (Polymer 2.11) ($CDCl_3$, 150 MHz).

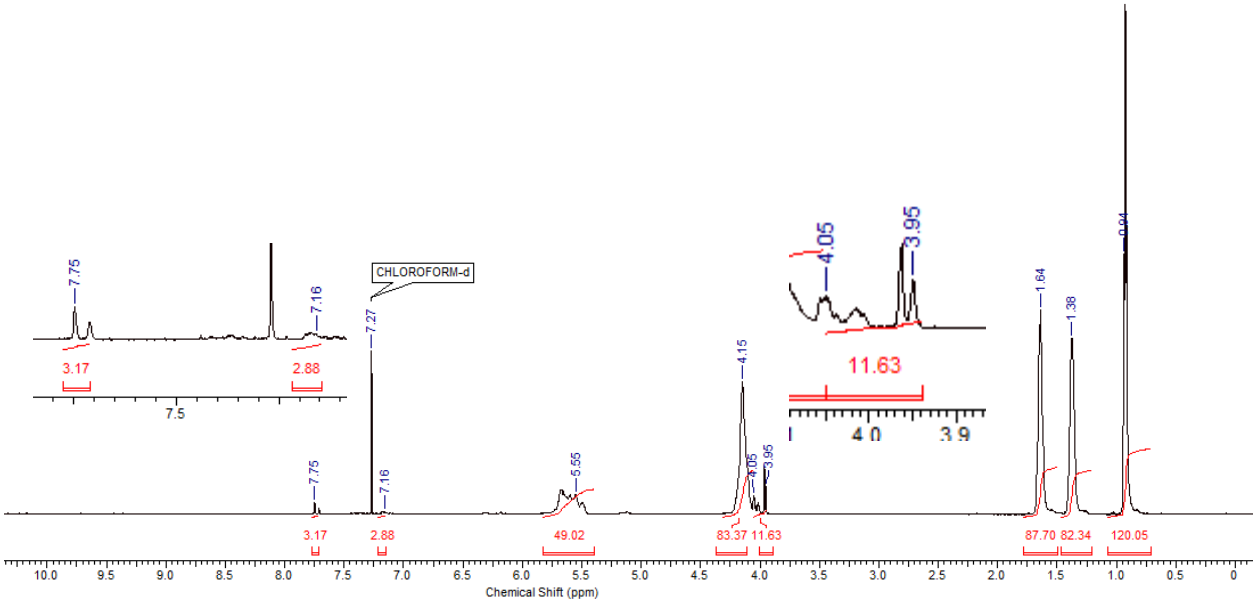

Figure A2. 16 ^{1}H NMR spectrum of poly(butyl glyoxylate) end-capped by NVOC-Cl (Polymer 2.12) ($CDCl_3$, 400 MHz).

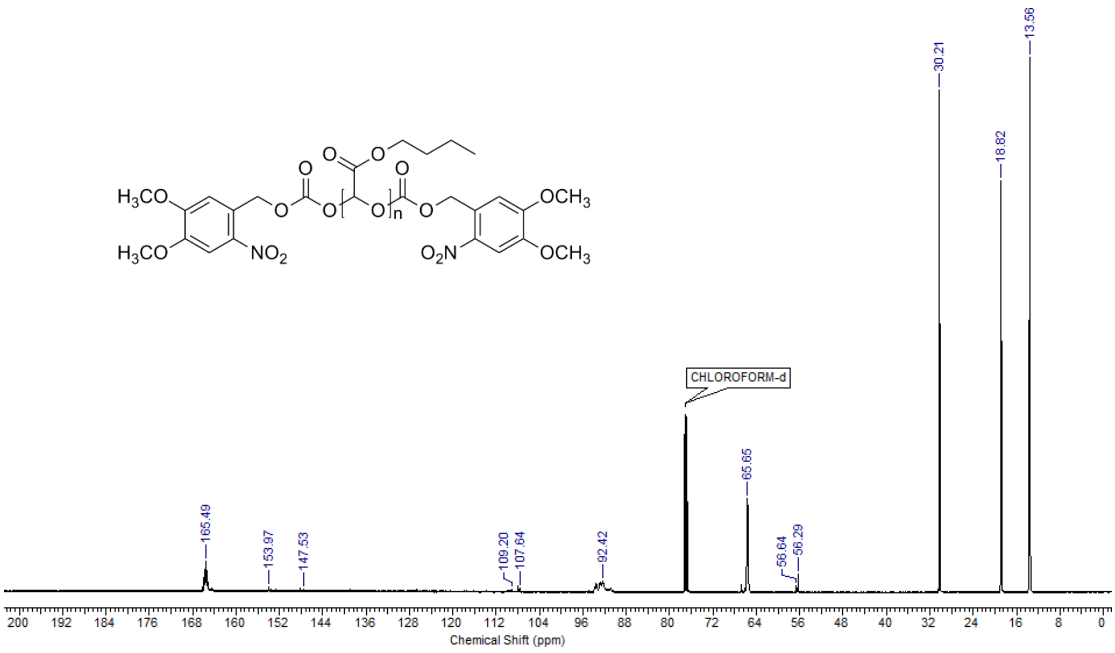

Figure A2. 17 ^{13}C NMR spectrum of poly(butyl glyoxylate) end-capped by NVOC-Cl (Polymer 2.12) ($CDCl_3$, 150 MHz).

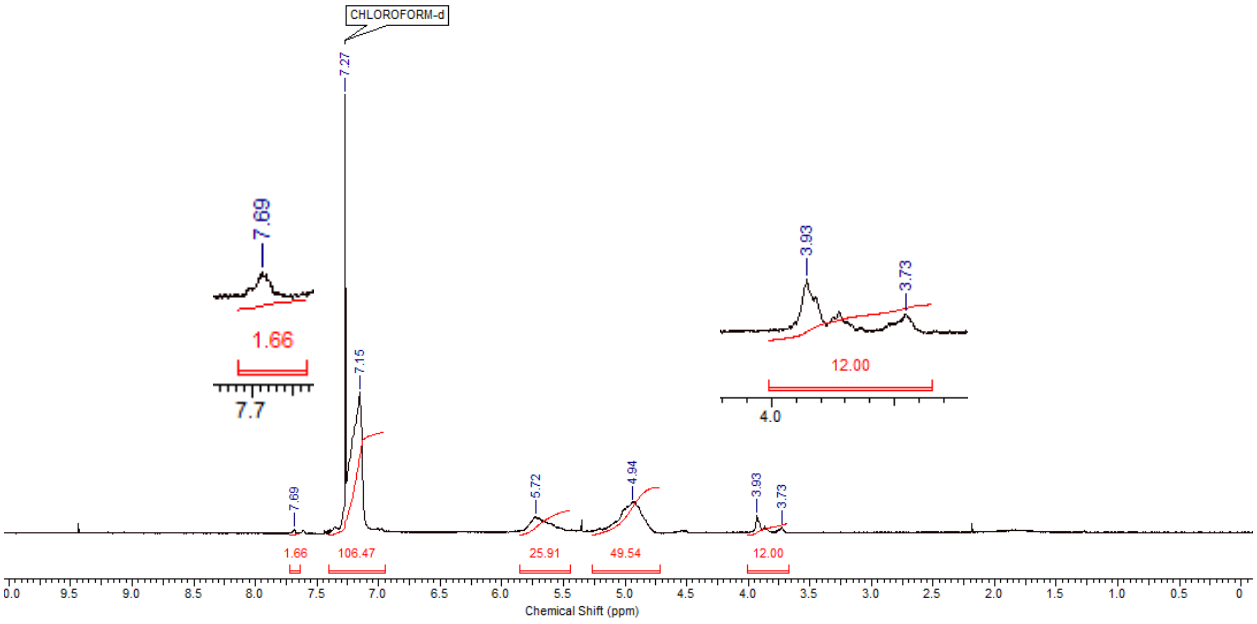

Figure A2. 18 ^{1}H NMR spectrum of poly(benzyl glyoxylate) end-capped by NVOC-Cl (Polymer 2.13) ($CDCl_3$, 400 MHz).

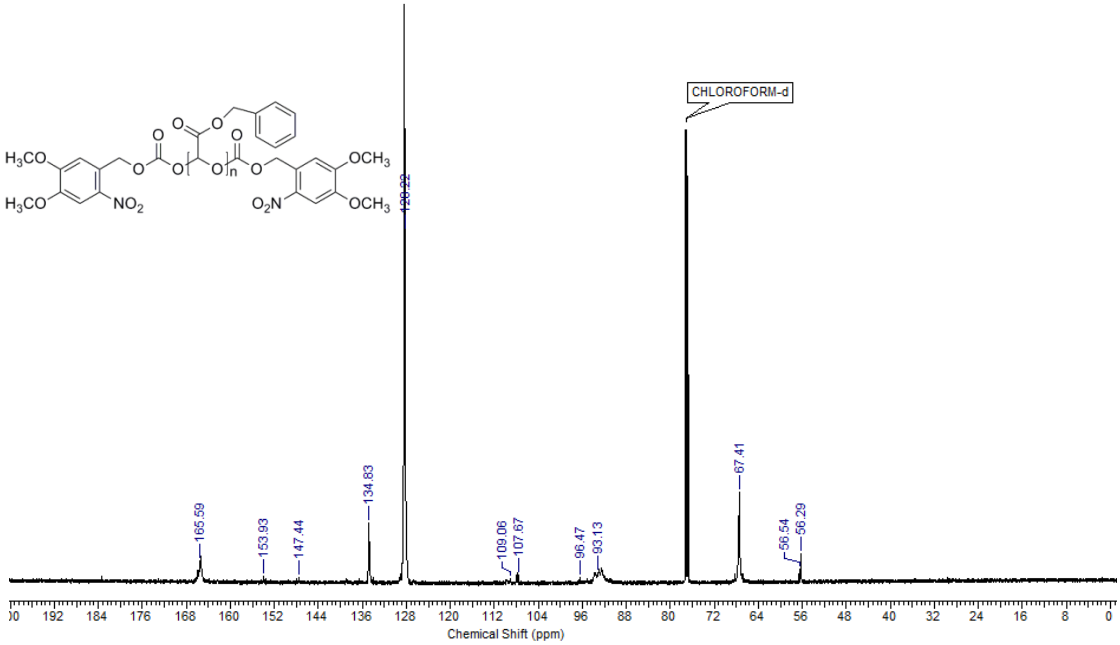

Figure A2. 19 ^{13}C NMR spectrum of poly(benzyl glyoxylate) end-capped by NVOC-Cl (Polymer 2.13) ($CDCl_3$, 150 MHz).

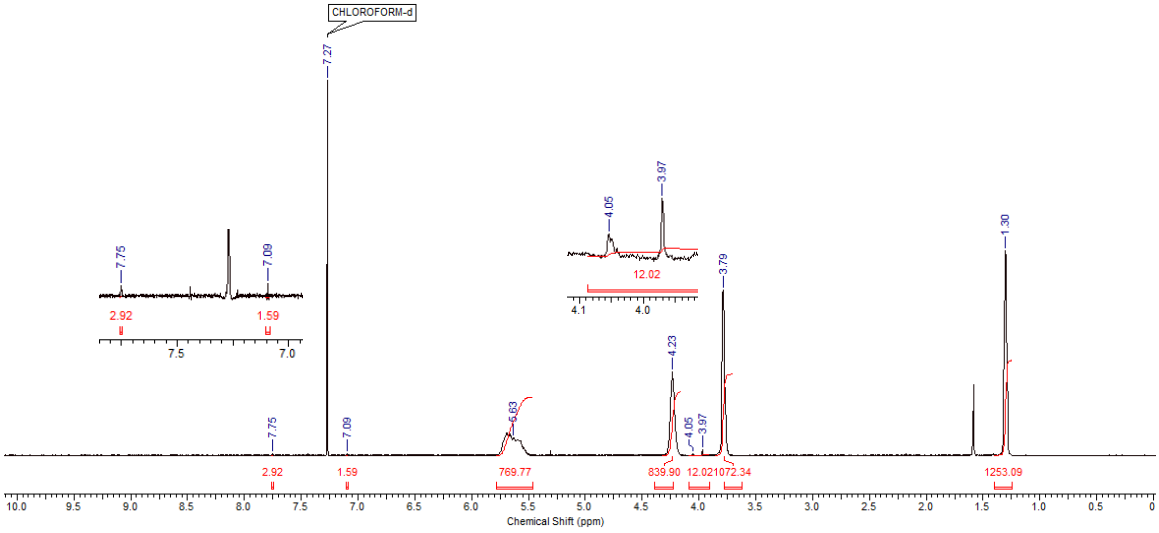

Figure A2. 20 ^{1}H NMR spectrum of poly(ethyl glyoxylate)-*co*-(methyl glyoxylate) end-capped by NVOC-Cl (Polymer 2.14) ($CDCl_3$, 400 MHz).

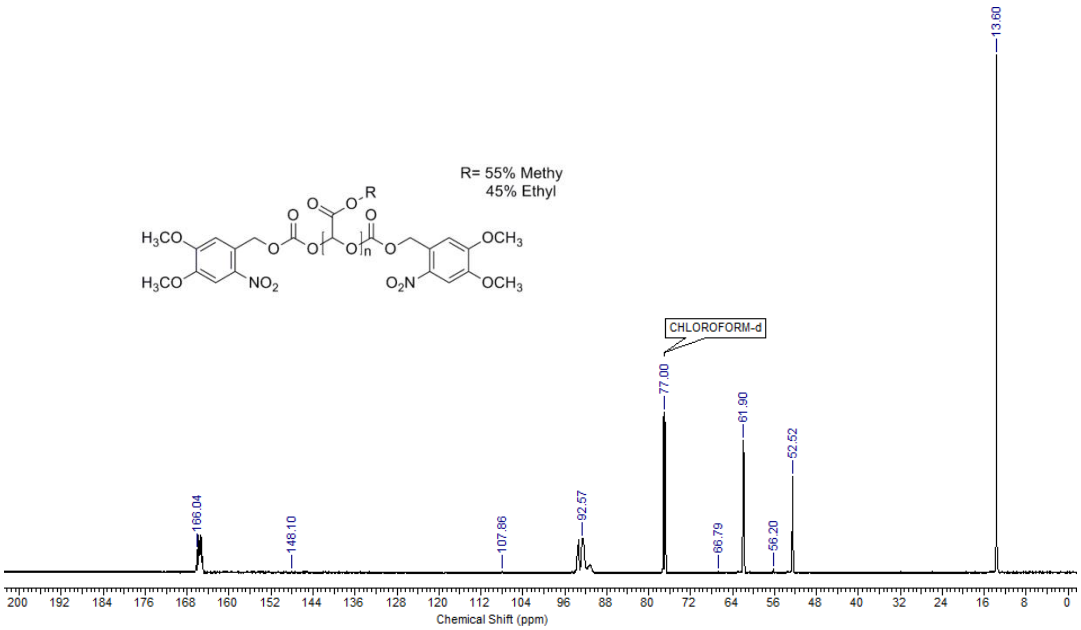

Figure A2. 21 ^{13}C NMR spectrum of poly(ethyl glyoxylate)-*co*-(methyl glyoxylate) end-capped by NVOC-Cl (Polymer 2.14) ($CDCl_3$, 150 MHz).

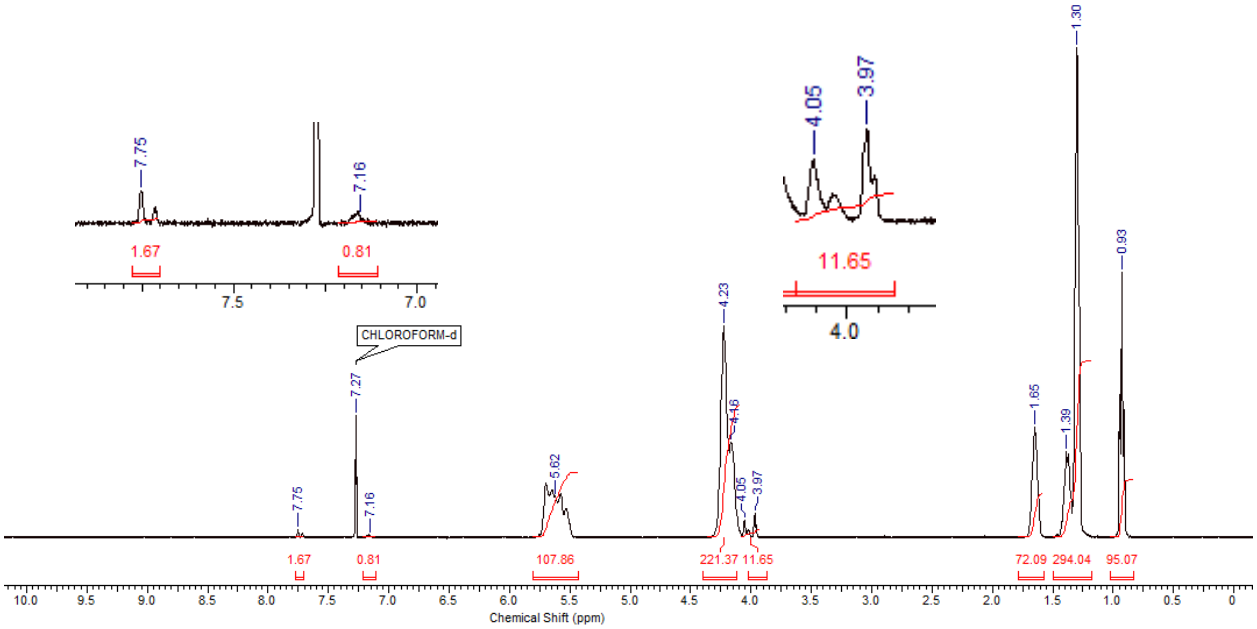

Figure A2. 22 ^{1}H NMR spectrum of poly(ethyl glyoxylate)-*co*-(butyl glyoxylate) end-capped by NVOC-Cl (Polymer 2.15) ($CDCl_3$, 400 MHz).

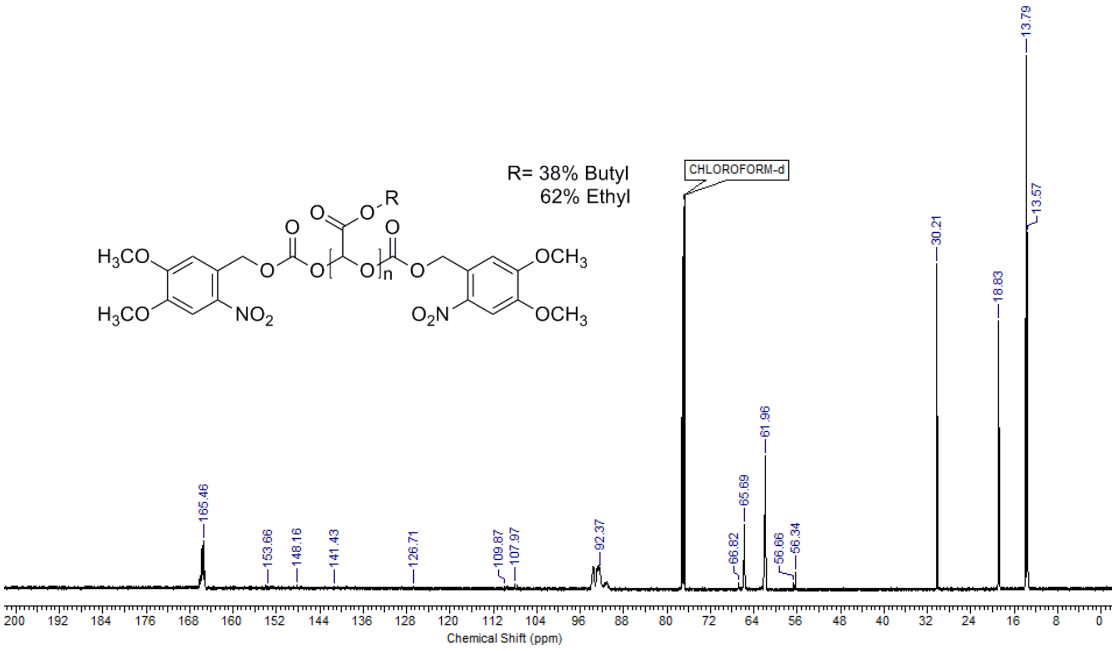

Figure A2. 23 ^{13}C NMR spectrum of poly(ethyl glyoxylate)-*co*-(butyl glyoxylate) end-capped by NVOC-Cl (Polymer 2.15) ($CDCl_3$, 150 MHz).

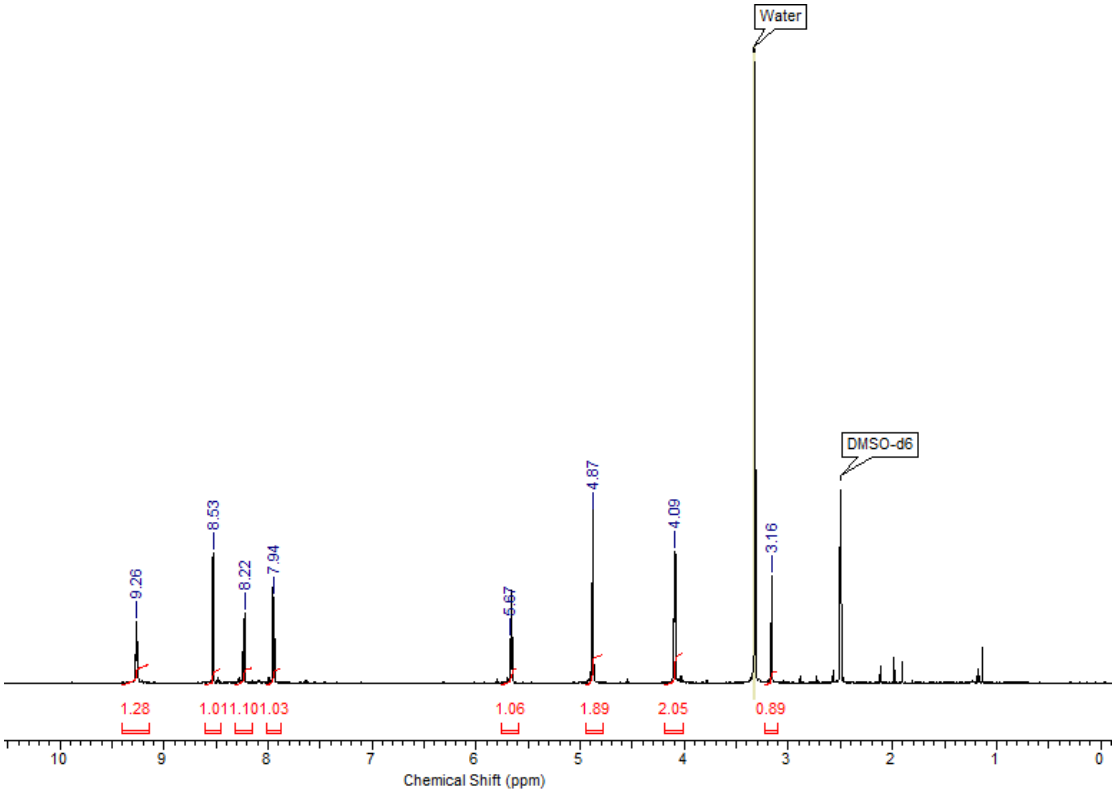

Figure A2. 24 ^{1}H NMR spectrum of compound 2.17 (DMSO-*d6*, 400 MHz).

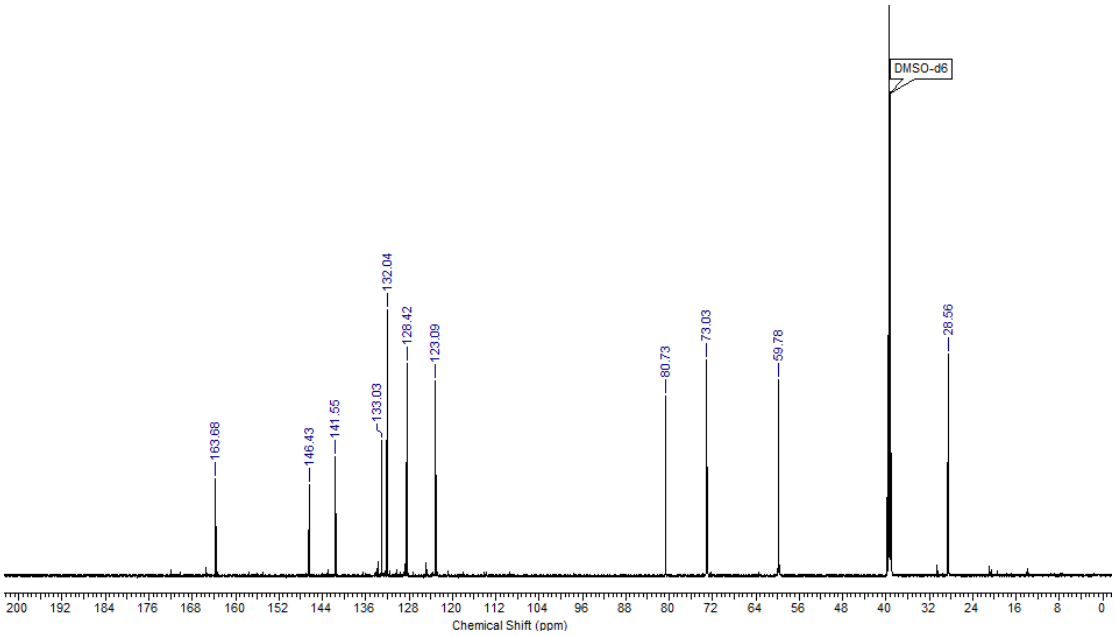

Figure A2. 25 ^{13}C NMR spectrum of compound 2.17 (DMSO-*d6*, 150 MHz).

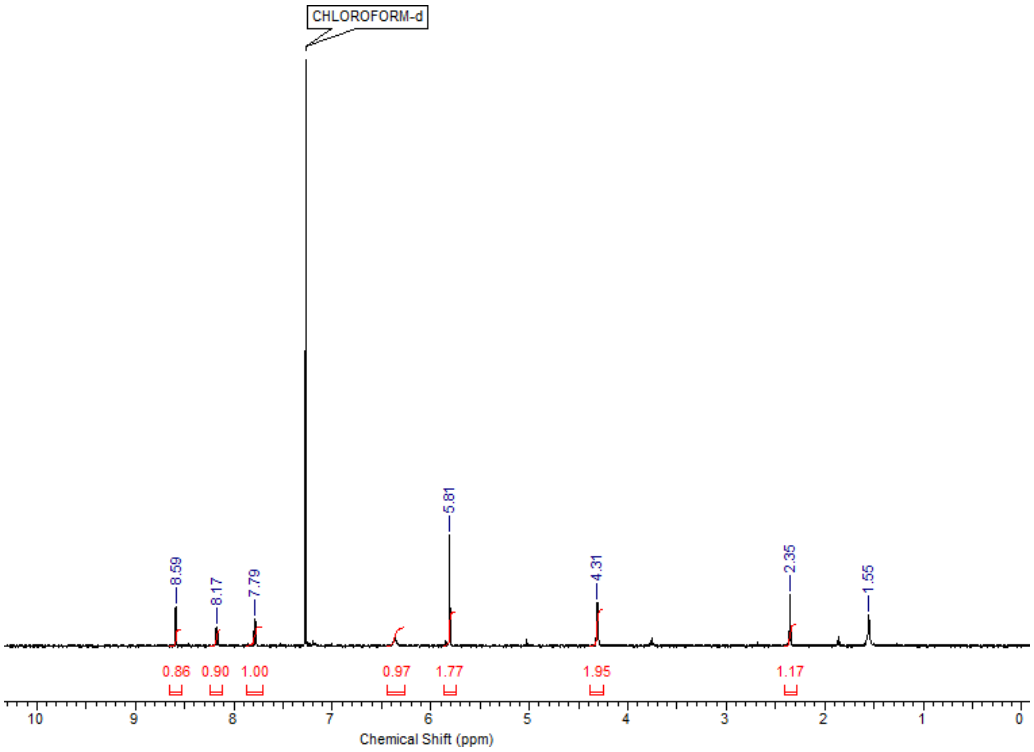

Figure A2. 26 ^{1}H NMR spectrum of compound 2.18 ($CDCl_3$, 400 MHz).

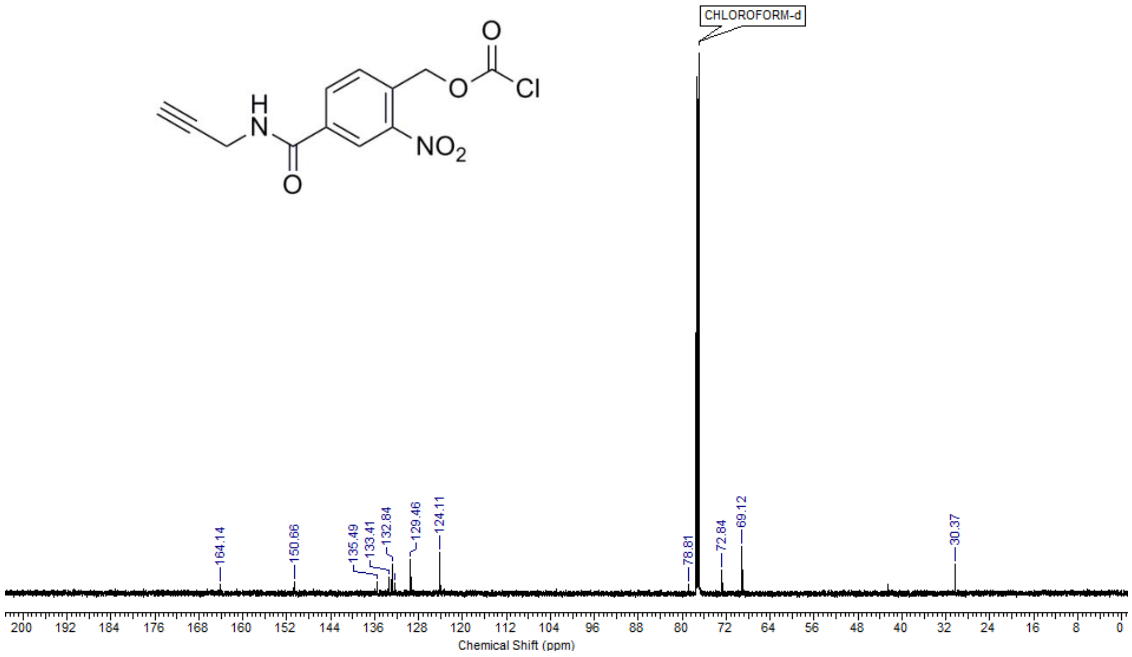

Figure A2. 27 ^{13}C NMR spectrum of compound 2.18 ($CDCl_3$, 150 MHz).

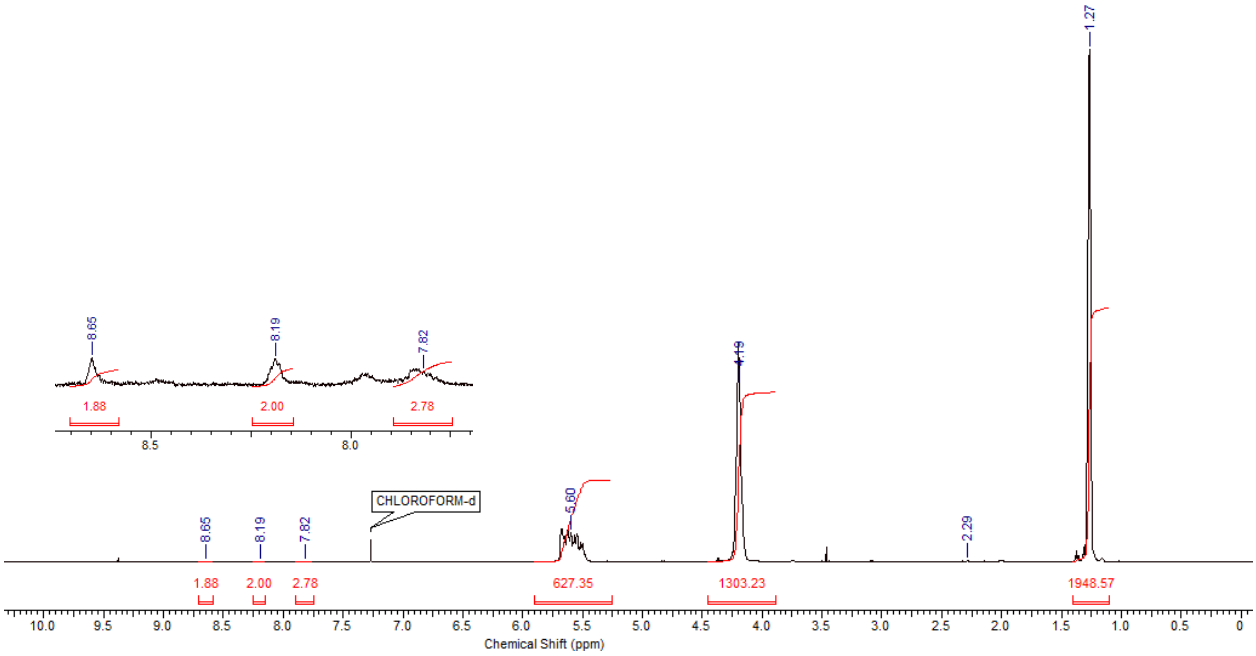

Figure A2. 28 ^{1}H NMR spectrum of poly(ethyl glyoxylate) end-capped by compound

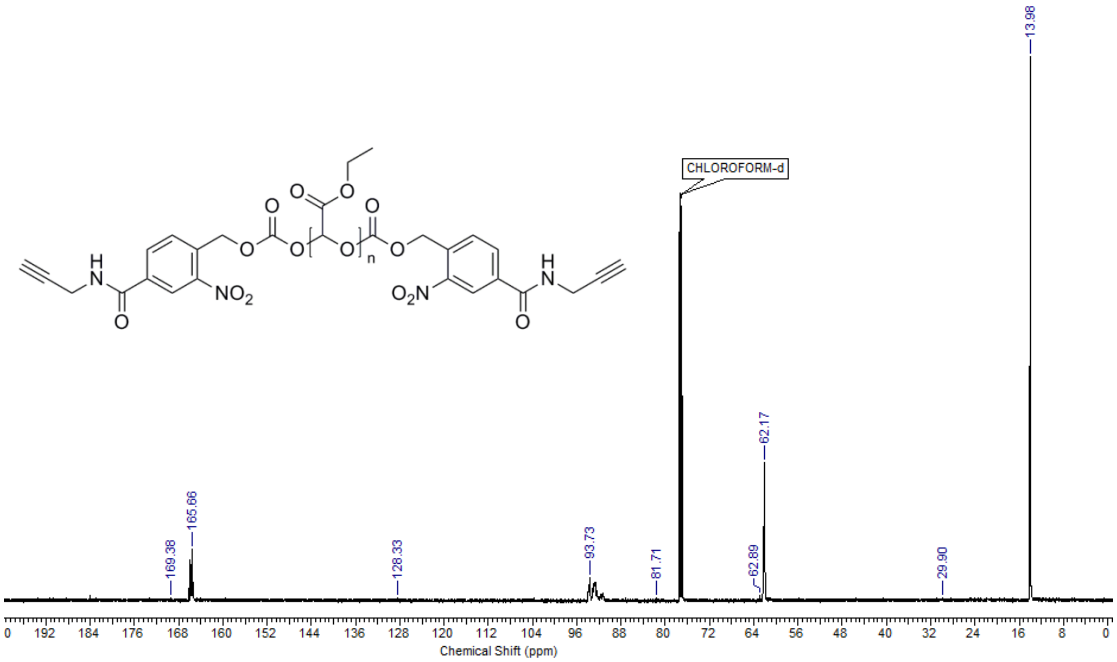

2.18 (Polymer 2.19) ($CDCl_3$, 400 MHz).

Figure A2. 29 ^{13}C NMR spectrum of poly(ethyl glyoxylate) end-capped by compound 2.18 (Polymer 2.19) ($CDCl_3$, 150 MHz).

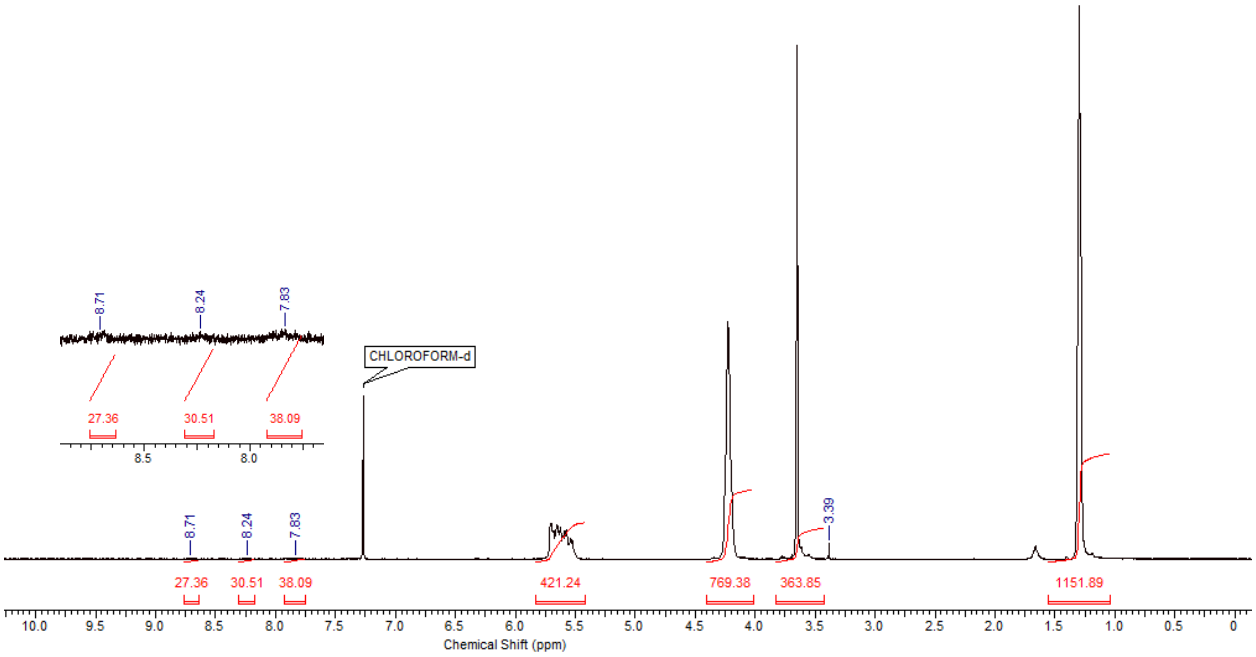

Figure A2. 30 ^{1}H NMR spectrum of block polymer (Polymer 2.21) ($CDCl_3$, 400MHz).

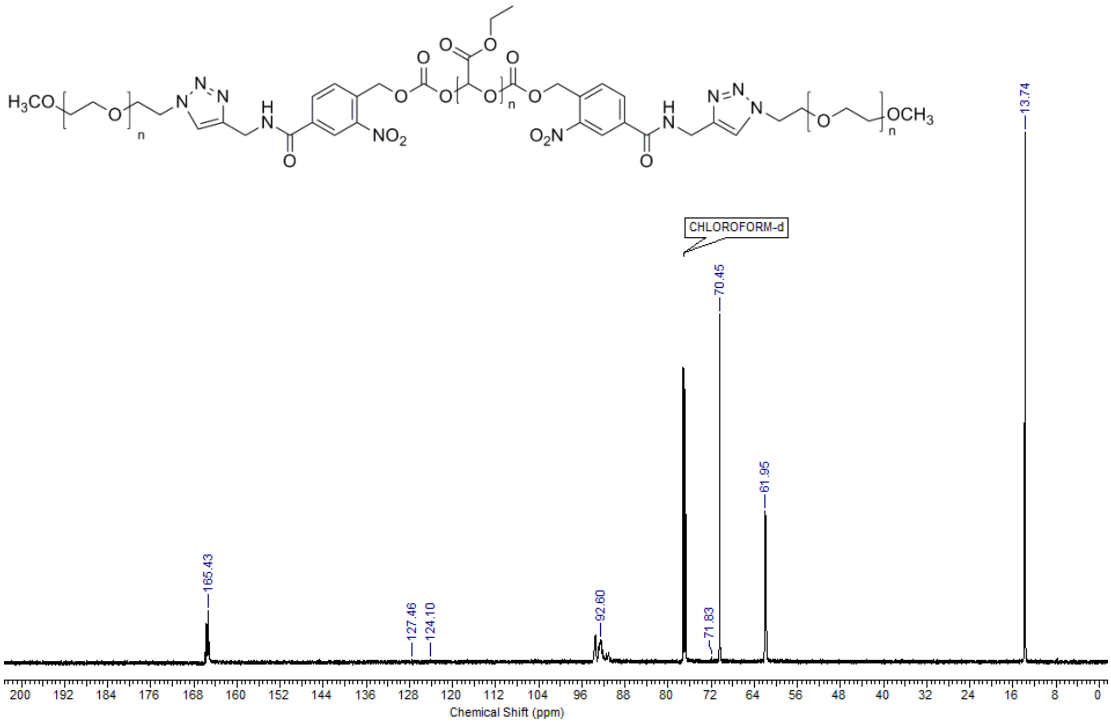

Figure A2. 31 ^{13}C NMR spectrum of block polymer (Polymer 2.21) ($CDCl_3$, 150 MHz).

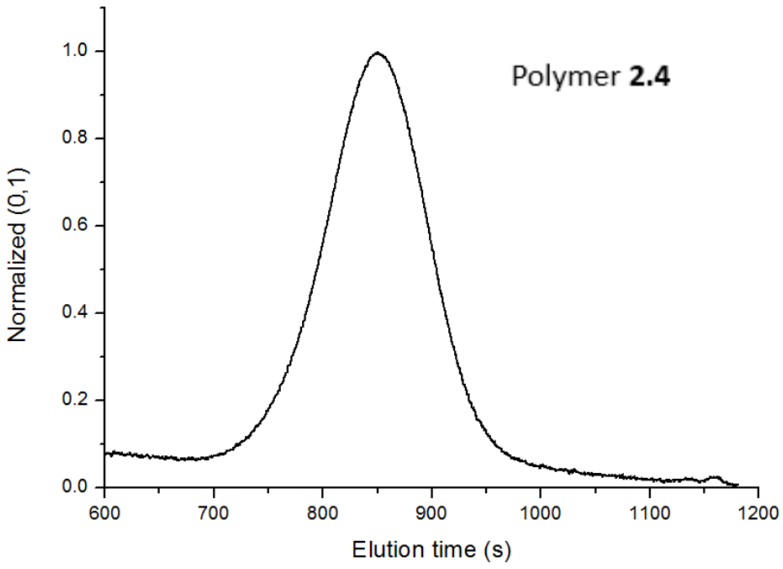

Figure A2. 32 SEC trace for Polymer 2.4

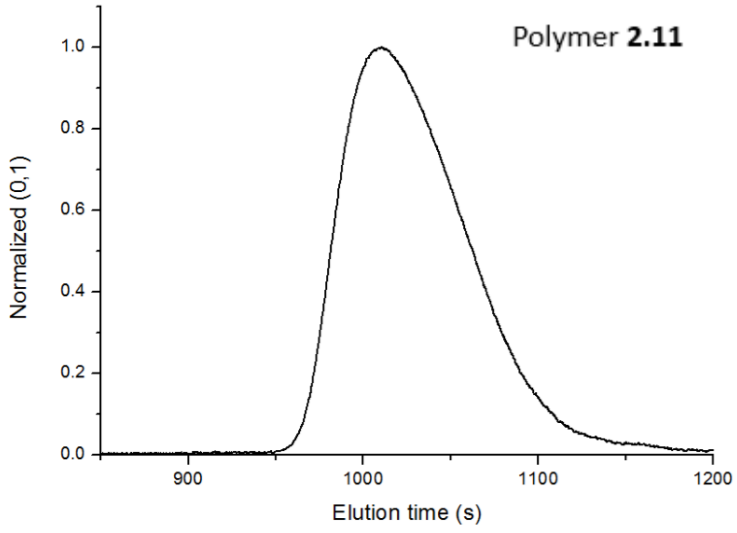

Figure A2. 33 SEC trace for Polymer 2.11

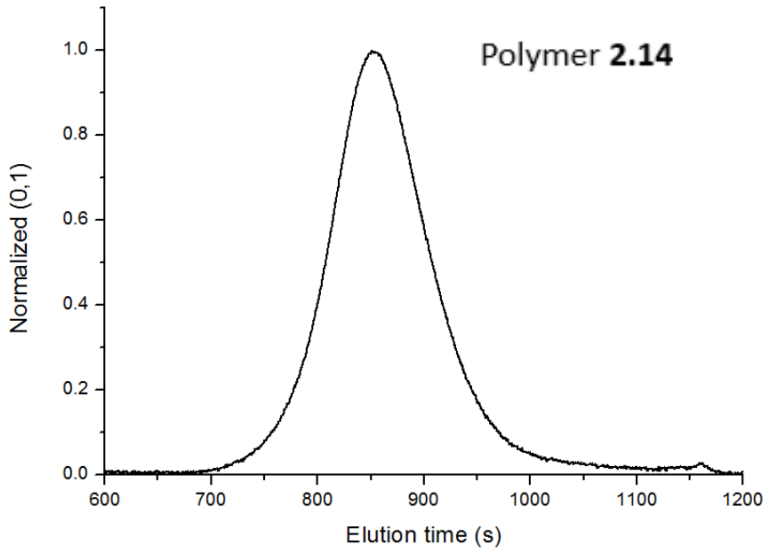

Figure A2. 34 SEC curve of Polymer 2.14

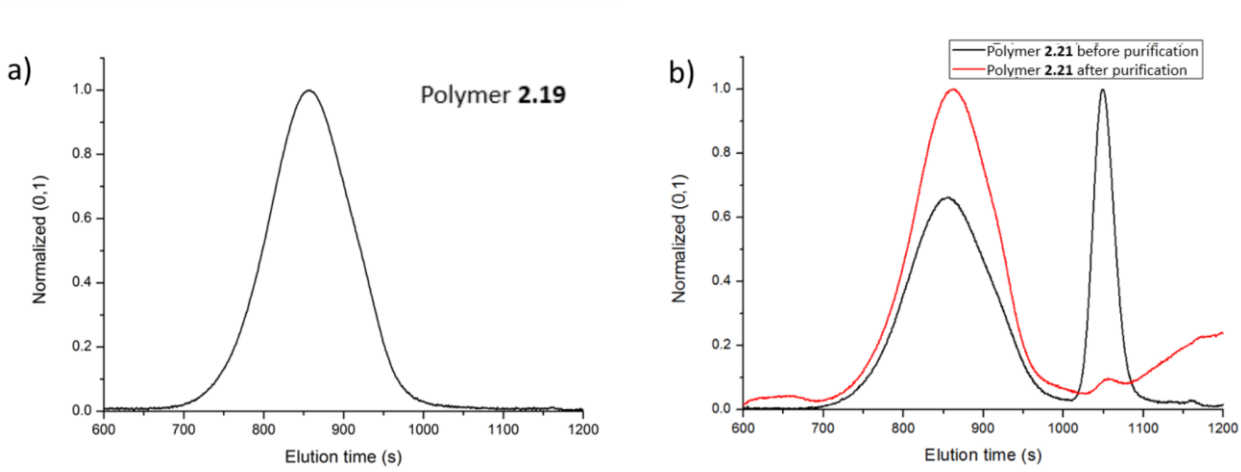

Figure A2. 35 SEC traces for Polymers 2.19 and 2.21

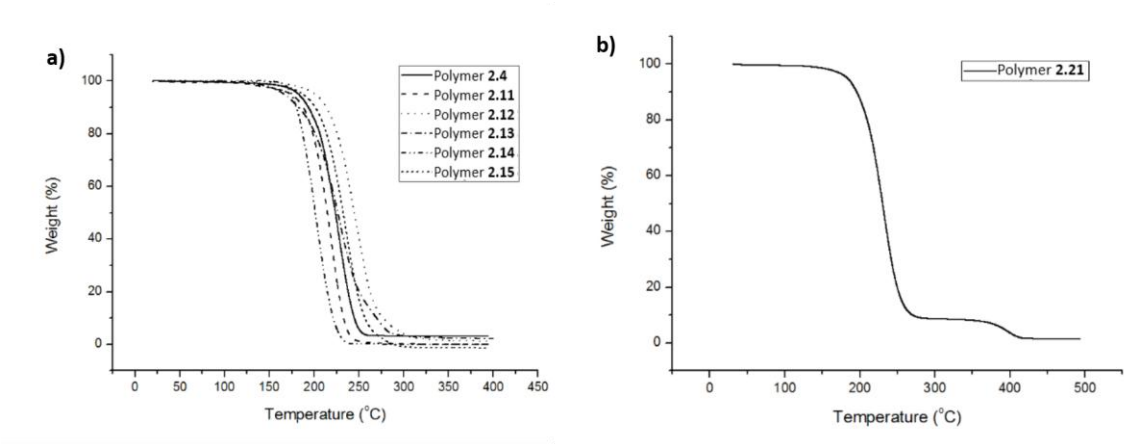

Figure A2. 36 TGA curves for: (a) polyglyoxylates 2.11-2.15 compared with PEtG 2.4; (b) triblock copolymer 2.21.

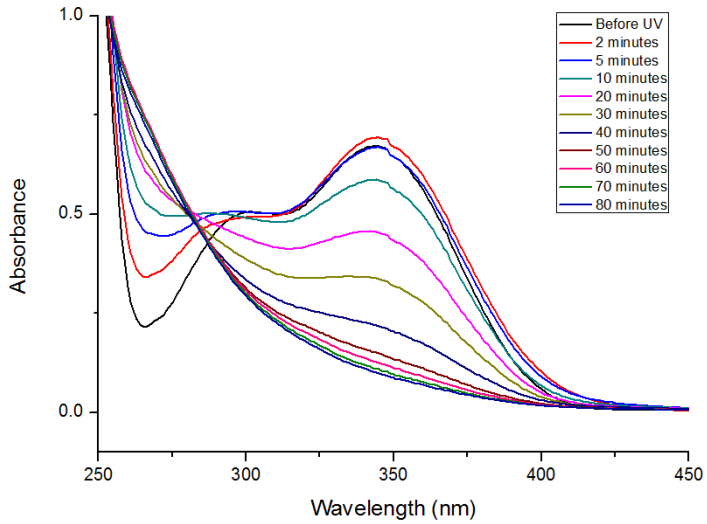

Figure A2. 37 UV-visible spectroscopy of polymer 2.4 and its end-cap cleavage following different irradiation time with UV light.

Degradation studies on polymer **2.3**.

To demonstrate that UV light was selective for cleaving the end-cap to initiate depolymerization rather than the polymer backbone, polymer **2.3** was treated as described in the manuscript for the study of PEtG **2.4** degradation in solution.

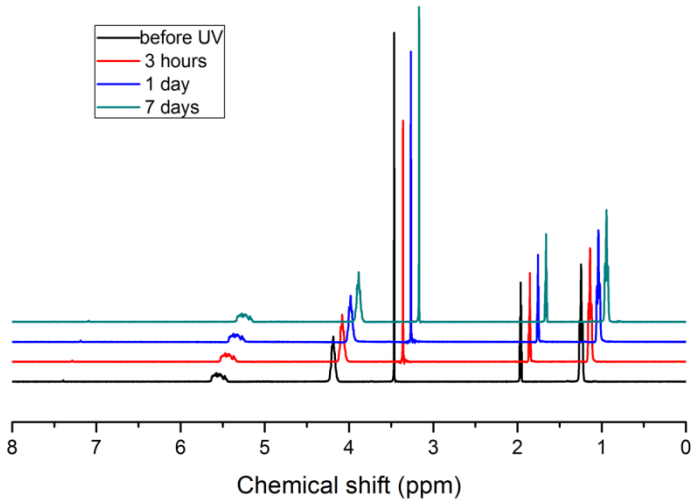

Figure A2. 38 ^{1}H NMR spectrum of polymer 2.3 after UV irradiation following the same procedure described for the study of polymer 2.4 (following incubation in 9:1 CD_3CN:D_2O). No changes were observed, indicating that the polymer is stable under these conditions and UV irradiation does not cleave the polymer backbone.

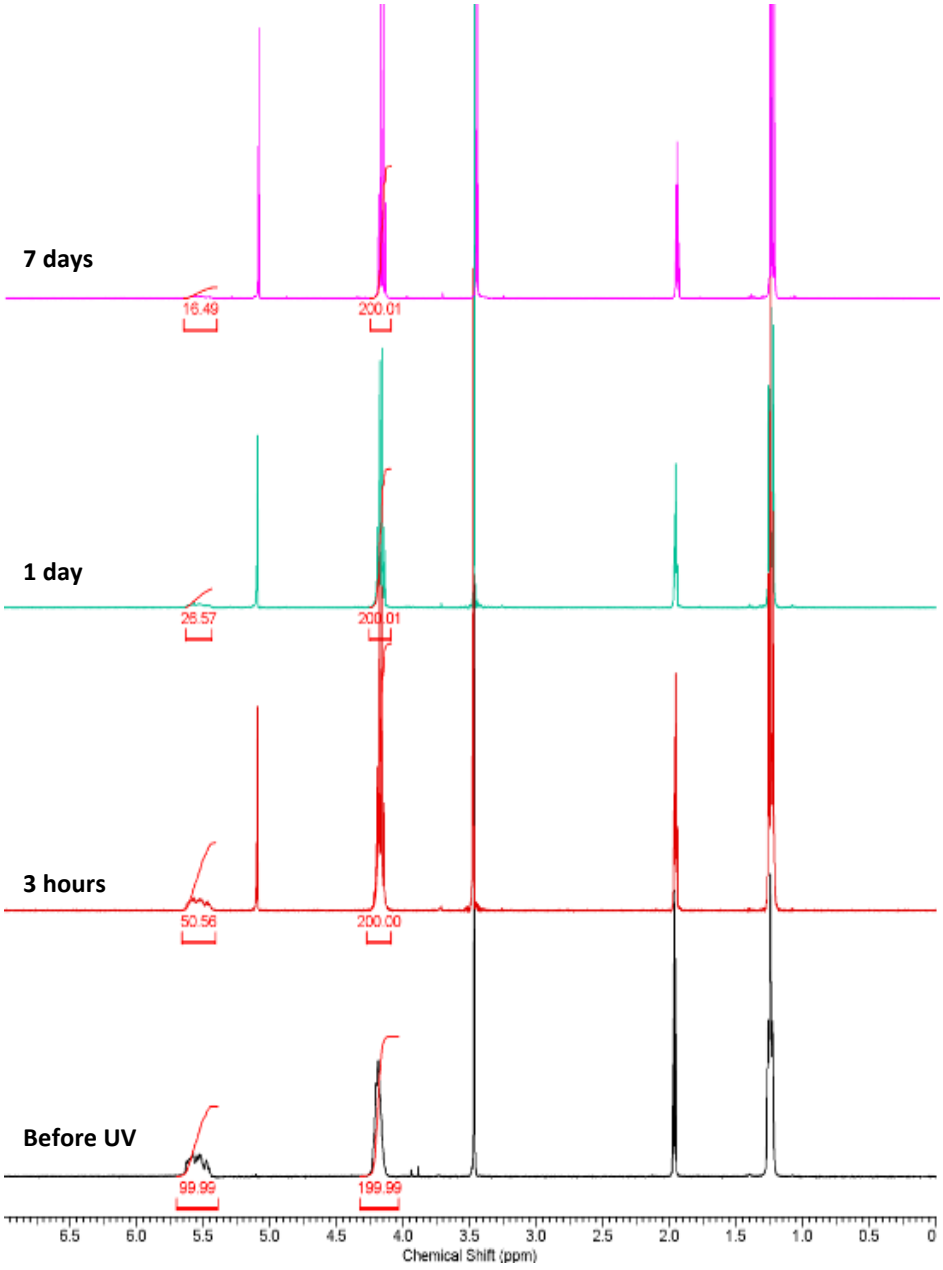

Figure A2. 39 Zoom of ^{1}H NMR spectra corresponding to Figure 2.2a from chapter 2, showing relative peak integrals that were used to calculate the % polymer remaining for Figure 2.4 of chapter 2. The initial integral (t = 0) for the peak at 5.6 ppm was set to 100 to indicate 100% polymer and it decreased over time. Integration of the peak at 4.2 ppm remained constant as it corresponds to the $CH_3C\underline{H}_2$-O- in both the polymer and degradation product.

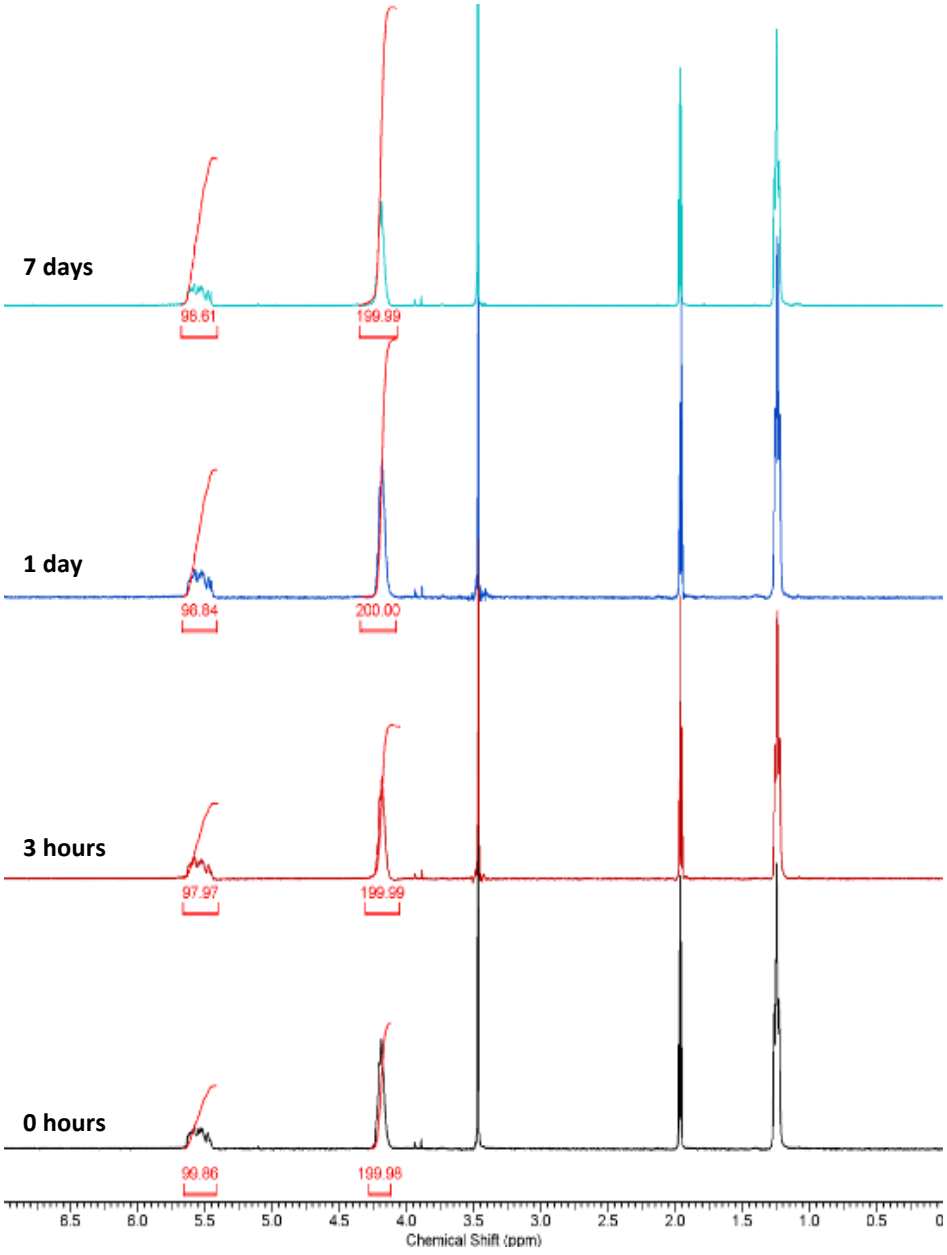

Figure A2. 40 Zoom of ^{1}H NMR spectra corresponding to Figure 2.2a from the manuscript, showing relative peak integrals that were used to calculate the % polymer remaining for Figure 2.4 of the manuscript. The initial integral (t = 0) for the peak at 5.6 ppm was set to 100 to indicate 100% polymer and it decreased over time. Integration of the peak at 4.2 ppm remained constant as it corresponds to the $CH_3C\underline{H}_2$-O- in both the polymer and degradation product.

Degradation studies on polymers **2.11** to **2.15** and **2.21**.

As for polymer **2.4,** before irradiation, the polymers showed broad peaks and several small peaks corresponding to the end-cap. However, following irradiation of a 9:1 $CD_3CN:D_2O$ solution of the polymer with UV light and incubation at ambient temperature (21 °C), the broad peak at 5.5 ppm started decreasing, and a new singlet at 5.1 ppm (alkyl glyoxylate hydrate) began increasing (a in Figures A2.51 – 2.56). Peaks associated with the alkyl/benzyl chains became sharper. In each case the control group (b in Figures A2.51 – 2.56) did not show any signs of significant degradation.

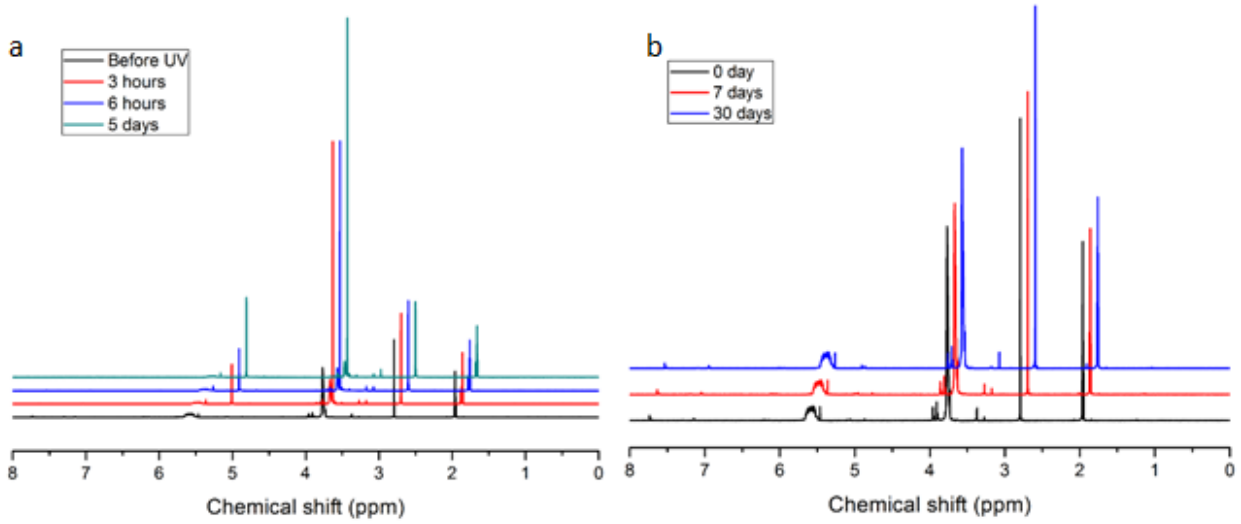

Figure A2. 41 (a) ^{1}H NMR spectra of polymer 2.11 after irradiation; (b) ^{1}H NMR spectra of polymer 2.11 without irradiation (following incubation in 9:1 $CD_3CN:D_2O$).

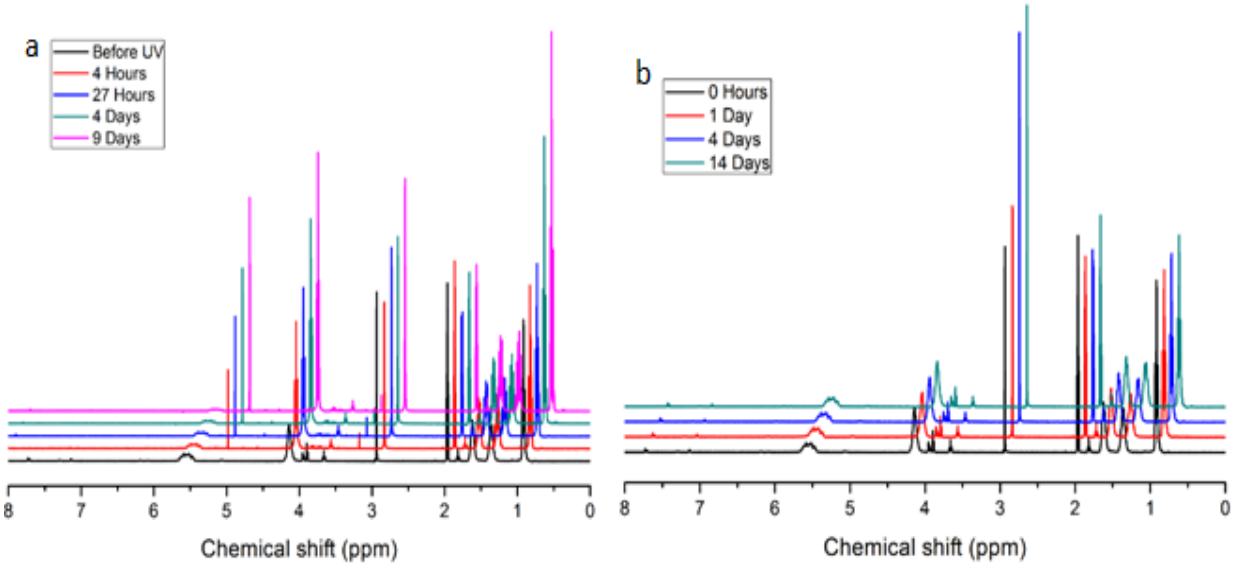

Figure A2. 42 (a) ^{1}H NMR spectra of polymer 2.12 after irradiation; (b) ^{1}H NMR spectra of polymer 2.12 without irradiation (following incubation in 9:1 $CD_3CN:D_2O$).

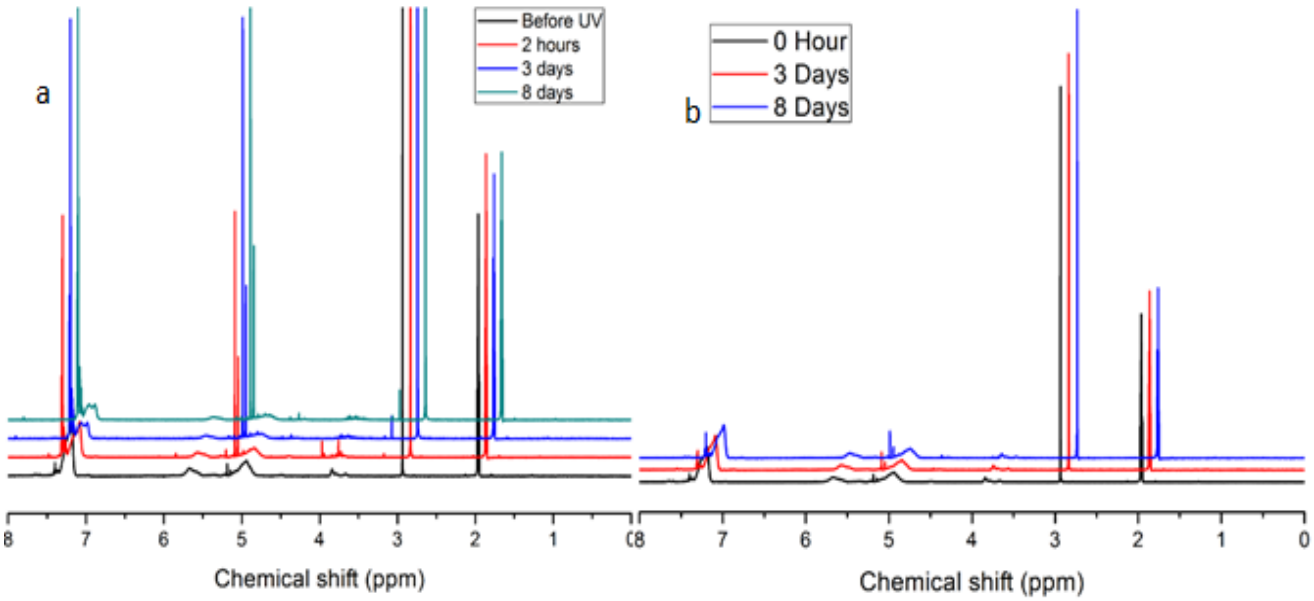

Figure A2. 43 (a) ^{1}H NMR spectra of polymer 2.13 after irradiation; (b) ^{1}H NMR spectra of polymer 2.13 without irradiation (following incubation in 9:1 $CD_3CN:D_2O$)

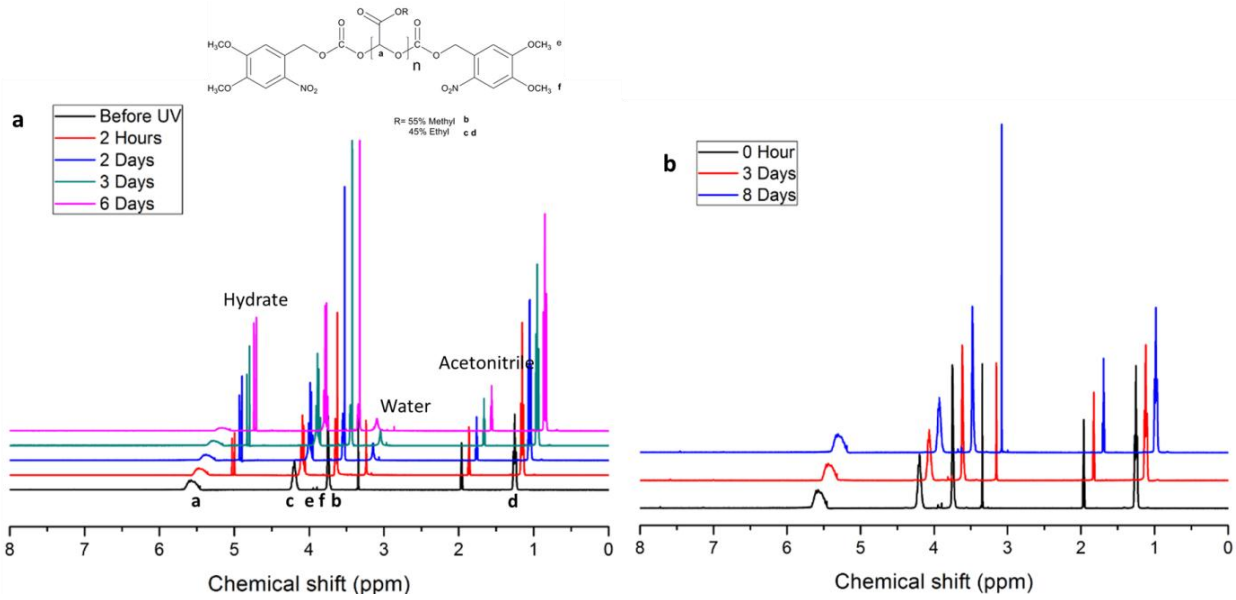

Figure A2. 44 (a) ^{1}H NMR spectra of polymer 2.14 after irradiation; (b) ^{1}H NMR spectra of polymer 2.14 without irradiation (following incubation in 9:1 CD_3CN:D_2O)

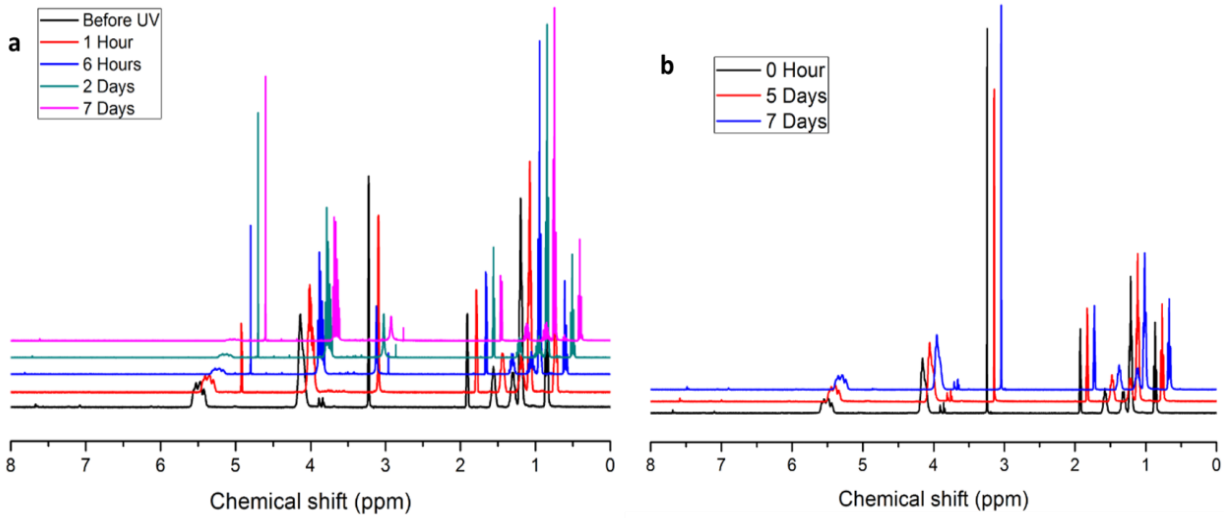

Figure A2. 45 (a) ^{1}H NMR spectra of polymer 2.15 after irradiation; (b) ^{1}H NMR spectra of polymer 2.15 without irradiation (following incubation in 9:1 CD_3CN:D_2O).

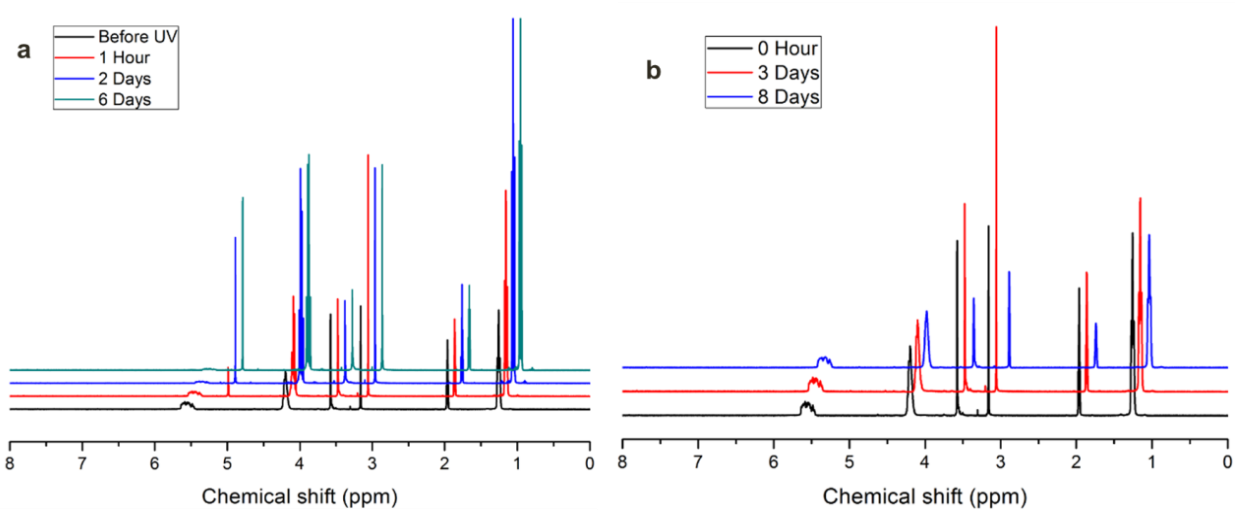

Figure A2. 46 (a) ^{1}H NMR spectra of polymer 2.21 after irradiation; (b) ^{1}H NMR spectra of polymer 2.21 without irradiation (following incubation in 9:1 CD_3CN:D_2O).

Depolymerization profiles of individual polyglyoxylates

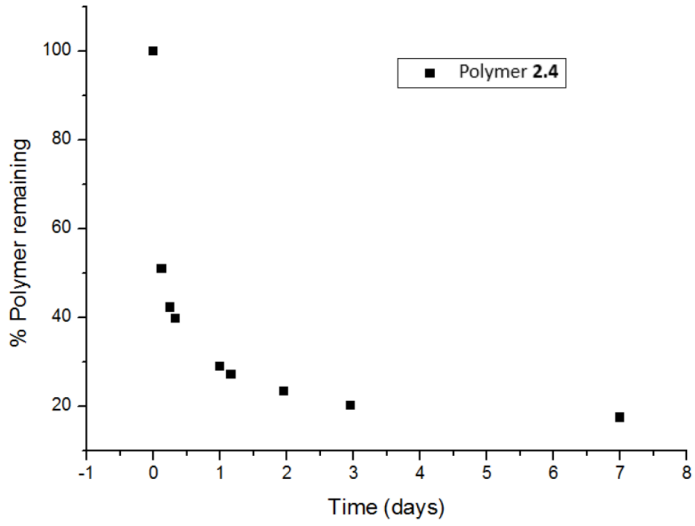

Figure A2. 47 Depolymerization of polymer 2.4 following cleavage of the NVOC end-caps by UV irradiation in 9:1 CD_3CN:D_2O following by incubation at ambient temperature (21°C).

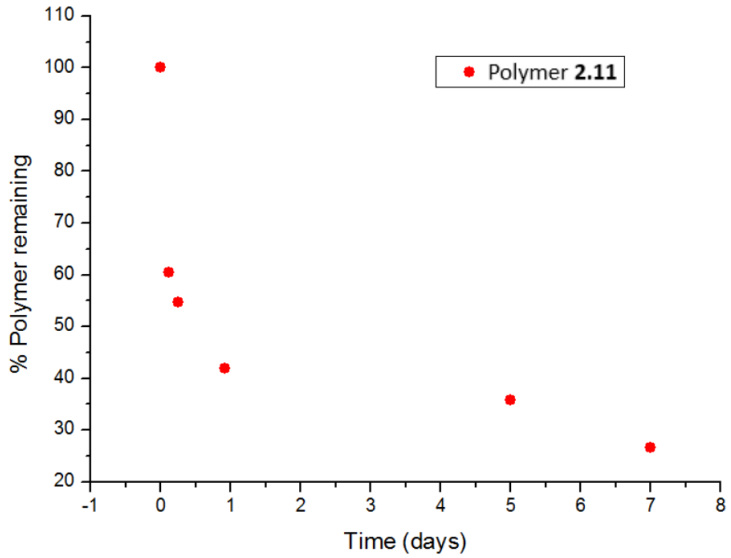

Figure A2. 48 Depolymerization of polymer 2.11 following cleavage of the NVOC end-caps by UV irradiation in 9:1 CD_3CN:D_2O following by incubation at ambient temperature (21°C).

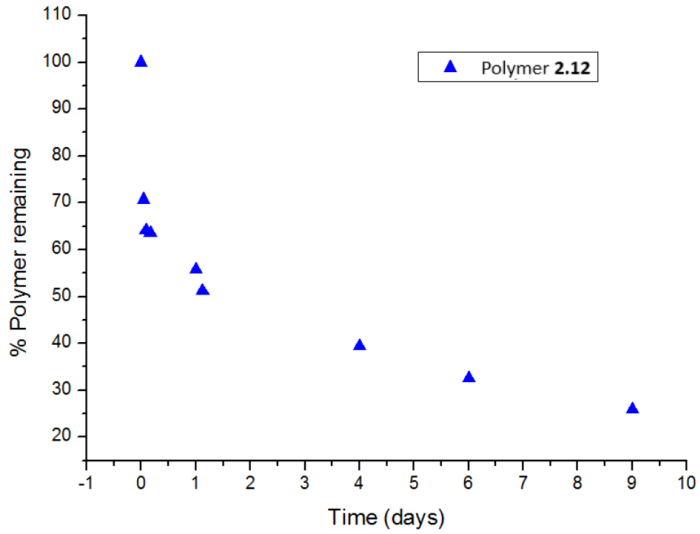

Figure A2. 49 Depolymerization of polymer 2.12 following cleavage of the NVOC end-caps by UV irradiation in 9:1 CD_3CN:D_2O following by incubation at ambient temperature (21°C).

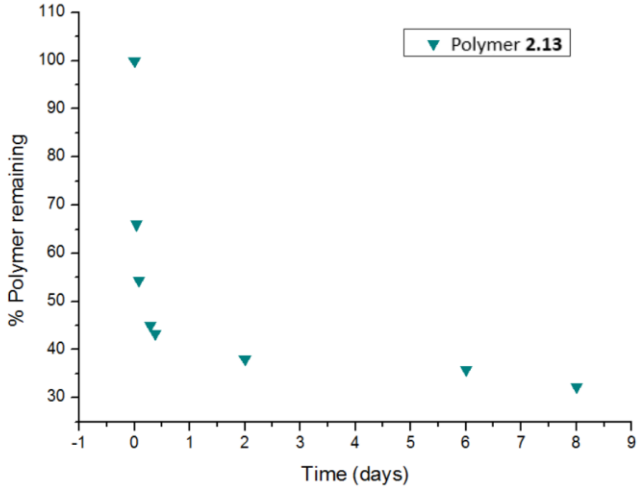

Figure A2. 50 Depolymerization of polymer 2.13 following cleavage of the NVOC end-caps by UV irradiation in 9:1 CD_3CN:D_2O following by incubation at ambient temperature (21°C).

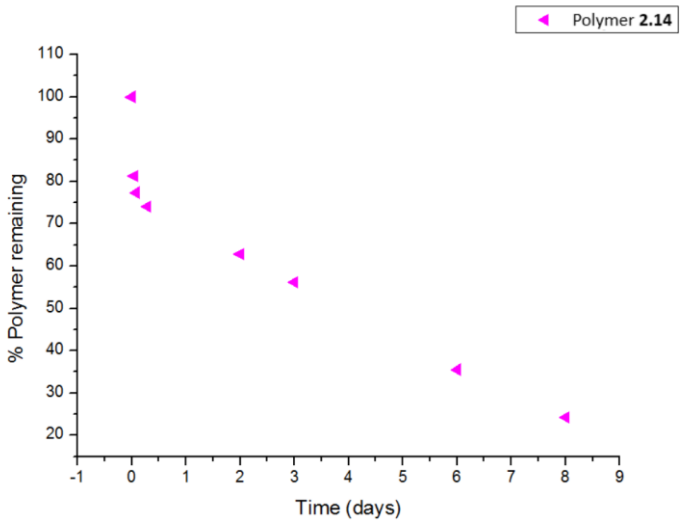

Figure A2. 51Figure SX. Depolymerization of polymer 2.14 following cleavage of the NVOC end-caps by UV irradiation in 9:1 CD3CN:D2O following by incubation at ambient temperature (21°C).

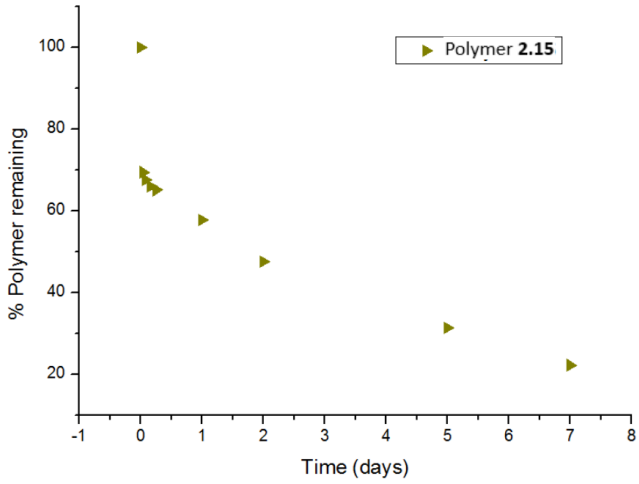

Figure A2. 52 Depolymerization of polymer 2.15 following cleavage of the NVOC end-caps by UV irradiation in 9:1 CD3CN:D2O following by incubation at ambient temperature (21°C).

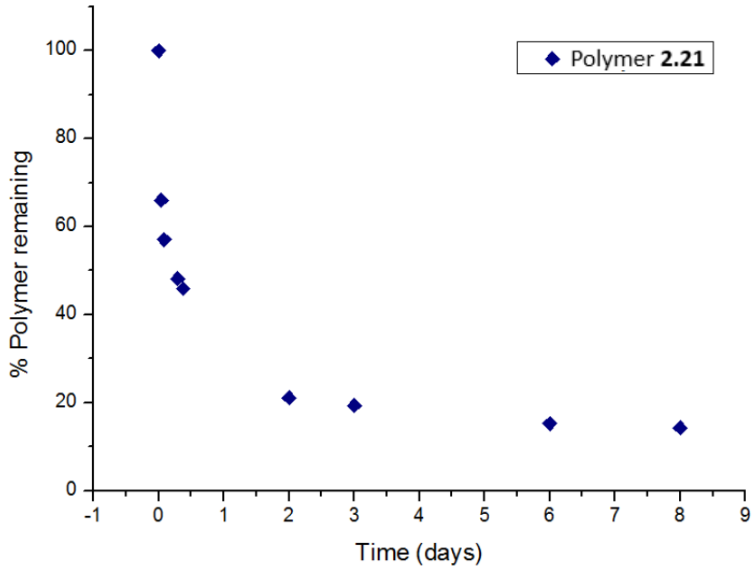

Figure A2. 53 Depolymerization of polymer 2.21 following cleavage of the NVOC end-caps by UV irradiation in 9:1 CD3CN:D2O following by incubation at ambient temperature (21°C).

Appendix 3: Supporting Information for Chapter 3

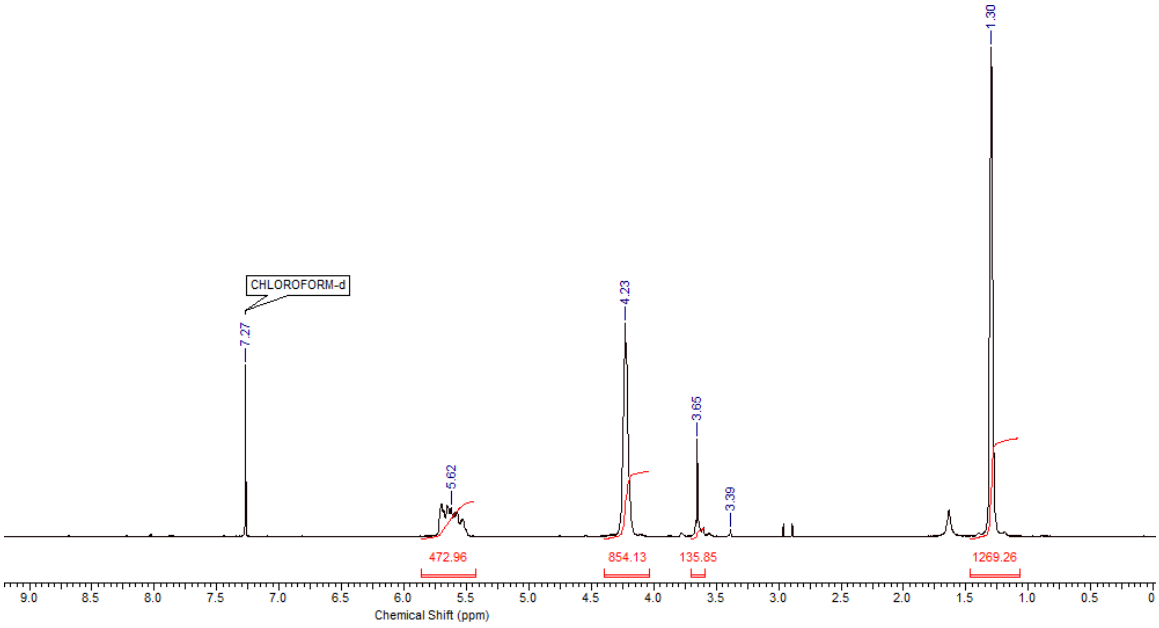

Figure A3. 1 ^{1}H NMR spectrum of block polymer (Polymer 3.1) ($CDCl_3$, 400MHz).

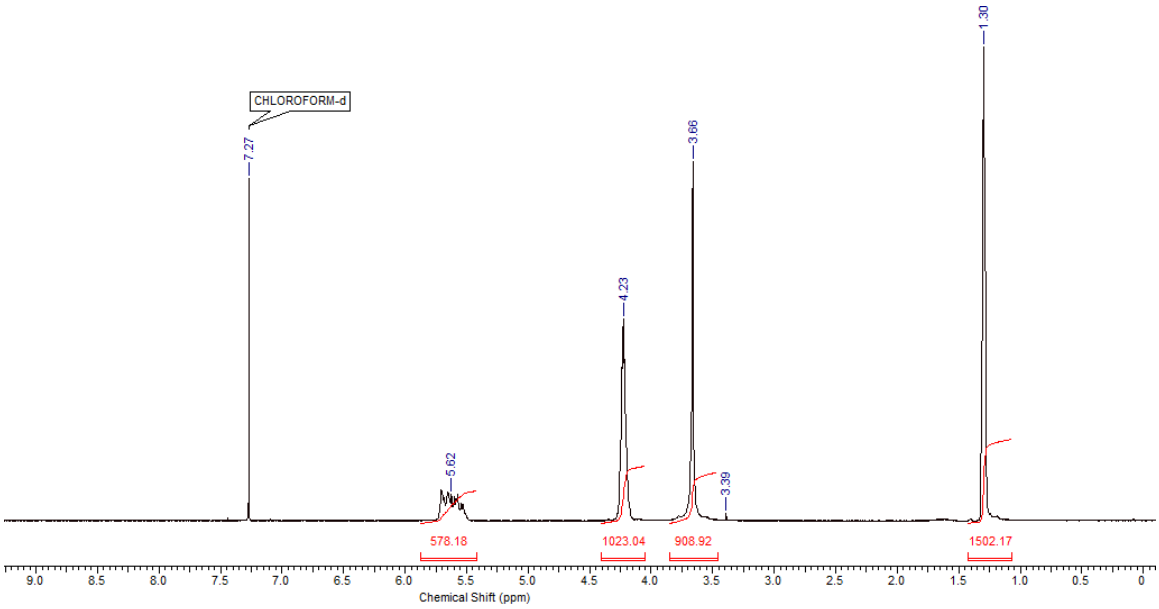

Figure A3. 2 ^{1}H NMR spectrum of block polymer (Polymer 3.3) ($CDCl_3$, 400MHz).

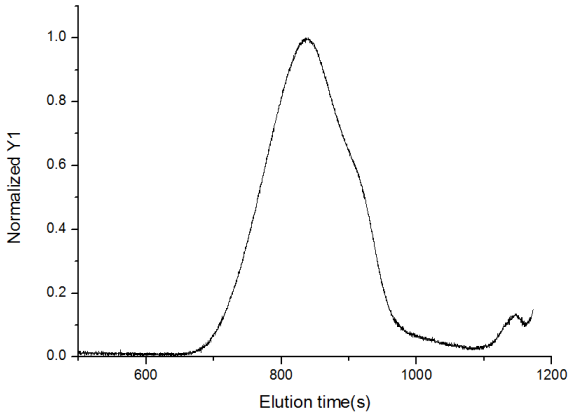

Figure A3. 3 SEC curve of polymer 3.1

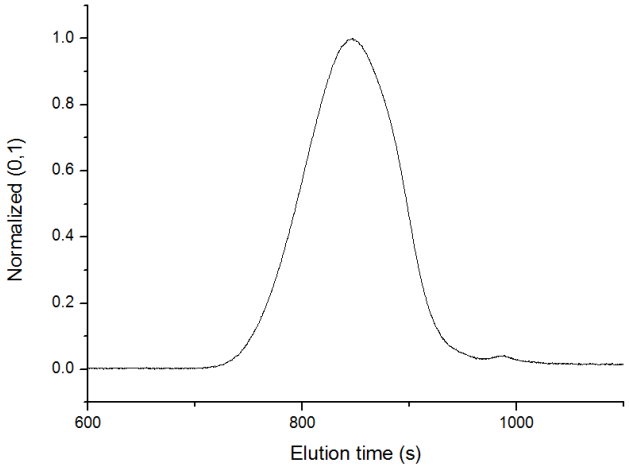

Figure A3. 4 SEC curve of polymer 3.3

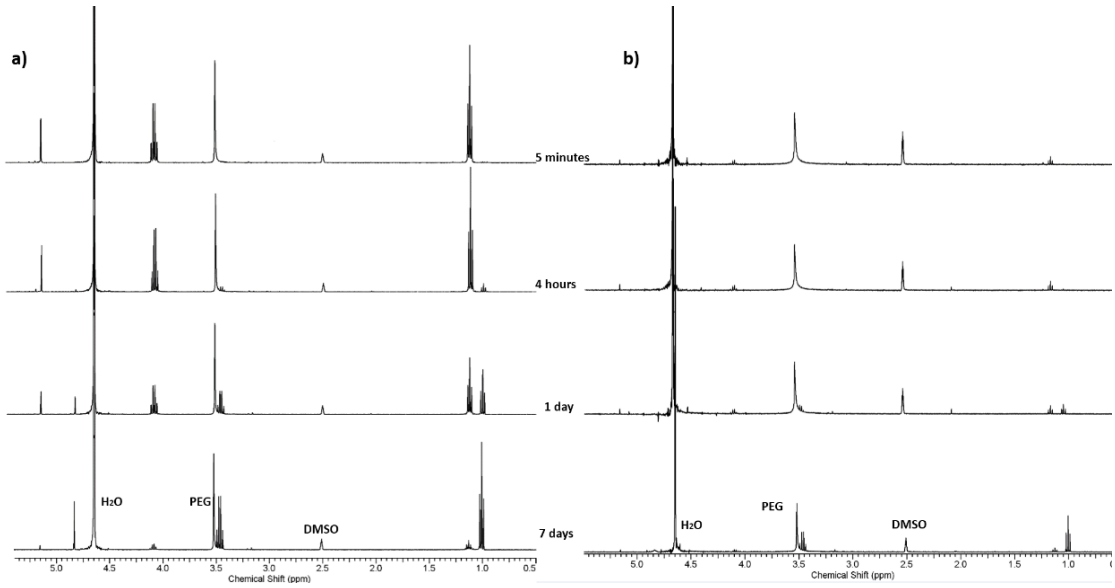

Figure A3. 5 NMR monitored micelle degradation at pH 7.4 and 37 ºC, a) with 10 minutes irradiation, b) without irradiation

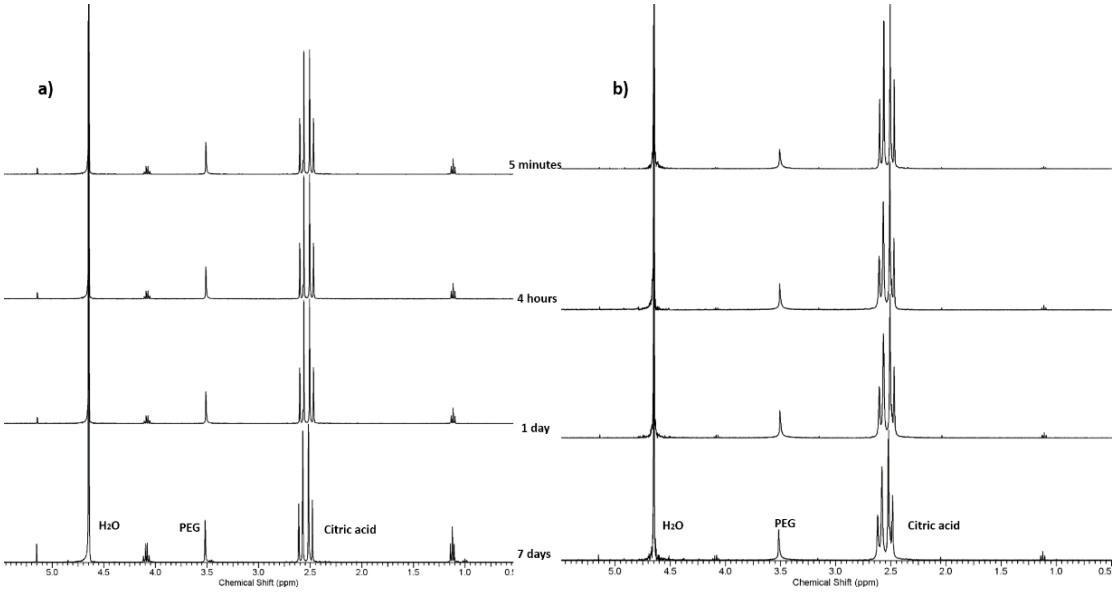

Figure A3. 6 NMR monitored micelle degradation at pH 5.0 and 37 ºC, a) with 10 minutes irradiation, b) without irradiation

Appendix 4: Supporting Information for Chapter 4

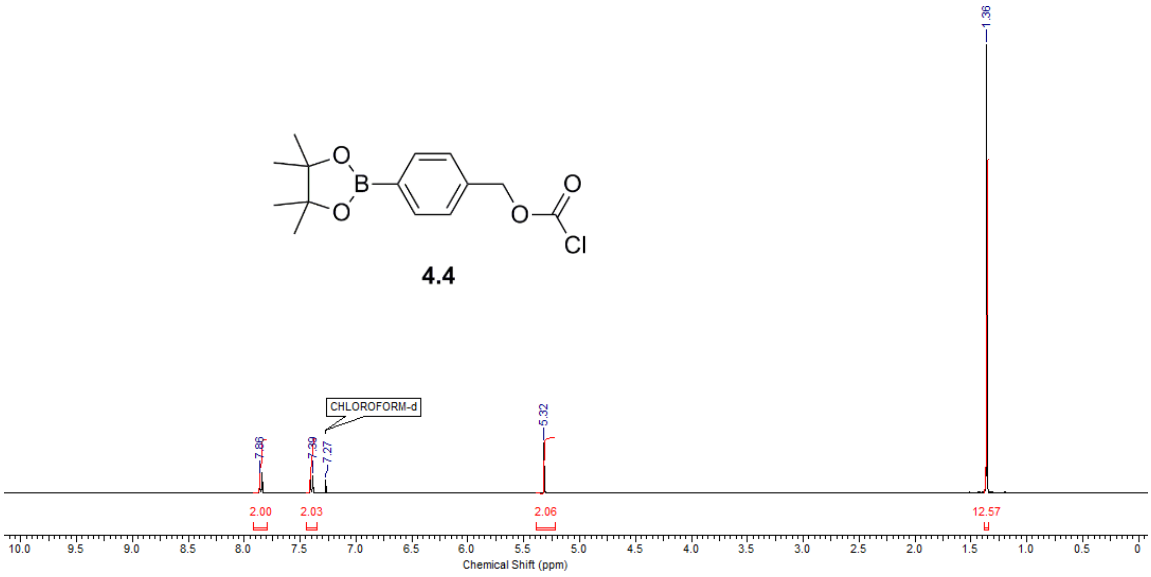

Figure A4. 1 ^{1}H NMR spectrum of Chloroformate 4.4 ($CDCl_3$, 400 MHz).

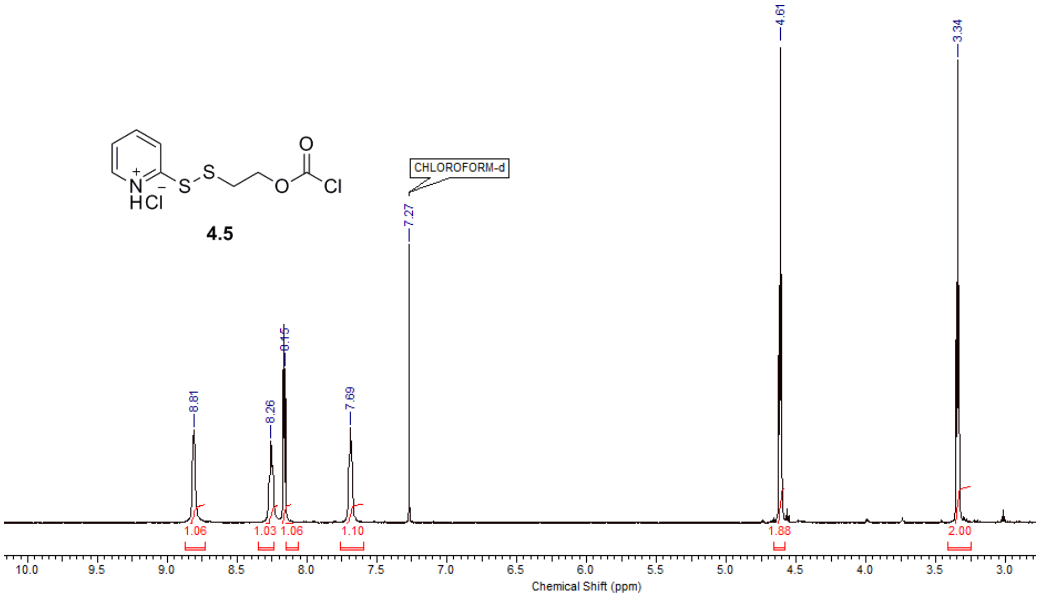

Figure A 4. 2 ^{1}H NMR spectrum of Chloroformate 4.5 ($CDCl_3$, 400 MHz).

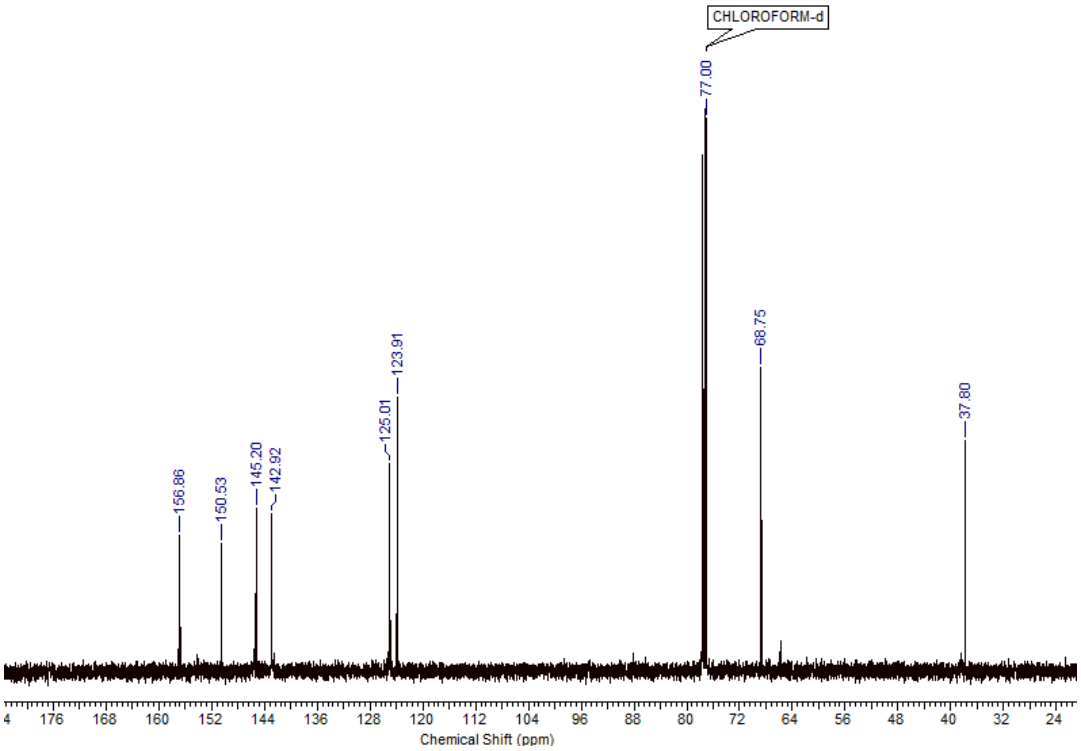

Figure A4. 3 ^{13}C NMR spectrum of Chloroformate 4. 5 ($CDCl_3$, 150 MHz).

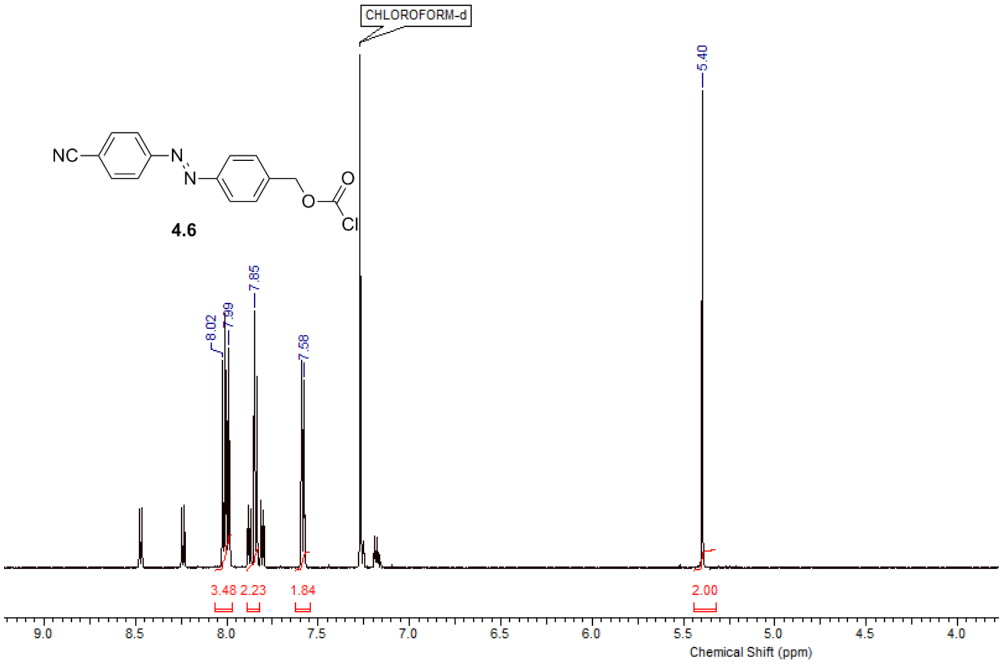

Figure A4. 4 ^{1}H NMR spectrum of Chloroformate 4.6 ($CDCl_3$, 400 MHz).

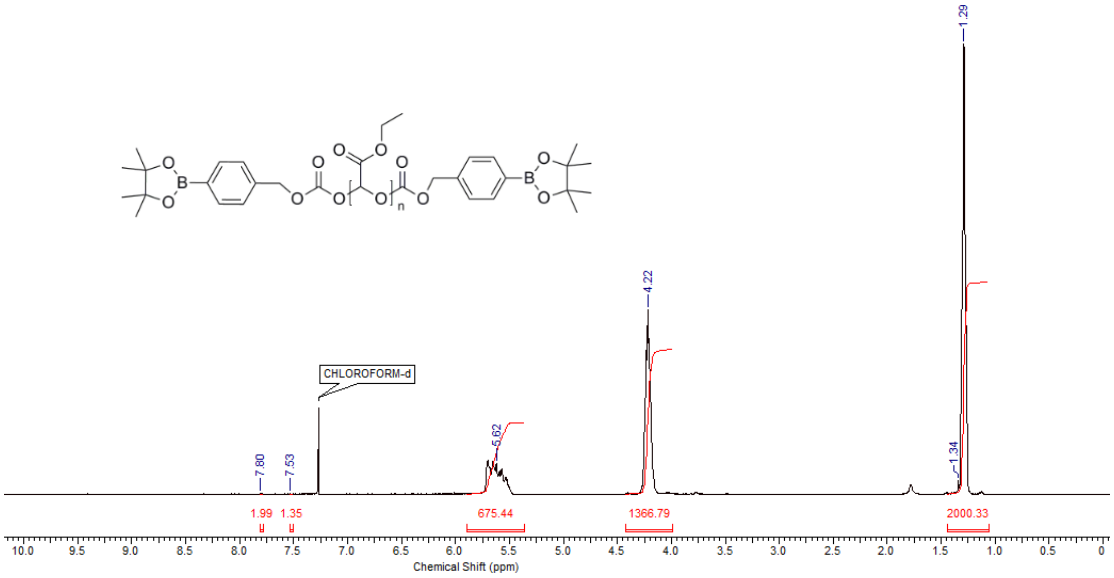

Figure A4. 5 ^{1}H NMR spectrum of Polymer 4.7 ($CDCl_3$, 400 MHz).

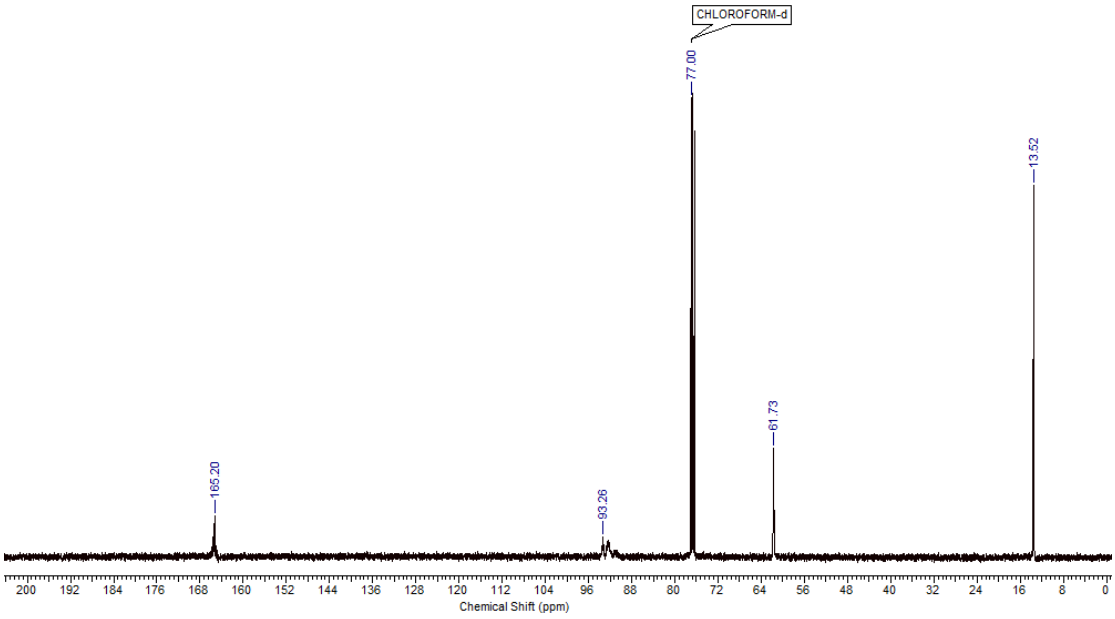

Figure A4. 6 ^{13}C NMR spectrum of Polymer 4.7 ($CDCl_3$, 150 MHz).

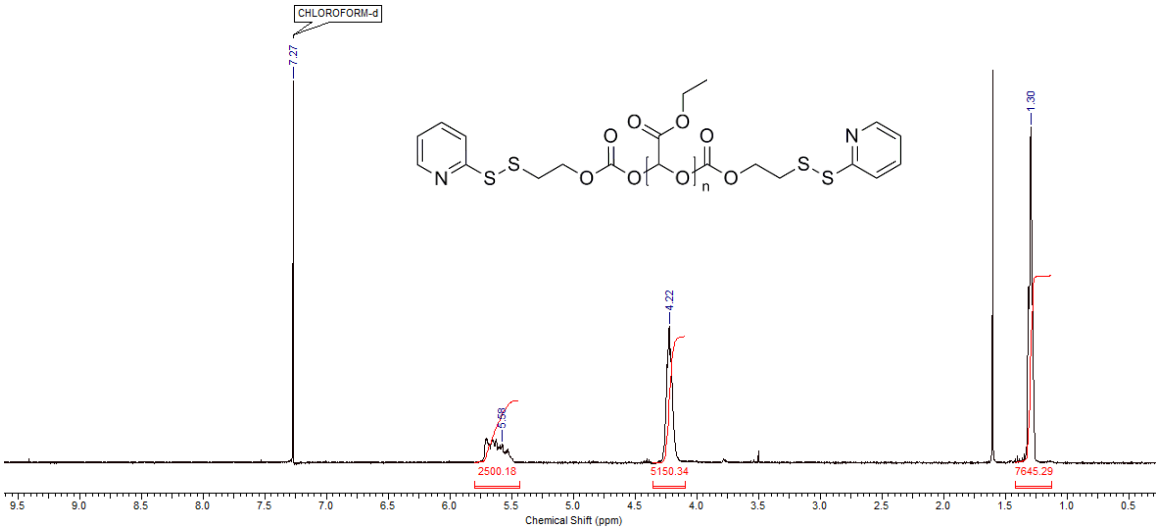

Figure A4. 7 ^{1}H NMR spectrum of Polymer 4.8 ($CDCl_3$, 400 MHz).

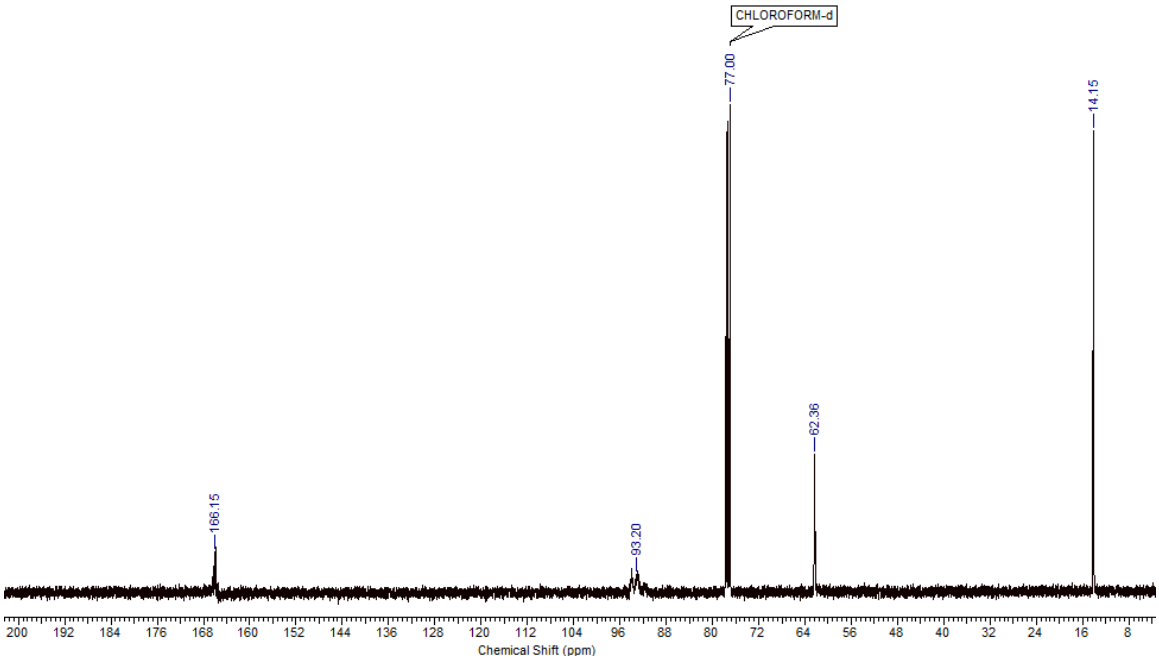

Figure A4. 8 ^{13}C NMR spectrum of Polymer 4.8 ($CDCl_3$, 150 MHz).

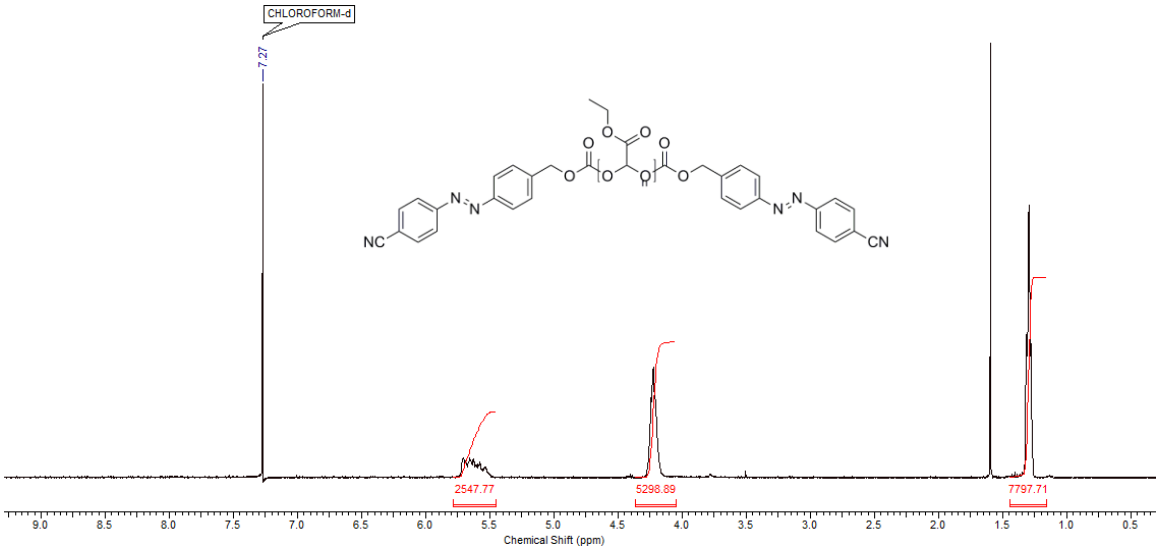

Figure A4. 9 ^{1}H NMR spectrum of Polymer 4.9 ($CDCl_3$, 400 MHz).

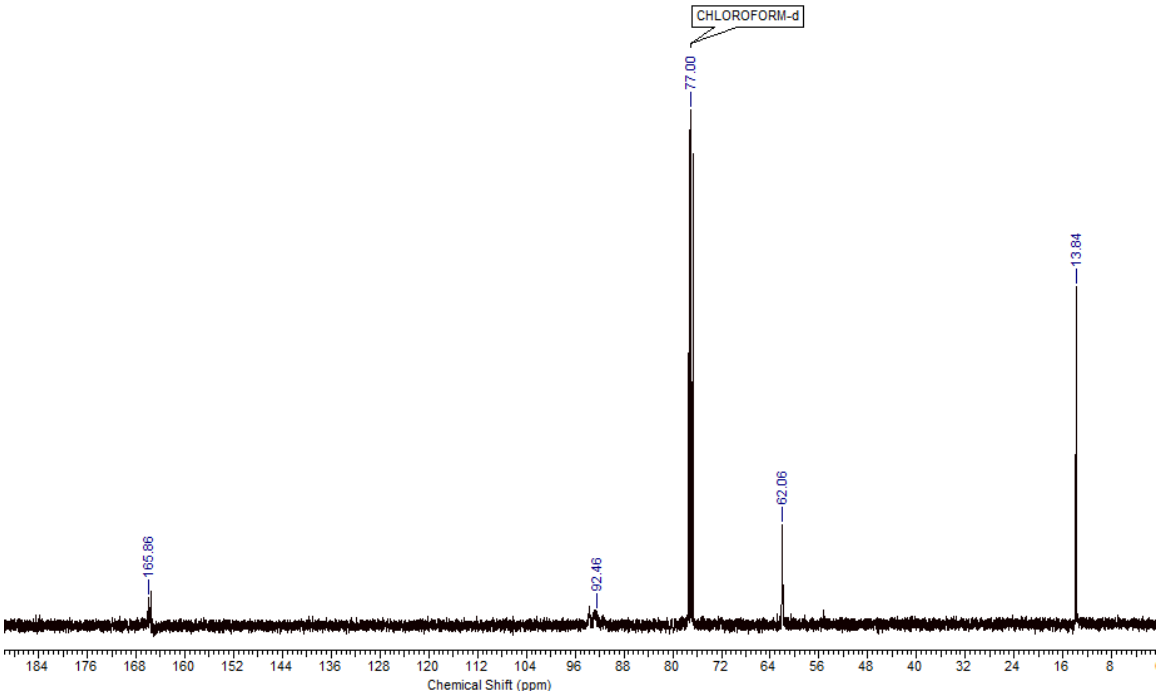

Figure A4. 10 ^{13}C NMR spectrum of Polymer 4.9 ($CDCl_3$, 150 MHz).

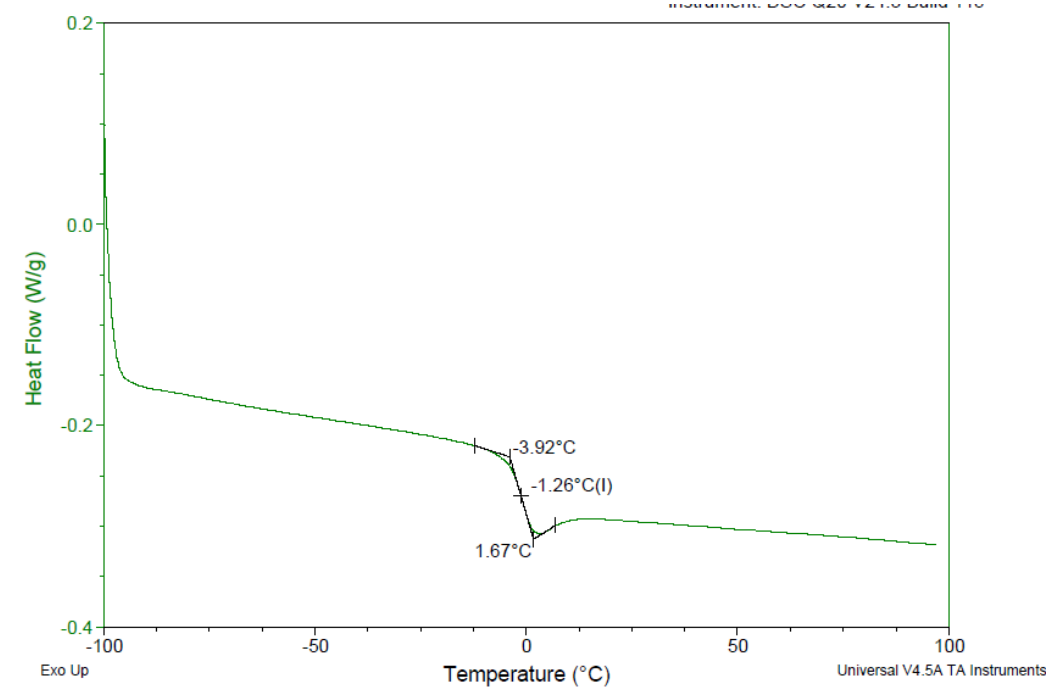

Figure A4. 11 DSC of Polymer 4.7.

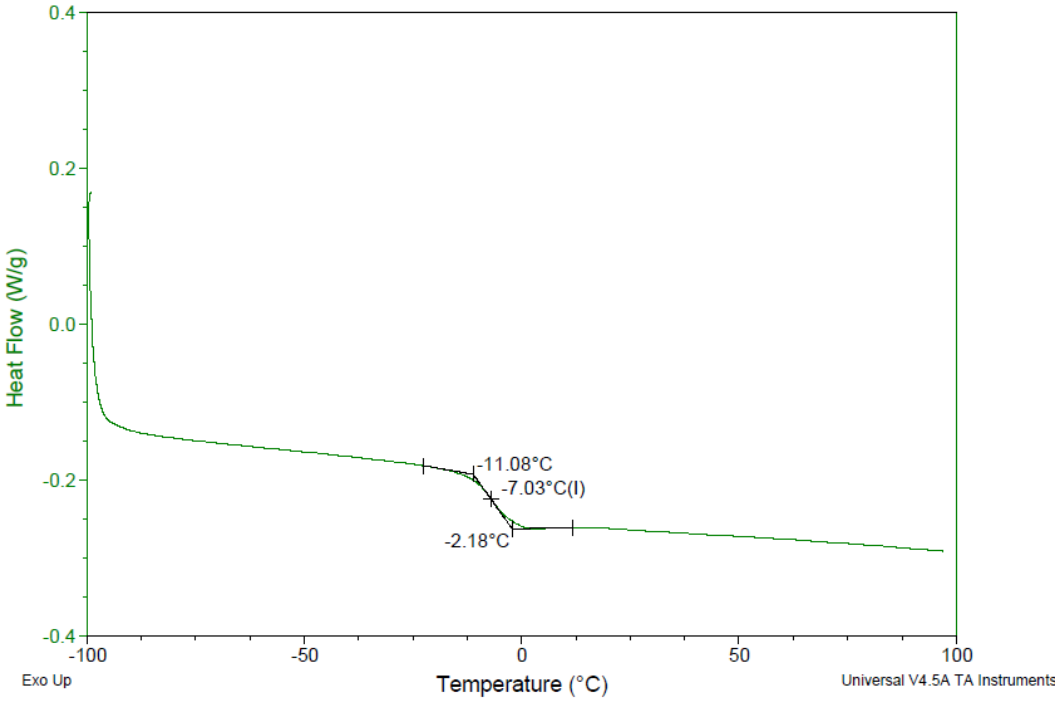

Figure A4. 12 DSC of Polymer 4.8.

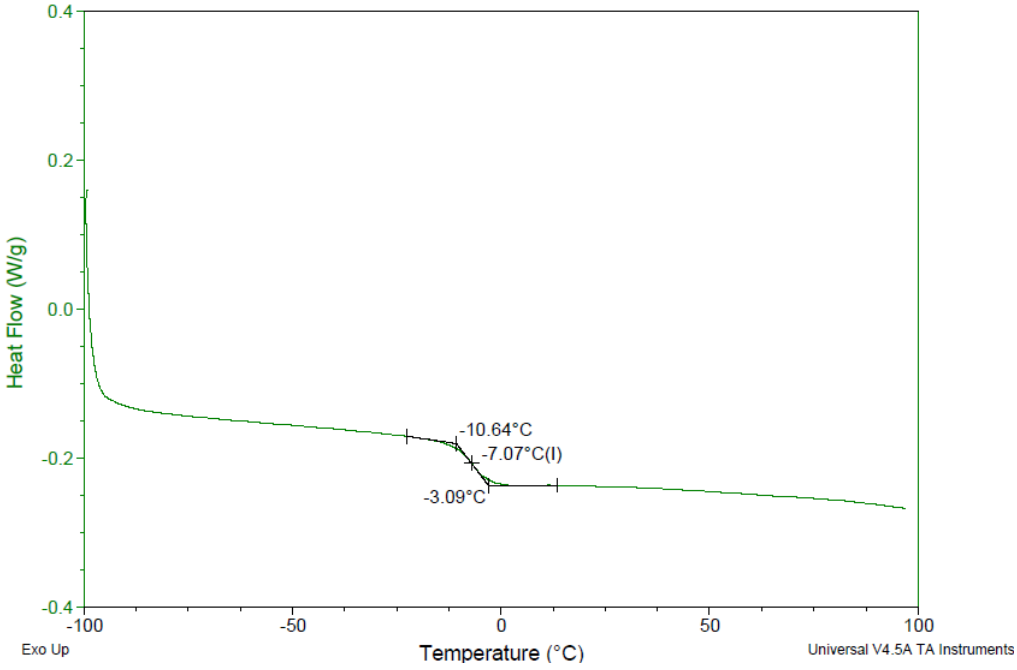

Figure A4. 13 DSC of Polymer 4.9.

Curriculum Vitae for Bo Fan

Education: **The University of Western Ontario**, London, ON 2013-2014

Master of Chemistry, The Department of Chemistry

- Supervisor: Dr. Elizabeth Gillies
- Thesis Project: Development of polyglyoxylates as a new calss of self-immolative polymers

Sichuan University, Chengdu, China 2008-2012

Bachelor of Engineering, The Department of Polymer Materials and Engineering

- Supervisor: Dr. Guangsu Huang
- Fourth year project: Synthesis and characterization of mono-functionalized polyhedral oligomeric silsesquioxanes

Honors and Awards:

International Students Scholarship, Western University, 2013-2014

Third prize Social Scholarship awarded by Shenzhen Senior Technology Material Co. LTD, Sichuan University, 2012

Excellent Volunteer of Academic Year, Sichuan University, 2011

First prize Scholarship of Academic Year, Sichuan University, 2010

Second prize Scholarship of Academic Year, Sichuan University, 2009

Publications:

Fan, B.; Trant, J. F.; Wong, A. D.; Gillies, E. R.* "*Polyglyoxylates: A versatile class of triggerable self-immolative polymers from readily accessible monomers*" J. Am. Chem. Soc. **2014**, 136, 10116-10123.

Patents:

Gillies, E. R.; Fan, B.; Trant, J. F.; Wong, A. D. "*Polyglyoxylates, manufacture and use thereof*" US Prov. Appl. (2014), No. 61/989,086.

Conference

Fan, B.; Trant, J. F.; Wong, A. D.; Gillies, E. R. "*Polyglyoxylate: A*

Presentation: *versatile class of triggerable self-immolative polymers from readily accessible monomers"* 36th Canadian High Polymer Forum, 2014, **Poster Presentation**

Professional Experience:

The University of Western Ontario, London, Ontario
Graduate Research Assistant, Gillies group 2013-2014

Sichuan University, Chengdu, China
4th year project, Huang's group 2011-2012

Teaching Experience:

The Univerity of Western Ontario, London, Ontario
Tutorial Teaching Assistant, First Year Chemistry (1024B)
01/2013-04/2013
Laboratory Teaching Assistant, Second Year Chemistry (2213A)
09/2013-12/2013
Laboratory Teaching Assistant, First Year Chemistry (1024B&1302B)
01/2014-04/2014
Laboratory Teaching Assistant, Second Year Chemistry (2213A)
05/2014-06/2014